



UNIVERSITÀ DEGLI STUDI DI PALERMO

Dottorato di ricerca in Scienze Agrarie, Alimentari, Forestali e Ambientali

Dipartimento Scienze Agrarie, Alimentari, Forestali e Ambientali

(SAAFA)

AGR/12 Patologia Vegetale

Molecular methods for the diagnosis and characterization of
phytopathogenic fungi of quarantine concern or causing
emerging plant diseases

PhD CANDIDATE

FRANCESCO ALOI

ADVISOR

PROF. SANTA OLGA CACCIOLA

COORDINATOR

PROF. VINCENZO BAGARELLO

CO ADVISOR

DR. LIVIO TORTA

SUPERVISOR

PROF. JULIO DIEZ CASEIRO

Acknowledgements

This thesis, far from being the final goal of my PhD course, is the expression of a human and scientific experience fertilized by the encounter with many people and special places. I met many leaders in my journey; each of them has dedicated precious time, discussing and finding answers to my questions, challenging my convictions and ideas. Here, I want to say thank you to all the people who have shared these years with me and this research project.

I will always thank Prof. Santa Olga Cacciola, my PhD tutor, to which goes my deepest gratitude for introducing me in the field of plant pathology both nationally and internationally. She has taught me that research work is a job build on sacrifice, commitment, dedication and study, but at the same time exciting and rewarding.

I would like to extend my appreciation to my co-tutor Dr. Livio Torta for scientific support but also for the kindness and availability.

I would also like to thank Prof. Antonella Pane for the valuable training in laboratory routines, the technical and scientific support.

I want to thank Professor Gaetano Magnano di San Lio for didactic and scientific aid, extraordinary availability, insights and above all for the shared experience at the Department of Plant Protection, of the University of Shiraz, Iran. Thanks to the immense hospitality of Prof. R. Mostowfizadeh-Ghalamfarsa and his PhD students Pegah, Bahar, Behnaz and Sahar. Yet, it remains one of the best experiences of my life.

I would like to thank the supervisor of this PhD thesis, Professor Julio Diez Caseiro for the extreme kindness, availability and hospitality and all his research group, in particular Dr Jorge Martin Garcia and Drs Cristina, Irene, Tamara and the laboratory technician Mariano. They were a central part of my experience abroad at the Escuela Técnica Superior de Ingenierías Agrarias of Palencia, Spain. It was long and intense, both for the repeated scientific evidence made and for having lived during the global pandemic of Covid-19.

I would also like to thank my friends of Palencia, in particular Sara, Aitor, Ana, Elena and Juan (Mis Amigos de las Rutas) and Carlota, Ana, Diego and Erik (Mis Amigos Palentino).

I would like to thank all my research group from the Molecular Plant Pathology laboratory of the Di3A, my small lab family. Maria, Federico, Mario and Rossana, thanks for having shared with me every moment of this experience.

Finally, my gratitude goes to the people who have been close to me and which believed in me for all of this time. They have made this "adventure" took on the right meaning and the right light in my life. A special thanks to my mother, my father and my brother Fabrizio for supporting me and encouraging me throughout my university career, for their affection and for never stopped believing in me.

“The best studies and research that can be done are those made to follow one's passions and satisfy one's curiosity. It is not essential to have bases or previous knowledge; the most important thing is to have passion and desire to understand and learn what we do not know. The curiosity to try to understand is the real engine of life.”

S.N.

Index

Abstract.....	1
Chapter 1. Introduction.....	5
1.1 General introduction: Molecular era in plant pathology.....	5
1.2 Objectives of the Ph.D. thesis.....	5
Chapter 2. <i>Fusarium circinatum</i> an emergent and quarantine pathogen of pine worldwide: its detection and its interaction with <i>Phytophthora</i> species (<i>P. cambivora</i> and <i>P. parvispora</i>) on <i>Pinus radiata</i> seedlings.....	6
2.1. Transferability of PCR-based diagnostic protocols: An international collaborative case study assessing protocols targeting the quarantine pine pathogen <i>Fusarium circinatum</i> . Published on Scientific Reports 2019, 9, 8195. DOI: 10.1038 / s41598-019-44672-8.	7
2.2. Co-infections by <i>Fusarium circinatum</i> and <i>Phytophthora</i> spp. on <i>Pinus radiata</i> , a case study of complex interactions in the Pine pitch canker disease	24
2.2.1 Introduction	24
2.2.2 Materials and Methods	25
2.2.2.1 Plant material.....	25
2.2.2.2 Fungal inoculum and inoculation methods.....	25
2.2.2.3 Evaluation of visual symptoms and internal necrosis length.....	26
2.2.2.4 Sample collection, RNA extraction and cDNA synthesis	27
2.2.2.5 Selection of primers and housekeeping genes	27
2.2.2.6 Relative expression of candidate genes	27
2.2.3 Results	28
2.2.3.1 Differences in disease symptoms progression.....	28
2.2.3.2 Housekeeping gene selection.....	29
2.2.3.3 Differential expression of candidate genes.....	30
2.2.4 Discussion.....	32
2.2.5 References.....	34
Chapter 3. Scabby canker caused by <i>Neofusicoccum batangarum</i> (<i>Botryosphaeriaceae</i>), an emergent disease of <i>Opuntia ficus-indica</i> in minor islands around Sicily: identification of the causative agent and characterization of both its phytotoxic metabolites and the genetic variability of its local population	39
3.1 New insights into scabby canker of <i>Opuntia ficus-indica</i> , caused by <i>Neofusicoccum batangarum</i> . Published on Mediterranean Phytopathology 2020, 59 (2): 269-284. DOI: 10.14601 / Phyto-11225.....	40

3.2 Phytotoxic Metabolites Isolated from <i>Neofusicoccum batangarum</i> , the Causal Agent of the Scabby Canker of Cactus Pear (<i>Opuntia ficus-indica</i> L.). Published on Toxins 2020, 12, 126. DOI: 10.3390 / toxins12020126	56
Chapter 4. Identification of <i>Neofusicoccum parvum</i> (<i>Botryosphaeriaceae</i>) as the causal agent of the bot gummosis disease of lemon (<i>Citrus × limon</i>) trees	69
4.1 Introduction	69
4.2 Materials and Methods	70
4.2.1 Fungal collections and isolations.....	70
4.2.2 Morphological characteristics and cardinal temperatures for growth of the isolates	72
4.2.3 Amplification and sequencing	72
4.2.4 Molecular identification and phylogenetic analyses.....	73
4.2.5 Pathogenicity tests	75
4.2.6 Statistical analyses of data	75
4.3 Results	75
4.3.1 Symptoms	75
4.3.2 Fungus isolation and morphological identification	77
4.3.3 Molecular identification.....	79
4.3.4 Pathogenicity tests	81
4.4 Discussion.....	83
4.5 References.....	85
Chapter 5. Characterization of <i>Alternaria</i> species associated with heart rot of pomegranate fruit.....	89
5.1 Introduction	89
5.2 Materials and Methods	90
5.2.1 <i>Alternaria</i> isolates.....	90
5.2.2 Symptoms, distribution, and incidence of the disease.....	93
5.2.2 Morphological characterization.....	94
5.2.3 Molecular characterization	94
5.2.4 Pathogenicity tests	96
5.2.5 Extraction and analyses of secondary metabolites	96
5.3 Results	97

5.3.1 Morphological characterization of isolates.....	97
5.3.2 Molecular characterization	97
5.3.3 Pathogenicity tests	100
5.3.5. Analyses of <i>Alternaria</i> mycotoxins	100
5.4 Discussion.....	102
5.5 References.....	104
Chapter 6. Shoot dieback of citrus, a new disease caused by <i>Colletotrichum</i> species. Published on <i>Cells</i> 2021, 10(2), 449; DOI: 10.3390/cells10020449.....	109
Chapter. 7 General conclusions	134
References.....	138

Abstract

In the context of molecular techniques applied to Plant Pathology, this Ph.D. thesis has pursued the following major objectives: i) to develop new diagnostic protocols for fungal pathogens; ii) to study the metabolic and physiological effects determined by new and emerging fungal pathogens; iii) to contribute to develop management strategies of diseases caused by quarantine and/or emerging fungi on plant species typical of the Mediterranean region. To fulfill these objectives, the following specific studies have been developed:

- “*Fusarium circinatum* an emergent and quarantine pathogen of pine worldwide: its detection and its interaction with *Phytophthora* species (*P. cambivora* and *P. parvispora*) on *Pinus radiata* seedlings.”

This study has been developed by two different lines of research:

- “Transferability of PCR-based diagnostic protocols: An international collaborative case study assessing protocols targeting the quarantine pine pathogen, *Fusarium circinatum*.”

In this study, different protocols for the molecular diagnosis of *F. circinatum* were compared and validated for the first time in 23 laboratories spread across Europe, South Africa and Chile, in the framework of the international collaborative study funded by COST Action FP1406 “Pine pitch canker - Strategies for management of *Gibberella circinata* in greenhouses and forests - PINESTRENGTH ". The protocols tested by the Laboratory of Molecular Plant Pathology of the Department of Agriculture, Food and Environment (Di3A) of the University of Catania were: (i) Real-time PCR by Lamarche et al. 2015 and (ii) real-time PCR by Luchi et al. 2018.

Results from the two tested protocols were illustrated in Ioos et al (2019), Scientific Reports 2019, 9, 8195. DOI: 10.1038 / s41598-019-44672-8.

- “Co-infections by *Fusarium circinatum* and *Phytophthora* spp. on *Pinus radiata*, a case study of complex interactions in the Pine pitch canker disease.”

This study investigated i. the phenotypic response of pine to the infective process and ii. the relative expression levels of genes of plant encoding for pathogenesis-related proteins and antifungal secondary metabolites. Results obtained in this research showed that the phenotypic response of pine to the simultaneous action of the aforementioned pathogens is manifested by an increase of the severity of the symptoms at the early stages of the infection, allowing then to speculate that *Phytophthora* spp. can realistically contribute to the severity of the disease. Results from gene expression suggest that a real synergic effect as the result of the effects of both pathogens it is not clearly evident.

- “Scabby canker caused by *Neofusicoccum batangarum* (*Botryosphaeriaceae*), an emergent disease of *Opuntia ficus-indica* in minor islands around Sicily: identification of the causal agent and characterization of both its phytotoxic secondary metabolites and the genetic variability of its local population.”

The specific objectives of this study were the following: i) determine the geographical distribution of the disease; ii) characterize *N. batangarum* isolates obtained from symptomatic plants of prickly pear in the smaller islands of Sicily; iii) check whether the range of potential host plants of this phytopathogenic fungus includes other Mediterranean species that could act as alternative hosts or as inoculum 'reservoir'; iv) determine the ability of *N. batangarum* to produce phytotoxic secondary metabolites (phytotoxins) in culture, which can play an active role in the pathogenesis of the disease; v) chemically identify the phytotoxins extracted from *N. batangarum* liquid filtrates and determine their phytotoxic effects on the host plant as well as on non-host plant species. In cross-pathogenicity tests, *N. batangarum* isolated from *Opuntia ficus-indica* plants was able to reproduce disease symptoms on the host plant and also infected other plant species. The fungus artificially inoculated by wounding induced cancers on several hosts. This result indicates that the pathogen has a very wide range of potential hosts. Six phytotoxins were obtained and identified from *Neofusicoccum batangarum* culture filtrates: (-) - (R) - mellein (1); (±) - botriisocoumarin A (2); (-) - (3R, 4R) - and (-) - (3R, 4S) - 4 hydroxymellin (3 and 4); (-) - terpestacin (5); and (+) - 3,4 - dihydro - 4,5,8 - trihydroxy - 3 - methylisocoumarin, renamed (+) - neoisocoumarin (6). All six metabolites have been shown to have phytotoxic activity on both the host and non-host plants. The most active compounds proved to be (±) - botriisocoumarin A (2), (-) - terpestacin (5) and (+) - neoisocoumarin (6).

Results from this study are part of two scientific publications: Masi et al., *Toxins* 2020, 12, 126. DOI: 10.3390/toxins12020126 and Aloï et al., *Mediterranean Phytopathology* 2020, 59 (2): 269-284. DOI: 10.14601/Phyto-11225.

- “Identification of *Neofusicoccum parvum* (*Botryosphaeriaceae*) as the causative agent of gummy cankers of lemon (*Citrus × limon*) trees.”

This study was aimed at identifying the causative agent of the observed disease. *Neofusicoccum parvum*, in the family *Botryosphaeriaceae*, was identified as the causal agent of bot gummosis of lemon (*Citrus x limon*) trees, in the two major lemon-producing regions in Italy. Gummy cankers on trunk and scaffold branches of mature trees were the most typical disease symptoms. *Neofusicoccum parvum* was the sole fungus constantly and consistently isolated from the canker bark of symptomatic lemon trees. It was identified on the basis of morphological characters and the phylogenetic analysis of three loci, i. e. the internal transcribed spacer of nuclear ribosomal DNA (ITS) as well as the translation elongation factor 1-alpha (*TEF1*) and β-tubulin (*TUB2*) genes. The pathogenicity of *N. parvum* was demonstrated by wound inoculating two lemon cultivars, ‘Femminello 2kr’ and ‘Monachello’, as well as citrange (*C. sinensis × Poncirus trifoliata*) ‘Carrizo’ rootstock. In artificial inoculations, the fungus was very aggressive on lemons and weakly virulent on citrange, consistently with symptoms observed in the field as a consequence of natural infections. This is the first report of *N. parvum*, both in a wide and in a strict taxonomic sense, as a pathogen of lemon in Italy.

- “Characterization of *Alternaria* species associated with heart rot of pomegranate fruit.”

This study was aimed at identifying *Alternaria* species associated with heart rot disease of pomegranate fruit in southern Italy and characterizing their mycotoxigenic profile. A total of 42 *Alternaria* isolates were characterized. They were obtained from pomegranate fruits with symptom of heart rot sampled in Apulia and Sicily and grouped into six distinct morphotypes based on macro- and microscopic features. According to multi-gene phylogenetic analysis, including internal transcribed spacer (ITS), translation elongation factor 1- α (EF-1 α), glyceraldehyde-3-phosphate dehydrogenase (GAPDH) and a SCAR marker (OPA10-2), 38 isolates of morphotypes 1 to 5 were identified as *A. alternata*, while isolates of morphotype 6, all from Sicily, clustered within the *A. arborescens* species complex. In particular, isolates of morphotype 1, the most numerous, clustered with the ex-type isolate of *A. alternata*, proving to belong to morphotype *alternata*. No difference in pathogenicity on pomegranate fruits was found between isolates of *A. alternata* and *A. arborescens* and among *A. alternata* isolates of different morphotypes. The toxigenic profile of isolates varied greatly: *in vitro*, all 42 isolates produced tenuazonic acid and most of them other mycotoxins including alternariol, alternariol monomethyl ether, altenuene and tentoxin.

- “Shoot dieback of citrus, a new disease caused by *Colletotrichum* species.”

This study was aimed at identifying the *Colletotrichum* species associated with twig and shoot dieback of citrus, a new disease occurring in the Mediterranean region and also reported as emerging in California. Overall, 119 *Colletotrichum* isolates were characterized. They were recovered from symptomatic trees of sweet orange, mandarin and mandarin-like during a survey of citrus groves in Albania and Sicily (southern Italy). The isolates were grouped into two distinct morphotypes. The grouping of isolates was supported by phylogenetic sequence analysis of two genetic markers, the internal transcribed spacer regions of rDNA (ITS) and β -tubulin (TUB2). The groups were identified as *Colletotrichum gloeosporioides* and *C. karstii*, respectively. The former accounted for more than 91% of isolates, while the latter was retrieved only occasionally in Sicily. Both species induced symptoms on artificially wound inoculated twigs. *C. gloeosporioides* was more aggressive than *C. karstii*. Winds and prolonged drought were the factor predisposing to *Colletotrichum* twig and shoot dieback. This is the first report of *C. gloeosporioides* and *C. karstii* as causal agents of twig and shoot dieback disease in the Mediterranean region and the first report of *C. gloeosporioides* as a citrus pathogen in Albania.

Chapter 1.

Introduction

1.1 General introduction: Molecular era in plant pathology

Polymerase Chain Reaction (PCR) was invented in the 1980s and represented a breakthrough in biochemistry and molecular biology (Bartlett and Stirling, 2003; Williams, 2009; Kaunitz, 2015). It took a few years to become a mature technology and during the last decades has tremendously impacted almost all scientific biological disciplines. Several fields of plant pathology have been revolutionized following the exploitation of this basic techniques, including diagnostics (Cooke et al., 2007; Schena et al., 2013; Sanzani et al., 2014; Raja et al., 2017), taxonomy (Crous, 2005; Crous et al., 2015; Guarnaccia et al., 2018; Ruvishika et al., 2020) and the study of plant pathogen interaction (Gupta et al., 2015; Peyraud et al., 2017; Frantzeskakis et al., 2020), just to mention those who have benefited most from this technology in terms of scientific publications and practical applications. The development of innovative molecular technologies, such as Next Generation Sequencing (NGS) (Lindahl et al., 2013; Barba et al., 2014; Adams et al., 2018) and the CRISPR–Cas genome editing systems (Chen et al., 2019; Muñoz et al., 2019; Schenke and Cai, 2020), along with the introduction of new concepts such as pathobiome, microbiome and, more in general, complex interactions between plants, pathogens, beneficial organisms and biotic as well as abiotic environment will determine a conceivable paradigm shift in plant pathology. However, despite the rapid progress of molecular biology and biotechnology the potential of more conventional molecular techniques for problem solving in plant pathology has not fully exploited. The aim of this study was to apply these techniques for the diagnosis and characterization of fungal plant pathogens of quarantine concern or causing emerging plant diseases in the Mediterranean region. Also, one of these pathogens was selected as a model-system to investigate preliminarily the plant-pathogen phenotypic and genetic interactions in multiple infections, a still scarcely explored field in plant pathology. Consistently with the aim, this thesis was conceived and structured as an anthology of case-studies.


1.2 Objectives of the Ph.D. thesis

Specific objectives of this PhD study were developed by the following studies: (i) *Fusarium circinatum* an emergent and quarantine pathogen of pine worldwide: its detection and its interaction with *Phytophthora* species (*P. cambivora* and *P. parvispora*) on *Pinus radiata* seedlings; (ii) scabby canker caused by *Neofusicoccum batangarum* (*Botryosphaeriaceae*), an emergent disease of *Opuntia ficus-indica* in minor islands around Sicily: identification of the causative agent and characterization of both its phytotoxic metabolites and the genetic variability of its local population; (iii) identification of *Neofusicoccum parvum* (*Botryosphaeriaceae*) as the causative agent of gummy cankers (bot gummosis) of lemon (*Citrus ×limon*) trees; (iv) characterization of *Alternaria* species associated with heart rot of pomegranate fruit; (v) Shoot dieback of citrus, a new disease caused by *Colletotrichum* species.

Chapter 2.









***Fusarium circinatum* an emergent and quarantine pathogen of pine worldwide: its detection and its interaction with *Phytophthora* species (*P. cambivora* and *P. parvispora*) on *Pinus radiata* seedlings.**

SCIENTIFIC REPORTS



OPEN

Transferability of PCR-based diagnostic protocols: An international collaborative case study assessing protocols targeting the quarantine pine pathogen *Fusarium circinatum*

Renaud Ios ¹, Francesco Aloj^{2,24}, Barbara Piškur³, Cécile Guinet¹, Martin Mullett^{4,22}, Mónica Berbegal⁵, Helena Bragança⁶, Santa Olga Cacciola², Funda Oskay⁷, Carolina Cornejo⁸, Kaleb Adamson⁹, Clovis Douanla-Meli ¹⁰, Audrius Kačergius¹¹, Pablo Martínez-Álvarez¹², Justyna Anna Nowakowska ¹³, Nicola Luchi¹⁴, Anna Maria Vettraino ¹⁵, Rodrigo Ahumada¹⁶, Matias Pasquali¹⁷, Gerda Fourie¹⁸, Loukas Kanetis¹⁹, Artur Alves ²⁰, Luisa Ghelardini ²¹, Miloň Dvořák²², Antonio Sanz-Ros²³, Julio J. Diez¹², Jeyaseelan Baskarathevan ²⁵ & Jaime Aguayo ¹

¹ANSES Laboratoire de la Santé des Végétaux, Unité de Mycologie, Domaine de Pixérécourt Bât. E, 54220, Malzéville, France. ²Department of Agriculture, Food and Environment, University of Catania, Via Santa Sofia, 100, Catania, 95123, Italy. ³Slovenian Forestry Institute, Department of Forest Protection, Večna pot 2, SI-1000, Ljubljana, Slovenia. ⁴Forest Research, Alice Holt Lodge, Farnham, Surrey, GU10 4LH, United Kingdom. ⁵Instituto Agroforestal Mediterráneo, Universitat Politècnica de València, Camino de Vera s/n, 46022, Valencia, Spain. ⁶Instituto Nacional de Investigação Agrária e Veterinária I.P. (INIAV I.P.), Quinta do Marquês, 2780-159, Oeiras, Portugal. ⁷Çankırı Karatekin University, Faculty of Forestry, 18200, Çankırı, Turkey. ⁸Swiss Federal Institute for Forest, Snow and Landscape Research WSL, Zuercherstrasse 111, 8903, Birmensdorf, Switzerland. ⁹Institute of Forestry and Rural Engineering, Estonian University of Life Sciences, 51006, Tartu, Estonia. ¹⁰Julius Kühn-Institut, Institute for National and International Plant Health, Messeweg 11-12, 38104, Braunschweig, Germany. ¹¹Lithuanian Research Centre for Agriculture and Forestry, Vokė Branch, Zalioji Sq. 2, 02232, Vilnius, Lithuania. ¹²Sustainable Forest Management Research Institute, University of Valladolid – INIA/Department of Vegetal Production and Forest Resources, University of Valladolid, 47011, Palencia, Spain. ¹³Cardinal Stefan Wyszyński University in Warsaw, Faculty of Biology and Environmental Sciences, Wóycickiego 1/3 Street, 01-938, Warsaw, Poland. ¹⁴Institute for Sustainable Plant Protection - National Research Council (IPSP-CNR), Via Madonna del Piano 10, I-50019, Sesto Fiorentino, Florence, Italy. ¹⁵Department for Innovation in Biological, Agro-food and Forest Systems (DIBAF), University of Tuscia, via S. Camillo de Lellis, snc, 01100, Viterbo, Italy. ¹⁶Bioforest S.A. Camino a Coronel km 155/N, 4030000, Concepción, Chile. ¹⁷Department of Food, Environmental and Nutritional Sciences, University of Milan, via Celoria 2, I-20133, Milano, Italy. ¹⁸Department of Biochemistry, Genetics and Microbiology, Forestry and Agricultural Biotechnology Institute (FABI), University of Pretoria, 0028 Hatfield, Pretoria, South Africa. ¹⁹Department of Agricultural Sciences, Biotechnology, and Food Science, Cyprus University of Technology, 3036, Limassol, Cyprus. ²⁰Departamento de Biologia, CESAM, Universidade de Aveiro, 3810-193, Aveiro, Portugal. ²¹Dipartimento di Scienze delle Produzioni Agroalimentari e dell'Ambiente (DISPAA), University of Florence, 50144, Florence, Italy. ²²Phytophthora Research Center, Department of Forest Protection and Wildlife Management, Faculty of Forestry and Wood Technology, Mendel University in Brno, Zemědělská 3, 613 00, Brno, Czech Republic. ²³Forest Health Center of Calabazanos, Regional Government of Castilla y León, JCyL, Polígono Industrial de Villamuriel, S/N, 30190, Villamuriel de Cerrato, Palencia, Spain. ²⁴Dipartimento di Scienze Agrarie, Alimentari e Forestali, Università degli Studi di Palermo, Viale delle Scienze, 90128, Palermo, Italy. ²⁵Plant Health & Environment Laboratory, Diagnostic and Surveillance Services, Biosecurity New Zealand, Ministry for Primary Industries, PO Box 2095, Auckland, 1140, New Zealand. Correspondence and requests for materials should be addressed to R.I. (email: renaud.ios@anses.fr)

Fusarium circinatum is a harmful pathogenic fungus mostly attacking *Pinus* species and also *Pseudotsuga menziesii*, causing cankers in trees of all ages, damping-off in seedlings, and mortality in cuttings and mother plants for clonal production. This fungus is listed as a quarantine pest in several parts of the world and the trade of potentially contaminated pine material such as cuttings, seedlings or seeds is restricted in order to prevent its spread to disease-free areas. Inspection of plant material often relies on DNA testing and several conventional or real-time PCR based tests targeting *F. circinatum* are available in the literature. In this work, an international collaborative study joined 23 partners to assess the transferability and the performance of nine molecular protocols, using a wide panel of DNA from 71 representative strains of *F. circinatum* and related *Fusarium* species. Diagnostic sensitivity, specificity and accuracy of the nine protocols all reached values >80%, and the diagnostic specificity was the only parameter differing significantly between protocols. The rates of false positives and of false negatives were computed and only the false positive rates differed significantly, ranging from 3.0% to 17.3%. The difference between protocols for some of the performance values were mainly due to cross-reactions with DNA from non-target species, which were either not tested or documented in the original articles. Considering that participating laboratories were free to use their own reagents and equipment, this study demonstrated that the diagnostic protocols for *F. circinatum* were not easily transferable to end-users. More generally, our results suggest that the use of protocols using conventional or real-time PCR outside their initial development and validation conditions should require careful characterization of the performance data prior to use under modified conditions (i.e. reagents and equipment). Suggestions to improve the transfer are proposed.

Fusarium circinatum Nelson Nirenberg & O'Donnell, formerly also known as *Gibberella circinata* Nirenberg & O'Donnell, is a harmful fungus causing pitch canker, a serious disease on pine trees. This pathogenic ascomycete attacks all *Pinus* species and *Pseudotsuga menziesii* (Mirb.) Franco, with varying levels of virulence¹⁻³. All stages of pine are susceptible to the pathogen: seedling blight and damping-off, dieback of branches and stems on young and mature trees, where the most conspicuous symptoms are cankers accompanied by sometimes copious resin exudate («pitch canker»)⁴. Dieback symptoms are also commonly observed in the crown due to the obstruction of water flow caused by the cankers and saturation of xylem by the excess resin produced by the tree. The multiplication of severe cankers on young or mature trees may lead to tree death⁵.

As for most tree pathogens, no economically and environmentally viable treatment is available to control or eradicate the fungus on a large scale. Management strategies are therefore focused on preventing the introduction of the pathogen, early detection and eradication of outbreaks in previously disease-free areas. *Fusarium circinatum* has been reported in different parts of the world, where it causes severe losses to the pine production industry (USA, South Africa, Korea, Japan, Spain) as well as in nurseries (Mexico, Haiti, Chile, Uruguay, Brazil, Colombia, South Africa) (EPPO Global database, <https://gd.eppo.int/>). In Europe, *F. circinatum* is officially present in Spain and Portugal in pine forests^{6,7}, while it is also occasionally found in pine nurseries. The pathogen has also been found in French nurseries⁸, and in a public garden in Italy⁹, but it is currently considered as officially eradicated in both countries (EPPO Global database, <https://gd.eppo.int/>). Since 2007, *F. circinatum* has been listed as a quarantine fungus for the EU, in order to prevent new introductions of infected material and further spread of the disease¹⁰. As a consequence of its quarantine status, a zero-tolerance policy is in force.

Management efforts should therefore focus on early detection of the pathogen in the different pathways of movement and introduction. Based on the pest risk assessment issued by the European Food and Environment Safety Agency (EFSA), the main pathways for the potential introduction of this fungus to disease-free areas are through contaminated pine seeds and seedlings⁸. To minimize the probability of an introduction and to reduce the cost associated with the eradication and control of this invasive pathogen, efficient management measures are needed¹¹. For these reasons, the development of reliable diagnostic protocols is fundamental for the early and accurate detection of *F. circinatum* in pine-related commodities which can harbor and consequently spread the pathogen (i.e. substrates) such as seeds, seedlings, plants, young and mature trees. The diagnostic protocols should therefore be as specific and sensitive as possible^{10,12}. False-negative detection results may lead to introduction of the pathogen in disease-free areas, while false-positive results may be responsible for unfair and inappropriate destruction of plant material, or a ban on trade with severe economic consequences.

Numerous diagnostic protocols targeting *F. circinatum* are currently available in the scientific literature and their use is suggested in international standard protocols by international bodies such as EPPO, ISTA or FAO-IPPC¹³⁻¹⁵. Despite most of them providing validation data supporting their accuracy, performance values are inconsistently reported or assessed in the original articles describing their development. Validation actions should be carried out to provide objective evidence that the test is suitable for the circumstances of use and can be considered for screening purposes¹⁶.

For instance, identification of *F. circinatum* may be achieved by isolation and morphological characterization of the pathogen, a common technique used in mycology. *Fusarium circinatum* displays several typical features, such as the presence of mono- and polyphialides as well as coiled sterile hyphae that aid diagnosis^{17,18}. However, a recent study based on the phenotypical characteristics of isolates from a wide geographical range (Europe, America, Africa, and Asia) found that coiled sterile hyphae may not be a reliable morphological trait of *F. circinatum*, as previously reported¹⁹. Recent description of new *Fusarium* species in Colombia, which are also pine pathogens and can produce similar coiled hyphae in culture, further challenges the specificity of this morphology-based technique²⁰. Additionally, morphological characterization is lengthy and requires

considerable mycological expertise, whilst also not being efficient for the detection of quiescent forms of the pathogen that can be encountered in seedlings²¹ or in seeds.

A number of conventional and real-time polymerase chain reaction (PCR) assays targeting *F. circinatum* have been developed^{13,22–28}, and another one is presented in the Supplementary Information section (Supplementary Information 1, hereafter referred to as Baskarathevan *et al.*, unpublished). In the original articles, variable levels of validation are presented. For instance, the assessment of specificity and inclusivity used a more or less exhaustive range of *Fusarium* strains, depending on the availability of testing material, which included numbers of *F. circinatum* strains from different continents and newly described species, genetically related to *F. circinatum*. Considering the paramount importance of the reliability of a test when dealing with a quarantine pathogen, efforts should be focused on the continuous verification of the specificity of the protocols. This is particularly relevant when a *Fusarium* species is targeted, since this genus includes a steadily increasing number of newly described and cryptic species^{20,29,30}. In addition, there is typically no data available to support the reliability of a given protocol when carried out in different laboratories, with different equipment and reagents than those described in the original papers. For instance, one may imagine that the specificity and the sensitivity of a test using conventional and real-time PCR may be altered by changing the brand of DNA polymerase enzyme, commercial ready-to-use master mix, or thermal-cycler/software. This in turn may affect the reliability of a diagnostic protocol targeting economically important pathogens such as *F. circinatum*^{31,32}. Validation of diagnostic protocols is therefore a key element in establishing reference methods and to assess a laboratory's competence and ability to produce reliable analytical data¹².

The currently ongoing European COST action FP1406 “Pine Pitch Canker Strategies for Management of *Gibberella circinata* in Green Houses and Forests” (PINESTRENGTH) brings together 34 countries to establish a European-focused network dedicated to the Pine Pitch Canker pathogen. The main objectives are to increase knowledge on the biology, ecology and spread pathways of *F. circinatum*, to evaluate the potential for the development of effective and environmentally friendly prevention and mitigation strategies and to deliver these outcomes to stakeholders and policy makers. Early and accurate detection of *F. circinatum* is essential to achieve these goals. In this study, we compared for the first time performance of existing molecular tools targeting *F. circinatum*, with a wide range of DNA from target and non-target *Fusarium* species, in a large panel of 23 laboratories from European countries, South Africa and Chile. This collaborative study enabled us to provide useful data for the transferability of the different molecular-based diagnostic protocols. We propose recommendations for the preparation and use of future standard diagnostic protocols using conventional or real-time PCR assays.

Results

Indeterminate results. All 23 participants carried out the tests as requested. However, a few samples could not be tested by some of the participants due to loss or shortage of DNA template after multiple PCR run failures and were thus not considered in the analyses.

All nine protocols generated indeterminate results (Table 1, Fig. 1A). The total number of indeterminate results was 58 (1.5% of the total analysis) and ranged from 0.42% for protocol p1 to 4.58% for protocol p6 (Table 1). The participants reported several reasons for rating results as indeterminate. These included late mean cycle threshold (Ct) values or inconsistent Ct values from the replicates for hydrolysis probe-based protocols, melting temperatures (Tm) and melting peaks slightly different from the positive control, or late mean Ct values for SYBR Green based protocols. Generally, laboratories performing conventional PCR protocols did not provide an explanation for indeterminate results. However, one participant sequenced each amplicon and rated the results as indeterminate when the sequence was not readable. Comparison of indeterminate results by Fisher's exact tests revealed significant differences ($P < 0.001$) between protocols (Table 1, Fig. 1A). In particular, protocol p6 based on SYBR Green real-time PCR, yielded significantly more indeterminate results than most of the other protocols. In this case, the melting peak analysis required by protocol p6 often revealed the presence of melting peaks slightly different from the positive control, the presence of double melting peaks, or only one out of two replicates were positive for some of the DNA extracts.

When indeterminate results were analyzed with only pure *Fusarium* strain DNA (no DNA extracts from inoculated seeds), 37 indeterminate results were reported (63.8% of the total number of indeterminate results). Fisher's exact tests revealed significant differences between protocols for these indeterminate results ($P < 0.001$, Table 1, Fig. 1B), and the rate of indeterminate ranged from 0.0% (protocol p5 and protocol p7) to 4.6% (protocol p6). In general, these indeterminate results mostly concerned non-target species (88.9% of the *Fusarium* strain DNA material indeterminate results).

Comparisons of indeterminate results between laboratories by protocol revealed significant differences for p2 (indeterminate data by laboratory ranging from 0% to 5.1%, $P = 0.02$), p5 (indeterminate data by laboratory ranging from 0% to 7.6%, $P = 0.002$), p6 (indeterminate data by laboratory ranging from 0% to 16.5%, $P < 0.001$), p8 (indeterminate data by laboratory ranging from 0% to 7.6%, $P < 0.001$) and p9 (indeterminate data by laboratory ranging from 0% to 5.1%, $P < 0.001$).

Positive and negative deviation rates. All nine protocols exhibited positive deviations (or false positives) and negative deviations (or false negatives) regardless of the data set used (Table 1, Fig. 1C–F). Analysis of DS1 (the dataset for which an indeterminate result is ultimately determined to be the expected result, see methods section) revealed positive deviation rates (PD) ranging from 3.0% (protocol p7) to 17.3% (protocol p8) (Table 1, Fig. 1C). Comparison of PD by Fisher's exact tests revealed significant differences ($P < 0.001$) between protocols (Table 1, Fig. 1C). Negative deviation rates (ND) in DS1 ranged from 14.5% (protocol p3) to 19.9% (protocol p8), but according to Fisher's exact tests, the ND rates between protocols were not different ($P = 0.71$) (Table 1, Fig. 1E). Concerning DS2 (the dataset for which an indeterminate result is ultimately determined to be the contrary of the expected result, see methods section), PD ranged from 3.0% (protocol p7) to 21.2% (protocol p6)

Protocol	End point PCR		SYBR Green real-time PCR			Hydrolysis probe real-time PCR				Significance of the difference between protocols
	p1	p9	p4	p5	p6	p2	p3	p7	p8	
Number of laboratories involved	6	6	6	5	4	6	6	4	6	
Number of samples analyzed and retained	474	472	473	393	393	474	474	316	473	
Number of indeterminate results ^{a,b}	2 A (2 AB)	4 A (2 AB)	7 A (4 AB)	6 A (0 A)	18 B (16 C)	5 A (1 AB)	5 A (4 AB)	3 A (0 AB)	9 AB (8 BC)	P < 0.001 (P < 0.001)
Negative Accord (NA) ^{b,c}	181 (180)	183 (179)	187 (183)	154 (154)	146 (130)	171 (171)	192 (191)	128 (128)	163 (161)	—
Positive Accord (PA) ^{b,c}	223 (221)	229 (231)	230 (227)	194 (189)	192 (191)	230 (226)	236 (232)	156 (153)	221 (220)	—
Negative Deviation (ND) ^{b,c}	53 (55)	43 (44)	45 (48)	34 (40)	35 (37)	46 (50)	40 (44)	28 (31)	55 (56)	—
Positive Deviation (PD) ^{b,c}	17 (18)	17 (19)	11 (15)	11 (11)	19 (35)	27 (27)	6 (7)	4 (4)	34 (37)	—
Diagnostic Sensitivity % (SE) ^{b,c}	80.8 (80.1)	84.3 (83.6)	83.6 (82.5)	85.0 (82.8)	84.0 (83.6)	83.3 (81.9)	85.5 (84.1)	84.8 (83.2)	80.1 (79.7)	P = 0.71 (P = 0.88)
Diagnostic Specificity % (SP) ^{b,c}	91.4 ABCD (90.9 AB)	92.4 ABCD (90.4 AB)	94.4 AC (92.4 AB)	93.3 ABC (93.3 AB)	88.5 ABD (78.8 C)	86.4 BD (86.4 AC)	97.0 C (96.6 B)	97.0 C (97.0 B)	82.6 D (81.6 C)	P < 0.001 (P < 0.001)
Diagnostic accuracy % (AC) ^{b,c}	85.2 AB (84.6 ABC)	87.7 AB (86.4 AB)	88.2 A (86.7 AB)	88.5 A (87.3 ACD)	85.9 AB (81.6 ABC)	84.6 AB (83.8 ABC)	90.3 A (89.2 B)	89.9 A (88.9 D)	81.2 B (80.5 CD)	P = 0.02 (P < 0.001)
Concordance level (%) ^b	96.8 A	93 C	96.8 A	93.7 C	74.6 D	88.5 B	93.2 C	97.7 A	93.5 C	P < 0.001
Positive deviation (PD) rate (%) ^{b,c}	8.6 ABC (9.1 AB)	8.5 ABC (9.6 AB)	5.6 BC (7.6 AB)	6.7 ABC (6.7 AB)	11.5 ACD (21.2 C)	13.6 AD (13.6 AC)	3.0 B (3.5 B)	3.0 B (3.0 B)	17.3 D (18.7 C)	P < 0.001 (P < 0.001)
Negative deviation (ND) rate % ^{b,c}	19.2 (19.9)	15.7 (16.1)	16.4 (17.5)	14.9 (17.5)	15.4 (16.2)	16.7 (18.1)	14.5 (15.9)	15.2 (16.8)	19.9 (20.3)	P = 0.716 (P = 0.89)

Table 1. Performance values obtained during the collaborative study. ^aNumbers outside brackets are the total number of indeterminate results, while those between brackets indicate the number of indeterminate results considering only pure *Fusarium* strain DNA (i.e. no DNA extracts from inoculated seeds). ^bValues followed by the same letter in a line are not significantly different ($P > 0.05$). ^cNumbers outside brackets are estimations for the DS1 dataset and those between brackets are estimations for the DS2 dataset.

(Table 1, Fig. 1D). Significant differences between protocols for PD rates were observed according to Fisher's exact tests ($P < 0.001$). ND in DS2 ranged from 15.9% (protocol p3) to 20.3% (protocol p8) (Table 1, Fig. 1F). ND comparisons between protocols using Fisher's exact tests did not reveal any significant differences ($P = 0.88$).

Comparisons between laboratories using DS1 revealed significant PD rate differences only for p2 (PD rate by laboratory ranging from 3.0% to 27.3%, $P = 0.007$) and p8 (PD rate by laboratory ranging from 9.1% to 37.5%, $P = 0.04$). Concerning the ND rate in DS1, significant differences were observed in p2 (ND rate by laboratory ranging from 6.5% to 32.6%, $P = 0.031$) and p6 (ND rate by laboratory ranging from 4.3% to 40.9%, $P < 0.001$). When comparisons were performed using DS2, significant differences between laboratories were revealed for p2 (PD rate by laboratory ranging from 3.0% to 27.3%, $P = 0.007$) and p6 (PD rate by laboratory ranging from 6.1% to 63.6%, $P < 0.001$), for the PD rate, and for p6 (ND rate by laboratory ranging from 6.5% to 40.9%, $P < 0.001$) for the ND rate.

Pattern of cross-reactions with non-target species. As shown previously, all protocols exhibited different levels of positive deviations (Table 1, Fig. 1C,D). Cross-reactions with DNA from strains of non-target *Fusarium* species were encountered for all nine protocols, but inconsistently between participating labs (Table 2). For many strains, a cross-reaction with the DNA extract was reported for only a single participant among the four, five, or six laboratories involved, which corresponds to a unique reagent/equipment/operator combination.

Fusarium subglutinans was the species that accounted for the most frequent cross-reactions, and its DNA yielded false-positive results for seven out of the nine protocols. Depending on the protocol, from three, up to six out of six laboratories observed cross-reaction with DNA of this species. *Fusarium temperatum* was the only, albeit consistent, cross-reaction observed with protocol p7. DNA from the newly-described species on pine from Colombia, i.e. *F. marasasanum*, *F. pinninemorale*, *F. sororula*, *F. fracticaudum*, and *F. parvisorum* also yielded frequent cross-reactions with four protocols (p1, p2, p8 and p9), and less frequently with protocol p6.

Reference sequences of target genes from species whose DNA cross-reacted with some of the PCR or real-time PCR tests were retrieved from GenBank and aligned with orthologous reference sequences of *F. circinatum*. The regions upstream and downstream of the forward and reverse PCR primers were removed. The alignments were manually scrutinized to check for the presence of interspecific polymorphism between the regions targeted by the primers. For some of the PCR or real-time PCR tests, it was shown that the presence of polymorphisms

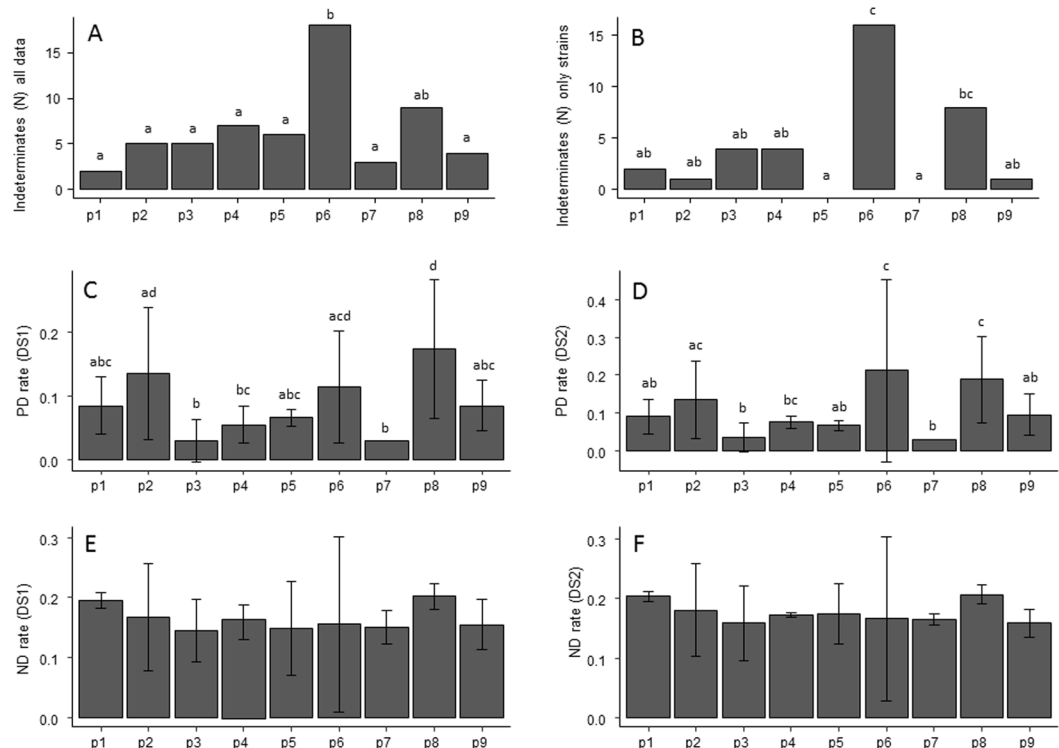


Figure 1. (A) Total number of indeterminate results by protocol considering all data (strains and inoculated seeds); (B) Total number of indeterminate results by protocol considering only strains (i.e. no inoculated seed data); (C) PD rate mean values and standard deviation by protocol for DS1 dataset; (D) PD rate mean values and standard deviation by protocol for DS2 dataset. (E) ND rate mean values and standard deviation by protocol for DS1 dataset; (F) ND rate mean values and standard deviation by protocol for DS2 dataset. The x – axis in all graphs represents the nine protocols tested in this study, from p1 to p9. Please refer to Table 4 for details of each protocol. Different letters indicate values are significantly different, according to Fisher's Exact Test, for count data with simulated P-values based on $1e + 05$ replicates.

after sequencing the amplicon would be helpful to confirm the occurrence of cross-reactions, and possible false-positive results (Table 2).

Inclusivity of the different protocols. In this work, inclusivity is defined as the ability of each protocol to detect DNA of the target species, regardless of the host plant, mating type, geographical origin and year of collection. Different patterns of inclusivity were observed between protocols. DNA from some of the *F. circinatum* strains yielded inconsistent negative results. Protocols p4, p7 and p9 successfully picked up all the 38 *F. circinatum* strains of both mating types included in the panel, regardless of the equipment, reagents and operator, thus supporting their excellent level of inclusivity. By contrast, protocols p1 and p8 almost systematically failed to yield positive results with DNA from the Japanese strain of *F. circinatum* NRRL2643. However, the rest of the false negative results were not reproducible between laboratories, and were only reported for one participant out of the four, five, or six involved, meaning that they were only observed for some operator/reagent/equipment combinations. Except for the Japanese strain of *F. circinatum* NRRL2643, these false negative results were observed with DNA from different *F. circinatum* strains originating from Spain, France, Chile, USA, and South Africa without any obvious pattern.

Performance criteria and reproducibility. Diagnostic sensitivity (SE) ranged from 80.1% (protocol p8) to 85.5% (protocol p3) and from 79.7% (protocol p8) to 84.1% (protocol p3) using the DS1 and DS2 datasets, respectively. Fisher's exact tests did not reveal significant differences for SE between the nine protocols either for DS1 ($P = 0.72$) or DS2 ($P = 0.88$) (Table 1, Fig. 2A,B). By contrast, diagnostic specificity (SP) differed significantly, using both datasets (both P -values < 0.001). SP ranged from 82.6% (protocol p8) to 97% (for both protocols p3 and p7) in DS1 (Table 1, Fig. 2C). When SP was assessed for DS2, it ranged from 78.8% (protocol p6) to 97% (protocol p7) (Table 1, Fig. 2D). Significant differences in Diagnostic accuracy (AC) were observed between protocols for both datasets ($P = 0.002$ and $P < 0.001$ for DS1 and DS2, respectively). AC ranged from 81.2% (protocol p8) to 90.3% (protocol p3) in DS1 and from 80.5% (protocol p8) to 89.2% (protocol p3) in DS2 (Table 1, Fig. 2E,F). Concordance ranged from 74.6% to 97.7% for p6 and p7, respectively. Fisher's exact tests revealed significant differences between methods ($P < 0.001$, Table 1).

Analytical sensitivity. The analytical sensitivity was assessed for each protocol using serial dilutions of DNA from *P. pinaster* seeds spiked with *F. circinatum* conidia. However, inconsistent results were obtained with the serial dilutions. For example, when analyses were performed with the DS1 scenario, seven out of the nine evaluated protocols were able to detect at least one of the samples containing *F. circinatum* DNA in seeds at the highest concentration, i.e. 2×10^5 conidia/mL of ground seed homogenate: p2, p3, p4, p5, p6, p7 and p9. Only p6 was able to give a positive result for all samples of this concentration. Similarly, these inconsistent results were also observed in data from DS2, and only p2, p3, p5 and p6 were able to detect at least one of the samples of the highest concentration of *F. circinatum* in seeds. This inconsistent behavior of inoculated material was observed for all of the serial dilution samples, in both datasets (Supplementary Dataset 1).

Discussion

To establish an international surveillance network for the detection of outbreaks of pine pitch canker across Europe and other disease-free areas, harmonization of protocols for *F. circinatum* diagnosis is needed. To our knowledge, two international diagnostic protocols targeting this pathogen already exist. Nevertheless, one of them is a list of protocols that the international community has agreed are satisfactory, with minimal validation data available^{13,15} and the other relies solely on techniques such as mycological plating, that were selected because of their low cost and ease of implementation¹⁴. Most of the protocols targeting *F. circinatum* described in the literature lack a comprehensive evaluation of some basic performance criteria, such as specificity, inclusivity and sensitivity. Additionally, in most cases, specificity has not been re-evaluated in light of newly emerged or described *Fusarium* species occurring on *Pinus* spp²⁰. In this study, we selected nine different detection protocols based on PCR and its variants. Their performance was assessed using a panel of 71 *Fusarium* strains and eight pine seed samples spiked with *F. circinatum* conidia. In order to achieve the best representation of *F. circinatum* strains (i.e. inclusivity), the panel included strains originating from six countries across four continents, and both mating types. Also included were recently-described *Fusarium* species isolated from pines, genetically related to *F. circinatum*, with overlapping morphological features, and some of them being pathogenic to *Pinus*²⁰. This large panel of strains was used to assess the performance and transferability of the different protocols through an international collaboration involving a broad consortium of 23 partners. Each protocol was evaluated by a minimum of four, and up to six laboratories therefore ensuring a robust dataset. Practical and technical constraints led to an unbalanced number of laboratories involved per protocol, which means that some of the results should be read with care. In particular, although significant differences were observed for some criteria between participant laboratories and some of the protocols, caution is required before generalizing the results regarding non-significance of some of the statistical tests. Indeed, non-significant differences between protocols means non-identification of a difference rather than the absence of a difference altogether.

Our results showed that all protocols presented acceptable performance values in both datasets (>75%) for diagnostic accuracy, specificity and sensitivity, with some laboratories obtaining individual values close to 100% (Supplementary Dataset 1). Yet diagnostic specificity and accuracy differed considerably between protocols, irrespective of the technology involved (i.e. end-point PCR or real-time PCR using SYBR Green dye or specific hydrolysis probes). These differences were principally linked to cross-reactions with non-target species (positive deviations), and less commonly to consistent or erratic negative deviations with particular strains of *F. circinatum*.

The cross-reactions with DNA from non-target species observed in our study have not been reported in the original articles describing the protocols. We included a broader and more comprehensive panel of strains, revealing more information about the level of specificity of these protocols. However, our panel is not exhaustive and of course does not cover the entire biological range of genetically related *Fusarium* strains. Other unexpected cross-reactions may therefore occur, particularly with DNA from as yet undescribed *Fusarium* taxa. Cross-reactions were observed in all protocols, although at different levels, depending on the laboratory involved. Some of the erratic cross-reactions and false negative results may have occurred because of issues such as pipetting errors, DNA shearing, among others. However, some of the cross-reactions were more frequent and were due to lack of specificity/sensitivity of the molecular markers toward strains that had not been assessed during the original validation step of the original protocol by the authors, such as for genetically related *F. temperatum* and *F. subglutinans*. From a practical point of view, the presence of some of the *Fusarium* species whose DNA yielded false positive results are very unlikely on pine tissue, but the recent finding of Herron *et al.*²⁰ showed that previously unknown species may be found on pine. In our experiment, a common DNA extraction procedure was followed for all the fungal strains, which sometimes differed from the original article describing each of the nine protocols. It cannot be ruled out that the DNA extraction procedure used in our study had an effect of PCR or real-time PCR specificity or inclusivity. Another aspect to consider is that for the sake of harmonization, a standard concentration of *Fusarium* DNA was used throughout the study (0.5 ng/ μ L). This may not always reflect the actual concentration that may occur when testing real pine samples contaminated with these *Fusarium* species, and the likelihood of cross-reactions with non-target DNA probably increases with higher concentrations. At the same time, certain strains of *F. circinatum* were 'missed' by some of the protocols (especially the *F. circinatum* strain from Japan), with false-negative results that were not reported in the original articles, except by Ramsfield *et al.* (2008) regarding protocol p1. This suggests that some of the *F. circinatum* strains travelling with plant material such as seeds might not be detected when using some of the protocols assessed here. Our data provide a first evaluation of the inclusivity of nine protocols, which can be useful for laboratories in charge of official analyses, by elucidating the level of uncertainty associated with some of the protocols used throughout the world. Although diagnostic specificity across all protocols was rather high (>75%), no protocol was 100% specific with the present panel of *F. circinatum* strains. These false-positives may not be acceptable when dealing with a pathogen subjected to strict phytosanitary regulations.

Protocol number	Cross-reactions*	Indeterminate or false negative result
		(<i>F. circinatum</i> strain, originating country)**
p1	<i>F. marasianum</i> (5/6) ^a	NRRL26431, Japan (5/6)
	<i>F. pinnemorale</i> (5/6) ^a	310/061, Spain (1/6)
	<i>F. sororula</i> (5/6) ^a	
	<i>F. temperatum</i> (2/6) ^a	
p2	<i>F. begoniae</i> (6/6) ^b	LSVM216, France (1/6)
	<i>F. concentricum</i> (1/6) ^b	LSVM1221, Spain (1/6)
	<i>F. culmorum</i> (1/6) ^b	FcCa01, Spain (1/6)
	<i>F. fracticaudum</i> (3/6) ^a	FcCa05, Spain (1/6)
	<i>F. parvisorum</i> (3/6) ^a	FcCa06, Spain (1/6)
	<i>F. pininemorale</i> (2/6) ^a	CSF-13, Spain (1/6)
	<i>F. sororula</i> (2/6) ^a	2306 BASA, Chile (1/6)
	<i>F. subglutinans</i> (4/6) ^b	
p3	<i>F. culmorum</i> (1/6) ^b	NRRL25708, USA (1/6)
	<i>F. subglutinans</i> (3/6) ^b	NRRL25333, S. Africa (1/6)
		FcCa06, Spain (1/6)
		CSF-18, Spain (1/6)
p4	<i>F. marasianum</i> (1/6) ^a	
	<i>F. proliferatum</i> (1/6) ^a	
	<i>F. subglutinans</i> (6/6) ^b	
p5	<i>F. proliferatum</i> (1/5) ^b	CSF8, Spain (1/5)
	<i>F. subglutinans</i> (6/5) ^b	CSF10, Spain (1/5)
		CSF11, Spain (1/5)
p6	<i>F. acuminatum</i> (1/5) ^a	NRRL25708, USA (1/5)
	<i>F. fracticaudum</i> (1/5) ^a	NRRL25331, USA (1/5)
	<i>F. graminearum</i> (1/5) ^b	NRRL25333, S. Africa (1/5)
	<i>F. incarnatum</i> (1/5) ^b	FcCa02, Spain (1/5)
	<i>F. mangiferae</i> (1/5) ^b	FcCa05, Spain (1/5)
	<i>F. marasianum</i> (3/5) ^a	FC042V, Spain (1/5)
	<i>F. parviporum</i> (1/5) ^a	FC035, Spain (1/5)
	<i>F. pininemorale</i> (1/5) ^a	CSF1, Spain (1/5)
	<i>F. reticulatum</i> (1/5) ^a	CSF2, Spain (1/5)
	<i>F. sacchari</i> (1/5) ^b	CSF3, Spain (1/5)
	<i>F. sororula</i> (1/5) ^a	CSF4, Spain (1/5)
	<i>F. sporotrichioides</i> (1/5) ^b	CSF7, Spain (1/5)
	<i>F. subglutinans</i> (4/5) ^b	CSF8, Spain (1/5)
	<i>F. torulosum</i> (1/5) ^a	CSF11, Spain (1/5)
	<i>F. thapsinum</i> (1/5) ^b	CSF12, Spain (1/5)
	<i>F. tricinctum</i> (2/5) ^b	CMW1219, S. Africa (1/5)
<i>F. verticillioides</i> (1/5) ^b		
p7	<i>F. temperatum</i> (4/4) ^c	
p8	<i>F. fracticaudum</i> (4/6) ^a	NRRL26431, Japan (6/6)
	<i>F. incarnatum</i> (1/6) ^a	LSVM211, France (1/6)
	<i>F. mangiferae</i> (1/6) ^a	LSVM216, France (1/6)
	<i>F. parvisorum</i> (4/6) ^a	
	<i>F. proliferatum</i> (1/6) ^a	
	<i>F. sacchari</i> (1/6) ^a	
	<i>F. sororula</i> (4/6) ^a	
	<i>F. subglutinans</i> (6/6) ^a	
	<i>F. temperatum</i> (5/6) ^a	
	<i>F. verticillioides</i> (1/6) ^a	

Continued

Protocol number	Cross-reactions*	Indeterminate or false negative result
		(<i>F. circinatum</i> strain, originating country)**
p9	<i>F. begoniae</i> (1/6) ^b	
	<i>F. concentricum</i> (2/6) ^b	
	<i>F. culmorum</i> (1/6) ^b	
	<i>F. fracticaudum</i> (5/6) ^a	
	<i>F. fractiflexum</i> (1/6) ^b	
	<i>F. marasianum</i> (1/6) ^a	
	<i>F. proliferatum</i> (1/6) ^b	
	<i>F. sororula</i> (1/6) ^a	
	<i>F. subglutinans</i> (5/6) ^b	
<i>F. torulosum</i> (1/6) ^a		

Table 2. Detailed list of the false positive and false negative results obtained with the panel DNA from target and non-target species in this study. *Number of participants for which a cross reaction was observed/number of participants involved. Species names in bold indicate a frequent cross-reaction was observed for the protocol with the 0.5 ng μ L⁻¹ DNA extract used. **Number of participants for which the 0.5 ng μ L⁻¹ DNA extract of the *F. circinatum* strain was not picked up by the protocol or yielded an indeterminate result/number of participants involved. ^aNo reference sequence is available for this marker on GenBank for comparison with amplicon sequence, at the time of this study. ^bComparison of the amplicon sequence with IGS *F. circinatum* reference sequences available on GenBank shows several polymorphisms in the region between primers. ^cComparison of the amplicon sequence with TEF 1alpha *F. circinatum* reference sequences available on GenBank shows no polymorphism in the region between primers.

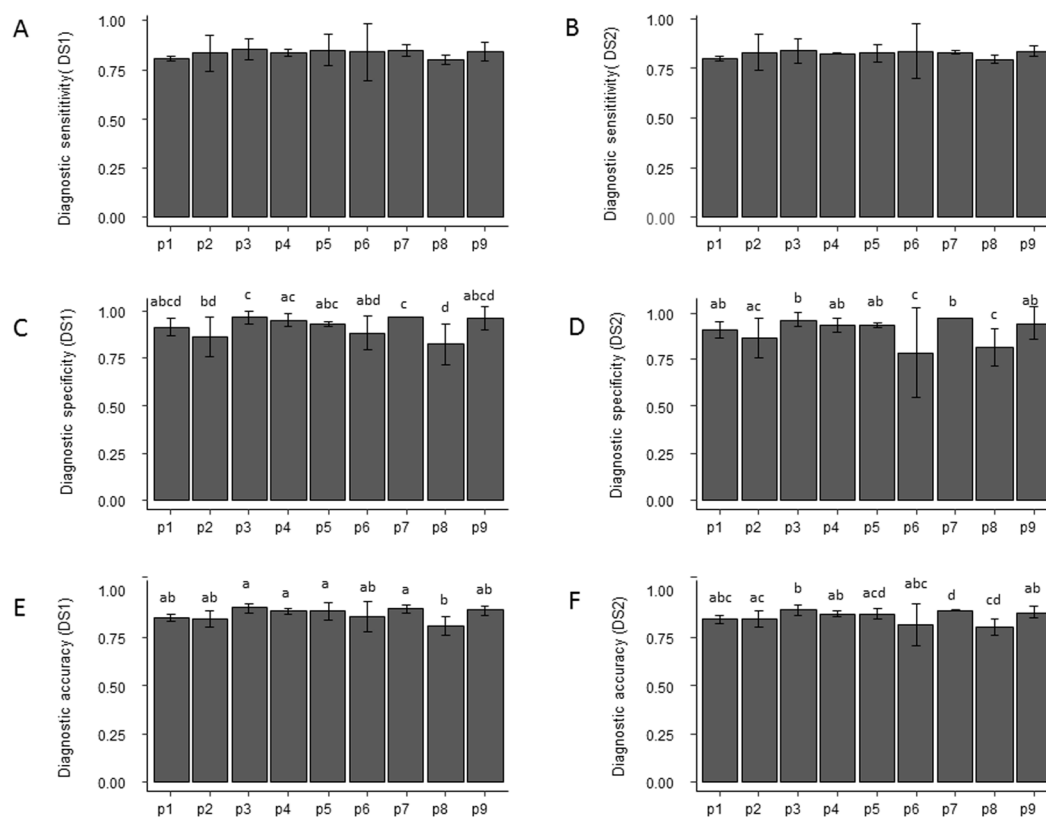


Figure 2. (A) Diagnostic sensitivity and standard deviation by protocol for the DS1 dataset. (B) Diagnostic sensitivity and standard deviation by protocol for the DS2 dataset. (C) Diagnostic specificity and standard deviation by protocol for the DS1 dataset. (D) Diagnostic specificity and standard deviation by protocol for the DS2 dataset. (E) Diagnostic accuracy and standard deviation by protocol for the DS1 dataset. (F) Diagnostic accuracy and standard deviation by protocol for the DS2 dataset. The x-axis in all graphs represents the 9 protocols tested in this study, from p1 to p9. Please refer to Table 4 for details of each protocol. Different letters indicate values are significantly different, according to Fisher's Exact Test, for count data with simulated P-values based on 1e + 05 replicates.

Concordance varied between protocols and ranged from 74.6 to 97.7%. Analysis of the differences between laboratories that tested the same protocol also showed that indeterminate results and negative and positive deviations differed significantly. These results suggest that molecular detection methods may not always be easily transferable. Basically, they clearly illustrate that deviations from the “original recipe”, i.e. the use of different equipment, consumables, but also operators, might compromise the stringency of the reactions, and therefore the specificity of the results. This is particularly important when dealing with a quarantine pathogen, with a zero-tolerance policy. Positive deviations may lead to the inappropriate destruction of goods, whereas negative deviations could fail to prevent introduction of the pathogen into disease-free areas.

We also showed that all the protocols exhibited some problems in result interpretation (indeterminate results), independently of the PCR technology used. However, end-point PCR generally yielded fewer indeterminate results, across all partners, probably linked to the simplicity of result interpretation, based on the observation of a band on an electrophoresis gel, with little room for doubt. Concerning the other PCR techniques, it can be suggested that interpretation of the melting curves was not straightforward when using the SYBR Green real-time PCR, and setting the fluorescence threshold for the calculation of the cycle threshold value when using a hydrolysis probe was sometimes done inconsistently between partners. In addition to this problem of result interpretation, some of the protocols required particular settings that may not have worked well under different conditions. For example, protocol p2²⁴ requires an unusually high hybridization temperature of 70 °C to ensure specificity, which seemed to cause a sensitivity problem when used in certain laboratories or with different reagents/equipment than the ones originally described. In this work, the statistical analysis of indeterminate results was enabled by processing data under two scenarios (DS1 and DS2). In all cases results from both datasets were consistent, leading consequently to the same conclusions. This is an important point because it means that differences in performance criteria between protocols were not influenced by indeterminate results, which represented less than 2% of the total results.

We did not evaluate and compare the sensitivity of a protocol based on mean Ct values, but rather on its ability to yield positive results with lower target concentrations. This approach enabled comparison of conventional PCR, for which no quantitative results are generated with real-time PCR protocols. Additionally, we chose not to provide cutoff values because the sensitivity of a test should not be dependent on Ct values, but rather on its ability to reliably amplify and detect a low concentration of target DNA³³. Late Ct values may still be valid and confidently used if the test specificity has been correctly designed and evaluated³⁴. Despite protocols p2, p3, p5 and p6 consistently yielding positive results for the highest conidia spiking quantity, the data of our study showed that positive results for lower concentrations were rarely obtained. This made it very difficult to compare the protocols to each other regarding analytical sensitivity with seeds. However, using protocols p2 and p6, successful detection of *F. circinatum* in naturally infected pine seeds has been reported by Ioos *et al.*²⁴ and Dreaden *et al.*²⁵, and protocol p2 has been used for years in ANSES for the interception of naturally infected imported seed lots (Guinet, C., ANSES, pers. Comm.). This suggests that the modified method used in our study for the preparation of artificially infected seed DNA was not able to provide samples with a sufficient level of contamination, probably inferior to what is expected with real-world samples. In this respect, a preliminary biologic enrichment of the seed in a broth of culture medium seems a very efficient method to improve detection of *F. circinatum* in seeds at low levels¹³.

One of the main recommendations resulting from the present study is that the transferability of a PCR or real-time PCR protocol should be thoroughly and continuously assessed before becoming a standard. In other words, the ability to yield accurate results when used under slightly different conditions should be checked. Indeed, it is very unlikely that all the specific brands of reagents and equipment described in the original scientific papers are available to end-users. In this study, partner laboratories were free to use their own real-time equipment and brand of reagents, such as DNA polymerases, PCR or real-time PCR master mixes. Discrepancies of results between laboratories regarding false positive and false negative rates, as well as the different analytical sensitivities confirm that changing the brand and type of DNA polymerase³⁵ and equipment^{31,36} may affect the reliability of the results. Changing the DNA polymerase may also generate the amplification of non-specific amplicons, especially when working with symptomatic pine DNA extracts (Piškur, B., pers. comm.). This observation is in line with Bustin & Huggett³³ who showed that the performance of a real-time PCR assay varied with different master mixes, probably due to differences in Mg²⁺ concentrations and the addition of undisclosed stabilizers to the buffer affecting primer and probe annealing.

Another parameter to be considered is that interpretation of the fluorescence levels yielded in the real-time PCR reactions requires the enforcement of decision rules, either by the operator, or the analysis software. In turn, the decision to rate a Ct value as a positive or indeterminate result may be influenced by internal rules, which are not the same between laboratories. In addition, slight variations induced by the operator or the equipment, such as pipetting errors, temperature drift or thermic heterogeneity of the thermal cycler block may have an effect on the stringency of the PCR reaction and thus, in turn may affect the analytical specificity and sensitivity^{33,37–39}.

In line with other guidelines proposed for testing genetically modified organisms⁴⁰, we therefore recommend that a preliminary assessment of the robustness and transferability of a new protocol should be carried out to provide an indication of its performance under different conditions than the ones used during its development. This assessment should be carried out in addition to the classical performance criteria assessed during the initial validation process. This may be achieved by, for instance, the organization of a collaborative study, using a large and representative panel of target and non-target taxa, and involving as many different reagent brands and thermal cycler types as possible. Therefore, the end users should bear in mind that the performance data of a conventional or real-time PCR protocol described in the original articles are intimately linked to the reagents, equipment and decision rules used. It is strongly suggested that individual laboratories should carry out their own characterization if these parameters are modified, and even if no parameter is modified at all. To this aim, a series of “reference samples” should be maintained and provided by a “reference laboratory” to any laboratory intending to establish and maintain an accurate diagnostic test⁴¹. The organization of training sessions by these reference laboratories

would also help to share experience and knowledge about the use of a given protocol, and would harmonize the practices and decision rules. This is of paramount importance when targeting a quarantine pathogen, for which very strict regulations are enforced.

We also advocate the continuous verification of the specificity of published protocols, in order to consider new taxa that are continuously described in the literature. This can be achieved by *in silico* evaluation, by blasting the primer and probe sequences on international DNA databases such as GenBank on a regular basis, and by wet lab testing of newly described strains. Another suggestion to ensure the accuracy of the positive results is to analyze the amplicon sequence and/or to use additional tests targeting other loci in the genome of the target organism. Currently, the two international protocols for the diagnosis of *F. circinatum*^{13,15} recommend sequencing of the amplicon after a positive result via conventional or SYBR Green real-time PCR using the CIRC1A-CIRC4A primers²². However, our study suggests that a similar procedure should also apply for the other available protocols targeting *F. circinatum*, even for those using hydrolysis probe-based methods. It is advisable that such a complementary approach should be followed to verify results of particular importance such as first reports in disease-free areas. For some of the protocols, analysis of the amplicon sequence, trimmed from the primers' sequences may help confirm the accuracy of the result. However, sequencing will not always be sufficient. Firstly, this is dependent on reference sequences being available in databases. Secondly, this approach will not work if undescribed species share a 100% match to *F. circinatum* (see Table 2 footnotes). Lastly, confirmation by sequencing is not always possible when the conventional or real-time PCR test targets a region of unknown function such as a Sequence Characterized Amplified Region (SCAR). Hence, no orthologous sequences for other *Fusarium* species are available for the SCAR targeted by protocol p1 and p8.

In addition, positive samples could be further processed in order to isolate the pathogen in pure culture, allowing the identification of the pathogen by both morphological and molecular features⁴². Combining molecular and morphological data would of course secure identification of the pathogen, particularly important for first reports, and will help to increase knowledge of the morphologic and genetic diversity of the pathogen. In this respect, it is necessary to establish protocols providing a representative sampling strategy, starting from plant tissue. With the exception of seeds, for which a strategy has been proposed⁴³, there is to our knowledge no standard for sampling plants or adult trees, tackling for instance the minimum number of samples that should be taken for assuring the absence of the pathogen, irrespective of the analysis technique chosen (molecular or isolation).

Methods

Participants and selection of protocols. An official call for participation was issued in 2016 in the framework of the COST action FP1406 PINESTRENGTH. In all, 23 laboratories representing 18 countries participated in the study (Table 3). Only laboratories with sufficient experience in molecular biology-based detection techniques and appropriate equipment were involved. Samples were sent to each participant on June 7th, 2017. The analyses were to be completed and results returned to the organizer by the end of August 2017.

At the time the project was started, a total of nine conventional or real-time PCR protocols targeting *F. circinatum* (p1 to p9) were available in the literature or were brought to our knowledge (Table 4). Protocols included several formats of PCR amplification and labeling. Protocols p1 and p9 use conventional or end-point PCR^{13,23}, p4, p5, and p6 use SYBR Green-based real-time PCR^{22,25,26}, and p2, p3, p7, and p8 use real-time PCR hydrolysis probe-based tests^{24,27,28}. In order to balance the comparison among the protocols and to provide a sufficient amount of data to compute the performance criteria, each protocol was assessed by at least four different partners.

Protocols were conducted following the description in the original article, observing the amplification parameters (cycling conditions, temperatures settings) and reaction mixtures (primers and probe concentrations, reaction and DNA template volumes) indicated by the authors and summarized in a reference document that was sent to each participant along with the DNA samples (Supplementary Information 2). However, if not available in the participant laboratory, the DNA polymerase or commercial real-time PCR master mix described in the original articles were replaced by the reagents typically used by the participant laboratory (for further information refer to Supplementary Information 3). Each participating laboratory was free to use its own PCR equipment.

***F. circinatum*-specific primers and probes.** Each partner provided the primers for the protocols using end-point PCR and SYBR Green real-time PCR, as described in the original articles. To cut down costs, the primers/probe combinations required for the different hydrolysis probe real-time PCR protocols were only purchased once by one of the partners and distributed to all the participants as ready-to-use aliquots of 30 μ M (primers) or 10 μ M (probe) solutions, in 1.5 mL amber microtubes. Primers/probe combinations for p2 and p7, p3, and p8 were custom made by Eurogentec (Seraing, Belgium), Integrated DNA technology (Skokie, Illinois), and Biosearch Technologies (Petaluma, California), respectively. Primers and probes were shipped at room temperature by a fast delivery service and kept in a freezer until used for testing.

Fungal strains and preparation of panels of DNA samples. A panel of 71 monosporic *Fusarium* spp. strains representing 29 distinct species was used (Table 5). Species identity was confirmed by EF1 alpha gene sequencing⁴⁴, if the strain was not obtained from an international fungal collection. It included 38 *F. circinatum* strains from different geographical origins, mating types, host tree species and environments, thus covering as much of the genetic diversity of the pathogen as possible. Thirty-three other *Fusarium* strains were also included. They represented species that are either genetically close to *F. circinatum*, or inhabit the same ecological niche, i.e. pine woody tissue, pine seeds, pine roots, or soil. Also included were recently described species of *Fusarium* associated with pine cankers in Colombia, i.e. *F. parvisorum*, *F. sororula*, *F. marasianum*, *F. pininemorale*, and *F. fracticaudum*²⁰. The strains were sent from different providers, and were kept on agar slants at 5 °C before handling. As *F. circinatum* is considered a quarantine organism for the European Union (EU), all strains from this species were maintained and manipulated in level 3 biohazard containment facilities in ANSES Plant Health

Partner Label	Institute/laboratory	Description	Country, city
1	Sustainable Forest Management Institute	University of Valladolid	Spain, Palencia
2	Institute of Forestry and Rural Engineering	Estonian University of Life Sciences	Estonia, Tartu
3	Institute for National and International Plant Health	Julius Kühn-Institute	Germany, Braunschweig
4	Voké Branch, Lab of Biotechnology	Lithuanian Research Centre for Agriculture and Forestry	Lithuania, Vilnius
5	Department for Innovation in Biological, Agro-food and Forest Systems (DIBAF),	University of Tuscia	Italy, Viterbo
6	Instituto Agroforestal Mediterráneo	Universitat Politècnica de València	Spain, Valencia
7	Laboratoire de la santé des végétaux	French Agency for food, environmental and occupational health safety (ANSES)	France, Malzéville
8	Faculty of Biology and Environmental Sciences	Cardinal Stefan Wyszyński University in Warsaw	Poland, Warsaw
9	Forest Health and Biotic Interactions/Phytopathology	Swiss Federal Institute for Forest, Snow and Landscape Research WSL	Switzerland, Birmensdorf
10	Instituto Nacional de Investigação Agrária e Veterinária I.P.,	State Laboratory of the Ministry of Agriculture, Forests and Rural Development	Portugal, Oeiras
11	Institute for Sustainable Plant Protection	National Research Council	Italy, Florence
12	Forest Research	Forestry Commission	United Kingdom, Farnham
13	Centro de Biotecnología	Universidad de Concepción	Chile, Concepción
14	Department of Food, Environmental and Nutritional Sciences	University of Milan	Italy, Milan
15	Forestry and Agricultural Biotechnology Institute	University of Pretoria	South Africa, Pretoria
16	Department of Agricultural Sciences, Biotechnology and Food Science	Cyprus University of Technology	Cyprus, Limassol
17	Department of Biology	University of Aveiro	Portugal, Aveiro
18	Dipartimento di Scienze delle Produzioni Agroalimentari e dell'Ambiente (DISPAA)	University of Florence	Italy, Florence.
19	Phytophthora Research Centre	Mendel University in Brno	Czech Republic, Brno
20	Laboratory of Forest Protection	Slovenian Forestry Institute	Slovenia, Ljubljana
21	Forest Health Center of Calabazanos	Regional Government of Castilla y León (JCyL)	Spain, Palencia
22	Faculty of Forestry, Forest Pathology Laboratories	Applied Sciences University of Isparta	Turkey, Isparta
23	Department of Agriculture, Food and Environment	University of Catania	Italy, Catania

Table 3. Partners involved in the collaborative project.

Laboratory (here named as ANSES), in Malzéville, France, in compliance with EU Directive 2008/61/EC. Taking into consideration that the *Fusarium* strains from Colombia are recently described species²⁰ not found in the EU, it was decided to manipulate them under the same conditions as *F. circinatum*.

To avoid biases generated by the involvement of different operators and laboratories and to minimize the risk of moving around living *F. circinatum* strains, all participants worked with DNA extracts rather than with living cultures. All strains were first gathered in ANSES and kept on site. For DNA extraction, the strains were first cultured on potato dextrose liquid media (PD Broth, DIFCO™), for approximately 5 days, after which 100 to 200 mg of fresh mycelium was harvested. Genomic DNA (gDNA) was extracted using the DNeasy plant mini kit™ (Qiagen, Courtaboeuf, France) following the manufacturer's guidelines, after grinding mycelium with a Lysis matrix A tube containing one 6-mm ceramic sphere and garnet matrix (MP Biomedicals, Santa Ana, CA, USA) and homogenized for 20 s at 6.5 U (m/sec) using a FASTprep 24 device (MP Biomedicals). DNA concentration was estimated using the Nanodrop 2000 Spectrophotometer™. For each strain, genomic DNA was produced from biological replicates and mixed/homogenized in order to obtain enough DNA to be tested in all of the different protocols and to supply to all of the partners. For each strain, the quality of the DNA extract was assessed by successful PCR amplification of the Internal Transcribed Spacer rDNA using the ITS1/ITS4 primer pair⁴⁵, and the DNA concentration normalized to 0.5 ng μL⁻¹ and distributed as 50-μL aliquots in individual 2-mL microtubes (F1 to F84, Table 5). In total, each laboratory received 38 *F. circinatum* DNA samples (target DNA) and 33 non-target DNA samples. All samples were anonymously labeled, shipped at room temperature by fast delivery service, and kept in a freezer until analysis.

A set of DNA from *F. circinatum*-artificially infected pine seeds was also prepared. Two strains of *F. circinatum* (F7 and F11) were cultured for 6 days at 22 °C under cool-white fluorescent lights with a 12-h light period on Spezieller Nährstoffarmer Agar (SNA) medium to allow macro- and microconidia production⁴⁶. Microconidia were harvested by washing the surface of cultures with 10 mL of deionized sterile water with 0.01% Tween 20. The resulting suspension was diluted with sterile water to obtain a final concentration of 2.52×10^3 and 1.90×10^3 conidia μL⁻¹ for F7 and F11, respectively, based on counts made using a hemocytometer. Healthy *Pinus pinaster*

Protocol number	Reference	Target in the <i>F. circinatum</i> genome	Type of assay
p1	Ramsfield <i>et al.</i> ²³	Two independent sequence characterized amplified regions (SCAR)	End-point PCR
p2	Ioos <i>et al.</i> ²⁴	rDNA Intergenic spacer (IGS)	Real-time PCR with hydrolysis probe
p3	Lamarche <i>et al.</i> ²⁷	rDNA Intergenic spacer (IGS)	Real-time PCR with hydrolysis probe
p4	Schweigkofler <i>et al.</i> ²²	rDNA Intergenic spacer (IGS)	Real-time PCR with SYBR Green staining
p5	Fourie <i>et al.</i> ²⁶	rDNA Intergenic spacer (IGS)	Real-time PCR with SYBR Green staining
p6	Dreaden <i>et al.</i> ²⁵	rDNA Intergenic spacer (IGS)	Real-time PCR with SYBR Green staining
p7	Luchi <i>et al.</i> ²⁸	Translation elongation factor 1-alpha gene (TEF)	Real-time PCR with hydrolysis probe
p8	Baskarathevan <i>et al.</i> (Supplementary Information 1)	Sequence characterized amplified region (SCAR)	Real-time PCR with hydrolysis probe
p9	EPPO ¹³ , appendix 4	rDNA Intergenic spacer (IGS)	End-point PCR

Table 4. List of *F. circinatum* diagnostic protocols assessed during the collaborative study.

seeds were first incubated in liquid PD Broth media as described by Ioos *et al.*²⁴, in order to simulate biological enrichment of natural samples, as is performed in routine detection analysis. Four replicates of one thousand healthy seeds each were incubated for 72 h at 22 °C in a sterile Easy flat flask containing 50 mL of PD Broth. After incubation, the contents of the Easy flask (healthy seeds + liquid medium) were aseptically transferred into a sterilized grinding bowl, and ground for 1 min using a Microtron MB 550 mixermill (Kinematica, Lucerne, Switzerland). Seventy subsamples of 500 µL of homogenate were collected using a micropipette and transferred into individual sterile 2-mL microtubes. For each of the two *F. circinatum* strains, 4 sets of 14 homogenized healthy seed subsamples were spiked with 1×10^5 , 1×10^4 , 1×10^3 , and 1×10^2 conidia, respectively. One set was spiked with sterile water to be used as negative control for the seeds. Total DNA was extracted from each spiked homogenate as described by Ioos *et al.*²⁴ using the Nucleospin Plant II miniprep (Macherey-Nagel) DNA extraction kit. For each level of contamination, all the DNA extracts were pooled, homogenized, and then distributed as 50 µL *F. circinatum* contaminated seed DNA to be used as template for PCR testing (F85 to F92, Table 5). In total, each laboratory received eight pine seed DNA extracts anonymously labeled, which were transported using a fast delivery service and kept in a freezer until analysis.

In total, each partner received an identical panel of 79 DNA extracts, to be tested in duplicate analysis for each protocol that was assessed.

Data generation and analysis. *Indeterminate results.* Data were processed anonymously, and no communication was allowed about the trials between partners before the end of the collaborative study. For each protocol, each participant tested all 79 DNA extracts in duplicate. For each sample, results of the tests were reported as either “positive” or “negative”, based on the duplicate analyses. With the exception of protocol p8 (where a $Ct < 36$ should be considered as a positive result), none of the five published real-time PCR protocols recommended a decision cut-off value. Therefore, the decision to rate a DNA sample as “positive” or “negative” was up to each participant, following the decision rules in force in the laboratory. However, in case of doubt or difficulty in interpretation of the results, “indeterminate result” could be reported. The participants were nevertheless encouraged to submit a brief description of the problem encountered. Indeterminate results between protocols, as reported by the participating laboratories, were compared by Fisher’s exact tests for count data.

Indeterminate results were also compared between laboratories by protocol using Fisher’s exact tests. Ideally, these comparisons would have been performed comparing all indeterminate results generated by laboratories, across all tests. However, it must be noted that not all participants implemented all nine protocols, and missing data for some partners exist in the datasets (for example laboratories that only participated in one test would not be included in the statistical test). Therefore, the decision was made to compare laboratories by protocol, in order to have an idea of potential differences that can exist for example between equipment, location or staff in charge of the tests. In both cases, Fisher’s exact tests were performed with simulated P-values based on 1×10^5 replicates.

Indeterminate results were then transformed following two scenarios as suggested by Chabirand *et al.*⁴⁷ and Loreti, *et al.*⁴⁸. The first scenario considered that an indeterminate result would be further assessed by the laboratory, and would always be rated “as expected” (i.e. a sample containing *F. circinatum* DNA would be rated as positive, and a sample not containing *F. circinatum* DNA would be rated as negative), so that the participant would always make the right decision, eventually. This dataset is here referred to as Dataset 1 (DS1). In the second scenario, an indeterminate result would always be rated “not as expected” (i.e. a sample containing *F. circinatum* DNA would be rated as negative, and a sample not containing *F. circinatum* DNA would be rated as positive), so that the participant would always make the wrong decision. This dataset is here referred to as Dataset 2 (DS2).

As the objective was to show the potential biases in the application of a protocol that may arise through differences between equipment, location or staff in charge of the analysis, identity of laboratories is not revealed and only the range of indeterminate results is shown.

Rates of false positive and false negative results. Results of the protocols were assessed by computing a number of parameters using both datasets: (i) PA, the number of positive accords or true positives, defined as the number of DNA samples from *F. circinatum* strains (or DNA from seed samples contaminated with *F. circinatum*) yielding positive results with the protocol; (ii) NA, the number of negative accords or true negatives, here defined as the

Code	Species	Strain	Mating type	Host	Origin	Environment	Provider
F1	<i>F. circinatum</i>	LSVM211	MAT-1	<i>P. menziesii</i>	France (Perpignan)	Private garden	R. Ioos
F2	<i>F. circinatum</i>	LSVM216	MAT-2	<i>P. radiata</i>	France (Vendée)	Nursery	R. Ioos
F3	<i>F. circinatum</i>	LSVM217	MAT-2	<i>P. radiata</i>	France (Côtes d'Armor)	Nursery	R. Ioos
F4	<i>F. circinatum</i>	LSVM1221	MAT-2	<i>P. radiata</i>	Espagne (Basque country)	Forest	J. Aguayo
F5	<i>F. circinatum</i>	NRRL26431	MAT-1	unkn.	Japan	unkn.	K. O'Donnell
F6	<i>F. circinatum</i>	NRRL25708	MAT-1	unkn.	USA	unkn.	K. O'Donnell
F7	<i>F. circinatum</i>	NRRL25331	MAT-1	unkn.	USA	unkn.	K. O'Donnell
F8	<i>F. circinatum</i>	NRRL25333	MAT-2	unkn.	S-Africa	unkn.	K. O'Donnell
F11	<i>F. circinatum</i>	FcCa01	MAT-2	<i>P. radiata</i>	Spain (Cantabria, Rionansa)	Forest	J. Diez
F12	<i>F. circinatum</i>	FcCa02	MAT-2	<i>P. radiata</i>	Spain (Cantabria, Castrouardiales)	Forest	J. Diez
F13	<i>F. circinatum</i>	FcCa05	MAT-2	<i>P. radiata</i>	Spain (Cantabria, Mazcuerras)	Forest	J. Diez
F14	<i>F. circinatum</i>	FcCa06	MAT-2	<i>P. radiata</i>	Spain (Cantabria, Comillas)	Forest	J. Diez
F15	<i>F. circinatum</i>	FC042v	MAT-2	<i>P. radiata</i>	Spain (Cantabria, Cabezón de la Sal)	Forest	J. Diez
F16	<i>F. circinatum</i>	FC035	MAT-2	<i>P. radiata</i>	Spain (Cantabria, Cabezón de la Sal)	Forest	J. Diez
F17	<i>F. circinatum</i>	CSF-1	MAT-1	<i>P. pinea</i>	Spain (Burgos)	Reforestation seedling	A. Sanz-Ros
F18	<i>F. circinatum</i>	CSF-2	MAT-1	<i>P. radiata</i>	Spain (León)	Insect (<i>Brachyderes</i> sp.)	A. Sanz-Ros
F19	<i>F. circinatum</i>	CSF-3	MAT-1	<i>P. radiata</i>	Spain (León)	Seed (cones)	A. Sanz-Ros
F20	<i>F. circinatum</i>	CSF-4	MAT-1	<i>P. radiata</i>	Spain (León)	Forest (twig)	A. Sanz-Ros
F22	<i>F. circinatum</i>	CSF-6	MAT-1	<i>P. radiata</i>	Spain (León)	Forest (stem)	A. Sanz-Ros
F23	<i>F. circinatum</i>	CSF-7	MAT-2	<i>P. radiata</i>	Spain (León)	Forest (stem)	A. Sanz-Ros
F24	<i>F. circinatum</i>	CSF-8	MAT-2	<i>P. nigra</i>	Spain (Palencia)	Reforestation seedling	A. Sanz-Ros
F26	<i>F. circinatum</i>	CSF-10	MAT-1	<i>P. nigra</i>	Spain (León)	Reforestation seedling	A. Sanz-Ros
F27	<i>F. circinatum</i>	CSF-11	MAT-1	<i>P. nigra</i>	Spain (Valladolid)	Nursery	A. Sanz-Ros
F28	<i>F. circinatum</i>	CSF-12	MAT-1	<i>P. sylvestris</i>	Spain (Valladolid)	Nursery	A. Sanz-Ros
F29	<i>F. circinatum</i>	CSF-13	MAT-2	<i>P. pinaster</i>	Spain (Valladolid)	Seeds	A. Sanz-Ros
F30	<i>F. circinatum</i>	116	MAT-2	<i>P. nigra</i>	Spain (Galicia)	Nursery	M. Berbegal
F31	<i>F. circinatum</i>	164	MAT-1	<i>P. sylvestris</i>	Spain (Asturias)	Nursery	M. Berbegal
F32	<i>F. circinatum</i>	221	MAT-2	<i>P. radiata</i>	Spain (Cantabria)	Nursery	M. Berbegal
F33	<i>F. circinatum</i>	253	MAT-1	<i>P. nigra</i>	Spain (Galicia)	Nursery	M. Berbegal
F34	<i>F. circinatum</i>	822	MAT-1	<i>P. pinaster</i>	Spain (Galicia)	Seeds	M. Berbegal
F35	<i>F. circinatum</i>	07/0649 1b	MAT-1	<i>P. pinaster</i>	Spain (Asturias)	Nursery	M. Berbegal
F36	<i>F. circinatum</i>	310/061	MAT-1	<i>P. palustris</i>	Spain (Asturias)	Nursery	M. Berbegal
F37	<i>F. circinatum</i>	2028	MAT-2	<i>P. radiata</i>	Chile	Nursery	R. Ahumada
F38	<i>F. circinatum</i>	2738	MAT-2	<i>P. radiata</i>	Chile	Nursery	R. Ahumada
F39	<i>F. circinatum</i>	INV19	MAT-2	<i>P. radiata</i>	Chile	Nursery	R. Ahumada
F40	<i>F. circinatum</i>	2306 BASA	MAT-2	<i>P. radiata</i>	Chile	Nursery	R. Ahumada
F41	<i>F. circinatum</i>	CMW 1219	MAT-2	<i>Pinus</i> sp.	South Africa	unkn.	MJ. Wingfield (FABI)
F42	<i>F. circinatum</i>	CMW 350	MAT-1	<i>Pinus</i> sp.	USA (California)	unkn.	MJ. Wingfield (FABI)
F51	<i>F. begoniae</i>	LSVM293	MAT-1	<i>Begonia elatior</i>	France		R. Ioos
F52	<i>F. concentricum</i>	NRRL 25181		unkn.	France		K. O'Donnell
F53	<i>F. fujikuroi</i>	LSV667	MAT-2	<i>Zea mays</i>	France		R. Ioos
F54	<i>F. mangiferae</i>	NRRL25226	MAT-2	unkn.	unkn.		K. O'Donnell
F55	<i>F. nygamai</i>	NRRL13448		unkn.	unkn.		K. O'Donnell
F56	<i>F. proliferatum</i>	LSVM673	MAT-2	<i>Populus</i> sp.	France		R. Ioos
F57	<i>F. sacchari</i>	NRRL13999		unkn.	unkn.		K. O'Donnell
F58	<i>F. subglutinans</i>	LSVM869	MAT-1	<i>Zea mays</i>	France		R. Ioos
F59	<i>F. subglutinans</i>	LSVM704	MAT-1	<i>Zea mays</i>	France		R. Ioos
F60	<i>F. temperatum</i>	LSVM870	MAT-2	<i>Zea mays</i>	France		R. Ioos
F61	<i>F. thapsinum</i>	NRRL22045		unkn.	unkn.		K. O'Donnell
F62	<i>F. verticillioides</i>	LSVM873		<i>Zea mays</i>	France		R. Ioos

Continued

Code	Species	Strain	Mating type	Host	Origin	Environment	Provider	
F63	<i>F. verticillioides</i>	437-6		<i>Glycine max</i>	Italy		M Pasquali	
F64	<i>F. fractiflexum</i>	NRRL28852	MAT-2	unkn.	unkn.		K. O'Donnell	
F65	<i>F. proliferatum</i>	FGSC 7421	MAT-2	unkn.	unkn.		J.F. Leslie	
F66	<i>F. parvisorum</i>	CMW 25267	MAT-2	<i>Pinus patula</i>	Columbia	Commercial nursery	MJ. Wingfield (FABI)	
F67	<i>F. sororula</i>	CMW 25254	MAT-2	<i>Pinus</i> spp.	Columbia	Commercial nursery	MJ. Wingfield (FABI)	
F68	<i>F. marasasanum</i>	CMW 25261	MAT-2	<i>Pinus patula</i>	Columbia	Commercial nursery	MJ. Wingfield (FABI)	
F69	<i>F. pininemorale</i>	CMW 25243	MAT-1	<i>Pinus tecunumanii</i>	Columbia	Plantation	MJ. Wingfield (FABI)	
F70	<i>F. fracticaudum</i>	CMW 25245	MAT-2	<i>Pinus maximinoi</i>	Columbia	Plantation	MJ. Wingfield (FABI)	
F72	<i>F. avenaceum</i>	Do_US_Nat_2_1		seed of <i>Douglasia</i> sp.	USA		WSL - Phytopathology	
F73	<i>F. incarnatum-equiseti</i> species complex	Do_US_Nat_3_1		seed of <i>Douglasia</i> sp.	USA		WSL - Phytopathology	
F74	<i>F. sporotrichioides</i>	Do_US_Nat_32_1		seed of <i>Douglasia</i> sp.	USA		WSL - Phytopathology	
F75	<i>F. tricinctum</i> species complex	Do_US_Sno_49_1		seed of <i>Douglasia</i> sp.	USA		WSL - Phytopathology	
F76	<i>F. acuminatum</i>	Do_US_VC_49_1		seed of <i>Douglasia</i> sp.	USA		WSL - Phytopathology	
F77	<i>F. torulosum</i>	Do_US_VC_5_1		seed of <i>Douglasia</i> sp.	USA		WSL - Phytopathology	
F78	<i>F. graminearum</i>	Do-Mur/17-1		seed of <i>D. menziesii</i>	USA		WSL - Phytopathology	
F79	<i>F. proliferatum</i>	FI-BOS/13-1		seed of <i>Picea</i> sp.	Switzerland		WSL - Phytopathology	
F80	<i>F. reticulatum negundis</i>	FI-BOS/14-1		seed of <i>Picea</i> sp.	Switzerland		WSL - Phytopathology	
F81	<i>F. redolens</i>	Do-D/11-1		seed of <i>Douglasia</i> sp.	Switzerland		WSL - Phytopathology	
F82	<i>F. culmorum</i>	CSF-14		<i>Pinus pinea</i>	Spain (Palencia)	reafforestation seedling	A. Sanz-Ros	
F83	<i>F. torulosum</i>	CSF-15		<i>Pinus nigra</i>	Spain (León)	reafforestation seedling	A. Sanz-Ros	
F84	<i>F. oxysporum</i>	CSF-16	MAT-2	<i>Pinus pinea</i>	Spain (Palencia)	reafforestation seedling	A. Sanz-Ros	
F85	<i>P. pinaster</i> seed spiked with 10 ⁵ conidia of strain F7						—	—
F86	<i>P. pinaster</i> seed spiked with 10 ⁴ conidia of strain F7						—	—
F87	<i>P. pinaster</i> seed spiked with 10 ³ conidia of strain F7						—	—
F88	<i>P. pinaster</i> seed spiked with 10 ² conidia of strain F7						—	—
F89	<i>P. pinaster</i> seed spiked with 10 ⁵ conidia of strain F11						—	—
F90	<i>P. pinaster</i> seed spiked with 10 ⁴ conidia of strain F11						—	—
F91	<i>P. pinaster</i> seed spiked with 10 ³ conidia of strain F11						—	—
F92	<i>P. pinaster</i> seed spiked with 10 ² conidia of strain F11						—	—

Table 5. List of *Fusarium* spp. strains used in the collaborative study.

number of DNA samples from other *Fusarium* species yielding negative results with the protocol; (iii) PD, the number of positive deviations or false positives, which takes into account the number of DNA samples from other *Fusarium* species (or DNA from seed samples not contaminated with *F. circinatum*) yielding positive results with the protocol; and iv) ND, the number of negative deviations or false negatives, which corresponds to the number of DNA samples from *F. circinatum* strains (or DNA from seed samples contaminated with *F. circinatum*) yielding negative results with the protocol.

Similarly, for both datasets, the performance of the protocols regarding specificity was assessed using the PD rate, computed as $PD\ rate = 100 \times (\text{number of misclassified known positive samples} / \text{total number of known negative samples})$, and the ND rate, computed as, $ND\ rate = 100 \times (\text{number of misclassified known negative samples} / \text{total number of known positive samples})$. As for indeterminate results, the PD and ND rates were compared between laboratories by protocol (in total nine comparisons) for both datasets.

All comparisons were performed using Fisher's exact tests for count data with simulated P-values based on 1×10^5 replicates.

Other performance criteria. For each protocol and for each participant the results obtained for the blind samples were processed according to EN ISO 16140 standard⁴⁹ and the PM7/98 (2) EPPO standard¹⁶. Three performance criteria were assessed: relative accuracy (AC), diagnostic specificity (SP) and diagnostic sensitivity (SE). AC

represents the agreement between the expected results and the results obtained using the protocol. SE provides an estimation of the ability of the procedure to detect the target when it is present (presence of *F. circinatum* DNA). SP provides an estimation of the ability of the procedure not to detect the target when it is not present (no *F. circinatum* DNA present in the sample). AC, SP and SE were estimated using PA, NA, PD and ND, described in the previous sections, as follows:

$$\begin{aligned} AC &= 100 * (PA + NA)/(NA + PA + PD + ND) \\ SP &= 100 * NA/(NA + PD); \\ SE &= 100 * PA/(PA + ND); \end{aligned}$$

Tests on the equality of SE, SP and AC between methods were performed using Fisher's exact test.

Qualitative reproducibility or concordance (CO) was also estimated for each protocol. Concordance is the probability that two identical test materials sent to different laboratories will both provide the same results (i.e. both found positive or both found negative)⁵⁰. Concordance for qualitative analyses is similar to reproducibility for quantitative analyses, and this performance criterion is a means to assess the ability of a protocol to provide consistent results with identical samples that are tested under different conditions: operator, equipment, master mix or DNA polymerase brand, location, time⁴⁹. In order to have a reliable estimation of CO, it was calculated for each protocol using the original data reported by the participating laboratories. This means that positive, negative and indeterminate results were included. CO between protocols was compared for both datasets using Fisher's exact tests for count data.

Statistical software for data analysis. All statistical tests were performed using the R statistical software version 3.4.0⁵¹. Statistical tests were considered as significant for estimated P-values with a confidence of less than 5%. All figures were produced using the R package "ggplot2"⁵².

Data Availability

All data generated or analyzed during this study are included in this published article (and its Supplementary Information and Dataset Files).

References

- Schmale, D. G. III & Gordon, T. R. Variation in susceptibility to pitch canker disease, caused by *Fusarium circinatum*, in native stands of *Pinus muricata*. *Plant Pathol.* **52**, 720–725 (2003).
- Gordon, T. R., Kirkpatrick, S. C., Aegerter, B. J., Wood, D. L. & Storer, A. J. Susceptibility of Douglas fir (*Pseudotsuga menziesii*) to pitch canker, caused by *Gibberella circinata* (anamorph = *Fusarium circinatum*). *Plant Pathol.* **55**, 231–237 (2006).
- Martínez-Álvarez, P., Pando, V. & Diez, J. J. Alternative species to replace Monterey pine plantations affected by pitch canker caused by *Fusarium circinatum* in northern Spain. *Plant Pathol.* **63**, 1086–1094, <https://doi.org/10.1111/ppa.12187> (2014).
- Wingfield, M. J. *et al.* Pitch canker caused by *Fusarium circinatum* - a growing threat to pine plantations and forests worldwide. *Australas. Plant Path.* **37**, 319–334 (2008).
- Bezos, D., Martínez-Alvarez, P., Fernández, M. & Diez, J. J. Epidemiology and management of pine pitch canker disease in Europe - a review. *Balt. For.* **23**, 279–293 (2017).
- Landeras, E. *et al.* Outbreak of pitch canker caused by *Fusarium circinatum* on Pinus spp. in Northern Spain. *Plant Dis.* **89**, 1015 (2005).
- Bragança, H., Diogo, E., Moniz, F. & Amaro, P. First report of pitch canker on pines caused by *Fusarium circinatum* in Portugal. *Plant Dis.* **93**, 1079–1079, <https://doi.org/10.1094/PDIS-93-10-1079A> (2009).
- EFSA. Risk assessment of *Gibberella circinata* for the EU territory and identification and evaluation of risk management options. *EFSA Journal* **8**, 1620 (2010).
- Carlucci, A., Colatruglio, L. & Frisullo, S. First report of pitch canker caused by *Fusarium circinatum* on *Pinus halepensis* and *P. pinea* in Apulia (Southern Italy). *Plant Dis.* **91**, 1683 (2007).
- Vettraino, A., Potting, R. & Raposo, R. EU legislation on forest plant health: an overview with a focus on *Fusarium circinatum*. *Forests* **9**, 568 (2018).
- Möykkynen, T., Capretti, P. & Pukkala, T. Modelling the potential spread of *Fusarium circinatum*, the causal agent of pitch canker in Europe. *Annals of Forest Sciences* **72**, 169–181 (2015).
- Bustin, S. A. *et al.* The MIQE guidelines: minimum information for publication of quantitative real-time PCR experiments. *Clin Chem* **55**, <https://doi.org/10.1373/clinchem.2008.112797> (2009).
- EPPO. PM 7/91(1): *Gibberella circinata*. *EPPO Bull.* **39**, 298–309 (2009).
- ISTA. 7-009: Detection of *Gibberella circinata* on Pinus spp. (pine) and *Pseudotsuga menziesii* (Douglas-fir) seed. *Validated Seed Health Testing Methods* (2015).
- IPPC. ISPM 27, Diagnostic protocols for regulated pests, DP 22: *Fusarium circinatum* (2017).
- EPPO. PM 7/98 (2) Specific requirements for laboratories preparing accreditation for a plant pest diagnostic activity. *EPPO Bull.* **44**, 117–147, <https://doi.org/10.1111/epp.12118> (2014).
- Nirenberg, H. I. & O'Donnell, K. New *Fusarium* species and combinations within the *Gibberella fujikuroi* species complex. *Mycologia* **90**, 434–458 (1998).
- Britz, H., Coutinho, T. A., Wingfield, M. J. & Marasas, W. F. O. Validation of the description of *Gibberella circinata* and morphological differentiation of the anamorph *Fusarium circinatum*. *Sydowia* **54**, 9–22 (2002).
- Mullett, M., Pérez-Sierra, A., Armengol, J. & Berbegal, M. Phenotypic and molecular characterisation of *Fusarium circinatum*: correlation with virulence and fungicide sensitivity. *Forests* **8**, 458 (2017).
- Herron, D. A. *et al.* Novel taxa in the *Fusarium fujikuroi* species complex from Pinus spp. *Stud. Mycol.* **80**, 131–150, <https://doi.org/10.1016/j.simyco.2014.12.001> (2015).
- Storer, G. & Clark, S. L. Association of the pitch canker fungus, *Fusarium subglutinans* f.sp. *pini*, with Monterey pine seeds and seedlings in California. *Plant Pathol.* **47**, 649–656, <https://doi.org/10.1046/j.1365-3059.1998.00288.x> (1998).
- Schweigkofler, W., O'Donnell, K. & Garbelotto, M. Detection and quantification of airborne conidia of *Fusarium circinatum*, the causal agent of pine pitch canker, from two California sites by using a real-time PCR approach combined with a simple spore trapping method. *Appl. Environ. Microbiol.* **70**, 3512–3520 (2004).
- Ramsfield, T. D., Dobbie, K., Dick, M. A. & Ball, R. D. Polymerase chain reaction-based detection of *Fusarium circinatum*, the causal agent of pitch canker disease. *Molecular Ecology Resources* **8**, 1270–1273 (2008).

24. Ioos, R., Fourrier, C., Iancu, G. & Gordon, T. R. Sensitive Detection of *Fusarium circinatum* in Pine Seed by Combining an Enrichment Procedure with a Real-Time Polymerase Chain Reaction Using Dual-Labeled Probe Chemistry. *Phytopathology* **99**, 582–590, <https://doi.org/10.1094/PHYTO-99-5-0582> (2009).
25. Dreaden, T. J., Smith, J. A., Barnard, E. L. & Blakeslee, G. Development and evaluation of a real-time PCR seed lot screening method for *Fusarium circinatum*, causal agent of pitch canker disease. *For. Path.* **42**, 405–411, <https://doi.org/10.1111/j.1439-0329.2012.00774.x> (2012).
26. Fourie, G. *et al.* Culture-independent detection and quantification of *Fusarium circinatum* in a pine-producing seedling nursery. *Southern Forests: a Journal of Forest Science* **76**, 137–143, <https://doi.org/10.2989/20702620.2014.899058> (2014).
27. Lamarche, J. *et al.* Molecular detection of 10 of the most unwanted alien forest pathogens in Canada using Real-Time PCR. *PLoS ONE* **10**, e0134265, <https://doi.org/10.1371/journal.pone.0134265> (2015).
28. Luchi, N., Pepori, A. L., Bartolini, P., Ioos, R. & Santini, A. Duplex real-time PCR assay for the simultaneous detection of *Caliciopsis pinea* and *Fusarium circinatum* in pine samples. *Applied Microbiology and Biotechnology* **102**, 7135–7146, <https://doi.org/10.1007/s00253-018-9184-1> (2018).
29. Sandoval-Denis, M., Swart, W. J. & Crous, P. W. New *Fusarium* species from the Kruger National Park, South Africa. *MycKeys* **34**, <https://doi.org/10.3897/mycokeys.34.25974> (2018).
30. Steenkamp, E. T., Wingfield, B. D., Desjardins, A. E., Marasas, W. F. & Wingfield, M. J. Cryptic speciation in *Fusarium* subglutinans. *Mycologia* **94**, 1032–1043 (2002).
31. Garcia-Benitez, C. *et al.* Proficiency of real-time PCR detection of latent *Monilinia* spp. infection in nectarine flowers and fruit. *Phytopathologia Mediterranea* **56**, 242–250 (2017).
32. Ebtentier, D. L. *et al.* Evaluation of the repeatability and reproducibility of a suite of qPCR-based microbial source tracking methods. *Water Research* **47**, 6839–6848, <https://doi.org/10.1016/j.watres.2013.01.060> (2013).
33. Bustin, S. & Huggett, J. qPCR primer design revisited. *Biomolecular Detection and Quantification* **14**, 19–28, <https://doi.org/10.1016/j.bdq.2017.11.001> (2017).
34. Grosdidier, M., Aguayo, J., Marçais, B. & Ioos, R. Detection of plant pathogens using real-time PCR: how reliable are late Ct values? *Plant Pathol.* **66**, 359–367, <https://doi.org/10.1111/ppa.12591> (2017).
35. Al-Soud, W. A. & Rådström, P. Capacity of nine thermostable DNA polymerases to mediate DNA amplification in the presence of PCR-inhibiting samples. *Applied and environmental microbiology* **64**, 3748–3753 (1998).
36. Saunders, G. C., Dukes, J., Parkes, H. C. & Cornett, J. H. Interlaboratory study on thermal cycler performance in controlled PCR and random amplified polymorphic DNA analyses. *Clinical chemistry* **47**, 47–55 (2001).
37. Boutigny, A.-L. *et al.* Optimization of a real-time PCR assay for the detection of the quarantine pathogen *Melampsora medusae* f. sp. *deltoidae*. *Fungal Biology* **117**, 389–398, <https://doi.org/10.1016/j.funbio.2013.04.001> (2013).
38. Guinet, C., Fourrier-Jeandel, C., Cerf-Wendling, I. & Ioos, R. One-step detection of *Monilinia fructicola*, *M. fructigena*, and *M. laxa* on *Prunus* and *Malus* by a multiplex real-time PCR assay. *Plant Dis.* **100**, 2465–2474, <https://doi.org/10.1094/PDIS-05-16-0655-RE> (2016).
39. Aguayo, J. *et al.* Development of a hydrolysis probe-based real-time assay for the detection of tropical strains of *Fusarium oxysporum* f. sp. *cubense* race 4. *PLoS ONE* **12**, e0171767, <https://doi.org/10.1371/journal.pone.0171767> (2017).
40. Broeders, S. *et al.* Guidelines for validation of qualitative real-time PCR methods. *Trends in Food Science & Technology* **37**, 115–126, <https://doi.org/10.1016/j.tifs.2014.03.008> (2014).
41. Pelloux, H. *et al.* A second European collaborative study on polymerase chain reaction for *Toxoplasma gondii*, involving 15 teams. *FEMS Microbiology Letters* **165**, 231–237, <https://doi.org/10.1111/j.1574-6968.1998.tb13151.x> (1998).
42. Leslie, J. F. & Summerell, B. A. *The Fusarium laboratory manual*. (Blackwell Publishing, 2006).
43. Ioos, R. *et al.* Test performance study of diagnostic procedures for identification and detection of *Gibberella circinata* in pine seeds in the framework of a EUPHRESKO project. *EPPO Bull.* **43**, 267–275, <https://doi.org/10.1111/epp.12037> (2013).
44. Geiser, D. M. FUSARIUM-ID v. 1.0: a DNA sequence database for identifying *Fusarium*. *Eur. J. Plant Pathol.* **110**, 473–479 (2004).
45. White, T. J., Bruns, T., Lee, S. & Taylor, J. In *PCR protocols: a guide to method and applications* (eds Gelfand, D. H., Innis M. A., Sninsky, J. J. and White, T. J.) 315–322 (Academic Press, 1990).
46. Nirenberg, H. I. A simplified method for identifying *Fusarium* spp. occurring on wheat. *Canadian Journal of Botany* **59**, 1599–1609 (1981).
47. Chabirand, A., Loiseau, M., Renaudin, I. & Poliakoff, F. Data processing of qualitative results from an interlaboratory comparison for the detection of “Flavescence dorée” phytoplasma: How the use of statistics can improve the reliability of the method validation process in plant pathology. *PLoS ONE* **12**, e0175247, <https://doi.org/10.1371/journal.pone.0175247> (2017).
48. Loreti, S. *et al.* Performance of diagnostic tests for the detection and identification of *Pseudomonas syringae* pv. *actinidiae* (Psa) from woody samples. *European Journal of Plant Pathology*, <https://doi.org/10.1007/s10658-018-1509-5> (2018).
49. International Standardization Organization. ISO 16140:2003 Microbiology of food and animal feeding stuffs - Protocol for the validation of alternative methods (2003).
50. Langton, S., Chevenement, R., Nagelkerke, N. & Lombard, B. Analysing collaborative trials for qualitative microbiological methods: concordance and concordance. *International Journal of Food Microbiology* **79**, 175–181 (2002).
51. R: A Language and Environment for Statistical Computing. R Foundation for Statistical Computing, Vienna (2014). R Foundation for Statistical Computing (2017).
52. Wickham, H. *ggplot2: elegant graphics for data analysis*. (Springer, 2016).

Acknowledgements

This work was supported by COST action FP1406 “Pinestrength”. The authors want to thank Laura Hernández Escribano (Instituto Nacional de Investigación y Tecnología Agraria y Alimentaria, Centro de Investigación Forestal INIA-CIFOR, Ctra. La Coruña, Km.7.5, 28040, Madrid, Spain), Špela Jagodic (Slovenian Forestry Institute), Dr. S. Markovskaja and J. Švediene (Lithuanian Nature Research Centre), Victoria Rodríguez (Centro de Biotecnología, Universidad de Concepción), Dr. Eugénia Andrade INIAV I.P., Portugal, Prof. Tadeusz Malewski (Museum and Institute of Zoology, Warsaw, Poland), Tuğba Doğmuş Lehtijarvi (Applied Sciences University of Isparta, Faculty of Forestry, Isparta, Turkey), Victoria Avgitidou (University of Milan, Maria Evoli (Department of Agriculture, Food and Environment, University of Catania, Italy), Gema Pérez, Paula Zamora, Ana Martín, Juan Carlos Domínguez, Miriam Dueñas, Africa Miravalles, Jorge Miranda, Eva Mayor, Alejandro González and Beltrán Álvarez (Calabazanos Forest Health Centre, JCyL), Tobias Wille (JKI, Institute for National and International Plant Health) and Michael Melek (Mendel university in Brno) for their technical contribution to this work. The work of the Estonian team was supported by the Estonian Science Foundation grants PSG136 and IUT21-04. The work of Portuguese team from INIAV was financed by INIAV I.P. Institute. The work at U. Aveiro (Portugal) was financed by European Funds through COMPETE and National Funds through the Portuguese Foundation for Science and Technology (FCT) to CESAM (UID/AMB/50017/2013 – POCI-01- 0145-FEDER-007638). The work of Slovenian team was financed through Slovenian Research Agency (P4-0107) and by the Slovenian Ministry of Agriculture, Forestry and Food (Public Forestry Service). The British work was

financially supported by the Forestry Commission, UK. The French work was financially supported by the French Agency for Food, environmental and occupational health safety (ANSES). The work in New Zealand was funded by Operational Research Programmes, Ministry for Primary Industries, New Zealand.

Author Contributions

R.I. conceived the project, and designed the study. B.P., C.G. and F.A. prepared and standardized the samples for comparison. All authors performed the experiments. R.I., J.A. and M.M. wrote the main manuscript text with inputs from coauthors. J.A. carried out the statistical analyses and prepared figures. All authors reviewed the manuscript.

Additional Information

Supplementary information accompanies this paper at <https://doi.org/10.1038/s41598-019-44672-8>.

Competing Interests: The authors declare no competing interests.

Publisher's note: Springer Nature remains neutral with regard to jurisdictional claims in published maps and institutional affiliations.



Open Access This article is licensed under a Creative Commons Attribution 4.0 International License, which permits use, sharing, adaptation, distribution and reproduction in any medium or format, as long as you give appropriate credit to the original author(s) and the source, provide a link to the Creative Commons license, and indicate if changes were made. The images or other third party material in this article are included in the article's Creative Commons license, unless indicated otherwise in a credit line to the material. If material is not included in the article's Creative Commons license and your intended use is not permitted by statutory regulation or exceeds the permitted use, you will need to obtain permission directly from the copyright holder. To view a copy of this license, visit <http://creativecommons.org/licenses/by/4.0/>.

© The Author(s) 2019

2.2. Co-infections by *Fusarium circinatum* and *Phytophthora* spp. on *Pinus radiata*, a case study of complex interactions in the Pine pitch canker disease

2.2.1 Introduction

Pinus radiata D. Don, originating from the southwestern United States, California, has been introduced in areas with a Mediterranean climate such as Australia, Chile, New Zealand, South Africa, Spain and Uruguay (Rogers, 2004). Thanks to the rapid growth and excellent quality of the wood, this pine species, of great interest for forestry, is mainly used for the production of timber (Guerrero & Bustamante 2007). The growth and productivity of *P. radiata* can be severely hampered by various parasites and diseases, resulting in significant economic losses. Several diseases of *P. radiata* have been described; among these stand out resinous canker of the pine, “pine pitch canker”, caused by *Fusarium circinatum*, considered as one of the most important diseases on the *Pinus* species in the world (Wingfield *et al.* 2008).

Fusarium circinatum, a necrotrophic fungus, included in the EPPO (European Plant Protection Organization) list among the quarantine pathogens, has been reported on over 60 species of *Pinus* and on *Pseudotsuga menziesii* (Hodge & Vorak 2000; Wingfield *et al.* 2008); *P. radiata* appears to be one of the most susceptible species (Gordon *et al.* 1998; Hodge & Vorak 2000).

The pathogen affects pines of all ages in any season of the year (Wingfield *et al.* 2008). It was first reported in the southeastern United States in 1946, on *Pinus virginiana* (Hepting & Roth 1946) and later in several countries including Haiti, Japan, South Africa, South Korea, Mexico, Chile, Spain, Italy, Uruguay, Portugal and Colombia (Viljoen *et al.* 1994, Lee *et al.* 2000). The disease originates from lesions that allow the penetration and development of *F. circinatum* (Thoungchaleun *et al.* 2008).

In nurseries, the symptoms consist of dying off of the seedlings (damping off), while in plantations the most common symptoms are the drying of the branches and cankers on the stems, with the formation of abundant resin (Viljoen *et al.* 1994; Gordon *et al.* 2001; Wingfield *et al.* 2008), which lead to the death of the apex of the plant, with consequent arrest of growth and reduction of the volume of the crown and of the stem consequent to these malformations.

Another group of important diseases of *Pinus* species are those caused by *Phytophthora* spp. The *Phytophthora* genus includes over 180 recognized species (Abad, 2014; Ruano-Rosa *et al.* 2018) including several very devastating phytopathogenic species (Brasier, 1999; Jung *et al.* 2018). *Phytophthora* spp. are able to cause leaf diseases, collar rot, stem cankers, fruit rot (Erwin & Ribeiro 1996) and in particular root rot which are among the most common symptoms (Migliorini *et al.* 2014), both in nurseries than in forests (Marcais *et al.* 2011, Jung *et al.* 2016).

Pinus seedlings, especially Scots pine, are susceptible to *P. cactorum*, *P. cambivora*, *P. plurivora* and *P. cinnamomi* (Chavarriaga *et al.* 2007; Jung *et al.* 2009; Jung *et al.* 2016; Tkaczyk *et al.* 2016; Cleary *et al.* 2017). Infected plants show growth reduction, chlorosis and decay caused by root rot and / or collar rot (Jung *et al.* 2018). The *Phytophthora* genus includes then pathogens with the greatest impact in the pine forests of Europe, and are believed to be among the main pathogens that occur together with *F. circinatum*. Infection by

these organisms appears to be facilitated by climatic factors such as high humidity, which is known to favor *Fusarium* spp.; therefore, interaction, including synergy, between these species should not be excluded (Elvira-Recuenco *et al.* 2020).

During the attack by the pathogens in the plant, different metabolic defense pathways are activated. These defense mechanisms are governed by a series of genes, individually or synergistically involved in the resistance traits of plants (Eyles *et al.* 2010).

Among the conifers, most commonly induced against pathogens are hypersensitive responses, early lignification of fibers and the production of phenolic compounds, terpenoids and alkaloids. These responses are produced after the recognition of a pathogen signal that triggers different signal transduction mechanisms which in turn stimulate secondary metabolic pathways for the production of defense compounds, which are the result of the expression of different genes (Franceschi *et al.* 2005; Eyles *et al.* 2010).

Previous studies have identified several genes associated with pathogen response to infections in coniferous species (Morse *et al.* 2004; Quesada *et al.* 2009). These include genes encoding for PR proteins, which have been classified as the largest group of defense-related proteins in plants as well as genes associated to secondary metabolites, such as ones related to the phenylalanine metabolic pathway, which are synthesized to generate compounds with a broad spectrum of antifungal properties (van Loon *et al.* 2006; Veluthakkal & Dasgupta 2010). In order to understand these defense mechanisms, it is necessary to evaluate the expression levels of the target genes that respond to the plant-pathogen interaction (Donoso *et al.* 2015).

In the *Pinus radiata-Fusarium circinatum-Phytophthora* spp. model system, this study investigated i. the phenotypic response of pine to the infective process and ii. the relative expression levels of genes of plant encoding for pathogenesis-related proteins and antifungal secondary metabolites.

2.2.2 Materials and Methods

2.2.2.1 Plant material

Ten-month-old *Pinus radiata* seedlings (Spanish provenance) were used for the experiment. Plants had an average height of 19.84 ± 1.8 cm and average diameter at the soil level of 0.34 ± 0.03 cm.

Seedlings were maintained in a greenhouse at 20 – 22°C and a photoperiod of 16 h light / 8 h darkness and inoculated after two weeks of acclimation.

2.2.2.2 Fungal inoculum and inoculation methods

One isolate of *F. circinatum* from *Pinus radiata* (Fc 072) sourced in Spain and two isolates of *Phytophthora*, *P. cambivora* from *Quercus ilex* (PH 14.012) recovered in Spain forest and *P. parvispora* from *Salix pedicellata* recovered in a Sicilian riparian forest were used for plant inoculation.

Spore suspension (*F. circinatum*-microconidia and *Phytophthora* species-zoospores) were used for inoculum. *Fusarium circinatum* was grown on potato dextrose agar (PDA) at 25°C in the dark until the mycelium covered at least 90% of the Petri dish. Three to five pieces of mycelium (5 mm diameter) were grown under agitation on potato dextrose broth (PDB) for at least 24 h. Obtained microconidia were then rinsed and suspended in

sterile distilled water. Finally, the spore concentration was measured with a hemocytometer and adjusted to 10^6 spores/ml.

Phytophthora cambivora and *P. parvispora* were first grown on V8 juice agar (V8A) at 20° C in the dark for seven days. For zoospore production, plug of agar and mycelium were taken from the colonies, flooded with sterile distilled water and incubated for 2-3 days at 20-22 °C with 16/8 h photoperiod. Sporangia formation was monitored during this incubation period and once sufficient mature sporangia were observed, the plates were cold shocked by incubation at 4°C for 45 min after which they were removed and left at room temperature for one hour to stimulate zoospore release. The zoospore suspension was removed from the plates, pooled together and used for inoculation.

Zoospore concentration was determined by using a hemocytometer and standardized to 10^6 zoospores/ml.

The experimental scheme consisted of the following treatments: i. wounded plants control (C); ii. plants inoculated with *F. circinatum* (FC); iii. plants inoculated with *P. cambivora* (PC); iv. plants inoculated with *P. parvispora* (PP); v. plants inoculated with *F. circinatum* * *P. cambivora* (FC x PC); vi. plants inoculated with *F. circinatum* * *P. parvispora* (FC x PP).

For the inoculation, stem surface of plants from all treatments was wounded by two cuts at the same height, in front and behind, by using a sterile scalpel; 10^6 spores (*F. circinatum*-microconidia and *Phytophthora* species-zoospores) were then applied at one of the two wounding point (the other wound received sterile distilled water in plants from treatments ii., iii. and iv., while each singular wound received singularly one of the two pathogens in plants from treatments v. and vi.). Wounds were then sealed with Parafilm® to prevent desiccation and contamination. Plants from control group were equally wounded and received an equal volume of sterile distilled water. After inoculation controls and inoculated plants were kept in separate climate chambers under controlled conditions at a temperature of 20 ± 2 °C, 40-50% relative humidity, a photoperiod of 16/8 h light/dark for 60 days and irrigated 30 min per day.

2.2.2.3 Evaluation of visual symptoms and internal necrosis length

The typical disease symptoms of tip dieback, needle wilting and browning and resin formation were evaluated and monitored one time per week; the seedlings were visually scored for disease symptoms following the empirical scale proposed by Correll *et al.* (1991): 0 = healthy plant or no symptoms; 1 = resin and/or necrosis at the point of inoculation and healthy foliage; 2 = resin and/or necrosis beyond the point of inoculation; 3 = accentuated wilting and appreciable dieback or damping off and 4 = dead plant. The above-mentioned evaluation was carried out at three time points (i.e. 7, 30, and 60 days post-inoculation – dpi). To confirm Koch's postulate, stem cuttings were plated onto PDA or V8A and incubated at 20-22°C for 7 days.

The internal stem lesion length (mm) was also measured in 4 cm longitudinal stem cuts of three biological replicates per treatment, when more of 50% of the inoculated plants expressed disease symptoms (14 dpi). Images of the necrosis were obtained using a zoom stereomicroscope.

Data were analyzed by using one-way ANOVA followed by Tukey's HSD test (Honestly Significant Difference) as a post-hoc test (R software). Differences at $P \leq 0.05$ were considered significant.

2.2.2.4 Sample collection, RNA extraction and cDNA synthesis

Stem fragments of approximately 4 cm from the inoculation point were sampled for RNA extraction at 4 and 11 dpi, using five seedlings per treatment at each of the evaluated time points.

Samples were immediately frozen in liquid nitrogen and then stored at -80°C until used for gene expression analyses.

Total RNA was extracted by using Spectrum™ Plant Total RNA Kit (Sigma-Aldrich) and quantified using a Qubit 4 Fluorometer (Invitrogen). Integrity of RNA samples was visualized by loading 5 µl of RNA on a 1.5% agarose gel stained with SYBR Safe.

cDNA was synthesized using Revert Aid Reverse Transcriptase (Thermo Fisher Scientific), random hexamers, and 1 µg of RNA in 20 µl reactions following the manufacturers specifications.

2.2.2.5 Selection of primers and housekeeping genes

The primers used to amplify the four candidate genes, namely PR3, PR5, PAL and PDC (Donoso *et al.* 2015, Amaral *et al.* 2019) and three housekeeping genes, namely actin (ACT), β-tubulin (TUB) and ubiquitin (UBQ) are shown in **Table 1**. Primers were selected on the basis of previous studies (Donoso *et al.* 2015, Amaral *et al.* 2019).

Housekeeping genes stability was analyzed using the geNORM v. 3.4 software (Vandesompele *et al.* 2002) and the comparative delta -Ct method (Silver *et al.* 2006). For the later, the reference gene analysis tool refFinder (<http://www.leonxie.com/referencegene.php>) was used. After the analysis, the one most stable reference gene was used for the normalization of the gene expression data.

2.2.2.6 Relative expression of candidate genes

Amplifications were performed by using the iCycler iQ™ Real-Time PCR Detection System (Biorad). Reactions were performed in a total volume of 20 µl by mixing 10 ng of cDNA with 1 µl of 10 µM of each primer and 10 µl of PowerUp™ SYBR™ Green Master Mix (2X) (Applied Biosystems). qRT-PCR experiments were carried out in triplicate. The thermo-cycling conditions were 2 min at 50° C (UDG activation), 2 min at 95° C (Dual-Lock™ DNA polymerase) followed by 40 cycles of two steps: 95 °C for 15 s (Denaturation) and 65 °C (annealing/extension) for 1 min. The quantification of gene expression was carried out by using the $2^{-\Delta\Delta Ct}$ method (Livak and Schmittgen, 2001) where $\Delta\Delta Ct = (Ct \text{ of target gene} - Ct \text{ of reference gene})_{\text{sample}} - (Ct \text{ of target gene} - Ct \text{ of reference gene})_{\text{calibrator}}$ and Ct is the threshold cycle of each transcript, defined as the point at which the amount of amplified target reaches a fixed threshold above the background fluorescence and using housekeeping genes for data normalization as described by Vandesompele *et al.*(2002).

Data on gene expression were analyzed by using oneway ANOVA followed by Dunnett's multiple comparisons test by using R software. Differences at $P \leq 0.05$ were considered significant.

Table 1. Primer sequences used for the housekeeping and candidate genes studied in the *Pinus radiata-Fusarium circinatum-Phytophthora* spp. model system.

Gene	Primer sequence	GenBank ID	Functions/Putative functions	Reference
Chitinase (PR3)	F: TGGCAACACGGACGCCATT R: ACCGGCGTCGTTTCTGTGCTT	HM219849.1	Hydrolyzation of chitin.	Amaral et al. 2019; Donoso et al. 2015; Collinge et al. 1993; Mauch et al. 1988
Thaumatin-like protein (PR5)	F: AGGAGCGCGTGTGATGCGTT R: TGAAAGTGCTGGTGGCGTCGT	JQ015859.1	Involved in cell wall damage and formation of pores on the plasma membrane.	Amaral et al. 2019; Donoso et al. 2015; Grenier et al. 1999; Roberts & Selitrennikoff, 1990
Phenylalanine ammonia lyase (PAL)	F: TGCTGGCCACTGTGAAGCAGA R: TCGCAGAAACGGCCTGGCAA	AY641535.1	Lignin and phenolic accumulation in plants. Cinamic acid synthesis	Amaral et al. 2019; Donoso et al. 2015; Campbell & Ellis, 1992; Liang et al. 1989
Pyruvate decarboxylase (PDC)	F: CCCGCAAACAATGACGTGGGGT R: TCGGAGCAGATGGTCCAGCA	JQ264496.1	Involved in aerobic fermentation.	Amaral et al. 2019; Mithran et al. 2013; Kürsteiner & Kuhlemeier, 2003
Actin (ACT)	F: TGGACCTTGCTGGGCGTGATCT R: ACAATCTCGCGCTCTGCGGT	GQ339779.1	Major component of cytoskeleton microfilaments.	Amaral et al. 2019; Donoso et al. 2015; Choi et al. 1991
β -Tubulin (TUB)	F: AAGGGGGTCAGTGTGGCAACCA R: ACAGCCC CGGAACAAACCT	KM496536.1	Structural units of the cytoskeleton microtubules	Amaral et al. 2019; Donoso et al. 2015; Jeong et al. 2006
Ubiquitin (UBQ)	F: AGCCCTTATGCCGAGGGGTTT R: AGTGCGGGACTCCACTGTTCTT	AF461687.1	Participates in protein recognition by the proteasome	Amaral et al. 2019; Donoso et al. 2015; Brunner et al. 2004

2.2.3 Results

2.2.3.1 Differences in disease symptoms progression

Results from the *in planta* inoculation trial evidenced that the most common symptom in inoculated plants from all the treatments was represented by the folding of the apex of the seedling (damping-off); needle wiltings as well as restricted resin exudations and necrotic responses in the cutting zones were also common symptoms observed at advanced stages of disease progression. Non-inoculated control plants remained healthy for all time course of the experiment.

The first symptom was the damping-off and appeared in plants from all treatments 7 dpi; at this time point, excluding seedlings inoculated with *F. circinatum* (FC) which showed the weakest symptoms of decay, plants from all other treatments appeared markedly equally symptomatic (**Fig. 1**).

Thirty days post inoculation, seedlings from all the treatments were in an advanced state of decay. The additional symptom was the marked wilting and browning of needles, which suggested the certain death of the plant (which occurred 60 dpi in all inoculated plants).

The temporal progression of symptoms severity is summarized in **Figure 1**.

Results from the analysis of the measures of the internal stem lesion evidenced that seedlings from all the inoculated treatments showed a marked necrotic area over the non-inoculated control, which did not show any symptom (**Fig. 2B**). The mean values of the internal stems lesions from different treatments have been determined at 14 dpi, namely at the time when more of the 50% of the inoculated plants of each treatments expressed disease symptoms. The statistical differences observed in seedlings from inoculated treatments (**Fig. 2A**) were in accordance with the visual symptoms evaluated 7 dpi (**Fig. 1**).

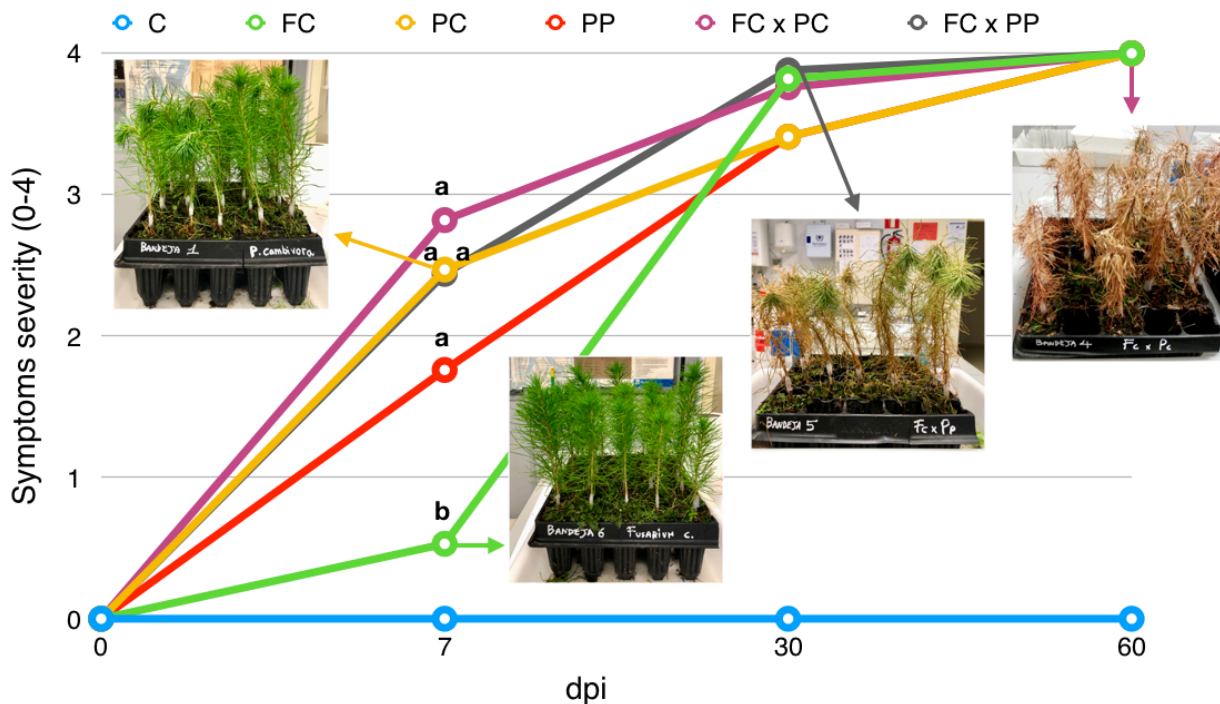


Figure 1 Temporal progression of symptoms severity (mean values) in *Pinus radiata* seedlings non-inoculated (C) or inoculated with *Fusarium circinatum* (FC), *P. cambivora* (PC), *P. parvispora* (PP), *F. circinatum** *P. cambivora* (FC x PC) and *F. circinatum** *P. parvispora* (FC x PP). Images representative of the symptoms at each time point are included. Days post-infection (d.p.i.). At each time point, values sharing same letters are not statistically different according to Tukey's honestly significant difference (HSD) test ($P \leq 0.05$).

2.2.3.2 Housekeeping gene selection

To obtain accurate results, the expression level of the target genes must be normalized using internal control genes, known as reference or housekeeping genes (Long *et al.*, 2010). The expression level of these genes is expected to be relatively stable between different samples and environmental conditions. To date, no housekeeping genes have been validated for gene expression studies on conifers infected by *F. circinatum* or similar necrotrophic fungi (Donoso *et al.*, 2015). The stability of the three housekeeping genes was assessed using the comparative delta Ct method and the software geNorm. Both methods showed that UBQ were the most stable housekeeping genes, while ACT and TUB had the highest delta Ct values and the highest M values after analysis with the geNorm software. The present study reveals that UBQ were the most stable housekeeping genes for *P. radiata* under *F. circinatum* or similar necrotrophic fungi infection, which coincides with the results of other studies of validation of reference genes on plants under biotic and abiotic stress conditions (Brunner *et al.*, 2004; Jarosova & Kundu, 2010; Donoso *et al.*, 2015; Amaral *et al.*, 2019).

In this study UBQ is suitable for normalizing qRT-PCR results, the use of this gene may provide more accurate and reliable results and could also be suitable for gene expression studies on other conifer species affected by necrotrophic fungi, however, a previous validation is always suggested. UBQ like housekeeping gene was used for the normalization of the subsequent qRT-PCR results.

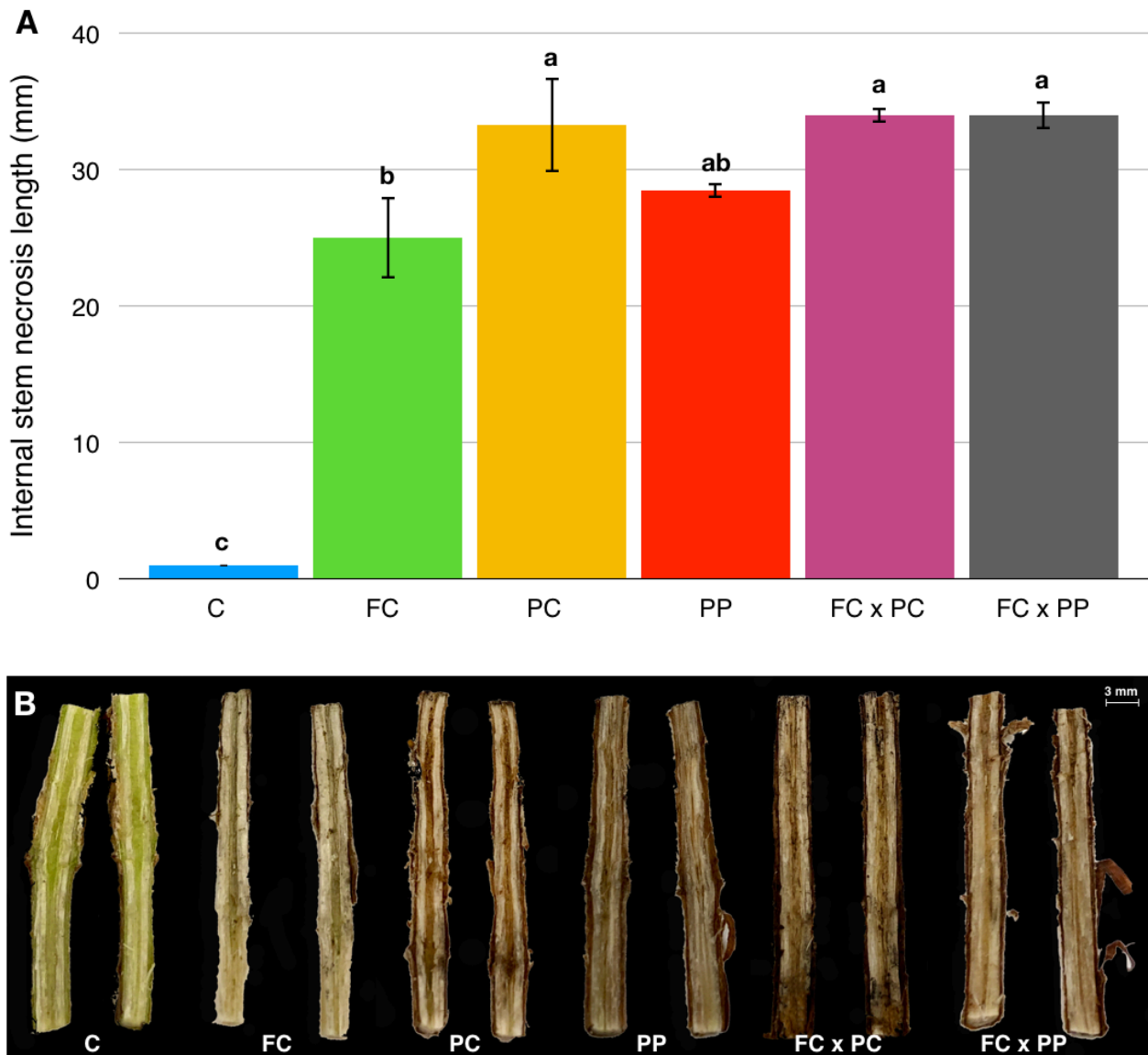


Figure 2 (A) Internal stem necrosis length (mean value) in *Pinus radiata* seedlings non-inoculated (C) or inoculated with *Fusarium circinatum* (FC), *P. cambivora* (PC), *P. parvispora* (PP), *F. circinatum** *P. cambivora* (FC x PC) and *F. circinatum** *P. parvispora* (FC x PP) when more of 50% of the inoculated plants of each treatments expressed disease symptoms (14 dpi). Data are presented as mean \pm SE of three biological replicates per treatment. Values sharing same letters are not statistically different according to Tukey's honestly significant difference (HSD) test ($P \leq 0.05$). (B) Stem internal necrosis from representative samples of *Pinus radiata* seedlings non-inoculated (C) or inoculated with *Fusarium circinatum* (FC), *P. cambivora* (PC), *P. parvispora* (PP), *F. circinatum** *P. cambivora* (FC x PC) and *F. circinatum** *P. parvispora* (FC x PP) observed using a zoom stereomicroscope when more of 50% of the inoculated plants of each treatments expressed disease symptoms (14 dpi).

2.2.3.3 Differential expression of candidate genes

The analysis of the transcriptomic profile of the studied candidate genes (PR3, PR5, PAL and PDC) evidenced different responses depending on both the treatment and the time point of measure.

With reference to the PR3-encoding gene, it resulted up-regulated in all the treatments at both time points of measure, with significant differences over the non-inoculated control in the treatment with *P. cambivora* (PC) (4 dpi) and *F. circinatum* (FC) (11 dpi) (**Fig. 3A**).

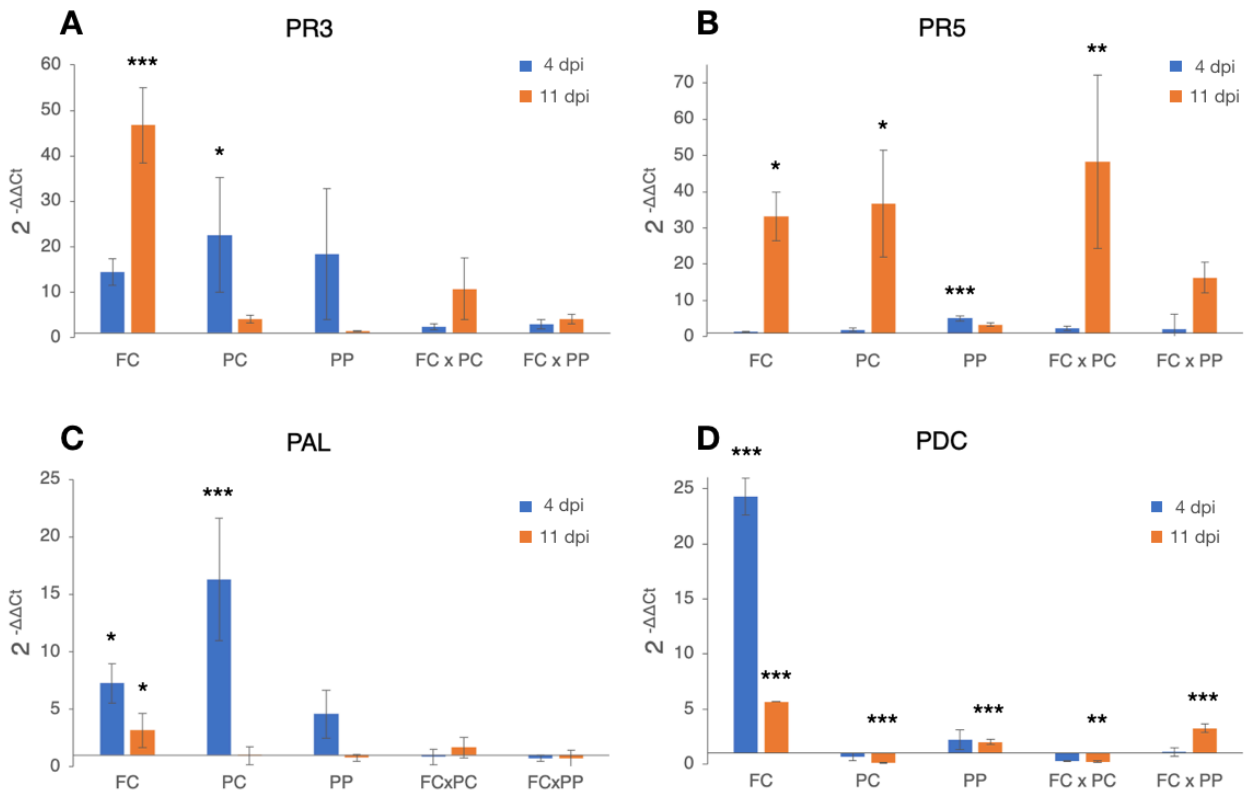


Figure 3 Differences in the expression levels of PR3- (A), PR5- (B), PAL- (C) and PDC- (D) -encoding genes in *Pinus radiata* seedlings at 4 (blue bars) and 11 (orange bars) days-post-inoculation (dpi) with *Fusarium circinatum* (FC), *P. cambivora* (PC), *P. parvispora* (PP), *F. circinatum** *P. cambivora* (FC x PC) and *F. circinatum** *P. parvispora* (FC x PP). Columns with asterisks are statistically different according to Dunnett's test (*P < 0.05, **P < 0.01, ***P < 0.001), compared to their calibrator (i.e. wounded and non-inoculated control seedlings).

As for PR3, the PR5-encoding gene had a generalized up-regulation, although it was markedly significant mainly at 11 dpi. In particular, 4 dpi a weak significant up-regulation was observed only in seedlings inoculated with *P. parvispora*, while at 11 dpi a marked up-regulation occurred in *F. circinatum*- (FC) and *P. cambivora*- (PC) -inoculated plants as well as in seedlings from their interaction system (FC x PC) (**Fig. 3B**).

The PAL-encoding gene resulted globally up-regulated 4 dpi only in treatments that received singularly the test pathogens (FC, PC, PP), although up-regulation was significant only in seedlings inoculated with *F. circinatum* (FC) and *P. cambivora* (PC). The only treatment significantly up-regulated at 11 dpi was FC (**Fig. 3C**).

Finally, the PDC-encoding gene was significantly modulated in all the treatments, although with opposite trends. The strongest up-regulations were observed in seedlings from treatments with the only *F. circinatum* (FC) at both time points (4-11 dpi). The gene was also up-regulated at both time points in the treatment with *P. parvispora* (PP), although the modulation was significant only at 11 dpi. Generalized significant down-

regulations were recorded in seedlings from treatments with the only *P. cambivora* (PC) and in its interaction system with *F. circinatum* (FC x PC). Finally, in the interaction system *F. circinatum* * *P. parvispora* (FC x PP) the gene was significantly up-regulated exclusively at 11 dpi (**Fig. 3D**).

2.2.4 Discussion

This study represents an additional contribute to the understanding of the complex of interactions plant-microorganisms which nowadays represent one of the main topics of modern Plant Pathology (La Spada et al., 2020). Within this framework, several studies started to investigate the mechanisms with whom microorganisms interact each other and affect the phenotypic and genetic-mediated response of plants as a consequence of their biotrophic activity (Tucci et al., 2011; Dalio et al., 2018; La Spada et al. 2020). In order to try to elucidate how the simultaneous action of different plant pathogens can affect the progression of a specific plant disease mainly attributed to a single pathogen, this study approached the plant-microorganism interaction within the framework of the “Pine pitch canker” by *Fusarium circinatum* under the additional influence of *Phytophthora* spp. Synergisms between microbial pathogens in plant disease complexes is an increasingly growing trend in Plant Pathology, with a special focus to fungi-fungi interactions (Lamichhane & Venturi, 2015). For example, the young grapevine decline disease is present across many regions worldwide, and is caused by the following fungal pathogens when present alone: *Ilyonectris* sp., *Phaeoconiella chlamydospora*, *Togninia* sp., and *Botryosphaeriaceae* sp. (Mugnai et al., 1999; Gramaje and Armengol, 2011). A recent study demonstrated that co-infection of several fungal species belonging to *Botryosphaeriaceae* sp. and *Ilyonectria* sp. results in very severe decline of young grafted grapevines in the field (Whitelaw-Weckert et al., 2013). Similarly, laboratory experiments further confirmed that co-inoculation of *Ilyonectria* and *Botryosphaeriaceae* isolates led to an increased disease severity compared to monoculture inoculations of *Ilyonectria* isolates (Whitelaw-Weckert et al., 2013).

In the present study the experimental approach carried out was aimed to investigate the phenotypic and genetic-mediated response of *Pinus* plants to an infective process due to the simultaneous action of two plant pathogens, namely *F. circinatum* and *Phytophthora cambivora* or *F. circinatum* and *Phytophthora parvispora*. Firstly, the phenotypic plant response to such a kind of infective process have been investigated. The synergic effects in the phenotypic response of a plant to a complex disease process involving *Fusarium* species and other fungal plant pathogens belonging to different genera have been previously reported for the cassava root rot (species involved: *Fusarium* sp. *Botryodiplodia theobromae* and *Armillaria* sp.) (Bandyopadhyay et al., 2006), the gray necrosis of hazelnut (species involved: *Alternaria* sp., *Fusarium* sp., and *Phomopsis* sp.) (Belisario et al., 2004), the root rot of strawberry (species involved: *Pythium* sp., *Fusarium* sp., *Cylindrocarpon* sp., *Rhizoctonia* sp.) (Wing et al., 1994) and the root disease of *Trifolium vesiculosum* (species involved: *Pythium* sp., *Rhizoctonia* sp., and *Fusarium* sp.) (Pemberton et al., 1998). With reference to pine disease involving *F. circinatum* and additional fungal pathogens, considering that the genera *Heterobasidion*, *Armillaria*, and *Phytophthora* include root and butt rot pathogens with the highest impact in pine forests in Europe and considering also that their infections are facilitated by factors such as high humidity (which is

known to favor also *Fusarium* spp.) (Garbelotto et al., 2013), it is expected that these species can co-occur with *F. circinatum*. However, to date the co-occurrence of *F. circinatum* with another fungal pathogen have been clearly recorded just a single time, namely together with *Diplodia sapinea* in wounds made by bark beetles (Bezoz et al., 2014, 2016).

Analyses carried out in the present study investigated for the first time the possible synergic action of *F. circinatum* and *Phytophthora* spp. in the “Pine pitch canker”. Results obtained here showed that the phenotypic response of pine to the simultaneous action of the aforementioned pathogens is manifested by an increasing of the severity of the symptoms at the early stages of the infection, allowing then to speculate that *Phytophthora* spp. can realistically contribute to the aggravation of the disease.

It is well known that a pathogenic infection triggers in plants the activation of a main resistance mechanism, namely the systemic acquired resistance (SAR), which provides long-term resistance throughout the plant to subsequent infection by different pathogens (La Spada et al., 2020). This kind of resistance is correlated with the synthesis of pathogenesis related (PR) proteins, which is mediated by the up-regulation of genes encoding enzymes involved in the biosynthesis of salicylic acid (SA) (Zhang et al., 2010). Plant cellular respiration is also usually stimulated after pathogenic infections (Amaral et al. 2019; Bolton, 2009). In such a kind of oxygen stress condition, it has been observed that plants respond by the synthesis of pyruvate decarboxylase (PDC), which in turn converts the pyruvate into acetaldehyde and CO₂ and then makes possible the production of energy (Bolton, 2009). In order to decrypt how the synergic action of *F. circinatum* and *Phytophthora* spp. affects the plant resistance response, this study described the modulation of the SAR and plant cellular respiration by the analysis of the transcriptomic profile of three genes encoding for pathogenesis-related proteins (namely, PR3, PR5 and PAL) as well as that of the pyruvate decarboxylase- (PDC) -encoding gene. Results obtained here from the interaction systems (namely, *F. circinatum* * *P. cambivora* and *F. circinatum* * *P. parvispora*) showed that, at the early stages of the infection (4 dpi), no one of the studied encoding genes had a significant modulation over the non-inoculated plants, while at 11 dpi significant up-regulations were exclusively reported for PR5 in the treatment *F. circinatum* * *P. cambivora* and PDC in *F. circinatum* * *P. parvispora*. Results from plants inoculated singularly with pathogens, globally evidenced that *F. circinatum* markedly stimulated the up-regulation of all the studied genes mainly at the late stages of infection, while between the two *Phytophthora* spp., only *P. cambivora* seems to stimulate significant up-regulations. This aspect suggests that a real synergic effect as the result of the sum of the effects of the singular pathogens it is not clearly evident. However, this result could be interpreted by considering a different aspect. Assuming that the interaction between the two pathogens mainly determined a competition for the infection site, the observed effect in gene expression could be determined by the delayed beginning of the infective process, which consequently could have led to a supposed delayed plant defensive response. Conversely, in plants inoculated with a single pathogen, the infective process could not have been delayed by the competition for the infective site, determining then a direct plant response. Considering that this is the first study that investigated the pine response to an infective process by the simultaneous attach of *F. circinatum* and *Phytophthora* spp., further researches are necessary to validate this hypothesis.

2.2.5 References

Abad, G.Z. The taxonomy of *Phytophthora*: What is done and what is needed for the correct identification and diagnostics of species in the genus. In Proceedings of the 7th International Union of Forest Research Organizations, IUFRO Working Party 7-02-09 Meeting, *Phytophthora* in Forests and Natural Ecosystems, Esquel, Argentina, 10–14 November 2014

Abdullah, A. S., Moffat, C. S., Lopez-Ruiz, F. J., Gibberd, M. R., Hamblin, J., & Zerihun, A. Host-Multi-Pathogen Warfare: Pathogen Interactions in Co-infected Plants. *Frontiers in plant science*. 2017, 8, 1806. <https://doi.org/10.3389/fpls.2017.01806>

Amaral J., Correia B., António C., Rodrigues A. M., Gómez-Cadenas A., Valledor L., Hancock R. D., Alves A., Pinto G. Pinus Susceptibility to Pitch Canker Triggers Specific Physiological Responses in Symptomatic Plants: An Integrated Approach. *Frontiers in Plant Science*. 2009, 10, 509 doi: 10.3389/fpls.2019.00509

Bandyopadhyay R., Mwangi M., Aigbe S. O., Leslie J. F. *Fusarium* species from the cassava root rot complex in west Africa. *Phytopathology*. (2006) 96 673–676. 10.1094/PHYTO-96-0673

Belisario A., Maccaroni M., Coramusi A., Corazza L., Pryor B. M., Figuli P. (2004). First report of *Alternaria* species groups involved in disease complexes of hazelnut and walnut fruit. *Plant Dis.* (2004) 88 426–426. 10.1094/PDIS.2004.88.4.426A

Bethune JE, Hepting Gh: Pitch Canker Damage to South Florida Slash Pine. Society of American Foresters. (accessed 16.03.15.).

Bezos, D.; Martínez-Álvarez, P.; Diez, J.J.; Fernández, M.M. Association levels between *Pityophthorus pubescens* and *Fusarium circinatum* in pitch canker disease affected plantations in northern Spain. *Entomol. Gen.* 2016, 36, 43–54.

Bezos, D.; Martínez-Álvarez, P.; Fernández-Fernández, M.M.; Diez, J.J. Fungi and insect diversity associated with *Pinus radiata* in pitch-canker-affected stands. *Int. For. Rev.* 2014, 16, 336.

Bolton, M. D. Primary metabolism and plant defense-fuel for the fire. *Mol. Plant Microbe Interact.* 2009, 22, 487–497. doi: 10.1094/MPMI-22-5-0487

Brasier, C.M. *Phytophthora* Pathogens of Trees: Their Rising Profile in Europe; Forestry Commission: Stockport, UK, 1999; p. 30.

Brunner, A.M., Yakovlev, I.A., Strauss, S.H. Validating internal controls for quantitative plant gene expression studies, *BMC Plant Biol.* 4 (2004) 14.

Campbell, M.M., Ellis, B.E. Fungal elicitor-mediated responses in pine cell cultures: III. Purification and Characterization of phenylalanine ammonialyase. *Plant Physiol.* 98 (1) (1992) 62e70.

Chavarriaga, D.; Bodles, W.J.A.; Leifert, C.; Belbahri, L.; Woodward, S. *Phytophthora cinnamomi* and other fine root pathogens in north temperate pine forests. *FEMS Microbiol. Lett.* 2007, 276, 67–74. <http://dx.doi.org/10.1111/j.1574-6968.2007.00914.x>

Choi, J.K., Holtzer, S., Chacko, S.A., Lin, Z.X., Hoffman, R.K., Holtzer, H. Phorbol esters selectively and reversibly inhibit a subset of myofibrillar genes responsible for the ongoing differentiation program of chick skeletal myotubes, *Mol. Cell Biol.* 11 (9) (1991) 4473e4482.

Cleary, M.; Blomquist, M.; Vetukuri, R.R.; Böhlenius, H.; Witzell, J. Susceptibility of common tree species in Sweden to *Phytophthora cambivora*, *P. plurivora* and *P. cactorum*. For. Pathol. 2017, 47, e12329. <http://dx.doi.org/10.1111/efp.12329>

Collinge, D.B., Kragh, K.M., Mikkelsen, J.D., Nielsen K.K., Rasmussen, U., Vad, K. Plant Chitinases, Plant J. 3 (1) (1993) 31e40.

Correll, J.C.; Gordon, T.R.; McCain, A.H.; Fox, J.W.; Koehler, C.S.; Wood, D.L.; Schultz, M.E. Pitch Canker Disease in California—Pathogenicity, Distribution, and Canker Development on Monterey Pine (*Pinus radiata*). Plant Dis. 1991, 75, 676–682. <http://dx.doi.org/10.1094/PD-75-0676>

Dalio, R. J. D., Máximo, H. J., Oliveira, T. S., Azevedo, T., de, M., Felizatti, H. L., et al.. molecular basis of *Citrus sunki* susceptibility and *Poncirus trifoliata* resistance upon *Phytophthora parasitica* attack. Mol. Plant Microb. Interact. (2018) 31, 386–398. doi: 10.1094/MPMI-05-17-0112-FI

Donoso, A., Rodriguez, V., Carrasco, A., Ahumada, R., Sanfuentes, E., and Valenzuela, S. Relative expression of seven candidate genes for pathogen resistance on *Pinus radiata* infected with *Fusarium circinatum*. Physiol. Mol. Plant Pathol. (2015) 92, 42–50. doi: 10.1016/j.pmp.2015.08.009

Elvira-Recuenco, M.; Cacciola, S.O.; Sanz-Ros, A.V.; Garbelotto, M.; Aguayo, J.; Solla, A.; Mullett, M.; Drenkhan, T.; Oskay, F.; Aday Kaya, A.G.; Iturritxa, E.; Cleary, M.; Witzell, J.; Georgieva, M.; Papazova-Anakieva, I.; Chira, D.; Paraschiv, M.; Musolin, D.L.; Selikhovkin, A.V.; Varentsova, E.Y.; Adamčíková, K.; Markovskaja, S.; Mesanza, N.; Davydenko, K.; Capretti, P.; Scanu, B.; Gonthier, P.; Tsopelas, P.; Martín-García, J.; Morales-Rodríguez, C.; Lehtijärvi, A.; Doğmuş Lehtijärvi, H.T.; Oszako, T.; Nowakowska, J.A.; Bragança, H.; Fernández-Fernández, M.; Hantula, J.; Díez, J.J. Potential Interactions between Invasive *Fusarium circinatum* and Other Pine Pathogens in Europe. *Forests* **2020**, *11*, 7.

Erwin, D.C.; Ribeiro, O.K. *Phytophthora Diseases Worldwide*; APS Press: Saint Paul, MN, USA, 1996; p. 562.

Eyles, A., Bonello, P., Ganley, R., Mohammed, C. Induced resistance to pests and pathogens in trees, *New Phytol.* 185 (4) (2010) 893e908.

Franceschi, V.R., Krokene, P., Christiansen, E., Krekling, T. Anatomical and chemical defenses of conifer bark against bark beetles and other pests, *New Phytologist* 167 (2) (2005) 353e375.

Garbelotto, M.; Gonthier, P. Biology, epidemiology and control of *Heterobasidion* species worldwide. *Annu.Rev. Phytopathol.* 2013, 51, 39–59.

Gordon, T.R., Storer, A.J., Wood, D.L. The pitch canker epidemic in California, *Plant Dis.* 85 (2001) 1128e1139.

Gordon, T.R., Wikler, R., Clark, K.R., Okamoto, S.L., Storer, D., Bonello, A.J. Resistance to pitch canker disease, caused by *Fusarium subglutinans* f. sp. pini, in Monterey pine (*Pinus radiata*), *Plant Pathol.* 47 (1998) 706e711.

Grenier, J., Potvin, C., Trudel, J., Asselin, A. Some thaumatin-like proteins hydrolyse polymeric b-1,3-glucans, *Plant J.* 19 (4) (1999) 473e480.

Grison, R., Grezes-Besset, B., Schneider, M., Lucante, N., Olsen, L., Leguay, J.J., Toppan, A. Field tolerance to fungal pathogens of *Brassica napus* constitutively expressing a chimeric chitinase gene, *Nat. Biotechnol.* 14 (5) (1996) 643e646.

Guerrero, P.C., Bustamante, R.O. Can native tree species regenerate in *Pinus radiata* plantations in Chile?: evidence from field and laboratory experiments, *For. Ecol. Manag.* 253 (1e3) (2007) 97e102.

Hepting, G.H., Roth, E.R. Pitch canker, a new disease of southern pines of Forestry, J. For. 44 (1946) 742e744.

Hodge, G., Dvorak, S. Differential responses of Central American and Mexican pine species and *Pinus radiata* to infection by the pitch canker fungus, New For. 19 (2000) 241e258.

Jarosova, J., Kundu, J.K. Validation of reference genes as internal control for studying viral infections in cereals by quantitative real-time RT-PCR, BMC Plant Biol. 10 (2010) 146.

Jeong, Y.-M., Mun, J.-H., Lee, I., Woo, J.C., Hong, C.B., Kim, S.-G. Distinct roles of the first introns on the expression of arabidopsis profilin gene family members, Plant Physiol. 140 (1) (2006) 196e209.

Jung, T.; Burgess, T.I. Re-evaluation of *Phytophthora citricola* isolates from multiple woody hosts in Europe and North America reveals a new species, *Phytophthora plurivora* sp. nov. Persoonia 2009, 22, 95–110. <http://dx.doi.org/10.3767/003158509X442612>

Jung, T.; Orlikowski, L.; Henricot, B.; Abad-Campos, P.; Aday Kaya, A.G.; Aguin Casal, O.; Bakonyi, J.; Cacciola, S.O.; Cech, T.; Chavarriaga, D.; et al. Widespread *Phytophthora* infestations in European nurseries put forest, semi-natural and horticultural ecosystems at high risk of *Phytophthora* diseases. For. Pathol. 2016. <http://dx.doi.org/10.1111/efp.12239>

Jung, T.; Pérez-Sierra, A.; Duran, A.; Horta Jung, M.; Balci, Y.; Scanu, B. Canker and decline diseases caused by soil-and airborne *Phytophthora* species in forests and woodlands. Persoonia 2018, 40, 180–220.

Kürsteiner O, Dupuis I, Kuhlemeier C. The pyruvate decarboxylase1 gene of Arabidopsis is required during anoxia but not other environmental stresses. *Plant Physiol.* 2003;132(2):968-978. doi:10.1104/pp.102.016907

La Spada F., Stracquadiano C., Riolo M., Pane A. and Cacciola S.O. *Trichoderma* Counteracts the Challenge of *Phytophthora nicotianae* Infections on Tomato by Modulating Plant Defense Mechanisms and the Expression of Crinkler, Necrosis-Inducing *Phytophthora* Protein 1, and Cellulose-Binding Elicitor Lectin Pathogenic Effectors. *Front. Plant Sci.* (2020) 11:583539. doi: 10.3389/fpls.2020.583539

Lamichhane JR, Venturi V. Synergisms between microbial pathogens in plant disease complexes: a growing trend. *Front Plant Sci.* 2015;6:385. Published 2015 May 27. doi:10.3389/fpls.2015.00385

Lee, J.K., Lee, S., Yang, S., Lee, Y. First report of pitch canker disease on *Pinus rigida* in Korea, Plant Pathol. 16 (2000) 52e54.

Liang, X., Dron, M., Cramer, C.L., Dixon, R.A., Lamb, C.J. Differential regulation of phenylalanine ammonia-lyase genes during plant development and by environmental cues, J. Biol. 264 (24) (1989) 14486e14492.

Livak, K.J., Schmittgen, T.D. Analysis of relative gene expression data using real-time quantitative PCR and the 2(-Delta Delta C(T)) method, *Methods* 25 (4) (2001) 402e408.

Long, X.Y., Wang, J.R., Ouellet, T., H. Rocheleau, H., Wei, Y.M., Pu, Z.E., Jiang, Q.T., Lan, X.J., Zheng, Y.L. Genome-wide identification and evaluation of novel internal control genes for Q-PCR based transcript normalization in wheat, *Plant Mol. Biol.* 74 (3) (2010) 307e311.

Marçais, B.; Caël, O.; Delatour, C. Interaction between root rot basidiomycetes and *Phytophthora* species on pedunculate oak. *Plant Pathol.* 2011, 60, 296–303. <http://dx.doi.org/10.1111/j.1365-3059.2010.02378.x>

Mauch, F., Mauch-Mani, B., Boller, T. Antifungal Hydrolases in Pea Tissue: II. Inhibition of Fungal Growth by Combinations of Chitinase and Beta-1,3-Glucanase, *Plant Physiol.* 88 (3) (1988) 936e942.

Migliorini, D.; Tondini, E.; Luchi, N.; Ghelardini, L.; Capretti, P.; Santini, A. Detection of *Phytophthora* species on different woody species in nurseries. In Proceedings of the 7th International Union of Forest Research Organizations, IUFRO Working Party 7-02-09 Meeting, Phytophthora in Forests and Natural Ecosystems, Esquel, Argentina, 10–14 November 2014.

Mitchell, R.G., Steenkamp, E.T., Coutinho, T.A., Wingfield, M.J. The pitch canker fungus, *Fusarium circinatum*: implications for South African forestry, South. For. A J. For. Sci. 73 (1) (2011) 1e13.

Mithran, M & Paparelli, Eleonora & Novi, Giacomo & Perata, Pierdomenico & Loreti, Elena. (2013). Analysis of the role of the pyruvate decarboxylase gene family in *Arabidopsis thaliana* under low-oxygen conditions. Plant biology (Stuttgart, Germany). 16. 10.1111/plb.12005.

Morse, A.M., Nelson, C.D., Covert, S.F., Holliday, A.G., Smith, K.E., Davis, J.M. Pine genes regulated by the necrotrophic pathogen *Fusarium circinatum*, TAG Theor. Appl. Genet. Theor. und Angewandte Genet. 109 (5) (2004) 922e932.

Nicot, N., Hausman, J.F., Hoffmann, L., Evers, D. Housekeeping gene selection for real-time RT-PCR normalization in potato during biotic and abiotic stress. J. Exp. Bot. 56 (421) (2005) 2907e2914.

Pemberton I. J., Smith G. R., Philley G. L., Rouquette F. M., Yuen G. Y. (1998). First Report of *Pythium ultimum*, *P. irregulare*, *Rhizoctonia solani* AG 4 and *Fusarium proliferatum* from Arrowleaf Clover (*Trifolium vesiculosum*): a disease complex. *Plant Dis.* 82 128.2.

Quesada, T., Gopal, V., Cumbie, W.P., Eckert, A.J., Wegrzyn, J.L., Neale, D.B., Goldfarb, B., Huber, D.A., Casella, G., Davis, J.M. Association mapping of quantitative disease resistance in a natural population of loblolly pine (*Pinus taeda* L.), *Genetics* 186 (2) (2010) 677e686.

Roberts, W.K., Selitrennikoff C.P. Zeamatin, an antifungal protein from maize with membrane-permeabilizing activity, *J. General Microbiol.* 136 (9) (1990) 1771e1778.

Rogers, D.L. In situ genetic conservation of a naturally restricted and commercially widespread species, *Pinus radiata*, *For. Ecol. Manag.* 197 (1e3) (2004) 311e322.

Ruano-Rosa, D.; Schena, L.; Agosteo, G.E.; Magnano di San Lio, G.; Cacciola, S.O. *Phytophthora oleae* sp. nov., causing fruit rot of olive in southern Italy. *Plant Pathol.* 2018, 67, 1362–1373. <http://dx.doi.org/10.1111/ppa.12836>

Silver, N., Best, S., Jiang, J., Thein, S.L. Selection of housekeeping genes for gene expression studies in human reticulocytes using real-time PCR, *BMC Mol. Biol.* 7 (2006) 33.

Thoungchaleun, V., Kim, K.W., Lee, D.K., Chang, C.S., Park, E.W. Pre-infection behavior of the pitch canker fungus *Fusarium circinatum* on pine stems, *Plant Pathol. J.* 24 (2) (2008) 112e117.

Tkaczyk, M.; Sikora, K.; Nowakowska, J.; Ani'sko, E.; Oszako, T.; Belbahri, L.; Milenkovi'c, I. Four different *Phytophthora* species that are able to infect Scots pine seedlings in laboratory conditions. *Folia For. Pol. Ser.* 2016, 58, 123–130. <http://dx.doi.org/10.1515/ffp-2016-0014>

Tucci, M., Ruocco, M., De Masi, L., De Palma, M., and Lorito, M. The beneficial effect of *Trichoderma* spp. on tomato is modulated by the plant genotype. *Mol. Plant Pathol.* (2011) 12, 341–354. doi: 10.1111/j.1364-3703.2010.00674.x

Turley, R.B. Expression of a phenylcoumaran benzylic ether reductase-like protein in the ovules of *Gossypium hirsutum*, *Biol. Plant.* 52 (2008) 759e762.

van Loon, L.C., Rep, M., Pieterse, C.M. Significance of inducible defense-related proteins in infected plants, *Annu. Rev. Phytopathol.* 44 (1) (2006) 135e162.

Vandesompele, J., De Preter, D., Pattyn, F., Poppe, B., Van Roy, N., De Paepe, A., F. S. Accurate normalization of real-time quantitative RT-PCR data by geometric averaging of multiple internal control genes, *Genome Biol.* 3 (2002) 7.

Veluthakkal, R., Dasgupta, M. Pathogenesis-related genes and proteins in forest tree species, *Trees* 24 (6) (2010) 993e1006.

Viljoen, A., Wingfield, M.J., W.F.O. Marasas, First report of *Fusarium subglutinans* f. sp. pini on seedlings in South Africa, *Plant Dis.* 78 (1994) 309e312.

Wing K. B., Pritts M. P., Wilcox W. F. (1994). Strawberry black root rot: a review. *Adv. Strawberry Res.* 13 13–19.

Wingfield, M.J., Hammerbacher, A., Ganley, R.J., Steenkamp, E.T., Gordon, T.R., Wingfield, B.D., Coutinho, T.A. Pitch canker caused by *Fusarium circinatum* -- a growing threat to pine plantations and forests worldwide, *Australas. Plant Pathol.* 37 (4) (2008) 319e334.

Zhang, Y., Xu, S., Ding, P., Wang, D., Cheng, Y. T., He, J., et al. Control of salicylic acid synthesis and systemic acquired resistance by two members of a plant-specific family of transcription factors. *Proc. Natl. Acad. Sci. U.S.A.* 2010, 107, 18220–18225. doi: 10.1073/pnas.100522 5107

Chapter 3.

Scabby canker caused by *Neofusicoccum batangarum* (*Botryosphaeriaceae*), an emergent disease of *Opuntia ficus-indica* in minor islands around Sicily: identification of the causative agent and characterization of both its phytotoxic metabolites and the genetic variability of its local population



Citation: F. Aloï, S. Giambra, L. Schena, G. Surico, A. Pane, G. Gusella, C. Stracquadiano, S. Burruano, S.O. Cacciola (2020) New insights into scabby canker of *Opuntia ficus-indica*, caused by *Neofusicoccum batangarum*. *Phytopathologia Mediterranea* 59(2): 269-284. DOI: 10.14601/Phyto-11225

Accepted: May 26, 2020

Published: August 31, 2020

Copyright: © 2020 F. Aloï, S. Giambra, L. Schena, G. Surico, A. Pane, G. Gusella, C. Stracquadiano, S. Burruano, S.O. Cacciola. This is an open access, peer-reviewed article published by Firenze University Press (<http://www.fupress.com/pm>) and distributed under the terms of the Creative Commons Attribution License, which permits unrestricted use, distribution, and reproduction in any medium, provided the original author and source are credited.

Data Availability Statement: All relevant data are within the paper and its Supporting Information files.

Competing Interests: The Author(s) declare(s) no conflict of interest.

Editor: Alan J.L. Phillips, University of Lisbon, Portugal.

Research Papers

New insights into scabby canker of *Opuntia ficus-indica*, caused by *Neofusicoccum batangarum*

FRANCESCO ALOI^{1,2,§}, SELENE GIAMBRA^{2,§}, LEONARDO SCHENA³, GIUSEPPE SURICO⁴, ANTONELLA PANE¹, GIORGIO GUSELLA², CLAUDIA STRACQUADANIO^{1,3}, SANTELLA BURRUANO², SANTA OLGA CACCIOLA^{1,*}

¹ Department of Agriculture, Food and Environment (Di3A), University of Catania, Via Santa Sofia 100, I-95123, Catania, Italy

² Department of Agricultural, Food and Forestry Sciences, University of Palermo, Viale delle Scienze 4, 90128 Palermo, Italy

³ Department of Agriculture, University Mediterranea of Reggio Calabria, Feo di Vito, 189122, Reggio Calabria, Italy

⁴ Department of Agrifood production and Environmental Sciences, University of Florence, Ple delle Cascine 18, I-50144, Firenze, Italy

§ These two authors contributed equally to the study

*Corresponding author: olga.cacciola@unict.it

Summary. This study characterizes a fungal disease of cactus pear (*Opuntia ficus-indica*, *Cactaceae*), reported from the minor islands of Sicily. The disease, originally named ‘gummy canker’, was first reported in 1973 from Linosa, a small island of the Pelagian archipelago, south of Sicily. The causal agent was identified as *Dothiorella ribis* (currently *Neofusicoccum ribis*, *Botryosphaeriaceae*). In a recent survey the disease has been found to be widespread in minor islands around Sicily, including Lampedusa, Linosa, Favignana and Ustica. The causal agent was identified in *Botryosphaeriaceae* as *Neofusicoccum batangarum* on the basis of the phylogenetic analysis of the DNA sequences from ITS, *tef1* and *tub2* sequences, and the disease was renamed ‘scabby canker’, which describes the typical symptoms on cactus pear cladodes. In artificial inoculations, *N. batangarum* induced symptoms on cactus pear cladodes identical to those observed in naturally infected plants. The fungus also induced cankers on artificially wound-inoculated stems of several common Mediterranean plants including Aleppo pine (*Pinus halepensis*), almond (*Prunus dulcis*), sweet orange (*Citrus × sinensis*), citrange (*Citrus sinensis* × *Poncirus trifoliata*) and holm oak (*Quercus ilex*), indicating that the pathogen has a wide potential host range. Isolates of *N. batangarum* from cactus pear from several small islands around Sicily were genetically uniform, as inferred from microsatellite primed (MSP)-PCR electrophoretic profiles, suggesting the pathogen populations in these islands have a common origin. A preliminary report of the identity of the causal agent of this disease has been published as the first record of *N. batangarum* in Europe and on cactus pear worldwide.

Keywords. *Botryosphaeriaceae*, cactus pear, phylogenetic analysis, marker genes, host range.

INTRODUCTION

Cactus pear [*Opuntia ficus-indica* (L.) Mill.] is probably native to Mexico (Kiesling and Metzger, 2017), and, after the discovery of America, this plant was introduced into the Mediterranean basin where it is naturalized (Ochoa and Barbera, 2017). In Sicily, cactus pear has become an economically important fruit crop and is a characteristic feature of the landscape. It is also cultivated in the Sardinia, Apulia, Calabria, and Basilicata regions of Italy, and this country is the second cactus pear fruit producer, after Mexico. Sicily produces approx. 90% of cactus pear fruit in the European Union. Cactus pear was introduced into the small islands around Sicily, where it is mainly grown as productive living fences. According to Pretto *et al.* (2012), *O. ficus-indica* was introduced into the small Mediterranean islands in the nineteenth century, as fodder or to fence fields.

Somma *et al.* (1973) reported a severe and unusual disease of *O. ficus-indica* on Linosa, a small island of the Pelagian archipelago, south of Sicily. The disease was named ‘gummy canker’, referring to the typical symptoms on cladodes, and the causal agent was identified as *Dothiorella ribis*, currently *Neofusicoccum ribis* (*Botryosphaeriaceae*). In a subsequent review of cactus pear diseases (Granata *et al.*, 2017), the ‘gummy canker’ described by Somma *et al.* (1973) was equated to a disease named ‘cladode and fruit rot’, and the causal agent was considered to be the cosmopolitan fungus *Lasiodiplodia theobromae* (Pat.) Giff. & Maubl. This fungus is in the same family as *N. ribis*. Recently, ‘gummy canker’ was seen to be destroying the cactus pear stands in Lampedusa, the southernmost island of the Pelagian archipelago, and the disease was also present in other minor islands near Sicily, including Favignana of the Aegadian archipelago, and Ustica, a small island around 67 km northwest of Palermo in the Tyrrhenian sea (Schena *et al.*, 2018). The name of the disease was changed to ‘scabby canker’, as this was more appropriate to describe the characteristic symptoms on cladodes. The fungus responsible for the disease was identified as *Neofusicoccum batangarum* Begoude, Jol. Roux & Slippers (Schena *et al.*, 2018), not previously reported in Europe (Phillips *et al.*, 2013; Dissanayake *et al.*, 2016a). This was the first report of *N. batangarum* on cactus pear, but there are records of this fungus in Brazil as a pathogen of cochineal cactus [*Nopalea cochenillifera* (L.) Salm-Dyck, syn. *Opuntia cochenillifera* (L.) Mill.], which is a close relative of cactus pear (Conforto *et al.*, 2016; Garcete-Gómez *et al.*, 2017).

The disease of cochineal cactus, named ‘cladode brown spot’, has some traits in common with ‘scabby

canker’ occurring in the minor Sicilian islands. However, other fungi, besides *N. batangarum*, are responsible for ‘cladode brown spot’ in Brazil (Conforto *et al.*, 2019; Feijo *et al.*, 2019). *Neofusicoccum batangarum* was first described as an endophyte of Indian almond (*Terminalia catappa* L., *Combretaceae*) in Africa (Begoude *et al.*, 2010, 2011). This fungus was also reported in Florida (USA) as a contaminant of seeds of *Schinus terebinthifolius*, the Brazilian pepper tree (Shetty *et al.*, 2011), and more recently as an aggressive pathogen causing stem cankers of fruit trees in the tropics (Netto *et al.*, 2017; Serrato-Diaz *et al.*, 2020). The distribution of *N. batangarum* includes Africa, Brazil, Puerto Rico and the United States of America (Phillips *et al.*, 2013; Dissanayake *et al.*, 2016a; Conforto *et al.*, 2019; Serrato-Diaz *et al.*, 2020).

The present study aimed to gain insights into the aetiology and epidemiology of ‘scabby canker’ that is destroying cactus pear on the minor islands of Sicily, and also poses a serious threat to cactus pear crops in Sicily. Specific objectives included: i) to determine the present distribution of ‘scabby canker’; ii) to characterize *N. batangarum* isolates from different minor islands of Sicily; and iii) to investigate if the potential host range of this fungus includes other Mediterranean plants which could act as alternative hosts or inoculum reservoirs for this pathogen.

MATERIALS AND METHODS

Fungus isolates, distribution and incidence of the disease

Samples were collected from 2013 to 2018, from the minor islands of Sicily, and a survey was carried out in the islands of Favignana, Lampedusa, Linosa and Ustica (Figure 1) to determine the distribution and the incidence of the disease. Since the extent of these islands is limited, all prickly pear hedges and plantations in each island were examined systematically. Isolations were made from the margins of active cankers developing on cladodes of the host plants. Pieces (5 mm) of diseased tissue were plated onto potato dextrose agar (PDA, Oxoid Limited) supplemented with 1 mg mL⁻¹ of streptomycin, and were incubated at 22°C. Isolates were also obtained as single conidium isolations from conidiomata emerging from cankers of diseased plants, as described by Phillips *et al.* (2013). A total of 26 representative isolates of *N. batangarum* from cactus pear were characterized in this study. Table 1 lists these isolates and their origins. Cultures were routinely grown and maintained on PDA in the collection of the Molecular Plant Pathology laboratory of the Di3A, University of Catania.



Figure 1. Sicily and the minor surrounding islands.

Morphological characteristics and cardinal temperatures for growth of the isolates

The isolates were induced to sporulate by plating them on PDA containing sterilized pine needles (Smith *et al.*, 1996), and incubating at room temperature (approx. 20 to 25°C) under diffused day light or near-UV light, until pycnidia developed. For microscopy, pycnidia and conidia were mounted in sterile distilled water or 100% lactic acid and observed microscopically at $\times 40$ and $\times 100$ magnifications, with an Axioskop (Zeiss) microscope. Images were captured with an AxioCam MRc5 camera (Zeiss), and measurements were made with the software AxioVision. For each isolate, 50 conidia were randomly selected and their lengths, widths and shape were recorded. For pycnidium dimensions, 20 measurements were made. Colony characters and pigment production were noted after 4 to 6 d of growth on PDA or malt extract agar (MEA) at 25°C, in the dark. Colony colours (upper and lower surfaces) were rated according to Rayner (1970).

Four isolates, one from each island, were deposited at Westerdijk Fungal Biodiversity Institute, with strain code numbers CBS 143023, CBS 143024, CBS 143025, and CBS 143026 (Schena *et al.*, 2018).

Radial growth rate and cardinal temperatures for radial growth were determined by growing the isolates on PDA in Petri dishes (9 cm diam.), and incubating at 5, 10, 15, 20, 25, 30 35°C, in the dark. Means of radial growth at the different temperatures were adjusted to a regression curve using Statgraphics Plus 5.1 software (Manugistics Inc.), and the best polynomial model was chosen based on parameter significance ($P < 0.05$) and coefficient of determination (R^2) to estimate the optimum growth temperature for each isolate. Four replicates of each isolate were evaluated and each experiment was repeated twice.

Amplification and sequencing of target genes

Genomic DNA was isolated from 1-week-old cultures grown on PDA at 25°C in the dark using the procedure of Schena and Cooke (2006). The internal transcribed spacer (ITS) region of the ribosomal DNA was amplified and sequenced with primers ITS5/ITS4 (White *et al.* 1990), part of the translation elongation factor 1 alpha gene (*tef1*) was sequenced and amplified with primers EF1-728F/EF1-986R (Carbone and Kohn, 1999), and the β -tubulin gene (*tub2*) was sequenced and amplified with Bt2a and Bt2b (Glass and Donaldson, 1995).

Amplified products with both forward and reverse primers were sequenced by MacroGen Europe. CHROMASPRO v. 1.5 (<http://www.technelysium.com.au/>) was used to evaluate reliability of sequences and to create consensus sequences. Unreliable sequences were re-sequenced.

Molecular identification and phylogenetic analyses

The preliminary identification of isolates and their association to *N. batangarum* were carried by BLAST analyses. For the accurate identification, sequences of ITS, *tef1* and *tub2* loci from the isolates obtained in the present study were phylogenetically analyzed along with validated sequences representative of *N. batangarum* and closely related species as defined by comprehensive phylogenetic studies (Slippers *et al.*, 2013; Lopes *et al.*, 2017; Yang *et al.*, 2017). Two additional isolates of *N. batangarum* for which ITS, *tef1* and *tub2* sequences were available in GenBank were included in the analysis. Table 2 lists the analyzed isolates. For all isolates, ITS, *tef1* and *tub2* sequences were trimmed to a common length and concatenated using the Sequence Matrix software (Vaidya *et al.*, 2011). Concatenated sequences were aligned with MUSCLE (Edgar, 2004) as implemented in Mega Version 7.0 (Kumar *et al.*, 2016), and edited manually for check-

Table 1. Identity of the *Neofusicoccum batangarum* isolates studied, and GenBank accession numbers, for isolates recovered from the small islands of Sicily.

Isolate	Species	Island origin	ITS	β -tubulin	EF1- α
FIF G	<i>N. batangarum</i>	Favignana	MF414731	MF414750	MF414769
FIF A	<i>N. batangarum</i>	Favignana	MF414732	MF414751	MF414770
FIF D	<i>N. batangarum</i>	Favignana	MF414730	MF414749	MF414768
FIF F1	<i>N. batangarum</i>	Favignana	MF414733	MF414752	MF414771
FIF E	<i>N. batangarum</i>	Favignana	MF414734	MF414753	MF414772
FIF F	<i>N. batangarum</i>	Favignana	MF414735	MF414754	MF414773
FIF I	<i>N. batangarum</i>	Favignana	MF414736	MF414755	MF414774
FIF H	<i>N. batangarum</i>	Favignana	MF414737	MF414756	MF414775
FILI F1	<i>N. batangarum</i>	Linosa	MF414747	MF414766	MF414785
OB43	<i>N. batangarum</i>	Linosa	MG609040	MG609057	MG609074
OB44	<i>N. batangarum</i>	Linosa	MG609041	MG609058	MG609075
OB46	<i>N. batangarum</i>	Linosa	MG609043	MG609060	MG609077
FIU 1	<i>N. batangarum</i>	Ustica	MF414739	MF414758	MF414777
FIU 1B	<i>N. batangarum</i>	Ustica	MF414738	MF414757	MF414776
FIU 2	<i>N. batangarum</i>	Ustica	MF414740	MF414759	MF414778
FIU 3	<i>N. batangarum</i>	Ustica	MF414741	MF414760	MF414779
FIU 3A	<i>N. batangarum</i>	Ustica	MF414742	MF414761	MF414780
FIU 3B	<i>N. batangarum</i>	Ustica	MF414743	MF414762	MF414781
FIU 4	<i>N. batangarum</i>	Ustica	MF414744	MF414763	MF414782
FIU 5	<i>N. batangarum</i>	Ustica	MF414745	MF414764	MF414783
FIU 6	<i>N. batangarum</i>	Ustica	MF414746	MF414765	MF414784
FILA 4	<i>N. batangarum</i>	Lampedusa	MF414748	MF414767	MF414786
OP5	<i>N. batangarum</i>	Lampedusa	MG609050	MG609067	MG609084
OP6	<i>N. batangarum</i>	Lampedusa	MG609051	MG609068	MG609085
OP9	<i>N. batangarum</i>	Lampedusa	MG609052	MG609069	MG609086
OB47	<i>N. batangarum</i>	Lampedusa	MG609053	MG609070	MG609087

ing indels and single nucleotide polymorphisms. Phylogenetic analyses were performed in Mega with the maximum likelihood method using the Tamura–Nei model and 1000 bootstrap replications (Tamura and Nei, 1993; Tamura *et al.*, 2013).

Analysis of genetic variability of isolates

Six representative isolates (FIU 1B, OP6, FIF D, FILA 4, OB43, and FILI F1) collected from four different islands were characterized according to their microsatellite-primed PCR (MSP-PCR) profiles using primer M13 (Meyer *et al.*, 1993; Santos and Phillips, 2009), (CAG)5 (Freeman and Shabi, 1996), and (GGA)5 (Uddin *et al.*, 1997). Each amplification was carried out in a total volume of 25 μ L, containing 1 μ L (50 ng) of fungal DNA, 1 μ M of primer, 2 mM [(primer (CAG)5 and (GGA)5) or 4 mM (primer M13) of MgCl₂ and 1U of GoTaq DNA Polymerase (Promega Corporation). Reactions were incubated for 2 min at 95°C, followed by 35 cycles of 30s at

95°C, 30 s at 49°C [primers (GGA)5 and M13] or 52°C [primer CAG)5] and 1 min at 72°C. All reactions ended with a final extension of 5 min at 72°C. PCR profiles were visualized on 2% agarose electrophoresis gels (Merck) in 1 \times TBE buffer stained with SYBR Safe DNA Gel Stain (Thermo Fisher Scientific).

Pathogenicity tests

Four *N. batangarum* isolates obtained from cactus pear cankers (isolates FIF D, FIU 1B, OP6 and OB43 from, respectively, Favignana, Ustica, Lampedusa and Linosa) were used in pathogenicity tests on cactus pear plants. These isolates were used to inoculate mature cladodes (cladodes of the previous year) and the stems of field-grown cactus pear plants (three plants per isolate and two cladodes per plant). On each cladode, two holes (5 mm diam.) were made 20 cm apart with a cork-borer, while only one hole was made on the stem. An agar plug from a 5-d-old colony grow-

Table 2. GenBank accession numbers of the *Neofusicoccum* spp. isolates of different country and host origins used as references in phylogenetic analyses

Species	Isolate	Country	Host	Source	GenBank accession number		
					ITS	tefl	β -tubulin
<i>N. algeriense</i>	CAA322	Portugal	<i>Malus domestica</i>	Lopes <i>et al.</i> , 2017	KX505906	KX505894	KX505916
<i>N. algeriense</i>	CBS137504	Algeria	<i>Vitis vinifera</i>	Lopes <i>et al.</i> , 2017	KJ657702	KX505893	KX505915
<i>N. batangarum</i>	CBS124922	Cameroon	<i>Terminalia catappa</i>	Yang <i>et al.</i> , 2017	FJ900606	FJ900652	FJ900633
<i>N. batangarum</i>	CBS127348	USA: Florida	<i>Schinus terebinthifolius</i>	Yang <i>et al.</i> , 2017	HM357636	KX464674	KX464952
<i>N. batangarum</i>	CMM4553	Brasil	<i>Anacardium</i> sp.	Unpublished	KI728917	KI728921	KI728913
<i>N. batangarum</i>	CBS124924 (ex-type)	Cameroon	<i>Terminalia catappa</i>	Lopes <i>et al.</i> , 2016	FJ900607	FJ900653	FJ900634
<i>N. batangarum</i>	CBS124923	Cameroon	<i>Terminalia catappa</i>	Lopes <i>et al.</i> , 2016	FJ900608	FJ900654	FJ900635
<i>N. brasiliense</i>	CMM1285	Brazil	<i>Mangifera indica</i>	Lopes <i>et al.</i> , 2016	JX513628	JX513608	KC794030
<i>N. brasiliense</i>	CMM1338	Brazil	<i>Mangifera indica</i>	Lopes <i>et al.</i> , 2016	JX513630	JX513610	KC794031
<i>N. cordaticola</i>	CBS123634	South Africa	<i>Syzygium cordatum</i>	Lopes <i>et al.</i> , 2016	EU821898	EU821868	EU821838
<i>N. cordaticola</i>	CBS123635	South Africa	<i>Syzygium cordatum</i>	Lopes <i>et al.</i> , 2016	EU821903	EU821873	EU821843
<i>N. kwambonambiense</i>	CBS123639	South Africa	<i>Syzygium cordatum</i>	Lopes <i>et al.</i> , 2016	EU821900	EU821870	EU821840
<i>N. kwambonambiense</i>	CBS123641	South Africa	<i>Syzygium cordatum</i>	Lopes <i>et al.</i> , 2016	EU821919	EU821889	EU821859
<i>N. macroclavatum</i>	CBS118223	Australia	<i>Eucalyptus globulus</i>	Lopes <i>et al.</i> , 2016	DQ093196	DQ093217	DQ093206
<i>N. macroclavatum</i>	WAC12445	Australia	<i>Eucalyptus globulus</i>	Lopes <i>et al.</i> , 2016	DQ093197	DQ093218	DQ093208
<i>N. occulatum</i>	CBS128008	Australia	<i>Eucalyptus grandis hybrid</i>	Lopes <i>et al.</i> , 2016	EU301030	EU339509	EU339472
<i>N. occulatum</i>	MUCC286	Australia	<i>Eucalyptus pellita</i>	Lopes <i>et al.</i> , 2016	EU736947	EU339511	EU339474
<i>N. parvum</i>	CBS110301	Portugal	<i>Vitis vinifera</i>	Lopes <i>et al.</i> , 2017	AY259098	AY573221	EU673095
<i>N. parvum</i>	CMW 9081	New Zealand	<i>Populus nigra</i>	Lopes <i>et al.</i> , 2017	AY236943	AY236888	AY236917
<i>N. ribis</i>	CBS115475	USA	<i>Ribes</i> sp.	Lopes <i>et al.</i> , 2016	AY236935	AY236877	AY236906
<i>N. umdonicola</i>	CBS123645	South Africa	<i>Syzygium cordatum</i>	Lopes <i>et al.</i> , 2016	EU821904	EU821874	EU821844
<i>N. umdonicola</i>	CBS123646	South Africa	<i>Syzygium cordatum</i>	Lopes <i>et al.</i> , 2016	EU821905	EU821875	EU821845
<i>Neofusicoccum</i> sp. 5	CBS15726	Sri Lanka	<i>Camellia sinensis</i>	Yang <i>et al.</i> , 2017	KX464214	KX464744	KX465034

ing on PDA was inserted into each hole. Three plants inoculated with sterile agar served as controls. Wounds were sealed with the excised tissues and inspected daily for 20 d after inoculation (a.i.). Lesion diameters was recorded 30 d a.i., and the size of the cankers on cladodes was calculated as the circle area. Inoculations were first performed in June 2014 in an experimental field at the University of Catania (Sicily), and these were repeated each year in June for three consecutive years on different healthy cactus pear plants. Commencing from 20 d a.i., inoculated plants were inspected each month to observe development of symptoms. Trials were also repeated in an experimental field at the University of Palermo (Sicily).

Isolates FIFD and FIU1B were also used to inoculate twigs and stems of 2-year-old trees of sweet orange 'Navelina' (*Citrus × sinensis*) grafted on citrange 'Carrizo' (*Citrus sinensis* × *Poncirus trifoliata*) rootstock, grown in a greenhouse maintained at 20 to 26°C. These isolates were also used to inoculate the stems of field-grown trees of woody plants typical of the Mediterranean region, in an experimental field at the University of Catania. These included 3-year-old trees of almond [*Prunus dulcis* (Mill.) D.A. Webb], 5-year-old trees of holm oak (*Quercus ilex* L.) and 6-year old trees of Aleppo pine (*Pinus halepensis* Mill.). Inoculations were performed in June 2016. On sweet orange (two twigs per tree) were inoculated (four trees per isolate). A hole in each twig was made with a 3 mm cork-borer. A 3 mm diam. mycelium plug from 5-d-old PDA culture was placed on the freshly wounded surface, the wound was covered with the excised bark disk and sealed with Parafilm®. The stem of each tree (the 'Carrizo' citrange rootstock) was inoculated 10 cm above soil level (a single hole per stem) using the same method. Four trees inoculated with sterile agar served as controls. The length and breadth of each resulting lesion were recorded 30 d a.i., and the outer surface areas of the bark cankers on twigs and stems were calculated as ellipses. Almond, holm oak and Aleppo pine trees were wound inoculated on the stems using a cork borer (5 mm diam.). Four trees per host species were inoculated (three holes per tree 60 cm apart), and the wounds were each covered with the excised bark disk. Four trees inoculated with sterile agar served as controls. The lengths and breadths of the lesions were recorded at 30 and 70 d a.i.

In all pathogenicity tests, re-isolations were made from lesions, and resulting fungal colonies were confirmed morphologically and by sequencing part of the ITS, *tef1* and *tub2* genes, as described above, to fulfill Koch's postulates.

Statistical analyses of data

Data from pathogenicity tests were analyzed using RStudio v.1.2.5 (R). When comparing the means of multiple groups, a one-way ANOVA followed by Tukey's HSD *post hoc* test was performed. Significant differences between groups ($P < 0.05$) were denoted with different letters. When comparing independent groups, Student's t-test was used. The significance level was reported as follows: * = $P < 0.05$, ** = $P < 0.01$, or *** = $P < 0.001$.

RESULTS

Symptoms, distribution and incidence of the disease

Symptoms were visible on cladodes and included radially expanding, crusty, concentric, silvery, perennial cankers, each with a leathery, brown halo (Figure 2A–C). Pycnidia were erumpent from the host epidermis, visible to the naked eye as minute, black dots, formed on the silver-coloured internal area of each canker (Figure 2C) The cankers had radial and tangential cracks (Figure 2B–C). A milky to buff-coloured abundant and viscous exudate of polysaccharide nature, caking on contact with air, oozed from active cankers and formed strips or cerebriform masses. The exudate, being water soluble, was partially washed away by rain, while masses of exudates that remained on the cankers became black due to the growth of sooty molds, giving the cankers an appearance of carbonaceous crusts. The cankers ceased to expand in the coldest season of each year. An individual canker rarely reached a maximum diameter of more than 25 cm, but cankers often coalesced and formed larger lesions extending to the whole cladode or up to its edge, causing wilting. The cladodes collapsed when the bases were girdled by cankers. Infections on thicker cladodes and stems gave rise to very prominent cankers and eruptions of solid exudates at scattered points far from the lesions. Cladodes and stems of heavily infected plants became senescent and the whole plants collapsed, appearing gray and ghostly. In a systematic survey of prickly pear hedges and plantations, symptoms were observed in all hedges and plantings with 80% of plants symptomatic in the island of Lampedusa (20.2 km²) and 40% of plants symptomatic plants on Linosa (5.43 km²). Conversely, on Favignana (19.8 km²), symptoms were observed at two sites three km apart, with incidences of 40% and 100% of plants with symptoms. On the island of Ustica (8.24 km²), symptoms were observed only at one site on the northern coast, overlooking the sea (Figure 2A). However, this disease out-



Figure 2. A. Cankers on cladodes incited by *Neofusicoccum batangarum* in a cactus pear hedge on the Island of Ustica, May 2014. B. Coalescing, concentric cankers incited by *Neofusicoccum batangarum* on a cactus pear cladode. C. Concentric expanding canker incited by *Neofusicoccum batangarum* on a cactus pear cladode. Note pycnidia, as small dark spots, and cracking on the silvery, intermediate area of the canker, the dark colour and the sooty appearance of the exudate after rain and the tan colour of the edge, indicating that the canker is still active. D. Mycelium emerging from conidiomata of *Neofusicoccum batangarum* formed on cankers (photograph taken using a stereomicroscope).

break was severe, with approx. 400 m of hedges containing 100% of plants with symptoms.

Morphological and molecular identification of the pathogen

A fungus with white aerial mycelium that turned gray with age was consistently recovered from canker tissues, with 100% of positive isolations. The same fungus was obtained by plating single conidia taken from conidiomata emerging individually or in groups from

cankers (Figure 2D). Colonies on MEA formed concentric rings. On PDA mycelium was white and became smoky gray to gray-olivaceous after 5 d (Figure 3A). The mycelium was fast-growing (Table 3) and covered the 9 cm diam. Petri dishes after 5 d incubation at 25°C in the dark. Optimum temperature for radial colony growth was between 25 and 30°C for all the isolates tested. Little growth was observed at 10 or 35°C. Stromatic conidiomata were produced in pine needle cultures within 14 d. The conidiomata were solitary, covered by mycelium, obpyriform to ampulliform, and each had

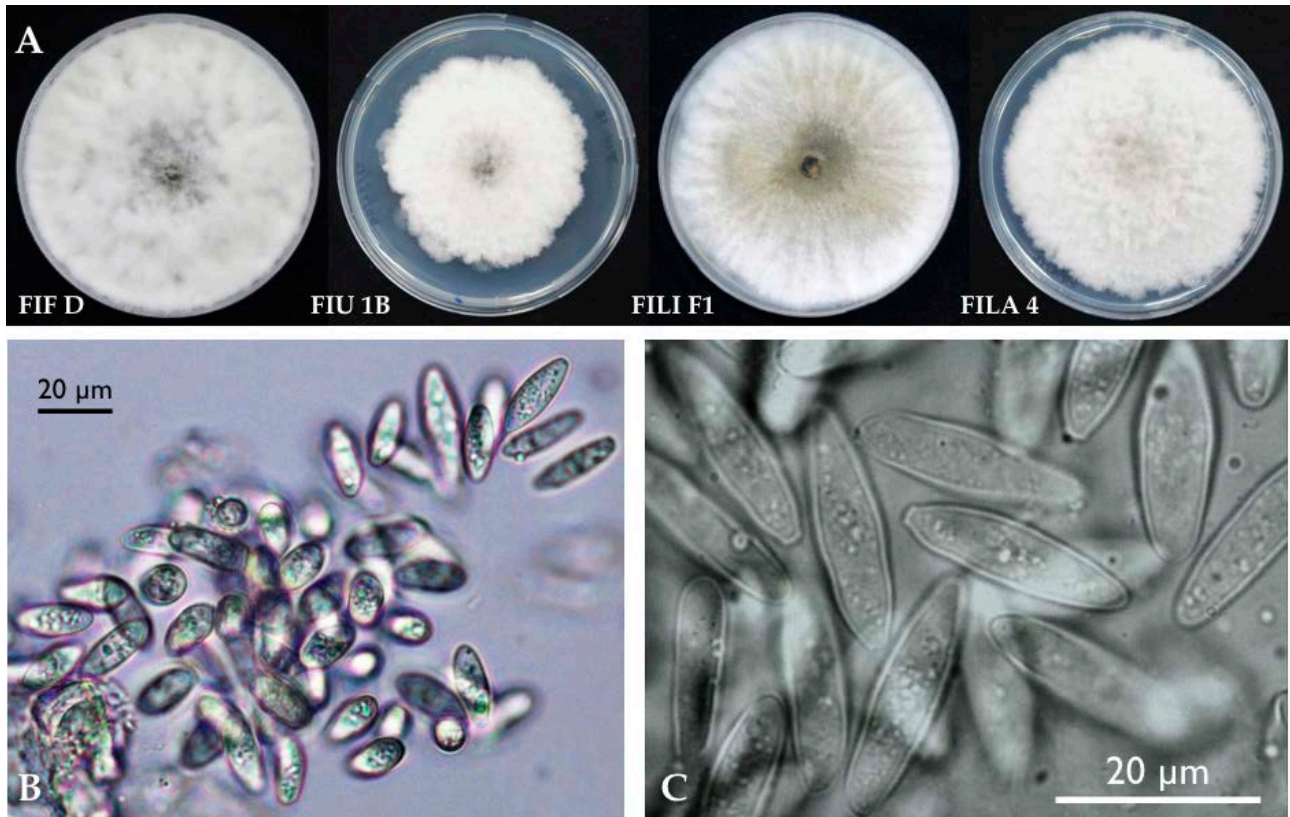


Figure 3. A. Four representative isolates of *Neofusicoccum batangarum* after 5 d of incubation on PDA at 25°C; CBS143023 (FIF D), CBS143024 (FIU 1B), CBS143025 (FILI F1), and CBS143026 (FILA 4). B and C. Unicellular, fusiform, thin-walled hyaline conidia of *Neofusicoccum batangarum*.

Table 3. Mean radial growth rates of colonies of *Neofusicoccum batangarum* isolates on PDA at three different temperatures, as determined after 3 d of incubation.

Isolates of <i>N. batangarum</i>	Island origin	15°C (mm d ⁻¹) mean ± S.D. ^a	25°C (mm d ⁻¹) mean ± S.D.	30°C (mm d ⁻¹) mean ± S.D.
FILI-F1	Linosa	3.83 ± 0.35	7.50 ± 0.00	5.90 ± 0.26
FILA 4	Lampedusa	3.97 ± 0.34	7.50 ± 0.00	7.50 ± 0.00
FIU-1B	Ustica	3.00 ± 0.58	6.53 ± 0.63	6.26 ± 0.42
FIF-D	Favignana	3.40 ± 0.41	7.50 ± 0.00	7.50 ± 0.00
OP5	Lampedusa	4.32 ± 0.05	9.77 ± 0.09	9.83 ± 0.06
OP6	Lampedusa	4.20 ± 0.21	12.94 ± 0.23	9.75 ± 0.13
OP9	Lampedusa	4.31 ± 0.09	13.00 ± 0.19	9.33 ± 0.24
OB44	Linosa	3.73 ± 0.81	12.83 ± 0.10	9.69 ± 0.06
OB46	Linosa	3.44 ± 0.44	13.03 ± 0.18	9.23 ± 0.42
OB47	Lampedusa	4.16 ± 0.10	12.94 ± 0.16	9.77 ± 0.11
OB43	Linosa	2.40 ± 0.22	7.82 ± 0.07	6.47 ± 0.06

^a Mean of four replicate Petri dishes.

a central and circular unilocular ostiole, and measured 250-300 μm in diameter. Conidia were non-septate (bi-cellular conidia were observed only very occasionally), hyaline, smooth, fusoid to ovoid, thin-walled, and measured 17.1-21.8 × 4.6-8.9 μm, with a mean length to width ratio = 2.9 (Figure 3B-C).

The isolates obtained had identical ITS, *tef1* and *tub2* sequences. Preliminary BLAST analyses of these three genes yielded several identical sequences of *Neofusicoccum* spp., deposited with different taxa names. Consequently, this analysis enabled the identification at the genus level, but did not provide reliable information on the species. The phylogenetic analysis of the combined data set of sequences from ITS, *tef1* and *tub2* sequences (Figure 4) produced trees with a high concordance with those reported by Lopes *et al.* (2017) and Yang *et al.* (2017). According to this analysis, isolates from cactus pear were identified as *N. batangarum*, since they clearly clustered with the ex-type (CBS 124924 from *Terminalia catappa*; Lopes *et al.*, 2016) and other reference isolates of this species, and were differentiated from other *Neofusicoccum* species, including

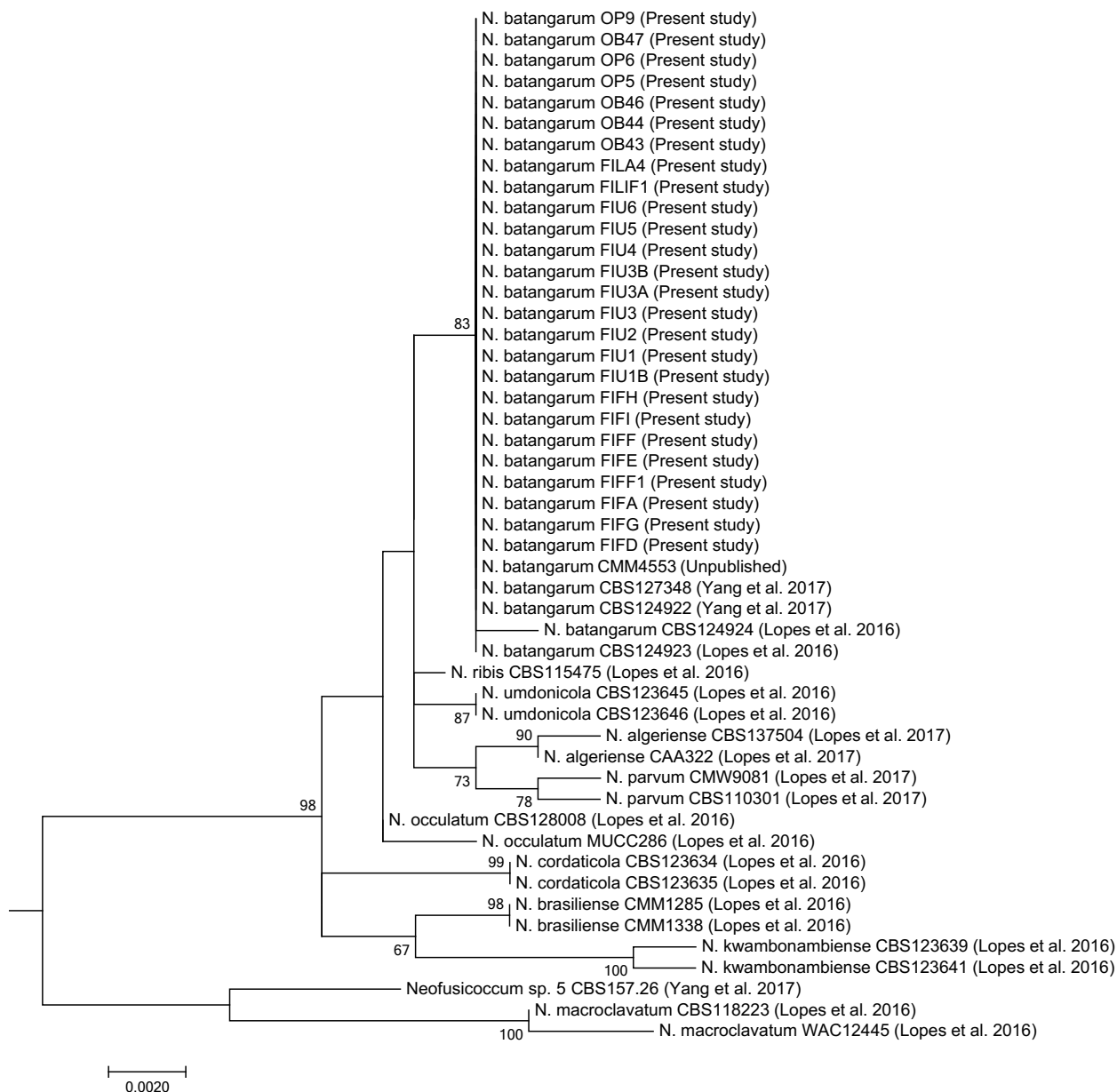


Figure 4. Phylogenetic tree of isolates of *Neofusicoccum* collected in the present study from *Opuntia ficus-indica*, and representative isolates of *Neofusicoccum batangarum* and closely related species as defined by in comprehensive phylogenetic studies (Tables 1 and 2). The tree was built using concatenated sequences of ITS-5.8S-ITS2 region, *tef1*- α gene and β -tubulin gene. Numbers on nodes indicate the posterior probabilities from the maximum likelihood method.

the closely related species *N. ribis*, *N. umdonicola*, and *N. occulatum* (Annex 1).

formity, since isolates showed identical banding patterns with the three tested primers (Annex 2).

Analysis of the genetic variability of isolates

The MSP-PCR characterization of the six representative isolates of *N. batangarum* revealed high genetic uni-

Pathogenicity tests

Four isolates, one from each island, were deposited at Westerdijk Fungal Biodiversity Institute [CBS 143023

Table 4. Mean lesion areas on cladodes of cactus pear (*Opuntia ficus-indica*) 30 d after wound inoculation with representative isolates of *Neofusicoccum batangarum* obtained from cactus pear from four minor islands of Sicily.

Isolate	Island origin	Mean lesion area (cm ²) ± S.D. ^{a,b}
FIF D	Favignana	4.4 ± 1.2
OP6	Lampedusa	4.4 ± 1.8
OB43	Linosa	4.5 ± 2.3
FIU 1B	Ustica	4.6 ± 0.6

^a Means of 12 replicate values.

^b ANOVA, $F_{(3,44)} = 0.372$, $P > 0.05$

Table 5. Mean lesion areas on stems of sweet orange ‘Navelina’ (*Citrus × sinensis*) trees grafted on ‘Carrizo’ Citrange (*C. sinensis* × *Poncirus trifoliata*) rootstock, 30 d after wound inoculation with representative isolates of *Neofusicoccum batangarum* from four minor islands of Sicily

Isolate ^f	Island origin	Mean lesion area (cm ²) ± S.D. ^a	
		rootstock ^{b,d}	scion ^{c,e}
FIF D***	Favignana	1.4 ± 0.18	1.8 ± 0.1
FIU 1B**	Ustica	1.4 ± 0.12	1.8 ± 0.2
FILI F1*	Linosa	1.4 ± 0.15	1.7 ± 0.2
FILA 4**	Lampedusa	1.5 ± 0.26	1.9 ± 0.4

^a Rootstock: means of four replicate values. Scion: means of eight replicate values.

^b Symptoms included barely noticeable gummy exudate.

^c Symptoms included abundant gummosis.

^d ANOVA rootstock, $F_{(3,12)} = 0$, $P > 0.05$.

^e ANOVA scion, $F_{(3,28)} = 0$, $P > 0.05$.

^f Comparing rootstock and scion according to Student’s t-test.

(* = $P < 0.05$, ** = $P < 0.01$, and *** = $P < 0.001$).

(FIF D), CBS 143024 (FIU 1B), CBS 143025 (FILI F1), and CBS 143026 (FILA 4)], and these were tested for their pathogenicity on cactus pear and other species of plants. Additional isolates from Lampedusa and Linosa were also included in the pathogenicity tests. Since the results of four inoculation series performed, respectively, in 2014, 2015, 2016 and 2017 were very similar, only the results of inoculations performed in 2014 are reported here in detail. All isolates were pathogenic on the inoculated plant species (Tables 4, 5, 6 and 7). The isolates induced cankers in all inoculated plants while no symptoms were observed on the controls.

On cactus pear plants, symptoms appeared after 4 d, as brown circular halos around the inoculation wounds with viscous exudates oozing from the lesions that consolidated in contact with the air to form long strips

Table 6. Mean lesion areas on stems of holm oak (*Quercus ilex*) trees 30 d and 70 d after wound inoculation with representative isolates of *Neofusicoccum batangarum* from two minor islands of Sicily.

Isolate	Island origin	Mean lesion area (cm ²) ± S.D. ^a	
		30 d ^b	70 d ^c
FIF D	Favignana	5.2 ± 1.3	8.2 ± 1.1
FIU 1B	Ustica	5.8 ± 2.4	10.0 ± 3.0

^a Means of six replicate values.

^b ANOVA 30 d, $F_{(1,10)} = 0.274$, $P > 0.05$.

^c ANOVA 70 d, $F_{(1,10)} = 1.517$, $P > 0.05$.

Table 7. Mean lesion areas on stems of Aleppo pine (*Pinus halepensis*) or almond (*Prunus dulcis*) trees 70 d after wound inoculations with representative isolates of *Neofusicoccum batangarum* from four minor islands of Sicily.

Isolate	Origin	Mean lesion area (cm ²) ± S.D. ^{a,f}	
		Aleppo pine ^{b,d}	Almond ^{c,e}
FIF D	Favignana	7.2 ± 0.6 a	4.9 ± 1.0 a
FIU 1B	Ustica	7.1 ± 0.9 ab	5.1 ± 1.4 a
FILA 4	Lampedusa	7.6 ± 2.8 ab	5.1 ± 1.7 a
FILI F1	Linosa	6.6 ± 0.6 b	5.8 ± 1.7 a

^a Means of six replicates.

^b Symptoms included resinous exudates.

^c Symptoms included abundant gummous exudates.

^d ANOVA Aleppo pine, $F_{(3,20)} = 6.015$, $P = 0.004$.

^e ANOVA Almond, $F_{(3,20)} = 2.783$, $P = 0.06$.

^f Means accompanied by the same letters are not statistically different ($P < 0.05$, Tukey’s HSD test).

(Figure 5A–B). Cankers expanded progressively and concentrically (Figure 5D). They were roughly circular, with irregular margins, identical or very similar to those observed on plants with natural infections, and the canker expansion reduced during the coldest months (late December to early February). Some cankers stopped growing permanently and healed, but most cankers resumed growth and the production of exudate when temperatures increased after winter. Table 4 presents the mean lesion areas induced on cactus pear cladodes by the four tested isolates 30 d after wound inoculation. Analysis of variance revealed no statistically significant differences in pathogenicity between the isolates. Five years after the first inoculation, most cankers were still active, and they continued to expand and produce abundant exudates (Figure 5D). In some cases, the cankers expanded more rapidly in one direction and became asymmetrical and irregular (Figure 5D). After rain, the cankers became dark, with a carbonaceous appearance.



Figure 5. A. Brown, circular lesions and waxy exudate oozing from lesions on a cactus pear cladode wound-inoculated with *Neofusicoccum batangarum*, 7 d after inoculation (a.i.) B. Brown lesion and exudate oozing from a lesion on a cactus pear cladode wound-inoculated with *N. batangarum*, 4 d a.i. C. A fusiform dry canker induced by wound-inoculation of *N. batangarum* on the stem of a holm oak tree 70 d a.i. D. A still active canker on a cactus pear cladode artificially inoculated with *Neofusicoccum batangarum* in the field, September 2019, 5 years a.i. E. A resinous canker induced by wound-inoculation with *N. batangarum* on the stem of an Aleppo pine tree, 70 d a.i. F. A gummy canker induced by wound-inoculation with *N. batangarum* on the stem of a young almond tree, 14 d a.i. G. A gummy canker induced by wound-inoculation with *N. batangarum* on the stem of a young 'Navelina' sweet orange tree, 14 d a.i. H. Pycnidia on a canker induced by wound-inoculation with *N. batangarum* on the stem of a young 'Navelina' sweet orange tree, 14 d a.i.

Pycnidia were visible on cankers 14-20 d a.i. From six months to 5 years a.i., small cankers and scattered eruptions of exudate, similar to runny wax, appeared on artificially inoculated cladodes approx. 10-20 cm from the inoculation points.

All four tested *N. batangarum* isolates induced necrotic lesions on the citrange rootstock and the sweet orange scion at 7 d a.i. Symptoms were more severe on

the sweet orange scions (Table 5) and included abundant gummosis (Figure 5G), while gummosis was much less abundant on citrange. Pycnidia emerged from the necrotic lesions on sweet orange stems from 10 to 14 d a.i. (Figure 5H). Differences in mean lesion size between the sweet orange scion and the citrange rootstock were significant ($P < 0.05$), according to Student's *t*-test. However, no statistically significant differences in patho-

genicity ($P > 0.05$) were observed among the fungal isolates on both citrus symbionts. No symptoms were observed on the controls.

On holm oak (Table 6), no gummy reaction was observed (Figure 5 C), but cankers expanded progressively along the stems and were still active 3 years after inoculation. No symptoms were observed on the controls. There were no significant differences ($P > 0.05$) among isolates in the pathogenicity test on holm oak at 30 d a.i. or 70 d a.i.

On almond and Aleppo pine (Table 7), *N. batangarum* isolates incited necrotic bark lesions with gummy exudates on almond (Figure 5F) and resinous exudates on Aleppo pine (Figure 5E). No symptoms were observed on the controls. Also on almond and Aleppo pine, cankers were still active 3 years a.i.

In the pathogenicity tests on almond and Aleppo pine there were small but statistically significant differences between the isolates on these two hosts (almond, $P = 0.06$; Aleppo pine, $P = 0.004$). All the *N. batangarum* isolates were re-isolated from inoculated plants, while no fungal pathogens were isolated from control plants, thus fulfilling Koch's postulates for the *N. batangarum* isolates.

DISCUSSION

Identification of the *Botryosphaeriaceae* prior to the application of DNA sequencing and phylogenetic inference should be considered with caution. The classification and nomenclature of these fungi have evolved rapidly and have been substantially revised, as previous classification based on morphological characters was confusing and most species were actually complexes of different taxa (Slippers *et al.*, 2004, 2013; Crous *et al.*, 2006; Phillips *et al.*, 2008, 2013; Crous *et al.*, 2017). According to the molecular taxonomy of the *Botryosphaeraceae*, *N. batangarum* is the appropriate name of the fungus responsible for the chronic disease observed on the cladodes of cactus pear in the minor islands of Sicily. *Neofusicoccum batangarum* was confirmed to be the sole causal agent of the 'scabby canker' disease. The fungus was consistently associated with symptomatic cactus pear plants and, when artificially inoculated onto this host, induced the same type of cankers as natural infections. From an etiological and ecological perspective, *N. batangarum* was the only fungus in the family *Botryosphaeriaceae* recovered from infected cactus pear in these small islands belonging to different archipelagos.

Several species of this family frequently occur together on the same host (Jami *et al.*, 2017), although

not all are able to cause disease (Lawrence *et al.*, 2017). In Brazil, *N. batangarum*, alone or in association with other fungi including several species of *Botryosphaeriaceae*, was reported to be responsible for 'brown spot' of cladodes, a severe disease of cochineal cactus that is grown as fodder for livestock in the semi-arid region of the north-east of that country (Conforto *et al.*, 2016, 2019). Although the syndromes of 'cladode brown spot' in north-eastern Brazil and 'scabby canker' in minor islands of Sicily have some traits in common, they are distinct. Differences between the symptoms of these diseases include the presence of crusty, silvery, perennial cankers, and exudates oozing from the cankers in the 'scabby canker' disease. However, differences might be due to environmental conditions, host plant and/or cultivation systems. In Brazil, cochineal cactus is pruned repeatedly for the production of fresh forage. The cactus pear fences in the minor islands near Sicily are pruned only occasionally, thus allowing the disease to become chronic on mature cladodes. The cladode brown spot in Brazil is also a complex disease and the causal agent may vary according to the season and the geographical region (Santana *et al.*, 2020).

For many years, *Botryosphaeriaceae*, which are widespread in tropical and temperate regions, were considered to be opportunistic pathogens infecting hosts exclusively through wounds or natural openings in their periderms. Since the late 1980s, however, these fungi have been recognized as endophytes that remain latent in woody host plants for long periods. With the onset of abiotic stress conditions (drought, physical damage, water-logging, frost and unsuitable environments for the growth) the latent pathogens cause disease (Slippers and Wingfield, 2007; Pavlic-Zupanc *et al.*, 2015; Marsberg *et al.*, 2017). The prolonged latent infection or endophytic phase implies that these fungi can easily pass undetected through phytosanitary controls or during the selection of propagation material.

The genus *Neofusicoccum* comprises species with widespread geographical and host distributions, and these fungi are typically endophytes, which in stressful environments can cause symptoms such as dieback, cankers and gummosis (Crous *et al.*, 2006; Lopes *et al.*, 2017; Zhang *et al.*, 2017; Burgess *et al.*, 2018). Wounds caused by hailstorms may have been the factor triggering the epidemic outbreak of *N. batangarum* on cactus pear in the small islands of Sicily. The climate of these islands is affected by the proximity to the sea, and this may have favoured the development of the disease and the survival of the inoculum. In *in vitro* tests, *N. batangarum* showed an optimum temperature for growth around 25°C, a minimum of approx. 10°C and a maxi-

imum of approx. 35°C. On artificially inoculated cladodes, the fungus formed pycnidia between 14 and 20 d a.i. In winter, conidia collected from pycnidia formed on cladodes artificially inoculated in the spring or autumn of the previous year were viable.

Most species of *Botryosphaeriaceae* have broad host ranges, and only very few have been described from a limited number of host species or are host specific (Slippers and Wingfield, 2007; Marsberg *et al.*, 2017). The ability to infect multiple hosts and to move among unrelated hosts facilitates the establishment and spread of species and genotypes of this family into new areas.

Neofusicoccum batangarum has been reported as an endophyte as well as a pathogen of several host plants in the tropics (Begoude *et al.*, 2010, 2011; Shetty *et al.*, 2011; Conforto *et al.*, 2016; Netto *et al.*, 2017). A very recent report has further expanded the known hosts (Serrato-Diaz *et al.*, 2020). Pathogenicity tests in the present study showed that this fungus has an even wider potential host range, encompassing woody forest and cultivated plants typical of the Mediterranean macro-region. These hosts include Aleppo pine, almond, citrus and holm oak. Like other *Botryosphaeriaceae*, *N. batangarum* can be regarded as a generalist pathogen, although in natural conditions the host affinity of polyphagous *Botryosphaeriaceae* species is strongly influenced by the environment (Slippers and Wingfield, 2007). On artificially inoculated sweet orange stems, *N. batangarum* induced the typical symptoms of 'gummy cankers' or 'bot gummosis', already known as 'Dothiorella gummosis'. These are minor, but widespread, diseases caused by diverse species of *Botryosphaeriaceae*, and they commonly occur in citrus groves in California and in the Mediterranean basin (Adesemoye *et al.*, 2014; Guarnaccia and Crous, 2017). Consistently with the typical symptoms of 'gummy canker' of citrus, in artificially inoculated symbiont citrus plant, symptoms were more severe on the sweet orange scion than on rootstock.

The polyphagy of *N. batangarum* may be related to its ability to produce non-host specific phytotoxins (Masi *et al.*, 2020). These toxins may have roles in pathogenicity as virulence factors and may also enhance the ecological fitness of the fungus by inhibiting other microorganisms competing in plant biospheres. Production of diffusible phytotoxins could also explain the systemic spread of symptoms on cactus pear cladodes and their appearance far from inoculation points (Masi *et al.* 2020).

Reports of *Botryosphaeriaceae* associated with various hosts have increased worldwide in recent years. In Italy, this family is common and widespread on a broad range of hosts, and is an increasing concern for agri-

cultural crops and urban and natural forest ecosystems (Burruano *et al.*, 2008; Linaldeddu *et al.*, 2014, 2016; Dissanayake *et al.*, 2016b). The disease of cactus pear caused by *N. batangarum* was noticed for the first time in Linosa more than 45 years ago (Somma *et al.*, 1973), and at that time it was widespread and had been established for many years. Similarly, the chronic nature of symptoms observed recently in Favignana, Lampedusa and Ustica and the widespread occurrence of the disease in Lampedusa, clearly indicate it has not emerged recently. During the last 50 years the disease has probably been favoured by the low frequency of cactus pear pruning as a consequence of the reduced importance of this plant as a crop, and the drastic reduction in the use of cladodes as fodder. Although Sicily is the main cactus pear fruit producer in Italy, with more than 3,500 ha of specialized culture (Ochoa and Barbera, 2017), this disease has not been reported in cactus pear cultivations in Sicily. The present study has shown that *N. batangarum* populations from Favignana, Lampedusa, Linosa and Ustica were genetically uniform, despite their geographical isolation.

It can be assumed that conidia and ascospores of *Botryosphaeriaceae* are dispersed by wind and rain only over short distances. The occurrence of *N. batangarum* only on cactus pear plantations of the minor islands, and the genetic uniformity of the fungus populations, may indicate that these populations have a common origin, and that the widespread distribution of a single genotype of the pathogen has resulted from anthropogenic activity. *Neofusicoccum batangarum*, as an endophytic or latent pathogen, may have been introduced with cactus pear cladodes collected in other geographical areas and used as propagation material. This hypothesis is consistent with cactus pear being introduced on a large scale into small islands of the Mediterranean Sea as fodder for livestock, for field fences or for edible fruit production, at one recent time (Pretto *et al.*, 2012). This was when more intensive colonization and exploitation of agriculture in these islands were promoted by the public authorities.

From an ecological perspective, the emergence of this disease in such an aggressive form, which has become a limiting factor for the cultivation of cactus pear in these small islands, may be partly due to the failure of the acclimatization of a non-native plant species. However, the occurrence of a serious disease of a crop of economic and landscaping relevance for Sicily in a restricted geographical area, but very close and frequently connected to the main island by tourist traffic, may have phytosanitary implications. Appropriate actions should be taken to prevent further spread and introduction of *N. batan-*

garum into areas where the non-native cactus pear host is naturalized and intensively cultivated.

LITERATURE CITED

- Adesemoye A. O., Mayorquin J. S., Wang D. H., Twizeyimana M., Lynch S. C., Eskalen A. 2014. Identification of species of Botryosphaeriaceae causing bot gummosis in citrus in California. *Plant Disease* 98:55–61.
- Begoude B.A.D., Slippers B., Wingfield M.J., Roux J. 2010. Botryosphaeriaceae associated with *Terminalia catappa* in Cameroon, South Africa and Madagascar. *Mycological Progress* 9: 101–123.
- Begoude B.A.D., Slippers B., Wingfield M.J., Roux J. 2011. The pathogenic potential of endophytic Botryosphaeriaceous fungi on *Terminalia* species in Cameroon. *Forest Pathology* 41: 281–292
- Burgess T.I., Tan Y.P., Garnas J., Edwards J., Scarlett K.A., ..., Jami F. 2018. Current status of the Botryosphaeriaceae in Australia. *Australasian Plant Pathology* DOI: 10.1007/s13313–018-0577-5
- Burruano S., Mondello V., Conigliaro G., Alfonzo A., Spagnolo A., Mugnai L. 2008. Grapevine decline in Italy caused by *Lasiodiplodia theobromae*. *Phytopathologia Mediterranea* 47: 132–136.
- Carbone I., Kohn L.M. 1999. A method for designing primer sets for speciation studies in filamentous ascomycetes. *Mycologia* 91: 553–556.
- Conforto C., Lima N.B., Garcete-Gómez J.M., Câmara M.P.S., Michereff S.J. 2016. First Report of Cladode Brown Spot in Cactus Prickly Pear Caused by *Neofusicoccum batangarum* in Brazil. *Plant Disease* 100: 1238.
- Conforto C., Lima N.B., Silva F.J.A., Câmara M.P.S., Maharachchikumbura S., Michereff S.J. 2019. Characterization of fungal species associated with cladode brown spot on *Nopalea cochenillifera* in Brazil. *European Journal of Plant Pathology* 155: 1179–1194.
- Crous P.W., Slippers B., Wingfield M.J., Rheeder J., Marasas W.F.O., ..., Groenewald J.Z. 2006. Phylogenetic lineages in the Botryosphaeriaceae. *Studies in Mycology* 55: 235–253.
- Crous P.W., Slippers B., Groenewald J.Z., Wingfield M.J. 2017. Botryosphaeriaceae: systematics, pathology, and genetics. *Fungal Biology* 121: 305–306.
- Dissanayake A.J., Phillips A.J.L., Li X.H., Hyde K.D. 2016a. *Botryosphaeriaceae*: Current status of genera and species. *Mycosphere* 7: 1001–1073.
- Dissanayake A.J., Camporesi E. Hyde K.D., Phillips A.J.L., Fu C.Y., ..., Li X.H. 2016b. *Dothiorella* species associated with woody hosts in Italy. *Mycosphere* 7: 51–63.
- Feijo F.M., Silva M.J.S., Nascimento A.D., Infante N.B., Ramos-Sobrinho R., ..., Lima G.S.A. 2019. Botryosphaeriaceae species associated with the prickly pear cactus, *Nopalea cochinellifera*. *Tropical Plant Pathology* 44: 452–459.
- Freeman S., Shabi, E.E. 1996 Cross-infection of subtropical and temperate fruits by *Colletotrichum* species from various hosts. *Physiological Molecular Plant Pathology* 49:395–404.
- Garcete-Gómez J.M., Conforto C., Domínguez-Monge S., Flores-Sánchez J.L.F., Mora-Aguilera G., Michereff S.J. 2017. Sample size for assessment of cladode brown spot in prickly pear cactus. *European Journal of Plant Pathology* 149: 759–763.
- Edgar R.C. 2004. Muscle: multiple sequence alignment with high accuracy and high throughput. *Nucleic Acids Research* 32: 1792–1797.
- Glass N.L., Donaldson G.C. 1995. Development of primer sets designed for use with the PCR to amplify conserved genes from filamentous ascomycetes. *Applied and Environmental Microbiology* 61: 1323–1330.
- Granata G., Faedda R., and Ochoa M.J. 2017. Diseases of cactus pear. In: Crop Ecology, Cultivation and user of Cactus pear (P. Inglese, C. Mondragon, A. Nefzaoui, C. Saenz, eds.), FAO and ICARDA, Rome, Italy, 115–126.
- Guarnaccia V., Crous P.W. 2017. Emerging citrus diseases in Europe caused by species of *Diaporthe*. *IMA Fungus* 8: 317–334.
- Jami F., Wingfield M.J., Gryenhout M., Slippers B. 2017. Diversity of tree-infecting Botryosphaeriales on native and non-native trees in South Africa and Namibia. *Australasian Plant Pathology* 46: 529–545.
- Kiesling R., Metzger D. 2017. Origin and Taxonomy of *Opuntia ficus-indica*. In: Crop Ecology, Cultivation and user of Cactus pear (P. Inglese, C. Mondragon, A. Nefzaoui, C. Saenz eds.), FAO and ICARDA, Rome, Italy, 14–19
- Kumar S., Stecher G., Tamura K. 2016. MEGA7: Molecular Evolutionary Genetics Analysis Version 7.0 for Bigger Datasets. *Molecular Biology and Evolution* 33: 1870–1874
- Lawrence P.D., Peduto Hand F., Gubler W.D., Trouillas F.T. 2017. *Botryosphaeriaceae* species associated with dieback and canker disease of bay laurel in northern California with the description of *Dothiorella californica* sp. nov. *Fungal Biology* 121: 347–360.
- Linaldeddu B.T., Scanu B., Maddau L., Franceschini A. 2014. *Diplodia corticola* and *Phytophthora cinnamomi*: the main pathogens involved in holm oak decline on Caprera island (Italy). *Forest Pathology* 44: 191–200.

- Linaldeddu B.T., Alves A., Phillips A.J.L. 2016. *Sardiniella urbana* gen. et sp. nov., a new member of the *Botryosphaeriaceae* isolated from declining *Celtis australis* trees in Sardinian streets capes. *Mycosphere* 7: 893–905.
- Lopes A., Barradas C., Phillips A.J.L., Alves A. 2016. Diversity and phylogeny of *Neofusicoccum* species occurring in forest and urban environments in Portugal. *Mycosphere* 7: 906–920.
- Lopes A., Phillips A.J.L., Alves A. 2017. Mating type genes in the genus *Neofusicoccum*: Mating strategies and usefulness in species delimitation. *Fungal Biology* 121, 394–404.
- Marsberg A., Kemler M., Jami F., Nagel J.H., Postma-Smidt A., ..., Slippers B., 2017. *Botryosphaeria dothidea*: a latent pathogen of global importance to woody plant health. *Molecular Plant Pathology* 18: 477–488.
- Masi M., Aloï F., Nocera P., Cacciola S.O., Surico G., Evidente A. 2020. Phytotoxic metabolites isolated from *Neofusicoccum batangarum*, the causal agent of the scabby canker of cactus pear (*Opuntia ficus-indica* L.). *Toxins* 12: 126; DOI: 10.3390/toxins12020126
- Meyer W., Mitchell T.G., Freedman E.Z., Vilgalys R. 1993. Hybridization probes for conventional DNA fingerprinting used as single primers in the polymerase chain reaction to distinguish strains of *Cryptococcus neoformans*. *Journal of Clinical Microbiology* 31: 2274–2280.
- Netto M.S.B., Lima W.G., Correia K.G., Da Silva C.F.B., Thon M., ... Câmara M.P.F. 2017. Analysis of phylogeny, distribution and pathogenicity of *Botryosphaeriaceae* species associated with gummosis of *Anacardium* in Brasil, with a new species of *Lasiodiplodia*. *Fungal Biology* 121: 437–451.
- Ochoa M.J., Barbera G., 2017. History and economic and agro-ecological importance. In: Crop Ecology, Cultivation and user of Cactus pear (P. Inglese, C. Mondragon, A. Nefzaoui, C. Saenz eds.), FAO and ICAR-DA, Rome, Italy, 1–12
- Pavlic-Zupanc D., Wingfield M.J., Boissin, E., Slippers, B. 2015. The distribution of genetic diversity in the *Neofusicoccum parvum*/*N. ribis* complex suggests structure correlated with level of disturbance. *Fungal Ecology* 13: 93–102.
- Phillips A.J.L., Alves A., Pennycook S. R., Johnston P.R., Ramaley A., ..., Crous P.W. 2008. Resolving the phylogenetic and taxonomic status of dark-spored teleomorph genera in the *Botryosphaeriaceae*. *Persoonia* 21: 29–55
- Phillips A.J.L., Alves A., Abdollahzadeh J., Slippers B., Wingfield M.J., ..., Crous P.W. 2013. The Botryosphaeriaceae: Genera and species known from culture. *Studies in Mycology* 76: 51–167
- Pretto F., Celesti-Grapow L., Carli E., Brundu G., Blasi C. 2012. Determinants of non-native plant species richness and composition across small Mediterranean islands. *Biological Invasions* 14: 2559–2572.
- Rayner R.W. 1970. *A Mycological Colour Chart*. Commonwealth Mycological Institute, Kew, Surrey, UK.
- Santana M.D., de Lima Leite I.C.H., da Silva Santos I.C., Michereff S.J., Freitas-Lopes R.do L., Lopes U.P. 2020. Reduction of cladode brown spot in cactus pear in semiarid growing areas and yield increase using fungicides. *Journal of Plant Pathology* DOI: 10.1007/s42161-019-00462-9
- Santos J.M., Phillips A.J.L. 2009. Resolving the complex of *Diaporthe* (*Phomopsis*) species occurring on *Foeniculum vulgare* in Portugal. *Fungal Diversity* 34: 111–125.
- Schena L., Cooke D.E.L., 2006. Assessing the potential of regions of the nuclear and mitochondrial genome to develop a “molecular tool box” for the detection and characterization of *Phytophthora* species. *Journal of Microbiological Methods* 67: 70–85.
- Schena L., Surico G., Burrano S., Giambra S., Pane A., ..., Cacciola S.O. 2018. First report of *Neofusicoccum batangarum* as causal agent of scabby cankers of cactus pear (*Opuntia ficus-indica*) in minor islands of Sicily. *Plant Disease* 102: 445.
- Serrato-Diaz L.M., Aviles-Noriega A., Soto-Bauzó A., Rivera-Vargas L.I., Goenaga R., Bayman P. 2020. Botryosphaeriaceae fungi as causal agents of dieback and corky bark in rambutan and longan. *Plant Disease* 104: 105–115.
- Shetty K.G., Minnis A.M., Rossman A.Y., Jayachandran K. 2011. The Brazilian peppertree seedborne pathogen, *Neofusicoccum batangarum*, a potential biocontrol agent. *Biological Control* 56: 91–97.
- Slippers B., Wingfield M.J. 2007. *Botryosphaeriaceae* as endophytes and latent pathogens of woody plants: diversity, ecology and impact. *Fungal Biology Reviews* 21: 90–106.
- Slippers B., Crous P.W., Denman S., Coutinho T.A., Wingfield B.D., Wingfield M.J. 2004. Combined multiple gene genealogies and phenotypic characters differentiate several species previously identified as *Botryosphaeria dothidea*. *Mycologia* 96: 83–101.
- Slippers B., Boissin E., Phillips A.J.L., Groenewald J.Z., Lombard L., ..., Crous P.W. 2013. Phylogenetic lineages in the *Botryosphaeriales*: a systematic and evolutionary framework. *Studies in Mycology* 76: 31–49.
- Smith H., Wingfield M.J., Crous P.W., Coutinho T.A., 1996. *Sphaeropsis sapinea* and *Botryosphaeria doth-*

- idea* endophytic in *Pinus* spp. and *Eucalyptus* spp. in South Africa. *South African Journal of Botany* 62: 86–88.
- Somma V., Rosciglione B., Martelli G.P. 1973. Preliminary observations on gummous canker, a new disease of prickly pear. *Tecnica Agricola* 25: 437–443.
- Tamura K., Nei M. 1993. Estimation of the number of nucleotide substitutions in the control region of mitochondrial DNA in humans and chimpanzees. *Molecular Biology and Evolution* 10: 512–526.
- Tamura K., Stecher G., Peterson D., Filipski A., Kumar S. 2013. MEGA6: Molecular Evolutionary Genetics Analysis Version 6.0. *Molecular Biology and Evolution* 30: 2725–2729.
- Uddin W., Stevenson, K.L., Pardo-Schultheiss R.A. 1997. Pathogenicity of a species of *Phomopsis* causing a shoot blight on peach in Georgia and evaluation of possible infection courts. *Plant Disease* 81: 983–998.
- Yang T., Groenewald J.Z., Cheewangkoon R., Jami F., Abdollahzadeh J., ... , Crous P.W. 2017. Families, genera, and species of *Botryosphaeriales*. *Fungal Biology* 121: 322–346.
- Vaidya N.H., Hadjicostis C.N., Dominguez-Garcia A.D. 2011. Distributed algorithms for consensus and coordination in the presence of packet-dropping communication links-part II: Coefficients of ergodicity analysis approach. arXiv preprint arXiv:1109.6392.
- White T. J., Bruns T. D., Lee S. B., Taylor J. W. 1990. Amplification and direct sequencing of fungal ribosomal RNA Genes for phylogenetics. In: *PCR - Protocols and Applications - A Laboratory Manual* (M.A. Innis, D.H. Gelfand, J.J. Sninsky, T.J White eds.), Academic Press Inc., New York, USA, 315–322.
- Zhang M., Lin S., He W., Zhang Y. 2017. Three species of *Neofusicoccum* (Botryosphaeriaceae, Botryosphaeriales) associated with woody plants from southern China. *Mycosphere* 8: 797–808.

Article

Phytotoxic Metabolites Isolated from *Neofusicoccum batangarum*, the Causal Agent of the Scabby Canker of Cactus Pear (*Opuntia ficus-indica* L.)

Marco Masi ¹, Francesco Aloï ^{2,3}, Paola Nocera ¹, Santa Olga Cacciola ^{3,*},
Giuseppe Surico ⁴ and Antonio Evidente ^{1,*}

- ¹ Dipartimento Scienze Chimiche, Università di Napoli Federico II, Complesso Universitario Monte S. Angelo, Via Cintia 4, 80126 Napoli, Italy; marco.masi@unina.it (M.M.); paola.nocera@unina.it (P.N.)
 - ² Dipartimento di Scienze Agrarie, Alimentari, Forestali e Ambientali, Università di Palermo, V. le delle Scienze 4, 90128 Palermo, Italy; francesco.aloi@unipa.it
 - ³ Dipartimento di Agricoltura, Alimentazione e Ambiente, Università di Catania, Via Santa Sofia 100, 95123 Catania, Italy
 - ⁴ Dipartimento di Scienze e Tecnologie Agrarie, Alimentari, Ambientali e Forestali, Sez. Patologia vegetale ed entomologia, Università di Firenze, Piazzale delle Cascine 28, 50144 Firenze, Italy; giuseppe.surico@unifi.it
- * Correspondence: evidente@unina.it (A.E.); olga.cacciola@unict.it (S.O.C.); Tel.: +39-081-2539178 (A.E.); +39-095-7147371 (S.O.C.)

Received: 24 January 2020; Accepted: 14 February 2020; Published: 18 February 2020

Abstract: Six phytotoxins were obtained from the culture filtrates of the ascomycete *Neofusicoccum batangarum*, the causal agent of the scabby canker of cactus pear (*Opuntia ficus-indica* L.) in minor Sicily islands. The phytotoxins were identified as (–)-(R)-mellein (**1**); (±)-botryoisocoumarin A (**2**); (–)-(3R,4R)- and (–)-(3R,4S)-4-hydroxymellein (**3** and **4**); (–)-terpestacin (**5**); and (+)-3,4-dihydro-4,5,8-trihydroxy-3-methylisocoumarin, which we named (+)-neoisocoumarin (**6**). This identification was done by comparing their spectral and optical data with those already reported in literature. The absolute configuration (3R,4S) to (+)-neoisocoumarin (**6**) was determined using the advanced Mosher method. All six metabolites were shown to have phytotoxicity on the host (cactus pear) and non-host (tomato) plants, and the most active compounds were (±)-botryoisocoumarin A (**2**), (–)-terpestacin (**5**), and (+)-neoisocoumarin (**6**).

Keywords: cactus pear; scabby cankers; *Neofusicoccum batangarum*; phytotoxins

Key Contribution: *Neofusicoccum batangarum*, the causal agent of the scabby canker of cactus pear (*Opuntia ficus-indica* L.) in minor Sicily islands, was grown *in vitro* to investigate its capacity to produce phytotoxic secondary metabolites. The bioguided purification of its organic extract allowed for the isolation of five low molecular weight compounds that showed phytotoxicity on host (cactus pear) and non-host (tomato) plants.

1. Introduction

Cactus pear (*Opuntia ficus-indica* (L.) Mill.), Cactaceae family, is believed to be native of Mexico [1], and after the discovery of America, it was introduced into the Mediterranean Basin where it is now naturalized [2]. In Sicily, it has become an economically important fruit crop and a characteristic feature of the landscape. Cactus pear is also cultivated, mostly as productive living fences, in minor islands around Sicily, and as a fruit crop in Sardinia, Apulia, Calabria, and Basilicata Italian regions. Countries where cactus pear is also cultivated include Mexico, United States of America, Chile, Brazil, North Africa, South Africa, Middle East, Turkey, Tunisia, Malta, etc.

Recently, a severe infectious disease of the plant was reported in some minor islands of Sicily: Lampedusa and Linosa of the Pelagie archipelago; Favignana of the Aegadian archipelago; and Ustica, a small island in the Tyrrhenian Sea [3]. Symptoms of this disease, which has been named scabby cankers, were visible on cladodes and included radially expanding, crusty, concentric, silvery, perennial cankers, with a leathery, brown halo (Figure 1). Characteristically, an abundant, milky, viscous exudate, caking on contact with air, leaked from cankers and formed strips or cerebriform masses (Figure 1). With time, the exudate in the central part of the canker became black, giving the cankers an appearance of carbonaceous crusts, and the cankers ceased to expand in the coldest season of the year.



Figure 1. Symptoms of scabby cankers on cladodes of pear cactus (*O. ficus-indica* L.), including radially expanding, crusty, concentric, silvery, perennial cankers, with a leathery, brown halo (**left panel**); and an abundant milky viscous exudate, caking on contact with air, which leaked from cankers and formed strips or cerebriform masses (**right panel**).

The causal agent of the scabby canker of cactus pear found in minor islands of Sicily was identified as *Neofusicoccum batangarum* Begoude, Jol. Roux & Slippers, a fungal species not reported previously in Europe, whose distribution includes Africa, Brazil, and USA [4–6]. In Brazil, *N. batangarum* was reported as an aggressive pathogen of cashew (*Anacardium occidentale*) and cochineal cactus (*Nopalea cochenillifera* (L.) Salm-Dyck, syn. *Opuntia cochenillifera* (L.) Mill.), a relative of cactus pear [6,7]. On cochineal cactus in Brazil, *N. batangarum*, alone or in association with other fungi, including different species of Botryosphaeriaceae, causes a disease that was named cladode brown spot and constitutes a serious threat to the cultivation of cochineal cactus as a fodder for livestock [7–10]. In preliminary cross-pathogenicity tests, the fungus isolated from infected cactus pear plants in minor islands of Sicily was able to reproduce the disease symptoms on the host plant and to induce a disease reaction on other plant species, such as Aleppo pine (*Pinus halepensis*), almond (*Prunus dulcis*), sweet orange (*Citrus sinensis*), citrange (*Citrus sinensis* *Poncirus trifoliata*), and holm oak (*Quercus ilex*) trees. These results show that *N. batangarum* has a wide host range like many other Botryosphaeriaceae species, which are frequently reported as causal agents of different important crop diseases, including the grapevine *Botryosphaeria* dieback [11–15].

The purpose of this study was to characterize the agent of the scabby canker of cactus pear for its ability to accumulate in culture biologically active substances, namely phytotoxins, which may have a role in the production of disease symptoms. The chemical identification of phytotoxins, obtained from the culture filtrates of *N. batangarum*, and their toxic effects on host and non-host plants are reported.

2. Results and Discussion

The organic extract of the *N. batangarum* culture was purified using both CC (Column Chromatography) and TLC (Thin Layer Chromatography) as reported in detail in the Materials and Methods, to produce five pure metabolites. They were identified, by comparing their ¹H NMR, MS, and specific optical rotation with the data reported in the literature, as (–)-(R)-mellein; (±)-botryosicoumarin A; (–)-(3R,4R)- and (–)-(3R,4S)-4-hydroxymellein; (–)-terpestacin; and

(+)-3,4-dihydro-4,5,8-trihydroxy-3-methylisocoumarin, which was named (+)-neoisocoumarin (**1–6**; Figure 2). The purity of compounds **1–6** was >95% as ascertained via ¹H NMR and HPLC analysis.

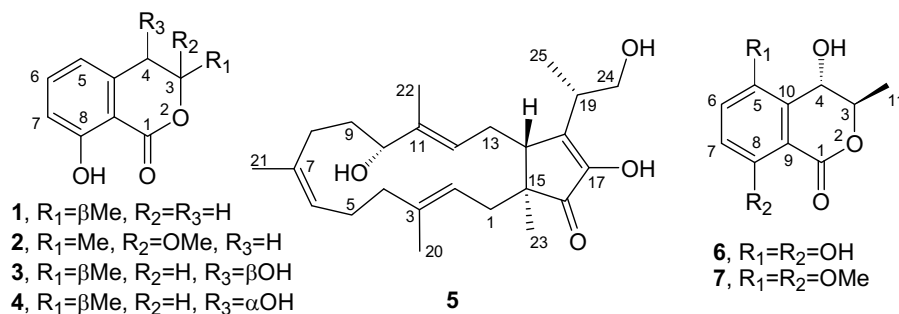


Figure 2. The structures of (–)-(R)-mellein (**1**), (±)-botryoisocoumarin A (**2**), (–)-(3R,4R)- and (–)-(3R,4S)-hydroxymellein (**3** and **4**), (–)-terpestacin (**5**), and (+)-neoisocoumarin (**6**).

These data were very similar to those previously reported in the literature for **1** [13,16–20], for **2** isolated in a racemic mixture [16], for **3** and **4** [17,21,22] for **5** [23–25], and for **6** [26]. Furthermore, **1** and **3–5** were also identified using TLC, performed in different conditions, in comparison using co-chromatography with standards.

(–)-(R)-Mellein (**1**) and its derivatives, including **3** and **4**, belong to the class of isocoumarins and are widely found in the fungal kingdom [13,15,19–21,27–31]; they have also been produced by plants and insects [32–35]. They are reported as phytotoxic metabolites of the fungi pathogen of forest and ornamental plants [36,37], and have been shown to possess a plethora of biological activities, including antiviral and antiparasitic activities [27,38–40]. Recently, in an advanced review of phytotoxins produced by grapevine pathogens [15], **1**, **3**, and **4** are reported as known phytotoxic metabolites synthesized by Botryosphaeriaceae species, inducing grapevine trunk disease, and **1** has also been found in infected grapevine wood [20]. These results suggested the potential use of these compounds as predictive biomarkers for early recognition of the disease [15]. However, the role of **1**, **3**, and **4** in the pathogenic process has not yet been clarified. Considering the potential application, some isocoumarins, such as cheniscoumarin, have been tested for the control of noxious weeds [41,42].

(±)-Botryoisocoumarin A (**2**) was isolated, together with 3,8-dihydroxy-3-methylisochroman-1-one and 4,8-dihydroxy-3-methylisochroman-1-one from *Botryosphaeria* sp. F00741 [16]. Then, it was also obtained together with five other metabolites from the mangrove *Kandelia candel*. This is an endophytic fungus *Botryosphaeria* sp. KcF6 studied during a screening carried out to find new metabolites for drug development. Compound **2** showed COX-2 inhibitory activity (IC₅₀ = 6.51 μM) but no cytotoxic activity. However, the structure drawn did not correspond to that of **2** [43]. Successively, **2** was isolated from the marine mangrove-derived fungus *Aspergillus ochraceus*, together with three new metabolites and another eleven known ones. In this study, some efforts were made to assign its absolute configuration (AC) at C-3 using X-ray methods but the results demonstrated the racemic nature of **2**, which was then named (±)-botryoisocoumarin A [44]. Compound **2**, together with a new acetate derivative and four already known compounds, were also isolated from *Aspergillus westerdijkiae* SCSIO 05233, a deep sea fungus, but **2** did not show antibiotic or cytotoxic activities [45].

(–)-Terpestacin (**5**) was isolated from the endophytic fungus *F. proliferatum* MA-84 [46] and from *Cleistothelobolus nipigonensis* and *Neogymnomyces virgineus* [25]. In addition, some key derivatives were hemi-synthesized from terpestacin and fusaproliferin. When they were tested against *Alternaria brassicicola*, *Botrytis cinerea* and *Fusarium graminearum* showed antifungal activity [25]. Recently, terpestacin was also isolated from *Rutstroemia capillus-albis* (Rutstroemiaceae, Helotiales, Leotiomyces), the causal agent of “bleach blonde syndrome” on the grass weed *Bromus tectorum* (cheatgrass) in North America [47]. When assayed on the host plant, **5** showed high phytotoxicity at 10^{−4} M, thus they should have a role in pathogenesis on *B. tectorum* [47].

(+)-3,4-Dihydro-4,5,8-trihydroxy-3-methylisocoumarin (**6**) was previously obtained, together with two already known compounds, from *Phomopsis* sp. (No. ZH-111) during a screening aimed at finding new compounds from endophytes of the South China Sea [26]. When assayed on zebrafish, the tetrasubstituted-3,4-dihydroisocoumarin significantly accelerates the growth of vessels but showed only weak cytotoxicity on the two cancer cell lines tested [26]. However, Yang et al. [26] assigned only the $3R^*,4S^*$ relative configuration to this compound based on the correlation measured in the NOESY spectrum. After recording the NOESY spectrum of **6** in the same conditions, we observed the expected correlations between H-6 and H-7, H-3 and Me-11, and H-4 and Me-11, and thus **6** had the same relative configuration that was assigned by Jang et al. [26].

Thus, to assign the absolute configuration at C-3 and C-4, **6** was firstly converted in the corresponding 5,8-*O,O'*-dimethyl ether derivative (**7**), whose spectroscopic data (^1H and ^{13}C NMR and ESI MS) were fully consistent with the structure of **6**. The ^1H NMR spectrum of **7** differed from that of **6** due to the two methoxy groups at δ 3.90 and 3.88. Its ESI MS spectrum exhibited the dimer sodiated form $[2\text{M} + \text{Na}]^+$, the potassium $[\text{M} + \text{K}]^+$ and sodium $[\text{M} + \text{Na}]^+$ clusters, and the protonated form $[\text{M} + \text{H}]^+$ at m/z 499, 277, 261, and 239, respectively. Furthermore, the protonated form generated the significant fragmentation ion $[\text{M} + \text{H} - \text{H}_2\text{O}]^+$ at m/z 193 via the loss of H_2O .

5,8-*O,O'*-dimethyl ether derivative of **6** (**7**) was transformed into the relative diastereomeric *S*-MTPA and *R*-MTPA monoesters (**8** and **9**, respectively) by reacting with *R*-(-)- α -methoxy- α -trifluoromethylphenylacetyl (MTPA) and *S*-(+)-MTPA chlorides. Surprisingly, the downfield shifts of H-3 ($\Delta\delta$ 0.48 and 0.47 in both **8** and **9**, respectively), instead of the expected downfield shift of H-4, was observed by comparing the ^1H NMR spectra of **8** and **9** with that of **7**. The reaction mechanism that could explain this result is reported in Figure 3. The driving force of the reaction was the hydroxyl anion generated from KOH where pyridine was preserved in non-dry conditions.

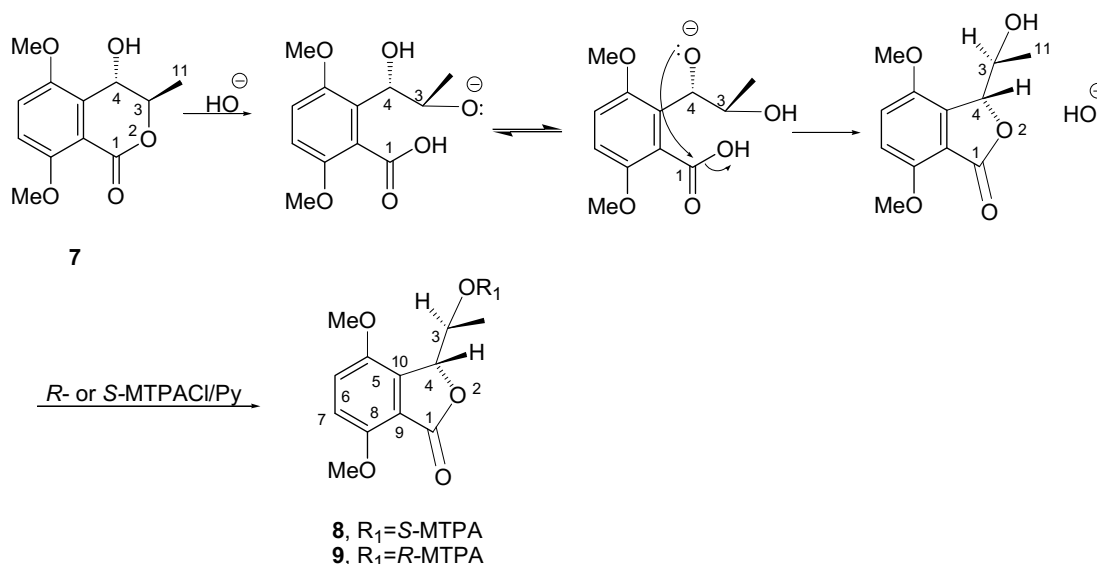


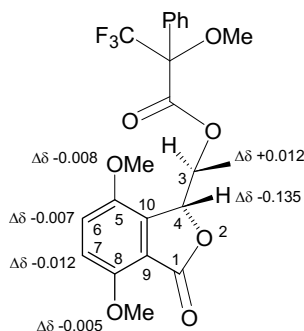
Figure 3. Mechanism of the conversion of the dimethylether of (+)-neoisocoumarin (**7**) into the corresponding diastereomeric benzofuranones (**8** and **9**) by reaction with *R*-(-)- α -methoxy- α -trifluoromethylphenylacetyl (MTPA) and *S*-(+)-MTPA chlorides.

However, the stereochemistry of C-3 and C-4 in the resulting benzofuranone did not change. The intermediate benzofuranone reacted with (*R*)-(-)- and (*S*)-(+)-MTPACl, yielding the corresponding monoesters **8** and **9**, respectively. Subtracting the chemical shifts of **9** from those of **8** (Table 1), the $\Delta\delta$ (**8–9**) values for all the protons were determined and reported in Figure 4.

Table 1. ^1H NMR data of 4-*O*-(*S*)- and 4-*O*-(*R*)-MTPA esters of 5,8-*O,O'*-dimethyl ether of (+)-neoisocoumarin (**8** and **9**, respectively).¹

Position	8	9
	δ_{H} (J in Hz)	δ_{H} (J in Hz)
3	5.960 (1H) dq (2.2, 6.6)	5.958 (1H) dq (2.2, 6.6)
4	5.694 (1H) d (2.2)	5.829 (1H) d (2.2)
6	7.361 (1H) d (8.9)	7.368 (1H) d (8.9)
7	7.129 (1H) d (8.9)	7.141 (1H) d (8.9)
Me-C3	1.092 (3H) d (6.6)	0.982 (3H) d (6.6)
OMe ²	3.950(3H) s	3.955 (3H) s
OMe ²	3.888 (3H) s	3.896 (3H) s
OMe	3.574 (3H) s	3.626 (3H) s
Ph	7.585–7.485 (5H) m	7.584–7.481 (5H) m

¹ The chemical shifts are in δ values (ppm) from TMS (Tetramethylsilane). ² These two signals could be exchanged.

**Figure 4.** Structures of 4-*O*-*S*- and 4-*O*-*R*-MTPA esters of 5,8-*O,O'*-dimethyl ether of (+)-neoisocoumarin (**8** and **9**, respectively), reporting the $\Delta\delta$ value of each proton system.

Applying model A as reported in Cimmino et al. [48], the (*R*) configuration was assigned at C-3, and consequently, on the basis of NOESY data, the (*S*) one was at C-4. Then, **6** was formulated as (+)-(3*R*,4*S*)-3,4 dihydro-4,5,8-trihydroxy-3-methylisocoumarin and named (+)-neoisocoumarin.

All the isolated compounds (**1–6**) were screened for phytotoxic activity as described in detail in Materials and Methods. All phytotoxins tested at the highest concentrations induced necrosis around inoculation points after 7 days, on cladodes of cactus pear (Figure 5), as well as on tomato leaves (Figure 6). However, **1**, **3**, and **4** were only phytotoxic at the highest concentrations on cactus pear and on non-host tomato plants (Tables 2 and 3). All three metabolites were found to be produced by *N. parvum*, another species in the genus, and other fungi in the Botryosphaeriaceae family associated with grapevine trunk diseases, confirming that they may be virulence factors in plant diseases caused by these fungi, although their role in the pathogenesis is still controversial [19,20]. (\pm)-Botryoisocoumarin A (**2**), (+)-neoisocoumarin (**6**), and (–)-terpestacin (**5**) showed phytotoxic activity, both on tomato (non-host) and cactus pear (host) plants in biological assays (Tables 2 and 3), even at the lowest concentrations used (1.2×10^{-4} for **5**, 2.4×10^{-4} M for **2** and **6**). The metabolites **2**, **5**, and **6** thus proved to have almost the same spectrum of phytotoxic activity as they showed a comparable activity against host and non-host plants.

Table 2. Phytotoxicity on tomato of 1–6 tested at various concentrations using the leaf puncture assay and evaluated based on the size of the necrotic lesions.

Compound	Concentration (M)	Mean Lesion Area (mm ²) ¹	Compound	Concentration (M)	Mean Lesion Area (mm ²) ¹
1	5.6×10^{-3}	2.75 ± 0.68	4	5.2×10^{-3}	3.14 ± 0.00
	2.8×10^{-3}	2.36 ± 0.79		2.6×10^{-3}	2.75 ± 0.68
	1.4×10^{-3}	0.00 ± 0.00		1.3×10^{-3}	0.00 ± 0.00
	5.6×10^{-4}	0.00 ± 0.00		5.2×10^{-4}	0.00 ± 0.00
	2.8×10^{-4}	0.00 ± 0.00		2.6×10^{-4}	0.00 ± 0.00
2	4.8×10^{-3}	7.98 ± 1.28	5	2.5×10^{-3}	5.10 ± 1.29
	2.4×10^{-3}	7.46 ± 1.5		1.2×10^{-3}	5.50 ± 1.04
	1.2×10^{-3}	6.67 ± 1.5		6.2×10^{-4}	4.81 ± 1.17
	4.8×10^{-4}	6.80 ± 1.71		2.4×10^{-4}	4.81 ± 1.3
	2.4×10^{-4}	6.28 ± 1.03		1.2×10^{-4}	4.61 ± 1.6
3	5.2×10^{-3}	3.14 ± 0.00	6	4.8×10^{-3}	7.98 ± 1.28
	2.6×10^{-3}	2.36 ± 1.36		2.4×10^{-3}	7.07 ± 1.26
	1.3×10^{-3}	0.00 ± 0.00		1.2×10^{-3}	6.67 ± 0.81
	5.2×10^{-4}	0.00 ± 0.00		4.8×10^{-4}	4.97 ± 1.55
	2.6×10^{-4}	0.00 ± 0.00		2.4×10^{-4}	5.36 ± 1.65

¹ Mean of 12 replications (three plants and four leaves per plant).

Table 3. Phytotoxicity on cactus pear of 1–6 tested at various concentrations with the cladode puncture method and evaluated based on the size of the necrotic lesions.

Compound	Concentration (M)	Mean Lesion Area (mm ²) ¹	Compound	Concentration (M)	Mean Lesion Area (mm ²) ¹
1	5.6×10^{-3}	3.14 ± 0.00	4	5.2×10^{-3}	6.28 ± 1.56
	2.8×10^{-3}	2.36 ± 0.79		2.6×10^{-3}	2.36 ± 0.79
	1.4×10^{-3}	2.75 ± 0.68		1.3×10^{-3}	3.14 ± 0.00
	5.6×10^{-4}	0.00 ± 0.00		5.2×10^{-4}	0.00 ± 0.00
	2.8×10^{-4}	0.00 ± 0.00		2.6×10^{-4}	0.00 ± 0.00
2	4.8×10^{-3}	11.00 ± 1.57	5	2.5×10^{-3}	11.58 ± 1.57
	2.4×10^{-3}	9.81 ± 1.75		1.2×10^{-3}	7.07 ± 1.67
	1.2×10^{-3}	11.78 ± 1.36		6.2×10^{-4}	6.28 ± 1.32
	4.8×10^{-4}	5.50 ± 0.79		2.4×10^{-4}	3.53 ± 0.68
	2.4×10^{-4}	7.07 ± 0.00		1.2×10^{-4}	2.94 ± 1.40
3	5.2×10^{-3}	3.14 ± 0.00	6	4.8×10^{-3}	11.78 ± 1.60
	2.6×10^{-3}	2.61 ± 0.93		2.4×10^{-3}	9.62 ± 1.55
	1.3×10^{-3}	3.14 ± 0.00		1.2×10^{-3}	9.62 ± 1.55
	5.2×10^{-4}	0.00 ± 0.00		4.8×10^{-4}	4.51 ± 1.61
	2.6×10^{-4}	0.00 ± 0.00		2.4×10^{-4}	3.50 ± 0.68

¹ Mean of eight replications (two cladodes from distinct plants and four punctures per each cladode).



Figure 5. Control cladode (MeOH 4%, *v/v*) (a), necrotic areas produced by (-)-(*R*)-mellein (1), (\pm)-botryoisocoumarin A (2), (-)-(*3R,4R*)-4-hydroxymellein (3), (-)-(*3R,4S*)-4-hydroxymellein (4), (-)-terpestacin (5), and (+)-neoisocoumarin (6) on cladodes of cactus pear.

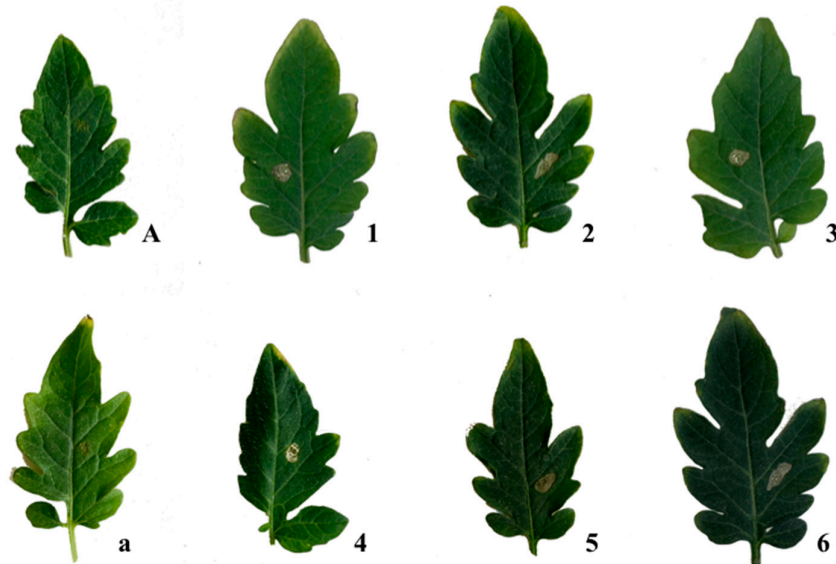


Figure 6. Control leaves with sterile distilled water (A) and MeOH (4% *v/v*) (a); necrotic areas produced by (-)-(*R*)-mellein (1), (\pm)-botryoisocoumarin A (2), (-)-(*3R,4R*)-4-hydroxymellein (3), (-)-(*3R,4S*)-4-hydroxymellein (4), (-)-terpestacin (5), and (+)-neoisocoumarin (6) on tomato leaves.

The results showed that (\pm)-botryoisocoumarin A (2), (-)-terpestacin (5), and (+)-neoisocoumarin (6) were by far more phytotoxic than melleins (1, 3, and 4) when tested on cladodes of cactus pear and tomato leaves. Compounds 2 and 6 were the most active at concentrations in a range from 10^{-3} M to 10^{-4} M, inducing a necrosis area around the inoculation points in both host and non-host plants, followed by 5. The ability of 2, 5, and 6 to induce large necrotic lesions on cactus pear cladodes

suggests that these toxins may be involved in the scabby cankers disease syndrome. These results also indicate the ability of fungi in the Botryosphaeriaceae family to produce phytotoxins that are active against non-taxonomically related plants, such as cactus pear and tomato, and could explain the wide host spectrum of many species in the family. Moreover, it can be speculated that the allelopathic, antifungal, and antibacterial activity of terpestacin demonstrated in previous studies [25,44] might enhance the ecological fitness of *N. batangarum* and might explain the ability of this fungus to rapidly colonize the cactus pear cladode and sporulate on infected tissues [3] before they are invaded by other saprophytes or opportunistic weak pathogens of the plant biosphere. Due to its allelopathic activity, *N. batangarum* was indicated as a potential biocontrol agent [49,50]. In a recent review, Masi et al. [51] questioned the possibility of using terpestacin as a biopesticide because of its toxicity and stressed that, although the functions of this mycotoxin in nature have not been clearly established, its allelopathic activity would suggest a role in eliminating other microorganisms competing in the same environment.

3. Conclusions

(-)-(R)-Mellein, (-)-(3R,4R)- and (-)-(3R,4S)-4-hydroxymellein, (±)-botryoisocoumarin A, (-)-terpestacin, and (+)-neoisocoumarin were obtained for the first time as phytotoxins of *N. batangarum*. The absolute configuration of (+)-neoisocoumarin was determined by using the advanced Mosher's method. Considering the phytotoxic activity on both host and non-host test plants, it can be deduced that all these metabolites were involved in the syndrome of scabby cankers disease of cactus pear, and like other Botryosphaeriaceae, *N. batangarum* has a wider host range than previously thought.

4. Materials and Methods

4.1. General Experimental Procedures

A Jasco P-1010 digital polarimeter (Jasco, Tokyo, Japan) was used to record the optical rotations in CHCl₃, or as stated otherwise. Electrospray ionization (ESI) mass spectrometry and liquid chromatography/mass spectrometry (LC/MS) analyses were performed using an LC/MS TOF system Agilent 6230B (Agilent Technologies, Milan, Italy), HPLC 1260 Infinity. A Phenomenex (Bologna, Italy) Luna (C₁₈ (2) 5 mm, 150 × 4.6 mm column) was used to perform the high-performance liquid chromatography (HPLC) separations. HPLC separation was carried out with the mobile phase used to elute the samples being MeCN-H₂O 85:15 at a flow rate of 0.3 mL/min at 25 °C, injecting 10 mL of a solution of 1 ppm for the pure compounds. Bruker 400 Anova Advance (Karlsruhe, Germany) and Varian Inova 500 MHz (Palo Alto, CA, USA) instruments were used to record the ¹H NMR spectra at 400 or 500 MHz in CDCl₃, if not otherwise noted, at 298 °K. Column chromatography (CC) was performed using silica gel (Merck, Kieselgel 60, 0.063–0.200 mm). Preparative and analytical TLC were carried out on silica gel (Kieselgel 60, F₂₅₄, 0.25 and 0.5 mm, respectively) plates (Merck, Darmstadt, Germany). The spots were visualized using the procedure previously described [47]. Sigma-Aldrich Co. (St. Louis, MO, USA) supplied all the reagents and the solvents.

4.2. Fungal Strain

The strains of *N. batangarum* used in this study were collected from infected host plant tissues on the islands of Favignana, Lampedusa, Linosa, and Ustica from 2013 to 2018 and maintained in potato dextrose agar (PDA, Fluka, Sigma-Aldrich Chemic GmbH, Buchs, Switzerland) and stored at 4 °C in the strain collection of the Dipartimento di Agricoltura, Alimentazione e Ambiente, Università di Catania, Catania, Italy. *N. batangarum* was obtained from scabby cankers on cladodes of cactus pear (*Opuntia ficus-indica* L.) recovered from minor islands of Sicily (Lampedusa, Linosa, Favignana, and Ustica). Four representative isolates, one from each island, were deposited at CBS-KNAW Biodiversity Centre, strains code nos. CBS143023, CBS143024, CBS143025, and CBS143026 [3].

4.3. Production, Extraction, and Isolation of Secondary Metabolites

The isolate CBS143023 (*Neofusicoccum batangarum*) was grown in liquid culture to obtain the liquid filtrate. In detail, the mycelium of fungal cultures, grown on potato dextrose agar for 5–7 days at 25 °C, was homogenized with sterile distilled water. Three milliliters of this suspension was distributed individually into 1 L Roux flasks containing 170 mL of modified Difco™ Czapeck-Dox (Benton, Dickinson and Company, Sparks, MD, USA) medium with 0.5% yeast and 0.5% malt extract (pH 5.75) and incubated at 25 °C for 28 days in the dark [15]. At harvest, the liquid cultures were filtered, initially with a double layer of gauze to reduce the fungal biomass, and subsequently with suction filters using porous membrane filter complexes Stericup Millipore® (pore diameter = 0.22 µm). A total of 20 L of culture filtrate was obtained and stored at –20 °C until use. It was concentrated under reduced pressure at 35 °C to 1 L and extracted with EtOAc (3 × 1 L). The combined organic extracts were dried (Na₂SO₄) and evaporated under reduced pressure. The oily residue (1.84 g) was fractionated via column chromatography eluted with chloroform/*iso*-propanol (9:1), obtaining twelve groups of homogeneous fractions. The residues (24.4 mg and 23.1 mg) of the first and second fractions were combined and further purified using preparative TLC eluted with hexane/ethyl acetate (8.5:1.5), yielding two pure metabolites as amorphous solids that were identified as (–)-(R)-mellein (**1**, 8.6 mg, 0.7 mg/L, R_f 0.4) and as (±)-botryoisocoumarin (**2**, 3.4 mg, 0.3 mg/L, R_f 0.3). The residue (41.6 mg) of the fourth fraction of the first column was purified using preparative TLC eluted with petroleum ether:acetone 8:2, producing two pure metabolites identified as (–)-(3R,4R)-4-hydroxymellein (**3**, 2.4 mg, 0.2 mg/L, R_f 0.3) and (–)-(3R,4S)-4-hydroxymellein (**4**, 3.6 mg, 0.3 mg/L, R_f 0.4). The residue (123.4 mg) of the fifth fraction of the original column was further purified using column chromatography on silica gel eluted with dichloromethane/*iso*-propanol (9.5:0.5), obtaining eleven groups of homogeneous fractions. The residues (17.5 mg and 10.0 mg) of the seventh and eighth fractions were combined and purified using analytical TLC eluted with dichloromethane/*iso*-propanol (9.5:0.5), obtaining a pure metabolite as an amorphous solid, which was identified as (–)-terpestacin (**5**, 6.0 mg, 0.5 mg/L, R_f 0.4). The residue (21.4 mg and 19.4 mg) of the fifth and sixth fractions were combined and purified using preparative TLC eluted with dichloromethane/*iso*-propanol (9.7:0.3), obtaining a pure compound identified as (+)-(3R*,4S*)-3,4-dihydro-4,5,8-trihydroxy-3methylisocoumarin, which was named (+)-neoisocoumarin (**6**, 8.0 mg, 0.7 mg/L, R_f 0.3).

(–)-(R)-Mellein (**1**): [α]²⁵_D –90 (c 0.2 CH₃OH); ¹H NMR, δ: 11.03 (s, HO-8), 7.41 (t, J = 8.4 Hz, H-6), 6.89 (d, J = 8.4 Hz, H-7), 6.69 (d, J = 8.4 Hz, H-5), 4.74 (tq, J = 6.9 and 6.3 Hz, H-3), 2.93 (d, J = 6.9 Hz, H₂-4), 1.53 (d, J = 6.3 Hz, Me-3). ESI MS (+) spectrum, m/z 179 [M + H]⁺. These data are in agreement with those previously reported [13,17–20].

(±)-Botryoisocoumarin (**2**): ¹H NMR, δ: 11.03 (s, HO-8), 7.41 (t, J = 8.3 Hz, H-6), 6.89 (d, J = 8.3 Hz, H-7), 6.69 (d, J = 8.3, H-5), 3.40 (OMe), 3.23 (d, J = 16.0 Hz, H-4A) 3.16 (d, J = 16.0 Hz, H-4B), 1.69 (s, Me-C3). These data are in agreement with those previously reported [16]. ESI MS (+) spectrum, m/z: 439 [2M + Na]⁺, 209 [M + H]⁺, 176 [MH - MeOH]⁺.

(–)-(3R,4R)-4-Hydroxymellein (**3**): [α]²⁵_D –29.0 (c 1.2 CH₃OH); ¹H NMR, δ: 10.99 (s, HO-8), 7.55 (t, J = 7.0 Hz, H-6), 7.03 (d, J = 7.0 Hz, H-7), 7.00 (d, J = 7.0 Hz, H-5), 4.68 (br q, J = 7.0 Hz, H-3), 4.60 (br s, H-4), 1.53 (d, J = 7.0 Hz, Me-C3). ESI MS (+) spectrum, m/z: 195 [M + H]⁺. These data are in agreement with the data previously reported [17–21].

(–)-(3R,4S)-4-Hydroxymellein (**4**): [α]²⁵_D –27.0 (c 1.1 CH₃OH); ¹H NMR and ESI MS (+) data were very similar to those of **3**. These data are also in agreement with the data previously reported [17–22].

(–)-Terpestacin (**5**): [α]²⁵_D –17.7 (c 0.4); ¹H NMR, δ: 5.38 (m, H-12), 5.25 (dd, J = 10.6 and 5.4 Hz, H-2), 5.13 (m, H-6), 4.07 (dd, J = 9.7 and 3.6 Hz, H-10), 3.85 (dd, J = 10.4 and 7.0 Hz, H-24A), 3.80 (dd, J = 10.4 and 5.5 Hz, H-24B), 2.66 (m, H-19), 2.36 (dd, J = 13.7 and 10.6 Hz, H-1A), 2.44 (d, J = 17.0 Hz, H-14), 2.26 and 2.11 (2H, both m, H₂-5), 2.24 and 2.10 (2H, both m, H₂-4), 2.18 and 1.78 (2H, both m, H₂-8), 1.92 (m, H-13A), 1.75 (m, H-1B), 1.75 and 1.70 (both m, H₂-9), 1.67 (s, Me-20), 1.64 (s, Me-21), 1.56 (s, Me-22), 1.29 (d, J = 7.3 Hz, Me-25), 0.99 (s, Me-23); ESI MS (+) spectrum, m/z 425 [M + Na]⁺. These data are in agreement with those previously reported [23–25].

(+)-Neoisocoumarin (**6**): $[\alpha]^{25}_D + 50$ (c 0.4); $^1\text{H NMR}$, δ : 10.68 (s, HO-8), 7.16 (d, $J = 9.0$ Hz, H-6), 6.84 (d, $J = 9.0$ Hz, H-7), 5.03 (d, $J = 4.1$ Hz, H-4), 4.90 (dq, $J = 6.7$ and 4.4 Hz, H-3), 1.35 (d, $J = 6.7$ Hz, Me-C3); ESI MS (+) spectrum, m/z 443 $[2M + Na]^+$, 233 $[M + Na]^+$, 211 $[M + H]^+$, 193 $[MH - H_2O]^+$, 175 $[MH - 2H_2O]^+$. These data were very similar to that already reported [23].

5,8-O,O-Dimethyl ether of (+)-neoisocoumarin (**7**): To (+)-neoisocoumarin (**6**, 1 mg) in methanol (200 mL), diazomethane in ether solution was added in excess. The reaction performed overnight at 25 °C was stopped by evaporating the solvent under a N_2 stream. The residue (1.2 mg) was purified using TLC, eluted with chloroform/*iso*-propanol 9.5:0.5 to yield **7** as a homogeneous oil (1.1 mg, R_f 0.4). Derivate **7** had the following: $^1\text{H NMR}$, δ : 7.29 (d, $J = 8.8$ Hz, H-6), 7.07 (d, $J = 8.8$ Hz, H-7), 5.49 (d, $J = 2.4$ Hz, H-4), 4.48 (dq, $J = 6.3$ and 2.4 Hz, H-3), 3.90 and 3.88 (s, 3H each $2 \times$ OMe), 0.85 (d, $J = 6.3$ Hz, Me-11); ESI MS (+) spectrum, m/z 499 $[2M + Na]^+$, 277 $[M + K]^+$, 261 $[M + Na]^+$, 239 $[M + H]^+$, 221 $[M + H - H_2O]^+$.

5-O-(S)- α -Methoxy- α -trifluoromethyl- α -phenylacetate (MTPA) ester of **7** (**8**). To **7** (1.1 mg) in pyridine (100 mL), (R)-(-)-MPTA-Cl (10 mL) was added. The mixture was carried out for 1 h at 25 °C and stopped by adding methanol and benzene. The mixture was evaporated using a N_2 stream. The residue (1.3 mg) was purified using analytical TLC eluted with dichloromethane/*iso*-propanol (9.7:0.3), yielding **8** as a homogeneous oil (0.6 mg, R_f 0.7). It had: $^1\text{H NMR}$, see Table 1; ESI MS (+) spectrum, m/z 477 $[M + Na]^+$, 455 $[M + H]^+$.

5-O-(R)- α -methoxy- α -trifluoromethyl- α -phenylacetate (MTPA) ester of **6** (**9**): To **7** (1.1 mg) in pyridine (100 mL), (S)-(+)-MPTA-Cl (10 mL) was added and the reaction was performed as previously reported. The crude residue (1.2 mg) was purified using analytical TLC eluted with dichloromethane/*iso*-propanol (9.7:0.3), producing **9** as a homogeneous oil (0.4 mg, R_f 0.7). Compound **9** had: $^1\text{H NMR}$, see Table 1; ESI MS (+) spectrum, m/z 477 $[M + Na]^+$, 455 $[M + H]^+$.

4.4. Biological Assays

The metabolites isolated (**1–6**) were tested on young cladodes of host plant cactus pear (*Opuntia ficus-indica* (L.) Mill.) and on non-host tomato plant (*Solanum lycopersicum* L.) leaves. Pure metabolites were first dissolved in methanol, and then diluted with distilled water (final concentration of methanol, 4%) up to the desired concentrations. For each metabolite, 50 μL of the solution were pipetted into cladodes at concentrations of 0.05, 0.1, 0.25, 0.5, or 1 mg/mL. The phytotoxicity of the pure metabolites of *N. batangarum* was also tested using a puncture assay on tomato leaves. A droplet (10 μL) of each metabolite, at concentrations of 0.05, 0.1, 0.25, 0.5, or 1 mg/mL, was placed on the leaf lamina previously punctured by a needle. One cladode of a single plant of cactus pear and four leaves of tomato were used as replicates, and the test was repeated twice. Methanol (4% *v/v*) and sterile distilled water were used as controls. Symptoms of phytotoxicity of inoculated cladodes and leaves, kept in a climatic chamber under controlled conditions, were observed each day for 7 days. The size (mm^2) of necrotic the area surrounding the punctures was measured.

Author Contributions: Conceptualization, A.E., S.O.C., and G.S.; Investigation, P.N., F.A., and M.M.; Writing—original draft, M.M., A.E., S.O.C., and G.S.; funding acquisition, M.M. All authors have read and agreed to the published version of the manuscript.

Funding: This work was funded by a grant awarded to M.M. by Programme STAR 2017 and MIUR - FFABR 2017 (S.O.C. grant, number 5A725192051), alongside financial support from Compagnia di San Paolo and University of Naples Federico II (grant number E62F16001250003). F. A. was supported by a Ph.D. fellowship provided by the University of Palermo.

Acknowledgments: A.E. is associated with the Istituto di Chimica Biomolecolare del CNR, Pozzuoli, Italy.

Conflicts of Interest: The authors declare no conflict of interest.

References

1. Kieling, R.; Metzger, D. Origin and Taxonomy of *Opuntia ficus-indica*. In *Crop Ecology, Cultivation and User of Cactus Pear*; Inglese, P., Mondragon, C., Nefzaoui, A., Saenz, C., Eds.; FAO and ICARDA: Rome, Italy, 2017; pp 14–19.
2. Ochoa, M.J.; Barbera, G. History and economic and agro-ecological importance. In *Crop Ecology, Cultivation and Uses of Cactus Pear*; Inglese, P.; Mondragon, C.; Nefzaoui, A.; Saenz, C., Eds.; FAO and ICARDA: Rome, Italy, 2017; pp 1–11.
3. Schena, L.; Surico, G.; Burruano, S.; Giambra, S.; Pane, A.; Evoli, M.; Cacciola, S.O. First report of *Neofusicoccum batangarum* as causal agent of scabby cankers of Cactus pear (*Opuntia ficus-indica*) in minor islands of Sicily. *Plant Dis.* **2018**, *102*, 445–445.
4. Phillips, A.J.L.; Alves, A.; Abdollahzadeh, J.; Slippers, B.; Wingfield, M.J.; Groenewald, J.Z.; Crous, P.W. The Botryosphaeriaceae: Genera and species known from culture. *Studies Mycol.* **2013**, *76*, 51–167.
5. Conforto, C.; Lima, N.B.; Garcete-Gómez, J.M.; Câmara, M.P.S.; Michereff, S.J. First report of cladode brown spot in cactus prickly pear caused by *Neofusicoccum batangarum* in Brazil. *Plant Dis.* **2016**, *100*, 1238.
6. Netto, M.S.B.; Lima W.G.; Correia K.G.; Da Silva, C.F.B.; Thon M.; Martins, R.B.; Miller, R.N.G.; Michereff, F.J.; Câmara, M.P.F. Analysis of phylogeny, distribution and pathogenicity of Botryosphaeriaceae species associated with gummosis of *Anacardium* in Brasil, with a new species of *Lasiodiplodia*. *Fungal Biol.* **2017**, *121*, 437–451.
7. Dissanayake, A.J.; Phillips, A.J.L.; Li, X.H.; Hyde, K.D. Botryosphaeriaceae: Current status of genera and species. *Mycosphere* **2016**, *7*, 1001–1073.
8. Garcete-Gómez, J.M.; Conforto, C.; Domínguez-Monge, S.; Flores-Sánchez, J.L.F.; Mora-Aguilera, G.; Michereff, S.J. Sample size for assessment of cladode brown spot in prickly pear cactus. *Eur. J. Plant Pathol.* **2017**, *149*, 759–763.
9. Conforto, C.; Lima, N.B.; Silva, F.J.A.; Câmara, M.P.S.; Maharachchikumbura, S.; Michereff, S.J. Characterization of fungal species associated with cladode brown spot on *Nopalea cochenillifera* in Brazil. *Eur. J. Plant Pathol.* **2019**, *155*, 1179–1194.
10. Feijo, F.M.; Silva, M.J.S.; Nascimento, A.D.; Infante, N.B.; Ramos-Sobrinho, R.; Assunção, I.P.; Lima, G.S.A. Botryosphaeriaceae species associated with the prickly pear cactus, *Nopalea cochinellifera*. *Trop. Plant Pathol.* **2019**, *44*, 452–459.
11. Dissanayake, A.J.; Camporesi, E.; Hyde, K.D.; Phillips, A.J.L.; Fu, C.Y.; Yan, J.Y.; Li, X.H. *Dothiorella* species associated with woody hosts in Italy. *Mycosphere* **2016**, *7*, 51–63.
12. Andolfi, A.; Maddau, L.; Cimmino, A.; Linaldeddu, B.T.; Basso, S.; Deidda, A.; Evidente, A. Lasiostasmonates A–C, three jasmonic acid esters produced by *Lasiodiplodia* sp., a grapevine pathogen. *Phytochemistry* **2014**, *103*, 145–153.
13. Cimmino, A.; Cinelli, T.; Masi, M.; Reveglia, P.; da Silva, M.A.; Mugnai, L.; Evidente, A. Phytotoxic lipophilic metabolites produced by grapevine strains of *Lasiodiplodia* species in Brazil. *J. Agric. Food Chem.* **2017**, *65*, 1102–1107.
14. Reveglia, P.; Savocchia, S.; Billones-Baaijens, R.; Masi, M.; Cimmino, A.; Evidente, A. Phytotoxic metabolites by nine species of Botryosphaeriaceae involved in grapevine dieback in Australia and identification of those produced by *Diplodia mutila*, *Diplodia seriata*, *Neofusicoccum australe* and *Neofusicoccum luteum*. *Nat. Prod. Res.* **2019**, *33*, 2223–2229.
15. Masi, M.; Cimmino, A.; Reveglia, P.; Mugnai, L.; Surico, G.; Evidente, A. Advances on fungal phytotoxins and their role in grapevine trunk diseases. *J. Agric. Food Chem.* **2018**, *66*, 5948–5958.
16. Xu, Y.; Lu, C.; Zheng, Z. A new 3,4-dihydroisocoumarin isolated from *Botryosphaeria* sp. F00741. *Chem. Nat. Compd.* **2012**, *48*, 205–207.
17. Cole R. J.; Cox R.H. *Handbook of Toxic Fungal Metabolites*. Academic Press: New York, NY, USA, 1981; Volume 3, pp. 623–624.
18. Cabras, A.; Mannoni, M.A.; Serra, S.; Andolfi, A.; Fiore, M.; Evidente, A. Occurrence, isolation and biological activity of phytotoxic metabolites produced *in vitro* by *Sphaeropsis sapinea*, pathogenic fungus of *Pinus radiata*. *Eur. J. Plant Pathol.* **2006**, *115*, 187–193.
19. Evidente, A.; Punzo, B.; Andolfi, A.; Cimmino, A.; Melck, D.; Luque, J. Lipophilic phytotoxins produced by *Neofusicoccum parvum*, a grapevine canker agent. *Phytopathol. Mediterr.* **2010**, *49*, 74–79.

20. Abou-Mansour, E.; Débieux, J.L.; Ramírez-Suero, M.; Bénard-Gellon, M.; Magnin-Robert, M.; Spagnolo, A.; Serrano, M. Phytotoxic metabolites from *Neofusicoccum parvum*, a pathogen of *Botryosphaeria dieback* of grapevine. *Phytochemistry*, **2015**, *115*, 207–215.
21. Djoukeng, J.D.; Polli, S.; Larignon, P.; Abou-Mansour, E. Identification of phytotoxins from *Botryosphaeria obtusa*, a pathogen of black dead arm disease of grapevine. *Eur. J. Plant. Pathol.* **2009**, *124*, 303–308.
22. Devys, M.; Barbier, M.; Bousquet, J.F.; Kollmann, A. Isolation of the new (–)-(3R, 4S)-4-hydroxymellein from the fungus *Septoria nodorum* Berk. *Z. Naturforsch., C, J. Biosci.* **1992**, *47*, 779–781.
23. Oka, M.; Iimura, S.; Tenmyo, O.; Sawada, Y.; Sugawara, M.; Ohkusa, N.; Oki, T. Terpestacin, a new syncytium formation inhibitor from *Arthrinium* sp. *J. Antibiot.* **1993**, *46*, 367–373.
24. Trost, B.M.; Dong, G.; Vance, J.A. A Diosphenol-based strategy for the total synthesis of (–)-terpestacin. *J. Am. Chem. Soc.* **2007**, *129*, 4540–4541.
25. Cimmino, A.; Sarrocco, S.; Masi, M.; Diquattro, S.; Evidente, M.; Vannacci, G.; Evidente, A. Fusaproliferin, terpestacin and their derivatives display variable allelopathic activity against some Ascomycetous fungi. *Chem Biodivers.* **2016**, *13*, 1593–1600.
26. Yang, J.X.; Chen, Y.; Huang, C.; She, Z.; Lin, Y. A new isochroman derivative from the marine fungus *Phomopsis* sp. (No. ZH-111). *Chem. Nat. Compd.*, **2011**, *47*, 13.
27. Krohn, K.; Bahramsari, R.; Flörke, U.; Ludewig, K.; Kliche-Spory, C.; Michel, A.; Antus, S. Dihydroisocoumarins from fungi: isolation, structure elucidation, circular dichroism and biological activity. *Phytochemistry* **1997**, *45*, 313–320.
28. Rukachaisirikul, V.; Arunpanichlert, J.; Sukpondma, Y.; Phongpaichit, S.; Sakayaroj, J. Metabolites from the endophytic fungi *Botryosphaeria rhodina* PSU-M35 and PSU-M114. *Tetrahedron* **2009**, *65*, 10590–10595.
29. Salazar, A.; Rios, I. *Sustainable Agriculture: Technology, Planning and Management*; Nova Science Publishers: New York, NY, USA, 2010.
30. Ramírez-Suero, M.; Bénard-Gellon, M.; Chong, J.; Laloue, H.; Stempien, E.; Abou-Mansour, E.; Bertsch, C. Extracellular compounds produced by fungi associated with *Botryosphaeria dieback* induce differential defence gene expression patterns and necrosis in *Vitis vinifera* cv. Chardonnay cells. *Protoplasma* **2014**, *251*, 1417–1426.
31. Cimmino, A.; Maddau, L.; Masi, M.; Linaldeddu, B.T.; Evidente, A. Secondary metabolites produced by *Sardiniella urbana*, a new emerging pathogen on European hackberry. *Nat. Prod. Res.* **2019**, *33*, 1862–1869.
32. Bestmann, H.J.; Kern, F.; Schäfer, D.; Witschel, M.C. 3, 4-dihydroisocoumarins, a new class of ant trail pheromones. *Angew. Chem.* **1992**, *31*, 795–796.
33. Kern, F.; Klein, R.W.; Janssen, E.; Bestmann, H.J.; Attygalle, A.B.; Schäfer, D.; Maschwitz, U. Mellein, a trail pheromone component of the ant *Lasius fuliginosus*. *J. Chem. Ecol.* **1997**, *23*, 779–792.
34. Manigaunha, A.; Ganesh, N.; Kharya, M.D. Morning glory: A new thirst in-search of *de-novo* therapeutic approach. *Int. J. Phytomedicine* **2010**, *2*, 18–21.
35. Herzner, G.; Schlecht, A.; Dollhofer, V.; Parzefall, C.; Harrar, K.; Kreuzer, A.; Ruther, J. Larvae of the parasitoid wasp *Ampulex compressa* sanitize their host, the American cockroach, with a blend of antimicrobials. *Proc. Natl. Acad. Sci. USA* **2013**, *110*, 1369–1374.
36. Cimmino, A.; Maddau, L.; Masi, M.; Linaldeddu, B.T.; Pescitelli, G.; Evidente, A. Fraxitoxin, a new isochromanone isolated from *Diplodia fraxini*. *Chem. Biodivers.* **2017**, *14*, e1700325.
37. Masi, M.; Maddau, L.; Linaldeddu, B.T.; Scanu, B.; Evidente, A.; Cimmino, A. Bioactive metabolites from pathogenic and endophytic fungi of forest trees. *Curr. Med. Chem.* **2018**, *25*, 208–252.
38. Höller, U.; König, G.M.; Wright, A.D. Three new metabolites from marine-derived fungi of the genera *Coniothyrium* and *Microsphaeropsis*. *J. Nat. Prod.* **1999**, *62*, 114–118.
39. Dai, J.R.; Carté, B.K.; Sidebottom, P.J.; Sek Yew, A.L.; Ng, S.B.; Huang, Y.; Butler, M.S. Circumdatin G, a new alkaloid from the fungus *Aspergillus ochraceus*. *J. Nat. Prod.* **2001**, *64*, 125–126.
40. Zhao, J.H.; Zhang, Y.L.; Wang, L.W.; Wang, J.Y.; Zhang, C.L. Bioactive secondary metabolites from *Nigrospora* sp. LLGLM003, an endophytic fungus of the medicinal plant *Moringa oleifera* Lam. *World J. Microbiol. Biotechnol.* **2012**, *28*, 2107–2112.
41. Cimmino, A.; Masi, M.; Evidente, M.; Superchi, S.; Evidente, A. Fungal phytotoxins with potential herbicidal activity: chemical and biological characterization. *Nat. Prod. Rep.* **2015**, *32*, 1629–1653.
42. Evidente, M.; Cimmino, A.; Zonno, M.C.; Masi, M.; Berestetskyi, A.; Santoro, E.; Evidente, A. Phytotoxins produced by *Phoma chenopodiicola*, a fungal pathogen of *Chenopodium album*. *Phytochemistry* **2015**, *117*, 482–488.

43. Ju, Z.; Lin, X.; Lu, X.; Tu, Z.; Wang, J.; Kaliyaperumal, K.; Liu, Y. Botryoisocoumarin A, a new COX-2 inhibitor from the mangrove *Kandelia candel* endophytic fungus *Botryosphaeria* sp. KcF6. *J. Antibiot.* **2015**, *68*, 653–656.
44. Liu, Y.; Li, X.M.; Meng, L.H.; Wang, B.G. Polyketides from the marine mangrove-derived fungus *Aspergillus ochraceus* MA-15 and their activity against aquatic pathogenic bacteria. *Phytochem. Lett.* **2015**, *12*, 232–236.
45. Fredimoses, M.; Zhou, X.; Ai, W.; Tian, X.; Yang, B.; Lin, X.; Liu, Y. Westerdijkina A, a new hydroxyphenylacetic acid derivative from deep sea fungus *Aspergillus westerdijkiae* SCSIO 05233. *Nat. Prod. Res.* **2015**, *29*, 158–162.
46. Liu, D.; Li, X.M.; Li, C.S.; Wang, B.G. Sesterterpenes and 2H-pyran-2-ones (= α -pyrones) from the mangrove-derived endophytic fungus *Fusarium proliferatum* MA84. *Helv. Chim. Acta*, **2013**, *96*, 437–444.
47. Masi, M.; Meyer, S.; Górecki, M.; Pescitelli, G.; Clement, S.; Cimmino, A.; Evidente, A. Phytotoxic activity of metabolites isolated from *Rutstroemia* sp. n., the causal agent of bleach blonde syndrome on cheatgrass (*Bromus tectorum*). *Molecules*, **2018**, *23*, 1734.
48. Cimmino, A.; Masi, M.; Evidente, M.; Superchi, S.; Evidente, A. Application of Mosher's method for absolute configuration assignment to bioactive plants and fungi metabolites. *J. Pharmaceut. Biomed.* **2017**, *144*, 59–89.
49. Shetty, K.G.; Minnis, A.M.; Rossman, A.Y.; Jayachandran, K. The Brazilian peppertree seedborne pathogen, *Neofusicoccum batangarum*. *Biol. Control* **2011**, *56*, 91–97.
50. Dawkins, K.; Esiobu, N. Emerging insights on Brazilian pepper tree (*Schinus terebinthifolius*) invasion: the potential role of soil microorganisms. *Front. Plant Sci.* **2016**, *7*, 712, doi: 10.3389/fpls.2016.00712.
51. Masi, M.; Nocera, P.; Reveglia, P.; Cimmino, A.; Evidente, A. Fungal metabolites antagonists towards plant pests and human pathogens: structure-activity relationship studies *Molecules* **2018**, *23*, 834, doi: 10.3390/molecules23040834.



© 2020 by the authors. Licensee MDPI, Basel, Switzerland. This article is an open access article distributed under the terms and conditions of the Creative Commons Attribution (CC BY) license (<http://creativecommons.org/licenses/by/4.0/>).

Chapter 4.

Identification of *Neofusicoccum parvum* (*Botryosphaeriaceae*) as the causal agent of the bot gummosis disease of lemon (*Citrus × limon*) trees

4.1 Introduction

Trunk and branch cankers caused by species of *Botryosphaeriaceae* on citrus were traditionally referred to as *Diplodia* gummosis and *Dothiorella* gummosis (Klotz, 1978; Scaramuzzi, 1965). More recently the comprehensive term bot gummosis was introduced to indicate trunk and branch cankers of citrus caused by fungi in the *Botryosphaeriaceae* family in California (Adesemoye et al., 2014). All common names of the disease refer to the most typical symptom, i. e. the gum exudate oozing from the bark cankers. Another typical symptom of the disease is a chocolate brown to dark brown discoloration of the wood which becomes evident after peeling the bark. Originally, the fungi causing *Diplodia* gummosis and *Dothiorella* gummosis were identified as *Diplodia natalensis* and *Dothiorella gregaria* (syn. *Botryosphaeria ribis*), respectively (Klotz, 1978). However, identifications of *Botryosphaeriaceae* species prior to the application of taxonomic criteria based on DNA sequencing and phylogenetic inference should be re-examined carefully as the taxonomy of this family of fungi has substantially changed during the last decade and is still evolving rapidly. As a matter of fact very recently new species have been described and species that were previously separated on the basis of both multi-loci phylogenetic analysis and morphological characters have been reduced to synonymy on the basis of same genetic markers previously regarded as discriminatory (Dissanayake et al., 2016; A. J.L. Phillips et al., 2013; Alan J.L. Phillips et al., 2019; Zhang et al., 2021). After the introduction of modern molecular taxonomy, several *Botryosphaeriaceae* species were reported to be associated to bot gummosis in California, including *Diplodia mutila*, *D. seriata*, *Dothiorella iberica* (very recently indicated as a possible synonym of *Do. sarmentorum*), *Spencermartinsia viticola* (syn. *Do. viticola*), *Lasiodiplodia parva*, *Neofusicoccum australe*, *N. luteum*, *N. mediterraneum*, *N. parvum* and *Neoscytalidium dimidiatum* (syn. *Ne. hyalinum*, formerly *Hendersonula toruloidea*) (Adesemoye et al., 2014; Adesemoye & Eskalen, 2011; Mayorquin et al., 2016). Moreover, *Dothiorella viticola* was reported to be responsible for bot gummosis of citrus in Tunisia (Hamrouni et al., 2018). Symptoms of bot gummosis were reproduced by artificially inoculating citrus trees with *Neofusicoccum batangarum* (very recently reduced to synonymy with *N. ribis*), the causal agent of a destructive disease of cactus pear in minor islands of Sicily (Aloi et al., 2020; Schena et al., 2018). In the island of Malta, about 80 marine miles south of Sicily, symptoms very similar to bot gummosis were reported on lemon (*Citrus × limon*) trees to be caused by species of *Diaporthe* (Guarnaccia & Crous, 2017).

During recent surveys in citrus growing areas in Sicily and Calabria, the two major citrus producer regions of Italy, symptoms of bot gummosis were observed to be common on mature, fruit-bearing lemon trees. This study was aimed at determining the etiology and the distribution of the disease in the major producing areas of lemon in Italy.

4.2 Materials and Methods

4.2.1 Fungal collections and isolations

Five citrus-growing areas in southern Italy, four in Sicily including the three Sicilian districts in the provinces of Catania, Messina and Syracuse to which the Protected Geographical Indication trademark was granted by EU, and one in Calabria (province of Reggio Calabria), were surveyed in 2017 and 2018 (**Figure 1**). The geographical map in Figure 1 also shows the close proximity between the surveyed areas and the major districts of Calabria and Sicily where citrus nursery plants production is concentrated.

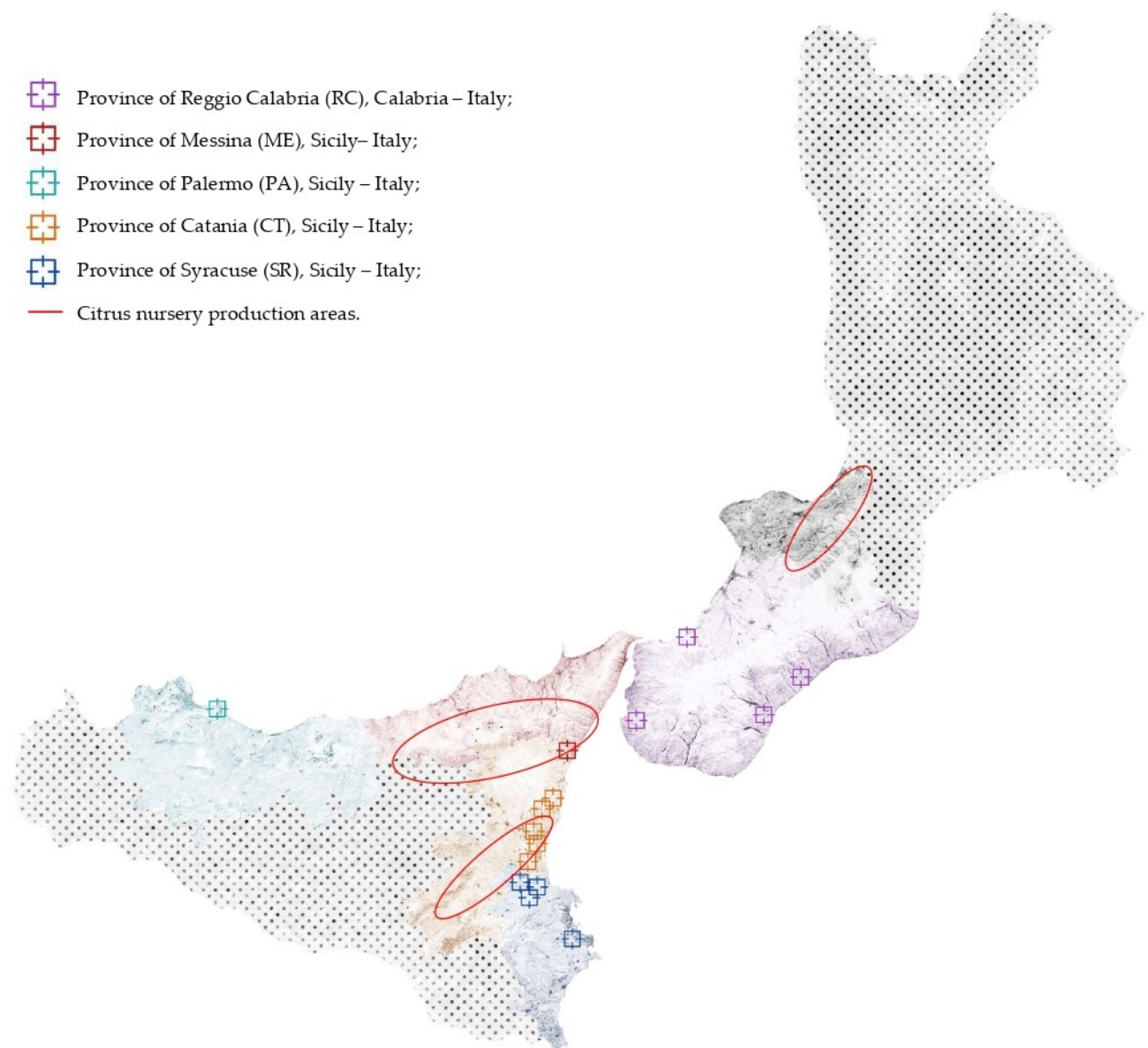


Figure 1. Map of southern Italy, including Sicily and Calabria, where sampling sites are indicated with colored squares (each color corresponds to a different province) while major citrus nursery production areas are indicated with circles.

Approximately 15 to 20 bark pieces from trunk and branch cankers were collected from 25 randomly selected trees (approximately 5 to 60 yr-old) in each area. Samples were transported in a cooler to the laboratory of

Molecular Plant Pathology at the Department of Agriculture, Food and Environment (Di3A) of the University of Catania, Italy.

Bark pieces with the typical brown discoloration of the wood were rinsed with deionized water to remove organic debris, blotted dry with paper towels, then briefly flamed after dipping in 95% ethanol for 3 s. Small sections (approximately 2 to 3 mm) from the inner face of necrotic bark were cut with a sterile scalpel and placed in Petri dishes onto potato dextrose agar (PDA; Difco Laboratories, Detroit, USA) amended with 100 µg/ml streptomycin (Sigma-Aldrich, Darmstadt, Germany). Cultures were incubated in the dark for 4 days at 25°C.

Pure cultures of fungal isolates were obtained by monoconidial cultures. The list of isolates characterized in this study is reported in **Table 1**.

Table 1. Identity of the *Neofusicoccum parvum* isolates studied, and GenBank accession numbers, for isolates obtained from gummy cankers of lemon (*Citrus × limon*) trees in southern Italy.

Isolate	Species	Origin	Host, variety	Accession numbers		
				ITS	β -tubulin	EF-1α
BOT 1A	<i>Neofusicoccum parvum</i>	Catania, Sicily-Italy	<i>Citrus x limon</i>	MW727244	MW789889	MW789904
BOT 1B	<i>N. parvum</i>	Catania, Sicily-Italy	<i>C. x limon</i>	MW727245	MW789890	MW789905
BOT 1C	<i>N. parvum</i>	Catania, Sicily-Italy	<i>C. x limon</i>	MW727246	MW789891	MW789906
BOT 1D	<i>N. parvum</i>	Catania, Sicily-Italy	<i>C. x limon</i>	MW727247	MW789892	MW789907
BOT 1E	<i>N. parvum</i>	Catania, Sicily-Italy	<i>C. x limon</i>	MW727248	MW789893	MW789908
BOT 2A	<i>N. parvum</i>	Syracuse, Sicily-Italy	<i>C. x limon</i>	MW727249	MW789894	MW789909
BOT 2B	<i>N. parvum</i>	Syracuse, Sicily-Italy	<i>C. x limon</i>	MW727250	MW789895	MW789910
BOT 2C	<i>N. parvum</i>	Syracuse, Sicily-Italy	<i>C. x limon</i>	MW727251	MW789896	MW789911
BOT 2D	<i>N. parvum</i>	Syracuse, Sicily-Italy	<i>C. x limon</i>	MW727252	MW789897	MW789912
BOT 2E	<i>N. parvum</i>	Syracuse, Sicily-Italy	<i>C. x limon</i>	MW727253	MW789898	MW789913
BOT 4A	<i>N. parvum</i>	Messina, Sicily-Italy	<i>C. x limon</i>	MW788562	MW789929	MW789919
BOT 4B	<i>N. parvum</i>	Messina, Sicily-Italy	<i>C. x limon</i>	MW788563	MW789930	MW789920
BOT 4C	<i>N. parvum</i>	Messina, Sicily-Italy	<i>C. x limon</i>	MW788564	MW789931	MW789921
BOT 4D	<i>N. parvum</i>	Messina, Sicily-Italy	<i>C. x limon</i>	MW788565	MW789932	MW789922
BOT 4E	<i>N. parvum</i>	Messina, Sicily-Italy	<i>C. x limon</i>	MW788566	MW789933	MW789923
BOT 5A	<i>N. parvum</i>	Palermo, Sicily-Italy	<i>C. x limon</i>	MW788567	MW789934	MW789924
BOT 5B	<i>N. parvum</i>	Palermo, Sicily-Italy	<i>C. x limon</i>	MW788568	MW789935	MW789925
BOT 5C	<i>N. parvum</i>	Palermo, Sicily-Italy	<i>C. x limon</i>	MW788569	MW789936	MW789926
BOT 5D	<i>N. parvum</i>	Palermo, Sicily-Italy	<i>C. x limon</i>	MW788570	MW789937	MW789927
BOT 5E	<i>N. parvum</i>	Palermo, Sicily-Italy	<i>C. x limon</i>	MW788571	MW789938	MW789928

BOT 3A	<i>N. parvum</i>	Reggio Calabria, Calabria-Italy	<i>C. x limon</i>	MW727254	MW789899	MW789914
BOT 3B	<i>N. parvum</i>	Reggio Calabria, Calabria-Italy	<i>C. x limon</i>	MW727255	MW789900	MW789915
BOT 3C	<i>N. parvum</i>	Reggio Calabria, Calabria-Italy	<i>C. x limon</i>	MW727256	MW789901	MW789916
BOT 3D	<i>N. parvum</i>	Reggio Calabria, Calabria-Italy	<i>C. x limon</i>	MW727257	MW789902	MW789917
BOT 3E	<i>N. parvum</i>	Reggio Calabria, Calabria-Italy	<i>C. x limon</i>	MW727258	MW789903	MW789918

4.2.2 Morphological characteristics and cardinal temperatures for growth of the isolates

The isolates were induced to sporulate by plating them on PDA containing sterilized pine needles (Smith et al., 1996), and incubating at room temperature (approx. 20 to 25°C) under diffused day light or near-UV light, until pycnidia developed. For microscopy, pycnidia and conidia were mounted in sterile distilled water or 100% lactic acid and observed microscopically at x40 and x100 magnifications, with an Axioskop (Zeiss) microscope. Images were captured with an AxioCam MRc5 camera (Zeiss), and measurements were made with the software AxioVision. For each isolate, 50 conidia were randomly selected and their lengths, widths and shape were recorded. For pycnidium dimensions, 20 measurements were made. Colony characters and pigment production were noted after 4 to 6 d of growth on PDA or malt extract agar (MEA) at 25°C, in the dark.

Colony colors (upper and lower surfaces) were rated according to Rayner (1970). The conidial characteristics observed were compared with those that were reported in previous studies (Crous et al., 2006; McDonald & Eskalen, 2011; Alan J.L. Phillips, 2002; Bernard Slippers et al., 2004; Wright & Harmon, 2010).

Radial growth rate and cardinal temperatures for radial growth were determined by growing the isolates on PDA in Petri dishes (9 cm diam.), and incubating at 5, 10, 15, 20, 25, 30, 35°C, in the dark. Means of radial growth at the different temperatures were adjusted to a regression curve using Statgraphics Plus 5.1 software (Manugistics Inc.), and the best polynomial model was chosen based on parameter significance ($P < 0.05$) and coefficient of determination (R^2) to estimate the optimum growth temperature for each isolate. Four replicates of each isolate were evaluated and each experiment was repeated twice.

4.2.3 Amplification and sequencing

Genomic DNA was isolated from 1-week-old cultures grown on PDA at 25°C in the dark using the procedure of Schena and Cooke (2006). The internal transcribed spacer (ITS) region of the ribosomal DNA was amplified and sequenced with primers ITS1/ITS4 (White et al. 1990), part of the translation elongation factor 1 alpha gene (*tef1*) was sequenced and amplified with primers EF1-728F/EF1-986R (Carbone and Kohn, 1999), and the β -tubulin gene (*tub2*) was sequenced and amplified with Bt2a and Bt2b (Glass and Donaldson, 1995).

The PCR amplifications were performed on a GeneAmp PCR System 9700 (Applied Biosystems, Monza-Brianza, Italy). All PCRs were performed by using the Taq DNA polymerase recombinant (Invitrogen™) and carried out in a total volume of 25 μ l contained the following: PCR Buffer (1X), dNTP mix (0,2 mM), MgCl₂ (1,5 mM), forward and reverse primers (0,5 μ M each), Taq DNA Polymerase (1 U) and 1 μ L of genomic DNA.

The reaction protocol for ITS and β -tubulin included an initial preheat at 94°C for 2 min; followed by 35 cycles of denaturation at 94°C for 15 s, annealing at 58°C for 15 s, and extension at 72°C for 45 s; and final extension at 72°C for 10 min (35). The translation EF α -1 included an initial denaturation at 95°C for 8 min; followed by 35 cycles of 95, 58, and 72°C for 15, 20, and 60 s, respectively; and a final extension at 72°C for 10 min (7). The amplicons were detected in 1% agarose gel and purified products were sequenced by MacroGen Europe (Amsterdam, The Netherlands). Sequences were analyzed by using FinchTV v.1.4.0 (<https://digitalworldbiology.com/FinchTV>) and MEGA7 (<https://www.megasoftware.net/>) and the consensus sequences were deposited in Genbank.

4.2.4 Molecular identification and phylogenetic analyses

Sequences of isolates were associated to a species by the application of BLAST algorithm on the NCBI nucleotide database. Species identity was confirmed by a multi-loci phylogenetical analysis including sequences from taxa that best matched the blast species identity (Anabela Lopes et al., 2017; B. Slippers et al., 2013; Yang et al., 2017). The list of compared isolates is reported in **Table 2**.

For all isolates, ITS, *tef1* and *tub2* sequences were trimmed to a common length and concatenated using the Sequence Matrix software (Vaidya et al., 2011). Concatenated sequences were aligned with MUSCLE (Edgar, 2004) as implemented in Mega Version 7.0 (Kumar et al., 2016), and edited manually for checking indels and single nucleotide polymorphisms. Phylogenetic analyses were performed in Mega with the maximum likelihood method using the Tamura–Nei model and 1000 bootstrap replications (Tamura et al., 2013). Obtained results are reported in **Figure 2**.

Table 2. GenBank accession numbers of sequences of the *Neofusicoccum* spp. isolates of different geographical and host origins used as references in phylogenetic analyses.

Species	Isolate	Origin	Host	Source	GenBank accession number		
					ITS	tef1	β-tubulin
<i>N. algeriense</i>	CAA 322	Portugal	<i>Malus domestica</i>	(A. Lopes et al., 2016)	KX505906	KX505894	KX505916
<i>N. algeriense</i>	CBS 137504	Algeria	<i>Vitis vinifera</i>	(A. Lopes et al., 2016)	KJ657702	KX505893	KX505915
<i>N. batangarum</i>	CBS 124922	Cameroon	<i>Terminalia catappa</i>	(Yang et al., 2017)	FJ900606	FJ900652	FJ900633
<i>N. batangarum</i>	CBS 143023	Italy, Favignana	<i>Opuntia ficus-indica</i>	(Aloi et al., 2020)	MF414730	MF414768	MF414749
<i>N. batangarum</i>	CBS 143025	Italy, Linosa	<i>Opuntia ficus-indica</i>	(Aloi et al., 2020)	MF414747	MF414785	MF414766
<i>N. batangarum</i>	CBS 127348	USA: Florida	<i>Schinus terebinthifolius</i>	(Yang et al., 2017)	HM357636	KX464674	KX464952
<i>N. batangarum</i>	CMM4553	Brasil	<i>Anacardium</i> sp.	Unpublished	KT728917	KT728921	KT728913
<i>N. batangarum</i>	CBS 124923	Cameroon	<i>Terminalia catappa</i>	(A. Lopes et al., 2016)	FJ900608	FJ900654	FJ900635
<i>N. batangarum</i>	CBS 124924	Cameroon	<i>Terminalia catappa</i>	(Yang et al., 2017)	FJ900607	FJ900653	FJ900634
<i>N. batangarum</i>	CBS 143026	Italy, Lampedusa	<i>Opuntia ficus-indica</i>	(Aloi et al., 2020)	MF414748	MF414786	MF414767
<i>N. batangarum</i>	CBS 143024	Italy, Ustica	<i>Opuntia ficus-indica</i>	(Aloi et al., 2020)	MF414738	MF414776	MF414757
<i>N. brasiliense</i>	CMM1285	Brazil	<i>Mangifera indica</i>	(A. Lopes et al., 2016)	JX513628	JX513608	KC794030
<i>N. cordaticola</i>	CBS 123634	South Africa	<i>Syzygium cordatum</i>	(A. Lopes et al., 2016)	EU821898	EU821868	EU821838
<i>N. kwambonambiense</i>	CBS 123639	South Africa	<i>Syzygium cordatum</i>	(A. Lopes et al., 2016)	EU821900	EU821870	EU821840
<i>N. macroclavatum</i>	CBS 118223	Australia	<i>Eucalyptus globulus</i>	(A. Lopes et al., 2016)	DQ093196	DQ093217	DQ093206
<i>N. parvum</i>	CBS 111994	Australia	<i>Telopea</i> sp.	(Yang et al., 2017)	AF452519	KX464702	KX464982
<i>N. parvum</i>	CAA 192	Portugal	<i>Ferula communis</i>	(A. Lopes et al., 2016)	KX505905	KX505892	KX505913
<i>N. parvum</i>	CBS 112930	South Africa	<i>Vitis vinifera</i>	(Yang et al., 2017)	AY343467	AY343359	KX464983
<i>N. parvum</i>	CBS 121486	Spain	<i>Vitis vinifera</i> cv. Parellada,	(Yang et al., 2017)	EU650672	KX464707	KX464992
<i>N. parvum</i>	CBS 114472	USA	<i>Leucadendron</i> sp.	(Yang et al., 2017)	AF452523	FJ150710	KX464987
<i>N. parvum</i>	CBS 111524	USA: Hawaii	<i>Protea cynaroides</i>	(Yang et al., 2017)	AF452524	FJ150709	KX465009
<i>N. parvum</i>	CBS 124492	Zambia	<i>Syzygium guineense</i>	(Yang et al., 2017)	FJ655000	KX464684	KX464962
<i>N. parvum</i>	CBS 110301 (ex-type)	Portugal	<i>Vitis vinifera</i>	(A. Lopes et al., 2016)	AY259098	AY573221	EU673095
<i>N. parvum</i>	CMW9081 (ex-type)	New Zealand	<i>Populus nigra</i>	(A. Lopes et al., 2016)	AY236943	AY236888	AY236917
<i>N. ribis</i>	CBS 115475	USA	<i>Ribes</i> sp.	(A. Lopes et al., 2016)	AY236935	AY236877	AY236906
<i>N. umdonicola</i>	CBS 123646	South Africa	<i>Syzygium cordatum</i>	(A. Lopes et al., 2016)	EU821905	EU821875	EU821845

4.2.5 Pathogenicity tests

The pathogenicity of an isolate of *Neofusicoccum parvum* (BOT 1D), obtained from lemon in Sicily, was assessed on twigs and stem of 2-year-old trees of three citrus varieties, *Citrus × limon* var. Monachello, *Citrus × limon* var. Feminello and Citrange Carrizo (*Citrus sinensis* Osbeck × *Poncirus trifoliata* Raf.), grown in a greenhouse maintained at 20 to 26°C.

Two plants per variety were inoculated in three points, on two twigs and on stem per tree. A hole in each twig was made with a 3 mm cork-borer. For the inoculation, a 3 mm diam. mycelium plug from 5-d-old PDA culture of the test isolate (BOT 1D) was placed on the freshly wounded surface; the wound was covered with the excised bark disk and sealed with Parafilm®. The stem of each tree was inoculated 10 cm above the soil level (a single hole per stem) using the method above reported. Two trees per each citrus variety were inoculated with sterile agar (Controls).

The length and breadth of each resulting lesion were recorded 30 d a.i. (day after inoculation), and the outer surface areas of the bark cankers on twigs and stems were calculated as ellipses.

In this pathogenicity test, re-isolation was made from lesions; the identity of resulting fungal colonies was confirmed by both morphological and molecular analysis (ITS, *tef1* and *tub2* genes were sequenced) as described above.

4.2.6 Statistical analyses of data

Data from pathogenicity tests were analyzed using RStudio v.1.2.5 (R). When comparing the means of multiple groups, a one-way ANOVA followed by Tukey's HSD post hoc test was performed. Significant differences between groups ($P < 0.05$) were denoted with different letters.

4.3 Results

4.3.1 Symptoms

Bot gummosis was detected on mature, fruit-bearing lemon trees, with an age ranging from approximately 5 to 60 years, both in commercial orchards and in trees planted singularly or in small groups in home gardens where trees were grown for both ornamental purposes and domestic consumption of fruits. The disease was common but usually in commercial orchards symptomatic trees were scattered. Exceptionally, in an orchard in the municipality of Lentini (Syracuse) 30 out of 400, 20-yr-old trees were symptomatic. Typically, symptoms, i.e. cankers with an abundant gummous exudate, were observed on the main trunk and scaffold branches (**Figure 2 A-E**) of trees. Another typical symptom was a chocolate to dark brown discoloration of the wood and the cambial face of the bark, which was visible after removing the bark (**Figure 2 C** and **Figure 3 B-D**). Cankers usually originated at the level of main branch scaffolding and progressively expanded upward to the secondary branches and downward to the grafting line between the scion and the rootstock (**Figures 2 A, C, D**). However, in most cases they were restricted to the lemon scion and only exceptionally and in any case to a limited extent they expanded on sour orange (*Citrus × aurantium*) or citrange (*Citrus sinensis* × *Poncirus trifoliata*) rootstock. In a few cases, as a consequence

of chronic long-lasting infections the cankers girdled the trunk. Old cankers either ceased to produce gum or produced it only on the expanding edge; they showed longitudinal bark splittings on secondary branches and irregular cracking and scaling of the bark on trunk and scaffold branches (**Figure 2 E** and **Figure 3 A, D**). Leaf yellowing, defoliation and dieback of single branches occurred commonly. Severely affected trees showed decline symptoms, including leaf chlorosis, severe crown thinning, branch and twig blight and dieback.



Figure 2. Symptoms of Bot gummosis on lemon trees: (**E**) old canker with bark scaling at the level of main branch scaffolding, expanding upward to the secondary branches and downward to the grafting line between the scion and the rootsstock; (**D**), gummous canker on a branch of lemon tree; (**C**) typical tan to brown discoloration of the wood beneath the bark of a canker; the discolored wood is visible after removing the bark; (**A** and **B**) cankers with abundant gummous exudate on scaffold branches of ‘Femminello Siracusano 2Kr’ lemon (*Citrus × limon*) tree.

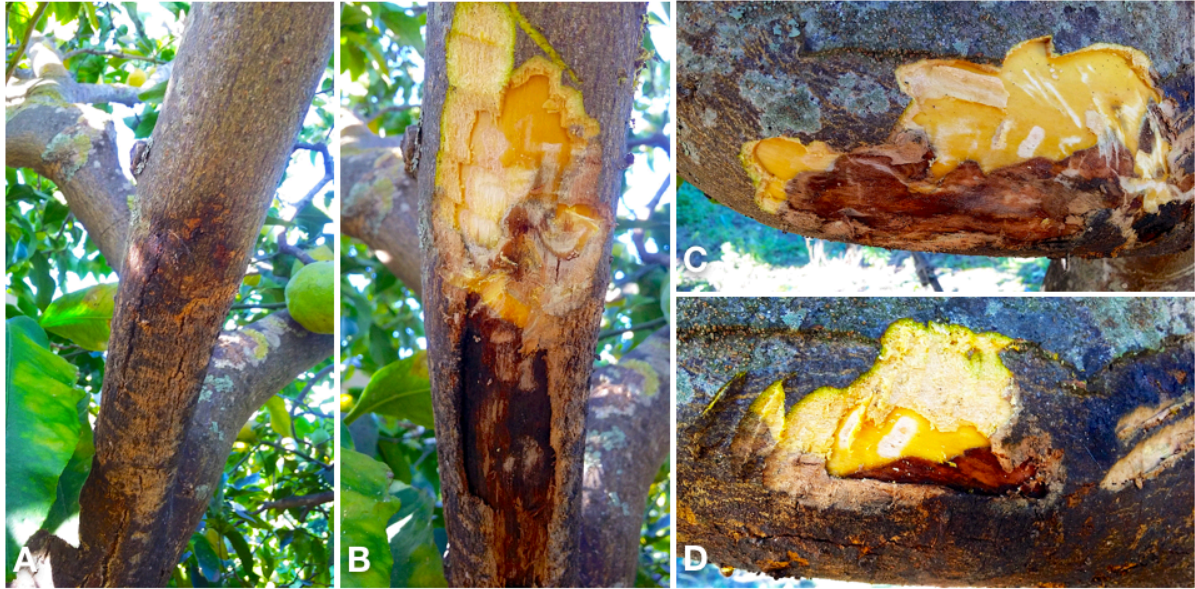


Figure 3. (A) old canker on a secondary branch of lemon tree with longitudinal bark splitting at the base of the branch and the gum exudate in the advancing upward front, indicating the canker is still active; (B) the same as (A) after peeling the bark to show the dark brown discoloration of the wood beneath the bark; (C) typical chocolate brown discoloration of the wood underneath the bark; (D) a detail showing the necrotic bark of the canker exuding gum and the typical chocolate brown wood discoloration beneath the bark.

4.3.2 Fungus isolation and morphological identification

A fungus with pale gray and rapidly growing colonies on potato-dextrose-agar (PDA) was constantly (from all samples and in all sampling sites) and consistently (around 100% of isolations) recovered from the inner bark with the typical brown discoloration. Based on the morphotype, i.e. colony morphology and conidial characteristics, all isolates were assigned to *Neofusicoccum*, a genus in the *Botryosphaeriaceae* family (Figure 5 A and B). A representative set of 17 isolates, was characterized further. A single isolate was selected from each sampling site, with the only exception of the site in the municipality of Lentini where due to the high incidence of the disease three isolates, each from a distinct tree, were selected.

Colonies on MEA of all 17 isolates developed an abundant grayish aerial mycelium, which produced black pycnidia after 2 weeks of incubation at 25 ° C. On PDA mycelium was white and became smoky gray to gray-olivaceous after 5 d (Figure 4 A). The mycelium was fast-growing and covered the 9 cm diam. Petri dishes after 5 d incubation at 25°C in the dark. Optimum temperature for radial colony growth was between 25 and 30°C for all the isolates tested (Table 3). Little growth was observed at 10 or 35°C. Stromatic conidiomata were produced in pine needle cultures within 14 d. The conidiomata were globose and non-papillate to pyriform with a short, acute papilla, entire locule lined with conidiogenous cells, and measured 150–250 µm in diameter. Conidia were ellipsoidal with apex round and base flat, unicellular and hyaline and measured 16.9–17.3 × 5.4–5.6 µm, with a mean length to width ratio = 3.2 (Figure 4 B). Old conidia becoming 1–2-septate hyaline, or light brown with the middle cell darker than the terminal cells.

Table 3. Mean radial growth rates of colonies of representative *Neofusicoccum parvum* isolates of different geographical origin on PDA at three different temperatures, as determined after 3 d of incubation.

Isolates of <i>N. parvum</i>	15°C (mm d-1) ± S.D. ^a	25°C (mm d-1) ± S.D. ^a	30°C (mm d-1) ± S.D. ^a
BOT 1A	3.73 ± 0.07	7.90 ± 1.08	6.71 ± 0.27
BOT 1D	3.11 ± 0.91	7.73 ± 0.28	7.38 ± 0.47
BOT 2A	3.41 ± 0.05	7.55 ± 0.32	7.06 ± 0.28
BOT 2D	3.53 ± 0.62	6.68 ± 0.90	5.58 ± 0.28
BOT 3A	3.45 ± 0.39	7.06 ± 0.28	6.23 ± 0.20
BOT 3D	3.30 ± 0.17	6.83 ± 0.32	6.63 ± 0.46
BOT 4A	3.42 ± 0.06	6.58 ± 0.62	7.38 ± 0.47
BOT 5D	3.28 ± 0.17	7.22 ± 0.42	5.37 ± 0.38

^a Mean of four replicate Petri dishes.

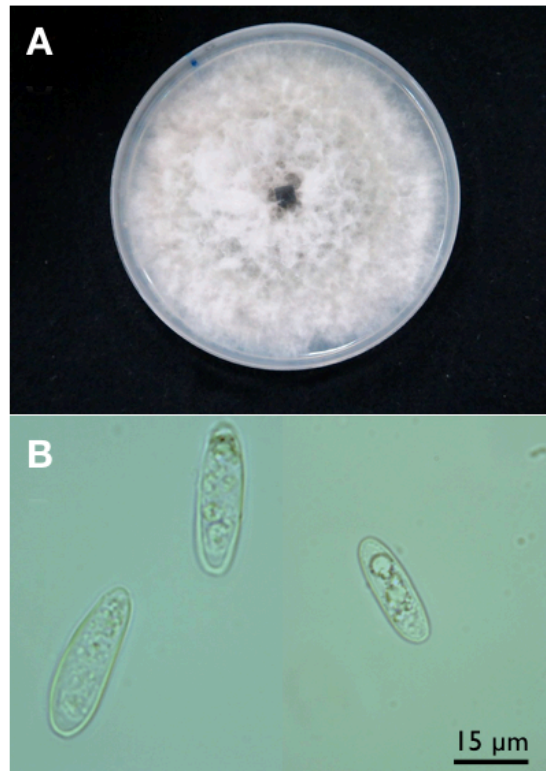


Figure 4. (A), Colony morphology of an isolate of *Neofusicoccum parvum* recovered from lemon on potato-dextrose-agar after 5 d incubation at 25°C; (B), Unicellular, ellipsoidal, thin-walled hyaline conidia of *Neofusicoccum parvum* mounted in sterile distilled water.

4.3.3 Molecular identification

The isolates obtained had identical ITS, *tef1* and *tub2* sequences. Preliminary BLAST analyses of these three gene regions yielded several identical sequences belonging to *Neofusicoccum* spp. but deposited with different taxa names. Consequently, this analysis enabled the identification at the genus level, but did not provide reliable information on the species. The phylogenetic analysis of the combined data set of sequences from ITS, *tef1* and *tub2* sequences (**Figure 5**) produced trees with a high concordance with those reported by Lopes et al. (2016), Lopes et al. (2017), Yang et al. (2017) and Zhang et al. (2021). According to this analysis, isolates obtained from gummy cankers of *Citrus x limon* were identified as *Neofusicoccum parvum sensu stricto* (*s.s.*), since they clearly clustered with the ex-type (CMW 9081 from *Populus nigra* (Lopes et al., 2016)) and other reference isolates of this species (CBS 111994 from *Telopea* sp. (Yang et al., 2017)) and were differentiated from other *Neofusicoccum* isolates in the *Neofusicoccum* species complex (Zhang et al., 2021).



Figure 5. Phylogenetic tree of isolates of *Neofusicoccum parvum* obtained from lemon trees in this study (in bold), and reference isolates of *Neofusicoccum parvum* (underlined) and other closely related *Neofusicoccum* species and isolates (Tables 1 and 2). The tree was built using concatenated sequences of ITS-5.8S-ITS2 region, tef1- α and β -tubulin genes. Numbers on nodes indicate the posterior probabilities from the maximum likelihood method.

4.3.4 Pathogenicity tests

In pathogenicity tests, *N. parvum* (isolate BOT 1D) induced gummy canker on twigs and stem of all three citrus varieties tested. Symptoms appeared at 14 days after inoculation (d.a.i.); they were more severe on lemon cultivars ‘Feminello 2kr’(lesion areas ranging from 8.4 to 8.9 cm² 30 d.a.i.), and ‘Monachello’ (lesion areas ranging from 6.5 to 6.8 cm² 30 d.a.i.) and included abundant gummosis (**Figure 6 A, B, C, D**), while gummosis was much less abundant on Citrange ‘Carrizo’ (lesion areas ranging from 3.1 to 3.3 cm² 30 d.a.i.) (**Figure 6 E, F**). Differences in mean lesion size between the three citrus varieties tested were significant, according to Tukey’s HSD (Honestly Significant Difference) test ($P < 0.05$) (**Figure 7**). No symptoms were observed on the controls.

The *N. parvum* test isolate was re-isolated from inoculated plants and identified by sequencing and multi-loci phylogenetic analysis, while no fungal pathogens were isolated from control plants, thus fulfilling Koch’s postulates.

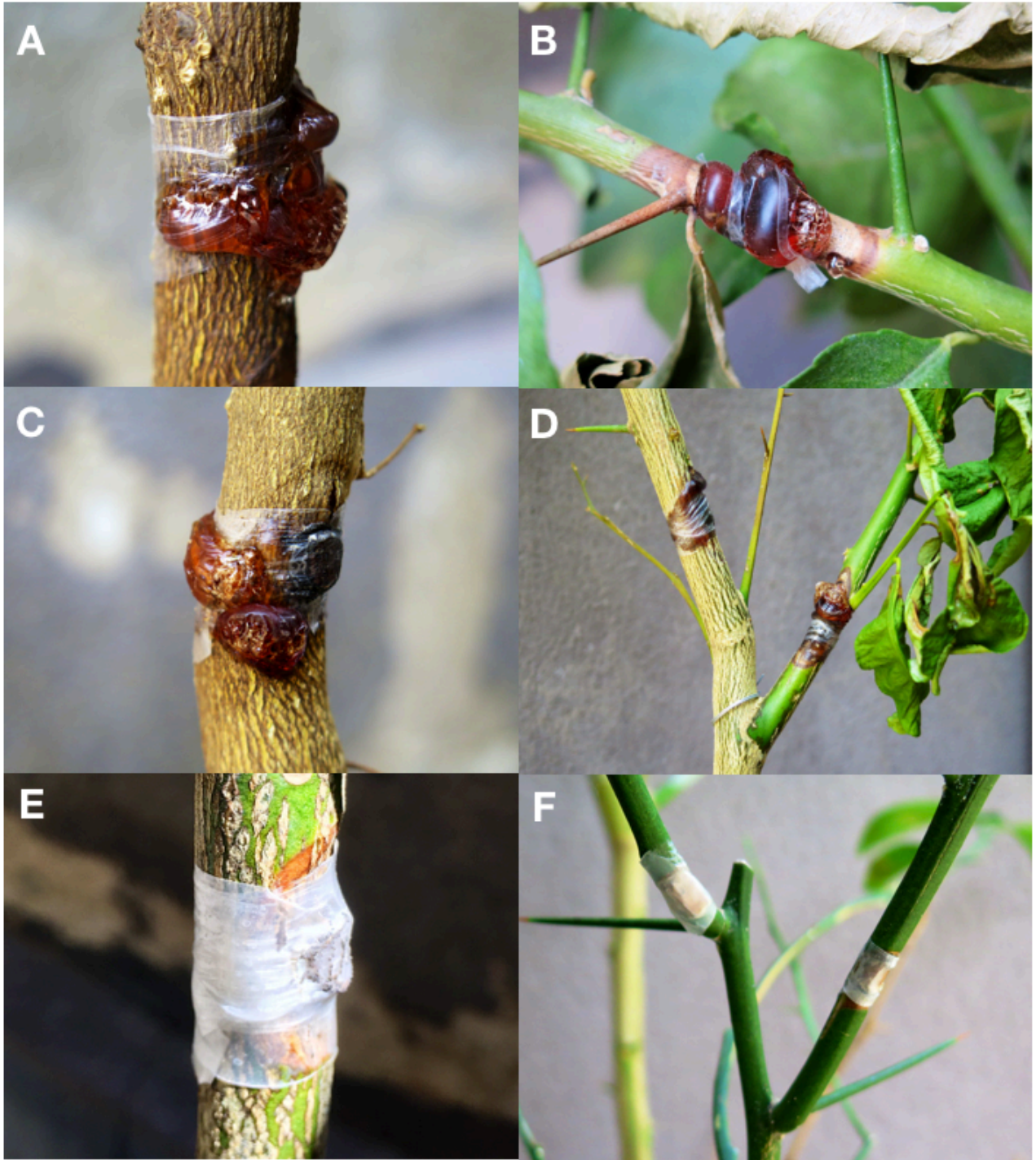


Figure 6. Gum exudate induced by wound-inoculation of *Neofusicoccum parvum* on stems and twigs of lemon 'Femminello 2kr' (A, B) and 'Monachello' (C, D), 14 d a.i.; necrotic lesions without gummous flux on inoculated Citrange 'Carrizo' (E, F).

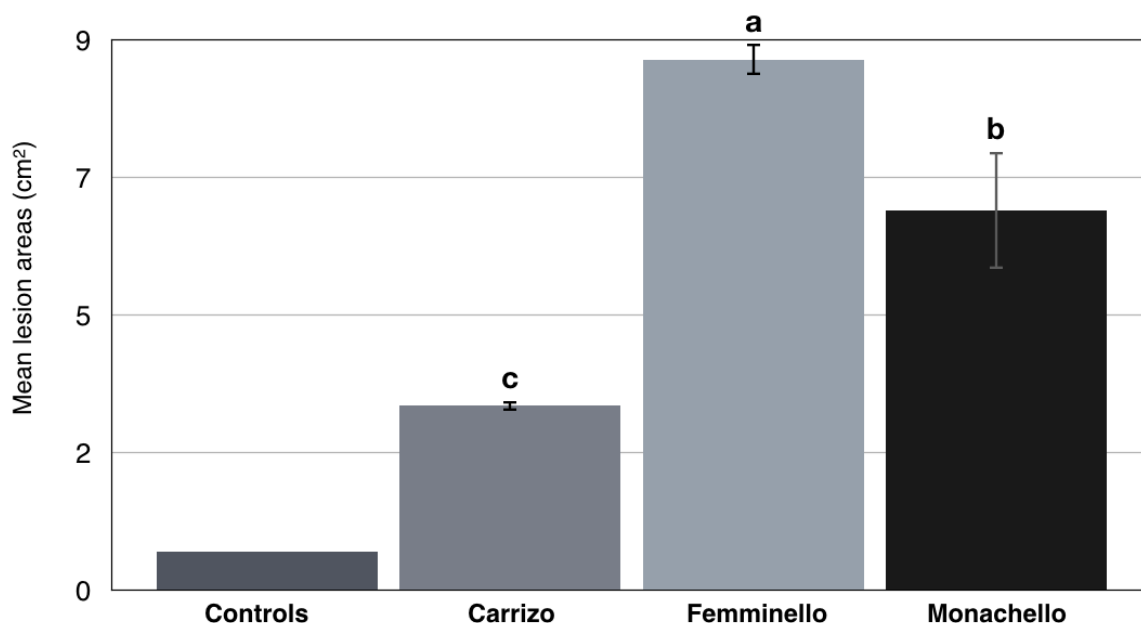


Figure 7. Mean lesion areas (cm²) on the stem of citrange (*Citrus sinensis* × *Poncirus trifoliata*)

‘Carrizo’ and lemon (*Citrus* × *limon*) cultivars ‘Femminello 2kr’ and ‘Monachello’, wound-inoculated with isolate BOT1D of *Neofusicoccum parvum*, 30 d.a.i. Controls (‘Femminello 2kr’ lemon, ‘Monachello’ lemon and ‘Carrizo’ citrange) stem inoculated with a sterile agar plug, showed no symptoms. Values sharing different letters are statistically different according to Tukey’s honestly significant difference, for P=0.05.

4.4 Discussion

Bot gummosis, traditionally regarded as a minor disease in citrus orchards (Timmer et al., n.d.), was found to be common and widespread in lemon groves of southern Italy. Although it is not as destructive as malsecco disease caused by the mitosporic fungus *Plenodomus tracheiphilus* (syn. *Phoma tracheiphila*) (Migheli et al., 2009), bot gummosis can be regarded as a major constraint for the lemon industry in this production area as it causes premature aging of trees and reduces their productivity. In this respect the impact of bot gummosis in commercial lemon orchards is more severe than wood rot disease caused by species of Basidiomycetes (Rocchetti et al., 2014). The present study provided evidence that *Neofusicoccum parvum* in the family *Botryosphaeriaceae* is responsible for bot gummosis of lemon trees in Sicily and Calabria, the two major lemon producing Italian regions. This fungus was the only species of this family associated to the typical disease symptoms in all surveyed areas and the two most popular Italian lemon cultivars, ‘Femminello 2kr’ and ‘Monachello’, were shown to be very susceptible to the infections by this pathogen in pathogenicity assays. Consistently with symptoms observed on naturally infected trees in the field, pathogenicity tests revealed that *N. parvum* was very aggressive on ‘Femminello 2kr’ and ‘Monachello’, which reacted to the infection with the abundant production of gum exudate, while it was weakly virulent on ‘Carrizo’ citrange, commonly used as a citrus rootstock. *Neofusicoccum parvum* is a generalist, cosmopolitan pathogen, occurring in various environments with a temperate, Mediterranean or

subtropical climate. The host range of this species encompasses at least 90 botanical entities, especially woody angiosperms, including conifers and many horticultural plants (Golzar & Burgess, 2011; Iturrutxa et al., 2011; Molina-Gayosso et al., 2012; Moral et al., 2019; A. J.L. Phillips et al., 2013; Sakalidis et al., 2013; Spagnolo et al., 2011; Úrbez-Torres & Gubler, 2011). In association with other fungal pathogens, including other *Botryosphaeriaceae* species, *N. parvum* is involved in the trunk disease complex of grapevine and is regarded as one of the most aggressive causal agent of this disease (Mondello et al., 2018; Úrbez-Torres & Gubler, 2009). It was also reported as a pathogen of citrus from Australia, California and Europe (Adesemoye & Eskalen, 2011; Bezerra et al., 2021; Cunnington et al., 2007). However, this is the first report of *N. parvum* as a pathogen of citrus in Italy.

In a previous study, it was shown that *N. parvum* is more aggressive than other *Botryosphaeriaceae* species associated to bot gummosis of citrus (Adesemoye et al., 2014). This may explain its prevalence on lemon, which is more susceptible to bot gummosis than other citrus species (Salerno & Cutuli, 1994). Like other species of *Neofusicoccum*, *N. parvum* produces phytotoxins, which probably act as virulence factors but none of them is host-specific (Abou-Mansour et al., 2015; Masi et al., 2020; Salvatore et al., 2021). Different *Neofusicoccum* species cause similar effects on plants, perhaps due to the production of these secondary metabolites. *Neofusicoccum parvum* e.g. when inoculated on cactus pear cladodes was able to induce on this host the same symptoms as *N. batagarum* (*data not shown*) and conversely in artificial inoculations *N. batagarum* induced on citrus plants the same symptoms as *N. parvum* (Aloi et al., 2020). In general, the *Botryosphaeriaceae*, like other opportunistic albeit aggressive plant pathogens such as *Colletotrichum* spp., behave as endophytes, saprobes or latent pathogens shifting to an aggressive pathogenic life style when the host-plant is stressed (Cacciola et al., 2020; Haridas et al., 2020; Pavlic-Zupanc et al., 2015; Riolo et al., 2021; Bernard Slippers & Wingfield, 2007). It has been suggested that the widespread occurrence of *N. parvum* and related species is due to their polyphagy and cross-infection potential as well as to their behaviour as endophytes or latent pathogens favoring a global spread through the movement of asymptomatic plants and plant propagation material (Pancher et al., 2012; Pérez et al., 2010; Sakalidis et al., 2013; Bernard Slippers & Wingfield, 2007). According with this hypothesis, it can be speculated that the widespread occurrence of *N. parvum* in lemon growing areas of southern Italy may also depend on their close proximity with districts where the nursery production of citrus plants is concentrated. As a consequence, it can be assumed that most lemon trees in these areas have a common origin and *N. parvum* has been spread as a latent pathogen with nursery plants. This study provided evidence that restricted outbreaks of bot gummosis may occur in lemon groves of southern Italy. Local emergence probably due to environmental stresses is typical of diseases caused by *Botryosphaeriaceae* (Aloi et al., 2020; Marsberg et al., 2017; Moral et al., 2019). Extreme temperatures and water deficit are suspected to be the most frequent stressors favoring bot gummosis of citrus. These environmental factors condition not only the disease onset and development, but also the severity of symptom expression. A better understanding of the factors favoring the emergence of the bot gummosis in lemon orchards would be useful to adopt appropriate management strategies to prevent the disease.

4.5 References

- Abou-Mansour, E., Débieux, J. L., Ramírez-Suero, M., Bénard-Gellon, M., Magnin-Robert, M., Spagnolo, A., Chong, J., Farine, S., Bertsch, C., L'Haridon, F., Serrano, M., Fontaine, F., Rego, C., & Larignon, P. (2015). Phytotoxic metabolites from *Neofusicoccum parvum*, a pathogen of *Botryosphaeria* dieback of grapevine. *Phytochemistry*, *115*, 2017–2215. <https://doi.org/10.1016/j.phytochem.2015.01.012>
- Adesemoye, A. O., & Eskalen, A. (2011). First Report of *Spencermartinsia viticola*, *Neofusicoccum australe*, and *N. parvum* Causing Branch Canker of Citrus in California. *Plant Disease*, *95*, 770. <https://doi.org/10.1094/pdis-02-11-0092>
- Adesemoye, A. O., Mayorquin, J. S., Wang, D. H., Twizeyimana, M., Lynch, S. C., & Eskalen, A. (2014). Identification of species of *Botryosphaeriaceae* causing Bot gummosis in citrus in California. *Plant Disease*, *98*, 55–61. <https://doi.org/10.1094/PDIS-05-13-0492-RE>
- Aloi, F., Giambra, S., Schena, L., Surico, G., Pane, A., Gusella, G., Stracquadanio, C., Burruano, S., & Cacciola, S. O. (2020). New insights into scabby canker of *Opuntia ficus-indica*, caused by *Neofusicoccum batangarum*. *Phytopathologia Mediterranea*, *59*, 269–284. <https://doi.org/10.14601/Phyto-11225>
- Bezerra, J. D. P., Crous, P. W., Aiello, D., Gullino, M. L., Polizzi, G., & Guarnaccia, V. (2021). Genetic diversity and pathogenicity of *Botryosphaeriaceae* species associated with symptomatic citrus plants in Europe. *Plants*, *10*(3), 492. <https://doi.org/10.3390/plants10030492>
- Cacciola, S. O., Gilardi, G., Faedda, R., Schena, L., Pane, A., Garibaldi, A., & Gullino, M. L. (2020). Characterization of *Colletotrichum ocimi* population associated with black spot of sweet basil (*Ocimum basilicum*) in Northern Italy. *Plants*, *9*(5), 654. <https://doi.org/10.3390/plants9050654>
- Carbone, I., & Kohn, L. M. (1999). A method for designing primer sets for speciation studies in filamentous ascomycetes. *Mycologia*, *91*, 553–556. <https://doi.org/10.2307/3761358>
- Crous, P. W., Slippers, B., Wingfield, M. J., Rheeder, J., Marasas, W. F. O., Phillips, A. J. L., Alves, A., Burgess, T., Barber, P., & Groenewald, J. Z. (2006). Phylogenetic lineages in the Botryosphaeriaceae. *Studies in Mycology*, *55*, 235–253. <https://doi.org/10.3114/sim.55.1.235>
- Cunnington, J. H., Priest, M. J., Powney, R. A., & Cother, N. J. (2007). Diversity of *Botryosphaeria* species on horticultural plants in Victoria and New South Wales. *Australasian Plant Pathology*, 157–159. <https://doi.org/10.1071/AP07002>
- Dissanayake, A. J., Camporesi, E., Hyde, K. D., Phillips, A. J. L., Fu, C. Y., Yan, J. Y., & Li, X. (2016). *Dothiorella* species associated with woody hosts in Italy. *Mycosphere*, *7*, 51–63. <https://doi.org/10.5943/MYCOSPHERE/7/1/6>
- Edgar, R. C. (2004). MUSCLE: Multiple sequence alignment with high accuracy and high throughput. *Nucleic Acids Research*, *32*, 1792–1797. <https://doi.org/10.1093/nar/gkh340>
- Glass, N. L., & Donaldson, G. C. (1995). Development of primer sets designed for use with the PCR to amplify conserved genes from filamentous ascomycetes. *Applied and Environmental Microbiology*, *61*(4), 1323–1330. <https://doi.org/10.1128/aem.61.4.1323-1330.1995>
- Golzar, H., & Burgess, T. I. (2011). *Neofusicoccum parvum*, a causal agent associated with cankers and decline of Norfolk Island pine in Australia. *Australasian Plant Pathology*, *40*, 484. <https://doi.org/10.1007/s13313-011-0068-4>
- Guarnaccia, V., & Crous, P. W. (2017). Emerging citrus diseases in Europe caused by species of *Diaporthe*. *IMA Fungus*, *8*, 317–334. <https://doi.org/10.5598/imafungus.2017.08.02.07>

- Hamrouni, N., Nouri, M. T., Trouillas, F. P., Said, A., Sadfi-Zouaoui, N., & Hajlaoui, M. R. (2018). Dothiorella gummosis caused by *Dothiorella viticola*, first record from citrus in Tunisia. *New Disease Reports*, 38, 10. <https://doi.org/10.5197/j.2044-0588.2018.038.010>
- Haridas, S., Albert, R., Binder, M., Bloem, J., LaButti, K., Salamov, A., Andreopoulos, B., Baker, S. E., Barry, K., Bills, G., Bluhm, B. H., Cannon, C., Castanera, R., Culley, D. E., Daum, C., Ezra, D., González, J. B., Henrissat, B., Kuo, A., ... Grigoriev, I. V. (2020). 101 Dothideomycetes genomes: A test case for predicting lifestyles and emergence of pathogens. *Studies in Mycology*, 96, 141–153. <https://doi.org/10.1016/j.simyco.2020.01.003>
- Iturrutxa, E., Slippers, B., Mesanza, N., & Wingfield, M. J. (2011). First report of *Neofusicoccum parvum* causing canker and die-back of Eucalyptus in Spain. *Australasian Plant Disease Notes*, 6, 57. <https://doi.org/10.1007/s13314-011-0019-5>
- Klotz, L. J. (1978). Fungal, bacterial, and nonparasitic diseases and injuries originating in the seedbed, nursery, and orchard. In *The Citrus Industry*. University of California (pp. 2–66).
- Kumar, S., Stecher, G., & Tamura K. (2016). MEGA7: Molecular Evolutionary Genetics Analysis Version 7.0 for Bigger Datasets. *Molecular Biology and Evolution*, 33, 1870–1874.
- Lopes, A., Barradas, C., Phillips, A. J. L., & Alves, A. (2016). Diversity and phylogeny of *Neofusicoccum* species occurring in forest and urban environments in Portugal. *Mycosphere*, 7(7), 906–920. <https://doi.org/10.5943/mycosphere/si/1b/10>
- Lopes, Anabela, Phillips, A. J. L., & Alves, A. (2017). Mating type genes in the genus *Neofusicoccum*: Mating strategies and usefulness in species delimitation. *Fungal Biology*, 121, 394–404. <https://doi.org/10.1016/j.funbio.2016.08.011>
- Marsberg, A., Kemler, M., Jami, F., Nagel, J. H., Postma-Smidt, A., Naidoo, S., Wingfield, M. J., Crous, P. W., Spatafora, J. W., Hesse, C. N., Robbertse, B., & Slippers, B. (2017). *Botryosphaeria dothidea*: a latent pathogen of global importance to woody plant health. *Molecular Plant Pathology*, 18, 477–488. <https://doi.org/10.1111/mpp.12495>
- Masi, M., Aloï, F., Nocera, P., Cacciola, S. O., Surico, G., & Evidente, A. (2020). Phytotoxic Metabolites Isolated from *Neofusicoccum batangarum*, the Causal Agent of the Scabby Canker of Cactus Pear (*Opuntia ficus-indica* L.). *Toxins*, 12, 126. <https://doi.org/10.3390/toxins12020126>
- Mayorquin, J. S., Wang, D. H., Twizeyimana, M., & Eskalen, A. (2016). Identification, distribution, and pathogenicity of Diatrypaceae and Botryosphaeriaceae associated with citrus branch canker in the Southern California desert. *Plant Disease*, 100, 2402–2413. <https://doi.org/10.1094/PDIS-03-16-0362-RE>
- McDonald, V., & Eskalen, A. (2011). Botryosphaeriaceae species associated with avocado branch cankers in California. *Plant Disease*, 95, 1465–1473. <https://doi.org/10.1094/PDIS-02-11-0136>
- Migheli, Q., Cacciola, S. O., Balmas, V., Pane, A., Ezra, D., & Di San Lio, G. M. (2009). Mal secco disease caused by *Phoma tracheiphila*: A potential threat to lemon production worldwide. *Plant Disease*, 93, 852–867. <https://doi.org/10.1094/PDIS-93-9-0852>
- Molina-Gayosso, E., Silva-Rojas, H. V., García-Morales, S., & Avila-Quezada, G. (2012). First Report of Black Spots on Avocado Fruit Caused by *Neofusicoccum parvum* in Mexico. *Plant Disease*, 96(2), 287. <https://doi.org/10.1094/pdis-08-11-0699>
- Mondello, V., Songy, A., Battiston, E., Pinto, C., Coppin, C., Trotel-Aziz, P., Clément, C., Mugnai, L., & Fontaine, F. (2018). Grapevine trunk diseases: A review of fifteen years of trials for their control with chemicals and biocontrol agents. *Plant Disease*, 102, 1189–1217. <https://doi.org/10.1094/PDIS-08-17-1181-FE>

- Moral, J., Morgan, D., Trapero, A., & Michailides, T. J. (2019). Ecology and epidemiology of diseases of nut crops and olives caused by Botryosphaeriaceae fungi in California and Spain. *Plant Disease*, *103*, 1809–1827. <https://doi.org/10.1094/PDIS-03-19-0622-FE>
- Pancher, M., Ceol, M., Corneo, P. E., Longa, C. M. O., Yousaf, S., Pertot, I., & Campisano, A. (2012). Fungal endophytic communities in grapevines (*Vitis vinifera* L.) Respond to crop management. *Applied and Environmental Microbiology*, *78*, 4308–4317. <https://doi.org/10.1128/AEM.07655-11>
- Pavlic-Zupanc, D., Wingfield, M. J., Boissin, E., & Slippers, B. (2015). The distribution of genetic diversity in the *Neofusicoccum parvum*/*N. ribis* complex suggests structure correlated with level of disturbance. *Fungal Ecology*, *13*, 93–102. <https://doi.org/10.1016/j.funeco.2014.09.002>
- Pérez, C. A., Wingfield, M. J., Slippers, B., Altier, N. A., & Blanchette, R. A. (2010). Endophytic and canker-associated Botryosphaeriaceae occurring on non-native Eucalyptus and native Myrtaceae trees in Uruguay. *Fungal Diversity*, *41*, 53. <https://doi.org/10.1007/s13225-009-0014-8>
- Phillips, A. J.L., Alves, A., Abdollahzadeh, J., Slippers, B., Wingfield, M. J., Groenewald, J. Z., & Crous, P. W. (2013). The Botryosphaeriaceae: Genera and species known from culture. *Studies in Mycology*, *76*, 51–167. <https://doi.org/10.3114/sim0021>
- Phillips, Alan J.L. (2002). Botryosphaeria species associated with diseases of grapevines in Portugal. *Phytopathologia Mediterranea*, *41*, 3–18. https://doi.org/10.14601/Phytopathol_Mediterr-1655
- Phillips, Alan J.L., Hyde, K. D., Alves, A., & Liu, J. K. (Jack). (2019). Families in Botryosphaeriales: a phylogenetic, morphological and evolutionary perspective. *Fungal Diversity*, *94*, 1–22. <https://doi.org/10.1007/s13225-018-0416-6>
- Riolo, M., Aloï, F., Pane, A., Cara, M., & Cacciola, S. O. (2021). Twig and Shoot Dieback of Citrus, a New Disease Caused by *Colletotrichum* Species. *Cells*, *10*(2), 449.
- Rocchetti, A., Schena, L., Sanzani, S. M., Cacciola, S. O., Mosca, S., Faedda, R., Ippolito, A., & Di San Lio, G. M. (2014). Characterization of basidiomycetes associated with wood rot of citrus in Southern Italy. *Phytopathology*, *104*, 851–858. <https://doi.org/10.1094/PHYTO-10-13-0272-R>
- Sakalidis, M. L., Slippers, B., Wingfield, B. D., Hardy, G. E. S. J., & Burgess, T. I. (2013). The challenge of understanding the origin, pathways and extent of fungal invasions: Global populations of the *Neofusicoccum parvum*-*N. ribis* species complex. *Diversity and Distributions*, *19*(8), 873–883. <https://doi.org/10.1111/ddi.12030>
- Salerno, M., & Cutuli, G. (1994). *Guida illustrate di patologia degli agrumi* (Edagrigo (ed.); Edizioni A).
- Salvatore, M. M., Alves, A., & Andolfi, A. (2021). Secondary Metabolites Produced by *Neofusicoccum* Species Associated with Plants: A Review. *Agriculture*, *11*(2), 149. <https://doi.org/10.3390/agriculture11020149>
- Scaramuzzi, G. (1965). *Le malattie degli agrumi* (Edizioni Agricole (ed.)).
- Schena, L., Burrano, S., Giambra, S., Surico, G., Pane, A., Evoli, M., Magnano Di San Lio, G., & Cacciola, S. O. (2018). First report of *Neofusicoccum batangarum* as causal agent of scabby cankers of cactus pear (*Opuntia ficus-indica*) in minor islands of sicily. *Plant Disease*, *102*, 445. <https://doi.org/10.1094/PDIS-07-17-1039-PDN>
- Schena, L., & Cooke, D. E. L. (2006). Assessing the potential of regions of the nuclear and mitochondrial genome to develop a “molecular tool box” for the detection and characterization of *Phytophthora* species. *Journal of Microbiological Methods*, *67*, 70–85. <https://doi.org/10.1016/j.mimet.2006.03.003>

Slippers, B., Boissin, E., Phillips, A. J. L., Groenewald, J. Z., Lombard, L., Wingfield, M. J., Postma, A., Burgess, T., & Crous, P. W. (2013). Phylogenetic lineages in the botryosphaeriales: A systematic and evolutionary framework. *Studies in Mycology*, *76*, 31–49. <https://doi.org/10.3114/sim0020>

Slippers, Bernard, Fourie, G., Crous, P. W., Coutinho, T. A., Wingfield, B. D., & Wingfield, M. J. (2004). Multiple gene sequences delimit *Botryosphaeria australis* sp. nov. from *B. lutea*. *Mycologia*, *96*, 1030–1041. <https://doi.org/10.1080/15572536.2005.11832903>

Slippers, Bernard, & Wingfield, M. J. (2007). Botryosphaeriaceae as endophytes and latent pathogens of woody plants: diversity, ecology and impact. *Fungal Biology Reviews*, *21*, 90–106. <https://doi.org/10.1016/j.fbr.2007.06.002>

Spagnolo, A., Marchi, G., Peduto, F., Phillips, A. J. L., & Surico, G. (2011). Detection of Botryosphaeriaceae species within grapevine woody tissues by nested PCR, with particular emphasis on the *Neofusicoccum parvum*/*N. ribis* complex. *European Journal of Plant Pathology*, *129*(3), 485–500. <https://doi.org/10.1007/s10658-010-9715-9>

Tamura, K., Stecher, G., Peterson, D., Filipiński, A., & Kumar, S. (2013). MEGA6: Molecular evolutionary genetics analysis version 6.0. *Molecular Biology and Evolution*, *30*, 2725–2729. <https://doi.org/10.1093/molbev/mst197>

Timmer, L. W., Garnsey, S. M., & Graham, J. . (n.d.). *Compendium of Citrus Diseases*.

Úrbez-Torres, J. R., & Gubler, W. D. (2009). Pathogenicity of Botryosphaeriaceae species isolated from grapevine cankers in California. *Plant Disease*, *93*, 584–592. <https://doi.org/10.1094/PDIS-93-6-0584>

Úrbez-Torres, J. R., & Gubler, W. D. (2011). Susceptibility of grapevine pruning wounds to infection by *Lasiodiplodia theobromae* and *Neofusicoccum parvum*. *Plant Pathology*, *60*, 261–270. <https://doi.org/10.1111/j.1365-3059.2010.02381.x>

Vaidya, N. H., Hadjicostis, C. N., & Dominguez-Garcia, A. D. (2011). Distributed Algorithms for Consensus and Coordination in the Presence of Packet-Dropping Communication Links - Part II: Coefficients of Ergodicity Analysis Approach. *ArXiv Preprint ArXiv:1109.6392*, *2208*, 1–23. <http://arxiv.org/abs/1109.6392>

White, T. J., Bruns, T., Lee, S., & Taylor, J. W. (1990). Amplification and direct sequencing of fungal ribosomal RNA genes for phylogenetics. In M. A. Innis, D. H. Gelfand, J. J. Sninsky, & T. J. White (Eds.), *PCR protocols: a guide to methods and applications* (Vol. 18, Issue 1, pp. 315–322). Academic Press, Inc. [http://msafungi.org/wp-content/uploads/Inoculum/64\(1\).pdf](http://msafungi.org/wp-content/uploads/Inoculum/64(1).pdf)

Wright, A. F., & Harmon, P. F. (2010). Identification of species in the Botryosphaeriaceae family causing stem blight on southern highbush blueberry in Florida. *Plant Disease*, *94*, 966–971. <https://doi.org/10.1094/PDIS-94-8-0966>

Yang, T., Groenewald, J. Z., Cheewangkoon, R., Jami, F., Abdollahzadeh, J., Lombard, L., & Crous, P. W. (2017). Families, genera, and species of *Botryosphaeriales*. *Fungal Biology*, *121*, 322–346. <https://doi.org/10.1016/j.funbio.2016.11.001>

Zhang, W., Groenewald, J. Z., Lombard, L., Schumacher, R. K., Phillips, A. J. L., & Crous, P. W. (2021). Evaluating species in *Botryosphaeriales*. *Persoonia - Molecular Phylogeny and Evolution of Fungi*, *46*, 63–115. <https://doi.org/10.3767/persoonia.2021.46.03>

Chapter 5.

Characterization of *Alternaria* species associated with heart rot of pomegranate fruit

5.1 Introduction

In Italy, the commercial cultivation of pomegranate is rapidly expanding and has grown from around 130 ha in 2013 to 1,234 ha in 2019 (Faedda et al., 2015; *Istat.it*, 2020). The most successful cultivar is Wonderful, originating from California and then introduced by Israeli in Italy, which is suitable for the consumption as fresh fruit and fresh-cut products as well as for processing to produce juice. Moreover, several industrial and medical applications of pomegranate peel extracts, e.g. as food preservatives, are being envisaged as pomegranate peel is rich in phenolic compounds, which are responsible for strong antioxidative and antimicrobial activity (Belgacem et al., 2019; Chen et al., 2020; Magangana et al., 2020; S. Pangallo et al., 2017; Sonia Pangallo et al., 2017, 2020; Tehranifar et al., 2011; R. Wang et al., 2010). Currently, a major constraint of pomegranate commercial production is constituted by heart rot, an emerging disease caused by *Alternaria* spp. and reported from California, India and several Mediterranean countries, including Cyprus, Greece, Egypt, Israel, and Italy (Benagi et al., 2011; Ezra et al., 2015; Faedda et al., 2015; Luo et al., 2017; Thomidis 2014; Tziros et al., 2008). The disease is also named *Alternaria* heart rot or black heart (Day & Wilkins, 2011; Zhang & McCarthy, 2012). No precise estimate of the damage caused yearly by heart rot to the pomegranate production in Italy is available. According with the first report of the disease in Italy, its incidence in commercial orchards varies from 1 to 9% of fruits (Faedda et al., 2015). However due to the difficulty in screening infected fruits on the basis of external symptoms and the unpleasant aspect of internal symptoms even the mere the presence of infected fruits causes a serious value loss of the whole fruit stock.

Different *Alternaria* species were identified as causative agents of pomegranate heart rot on the basis of morphological characteristics and multi-loci phylogenetic analyses (Ezra et al., 2015; Faedda et al., 2015; Garganese et al., 2016; Michailides et al., 2008). Airborne spores of the pathogen are thought to cause flower infections (David Ezra et al., 2015; Michailides et al., 2008). Following fruit onset, infections can remain latent for most of the growing season until the establishment of favorable conditions (David Ezra et al., 2015). Since the affected fruits are more prone to fall, one of the preventive agronomic practices is the shaking of the trees before harvesting (Zhang & McCarthy, 2012). Precise identification of the causative agent of heart rot is crucial for all aspects concerning the epidemiology and management of the disease. Unfortunately, the taxonomy of *Alternaria* is problematic and has undergone several revisions (Lawrence et al., 2016; Patriarca, 2016; Woudenberg et al., 2015). The difficulties in the identification of this genus at species level are related to the considerable morphological plasticity of most of the recognized *Alternaria* species. Historically, the identification of *Alternaria* spp. was based on morphological characteristics, including cultural features, size and shape of conidia, and branching patterns of conidial chains (Simmons, 1999, 2007). Although the main sections of *Alternaria* can be differentiated using these features, this approach is not sufficient for distinguishing closely related species (Andrew et al., 2009; Armitage et al.,

2015). In the past, the production of host-specific toxins (HSTs) has been used to distinguish among species (Kusaba & Tsuge, 1995), but this criterion proved unreliable since HST biosynthetic gene clusters are located on small conditionally dispensable chromosomes, which can be lost or gained (Johnson et al., 2001). Molecular identification based on ribosomal DNA (rDNA), a genomic region typically used in fungal systematics, failed to differentiate small-spored *Alternaria* species (Peever et al., 2004; B. M. Pryor & Gilbertson, 2000; Barry M. Pryor & Bigelow, 2003). Furthermore, the poor resolution obtained even using more variable genetic loci, generated debate on which species should be kept within the *Alternaria* section *Alternaria* (i.e. *A. alternata*, *A. tenuissima*, *A. arborescens*, *A. mali*, and *A. gaisen*), suggesting to combine *A. alternata* and *A. tenuissima* or to merge the latter two species with *A. arborescens* (Andrew et al., 2009; Armitage et al., 2015; Woudenberg et al., 2015).

The analysis of secondary metabolites has also been proposed as a mean to support species identification within the genus (Andersen et al., 2015; Patriarca, 2016). *Alternaria* is one of the major mycotoxigenic fungal genera (Andersen et al., 2015; Escrivá et al., 2017; Fraeyman et al., 2017; Hickert et al., 2016; Logrieco et al., 2009; Masiello et al., 2020; Patriarca, 2016; Prella et al., 2013; Siciliano et al., 2015). Furthermore, it produces more than 70 phytotoxic metabolites, including host-specific toxins and non-host-specific toxins (Thomma, 2003). However, only a few mycotoxins (e.g. tenuazonic acid, alternariol, alternariol monomethyl ether) may be found in food and are of major toxicological concern. These toxins are suspected to exert both acute and chronic detrimental effects (“Scientific Opinion on the risks for animal and public health related to the presence of *Alternaria* toxins in feed and food,” 2011). As a consequence, their presence as contaminants in pomegranate fruits and juice may represent a threat to human health.

This study aimed at the characterization of *Alternaria* isolates obtained from pomegranate fruit with symptoms of heart rot in southern Italy and at determining their mycotoxigenic profile.

5.2 Materials and Methods

5.2.1 *Alternaria* isolates

Overall, 42 *Alternaria* isolates obtained from pomegranate fruit with symptoms of heart rot were included in this study (**Table 1**).

Table 1. *Alternaria* isolates from pomegranate fruits characterized in this study, their geographical origins and accession numbers of their ITS, EF-1 α , GAPDH and OPA 10-2 sequences in GenBank.

Isolate	Morphotype	Location	Host, cultivar	Accession numbers			
				ITS	EF-1 α	GAPDH	OPA 10-2
AaMR7	1	Italy, Sicily	<i>Punica granatum</i> cv. Wonderful	MW580732	MW585113	MW590491	MW590533
AaMP7a	1	Italy, Sicily	<i>Punica granatum</i> cv. Wonderful	MW580733	MW585114	MW590492	MW590534
AaMP10	1	Italy, Sicily	<i>Punica granatum</i> cv. Wonderful	MW580734	MW585115	MW590493	MW590535
AaMR11	1	Italy, Sicily	<i>Punica granatum</i> cv. Wonderful	MW580735	MW585116	MW590494	MW590536
AaMMH6e	1	Italy, Sicily	<i>Punica granatum</i> cv. Mollar de Helche	MW580743	MW585121	MW590502	MW590544
AaMP3	1	Italy, Sicily	<i>Punica granatum</i> cv. Wonderful	MW580745	MW585123	MW590504	MW590546
AaMR9a	1	Italy, Sicily	<i>Punica granatum</i> cv. Wonderful	MW580747	MW585125	MW590506	MW590548
AaMP9	1	Italy, Sicily	<i>Punica granatum</i> cv. Wonderful	MW580748	MW585126	MW590507	MW590549
AaMDc5b	1	Italy, Sicily	<i>Punica granatum</i> cv. Dente di cavallo	MW580754	MW585132	MW590513	MW590555
AaMDc5d	1	Italy, Sicily	<i>Punica granatum</i> cv. Dente di cavallo	MW580755	MW585133	MW590514	MW590556
AaMMH6b	1	Italy, Sicily	<i>Punica granatum</i> cv. Mollar de Helche	MW580756	MW585134	MW590515	MW590557
AaMMH7a	1	Italy, Sicily	<i>Punica granatum</i> cv. Mollar de Helche	MW580757	MW585135	MW590516	MW590558
AaMMH7d	1	Italy, Sicily	<i>Punica granatum</i> cv. Mollar de Helche	MW580758	MW585136	MW590517	MW590559
AaMMH6a	1	Italy, Sicily	<i>Punica granatum</i> cv. Dente di cavallo	MW580763	MW585140	MW590522	MW590564
AaMMH6d	1	Italy, Sicily	<i>Punica granatum</i> cv. Mollar de Helche	MW580764	MW585141	MW590523	MW590565
AaMMH7b	1	Italy, Sicily	<i>Punica granatum</i> cv. Mollar de Helche	MW580765	MW585142	MW590524	MW590566
M24-BB1	1	Italy, Apulia	<i>Punica granatum</i> cv. Dente di cavallo	MW580768	MW585145	MW590527	MW590569
M95 A2	1	Italy, Apulia	<i>Punica granatum</i> cv. Wonderful	MW580770	MW585147	MW590529	MW590571
M103 A2-1	1	Italy, Apulia	<i>Punica granatum</i> cv. Wonderful	MW580771	MW585148	MW590530	MW590572
M109 3	1	Italy, Apulia	<i>Punica granatum</i> cv. Wonderful	MW580772	MW585149	MW590531	MW590573
AaMR4	2	Italy, Sicily	<i>Punica granatum</i> cv. Wonderful	MW580739	MW585117	MW590498	MW590540
AaMR12	2	Italy, Sicily	<i>Punica granatum</i> cv. Wonderful	MW580742	MW585120	MW590501	MW590543
AaMR2b	2	Italy, Sicily	<i>Punica granatum</i> cv. Wonderful	MW580744	MW585122	MW590503	MW590545
AaMP4	2	Italy, Sicily	<i>Punica granatum</i> cv. Wonderful	MW580746	MW585124	MW590505	MW590547
AaMR14b	2	Italy, Sicily	<i>Punica granatum</i> cv. Wonderful	MW580760	MW585137	MW590519	MW590561
AaMP14a	2	Italy, Sicily	<i>Punica granatum</i> cv. Wonderful	MW580761	MW585138	MW590520	MW590562
AaMR14a	2	Italy, Sicily	<i>Punica granatum</i> cv. Wonderful	MW580766	MW585143	MW590525	MW590567
AaMP14b	2	Italy, Sicily	<i>Punica granatum</i> cv. Wonderful	MW580767	MW585144	MW590526	MW590568
M80 B5	2	Italy, Apulia	<i>Punica granatum</i> cv. Wonderful	MW580769	MW585146	MW590528	MW590570
AaMR5b	3	Italy, Sicily	<i>Punica granatum</i> cv. Wonderful	MW580731	MW585112	MW590490	MW590532
AaMDc3a	4	Italy, Sicily	<i>Punica granatum</i> cv. Dente di cavallo	MW580751	MW585129	MW590510	MW590552
AaMDc3b	4	Italy, Sicily	<i>Punica granatum</i> cv. Dente di cavallo	MW580752	MW585130	MW590511	MW590553
AaMDc3c	4	Italy, Sicily	<i>Punica granatum</i> cv. Dente di cavallo	MW580753	MW585131	MW590512	MW590554
AaMDc3d	4	Italy, Sicily	<i>Punica granatum</i> cv. Wonderful	MW580762	MW585139	MW590521	MW590563
AaMR6b	5	Italy, Sicily	<i>Punica granatum</i> cv. Wonderful	MW580740	MW585118	MW590499	MW590541
AaMP6b	5	Italy, Sicily	<i>Punica granatum</i> cv. Wonderful	MW580741	MW585119	MW590500	MW590542
AaMDc2a	5	Italy, Sicily	<i>Punica granatum</i> cv. Dente di cavallo	MW580749	MW585127	MW590508	MW590550
AaMDc2b	5	Italy, Sicily	<i>Punica granatum</i> cv. Dente di cavallo	MW580750	MW585128	MW590509	MW590551
AaMDc1a	6	Italy, Sicily	<i>Punica granatum</i> cv. Dente di cavallo	MW580736	MW585150	MW590495	MW590537
AaMDc1b	6	Italy, Sicily	<i>Punica granatum</i> cv. Dente di cavallo	MW580737	MW585151	MW590496	MW590538
AaMDc1d	6	Italy, Sicily	<i>Punica granatum</i> cv. Dente di cavallo	MW580738	MW585152	MW590497	MW590539

They were sourced from fruits of the three pomegranate cultivars Wonderful (Californian/Israeli origin), Mollar de Elche (Spanish origin) and Dente di Cavallo (Italian origin) (Holland et al., 2009; Pareek et al., 2015), picked up in commercial pomegranate orchards in Apulia and Sicily from 2015 to 2016.

Isolates were preserved in the collection of the laboratory of Molecular Plant Pathology at the Department of Agriculture, Food and Environment (Di3A) of the University of Catania, Italy. Reference strains of *A. alternata* and *A. arborescens* from CBS-KNAW were included for comparison (**Table 2**).

Table 2. GenBank accession numbers of sequences of the *Alternaria* spp. isolates of different country and host origins used as references in phylogenetic analyses.

Species	Isolate	Country	Host	Accession numbers ^a			
				ITS	EF-1 α	GPDH	OPA 10-2
<i>Alternaria alternata</i> (ex <i>A. citri</i>)	CBS 102.47	USA	<i>Citrus sinensis</i>	KP124304	KP125080	KP124161	KP124610
<i>Alternaria alternata</i> (ex-type)	CBS 916.96	India	<i>Arachis hypogaea</i>	AF347031	KC584634	AY278808	KP124632
<i>Alternaria alternata</i> (ex <i>A. limoniasperae</i>)	CBS 102595	USA	<i>Citrus jambhiri</i>	FJ266476	KC584666	AY562411	KP124636
<i>Alternaria alternata</i> (ex <i>A. tenuissima</i>)	CBS 112252	-	-	KP124340	KP125116	KP124194	KP124650
<i>Alternaria alternata</i> (ex <i>A. godetiae</i>)	CBS 117.44	Denmark	<i>Godetia</i> sp.	KP124303	KP125079	KP124160	KP124609
<i>Alternaria gaisen</i>	CBS 118488	Japan	<i>Pyrus pyrifolia</i>	KP124427	KP124278	KP125206	KP124743
<i>Alternaria alstroemeriae</i>	CBS 118808	USA	<i>Alstroemeria</i> sp.	KP124296	KP125071	KP124153	KP124601
<i>Alternaria iridialustralis</i>	CBS 118487	Australia	<i>Iris</i> sp.	KP124436	KP125215	KP124285	KP124752
<i>Alternaria jacinthicola</i>	CBS 878.95	Mauritius	<i>Arachis hypogaea</i>	KP124437	KP125216	KP124286	KP124753
<i>Alternaria tomato</i>	CBS 103.30	-	<i>Solanum lycopersicum</i>	KP124445	KP125224	KP124294	KP124762
<i>Alternaria burnsii</i>	CBS 107.38	India	<i>Cuminum cyminum</i>	KP124420	JQ646305	KP125198	KP124734
<i>Alternaria alternata</i> (ex <i>A. toxicogenica</i>)	CBS 102600	USA	<i>Citrus reticulata</i>	KP124331	KP125107	KP124186	KP124640
<i>Alternaria longipes</i>	CBS 540.94	USA	<i>Nicotiana tabacum</i>	AY278835	KC584667	AY278811	KP124758
<i>Alternaria alternata</i>	CBS 109803	Germany	human skin	KP124336	KP125112	KP124190	KP124645
<i>Alternaria betae-kenyensis</i>	CBS 118810	Kenya	<i>Beta vulgaris</i> var. <i>cicla</i>	KP124419	KP125197	KP124270	KP124733
<i>Alternaria eichhorniae</i>	CBS 119778	Indonesia	<i>Eichhornia crassipes</i>	KP124426	KP125205	KP124277	KP124741
<i>Alternaria arborescens</i>	CBS 109730	USA	<i>Solanum lycopersicum</i>	KP124399	KP125177	KP124251	KP124713
<i>Alternaria arborescens</i>	CBS 105.24	-	<i>Solanum tuberosum</i>	KP124393	KP125171	KP124245	KP124706
<i>Alternaria arborescens</i>	CBS 108.41	-	wood	KP124394	KP125172	KP124246	KP124707
<i>Alternaria arborescens</i>	CBS 112749	South Africa	<i>Malus domestica</i>	KP124401	KP125179	KP124253	KP124715
<i>Alternaria arborescens</i>	CBS 118389	Japan	<i>Pyrus pyrifolia</i>	KP124407	KP125185	KP124259	KP124721
<i>Alternaria arborescens</i>	CBS 115517	South Africa	<i>Malus domestica</i>	KP124404	KP125182	KP124256	KP124718

^a source (Woudenberg et al., 2015).

5.2.2 Symptoms, distribution, and incidence of the disease

Infected fruits were characterized by a brown to black, soft to dry rot of the arils, visible when the fruit was cut open. Typically, the rot was confined to some aril compartments (**Figure 1 C**) and did not affect the peel and compartment membranes (septa). The outer peel (epicarp) in correspondence of the internal rot showed symptoms difficult to recognize, such as a dark-red discoloration and wrinkling of the peel (**Figure 1 A, B**).



Figure 1. (A, B) External symptoms of heart rot in pomegranate fruit: dark-red discoloration and wrinkling of the peel. (C) Cut open fruit of pomegranate with typical symptoms of heart rot. Note the dark brown mass of conidia produced by *Alternaria* sporulating on rotten arils within the fruit. Symptoms were restricted by membranes that separate the fruit compartments.

Heavily affected fruits were asymmetric and lighter in weight. The incidence of fruits affected by heart rot in southern Italy was estimated to vary from 1 to 9% (Faedda et al., 2015), although it might have been higher under favorable conditions, such as rainy and warm weather during flowering and early fruit development (Prasad et al., 2010). Heart rot is considered a serious postharvest problem due to the difficulty in recognizing affected fruits from external symptoms (David Ezra et al., 2015; Faedda et al., 2015; Prasad et al., 2010; Zhang & McCarthy, 2012).

5.2.2 Morphological characterization

Isolates were grown in Petri dishes on Potato Dextrose Agar (PDA; Oxoid Ltd., Basingstoke, UK) and Malt Extract Agar (MEA; Sigma-Aldrich, United States), prepared according to CBS-KNAW Fungal Biodiversity Centre (Utrecht, The Netherlands) (Crous et al., 2009). Dishes were incubated for 7 days at $25\pm 1^\circ\text{C}$ in the dark (**Figure 2**).

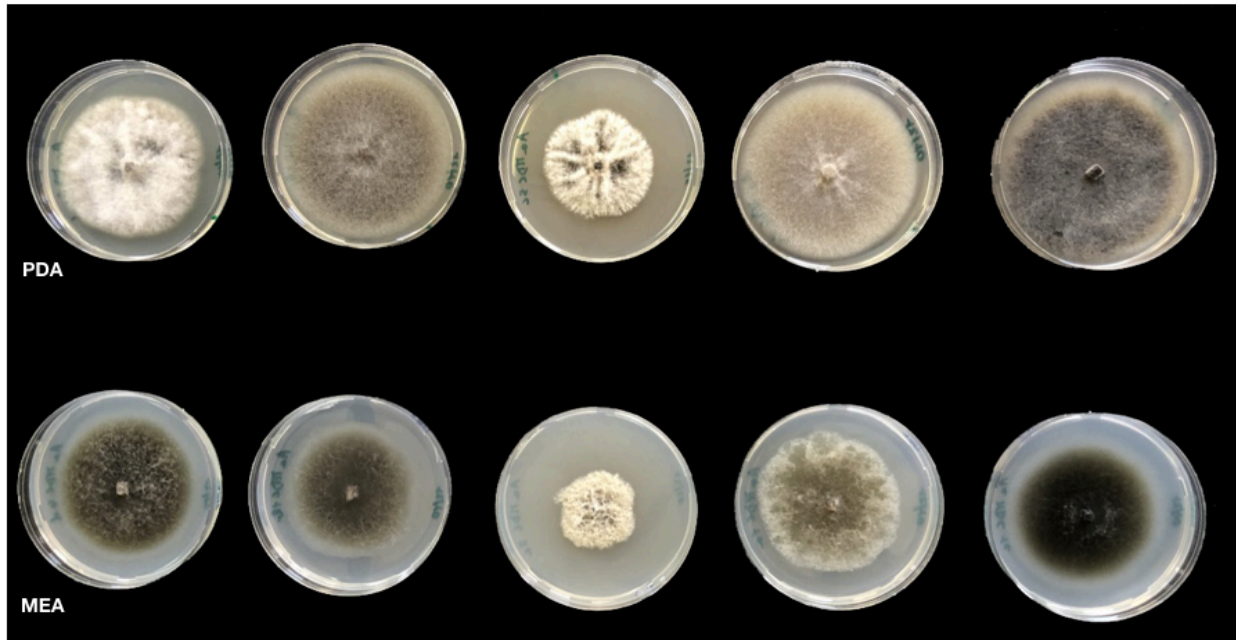


Figure 2. Growth pattern and colony morphology of isolates of *Alternaria* spp. obtained from pomegranate fruits with symptoms of heart rot collected from different Sicilian and Apulian orchards. From left to right: AaMDc1a, AaMP4, AaMRa1, AaMR4, and AaMDc5d. All the *Alternaria* isolated were grown on PDA and MEA culture media and incubated at $25\pm 1^\circ\text{C}$ for 7 days in the dark.

The macroscopic characteristics (color, margin, diameter, and texture) of colonies were examined according to Pryor and Michailides (Barry M. Pryor & Michailides, 2002), whereas microscopic features (conidium and conidiophore branch morphology) according to Simmons (Simmons, 2007).

5.2.3 Molecular characterization

Isolates were grown on PDA for 7 days at $25\pm 1^\circ\text{C}$. Mycelium of each isolate was harvested with a sterile scalpel, and the genomic DNA was extracted using PowerPlant® Pro DNA isolation Kit (MO BIO Laboratories, Inc., Carlsbad, CA, USA), following the manufacturer's protocol. The DNA was preserved at -20°C . A multilocus approach was adopted to characterize and determine the phylogenetic allocation of the 42 isolates from pomegranate fruit.

Portions of four *Alternaria* barcoding genes/regions, i.e. internal transcribed spacer (ITS), translation elongation factor 1- α (EF-1 α), glyceraldehyde-3-phosphate dehydrogenase (GAPDH) and one SCAR marker (OPA10-2), were sequenced (Woudenberg et al., 2015). The primers used for amplifying these genes/regions were: ITS1/ITS4 for ITS (White et al., 1990), EF1-728F/EF1-986R for EF-1 α (Carbone &

Kohn, 1999), GPD1/GPD2 for GAPDH (Berbee et al., 1999) and OPA10-2R/OPA10-2L for OPA10-2 (Andrew et al., 2009)(Table 3).

Table 3. Primers used in this study

Primer	Primer DNA sequence	PCR conditions	Reference
ITS1	5' TCC GTA GGT GAA CCT GCG G 3'	94°C for 3 min; 94°C for 30 s, 55°C for 30 s, 72°C for 30 s for 35 cycles and final extension at 72°C for 10 min	(White et al., 1990)
ITS4	5' GCT GCG TTC TTC ATC GAT GC 3'		
EF1-728F	5' CAT CGA GAA GTT CGA GAA GG 3'	94°C for 3 min; 94°C for 30 s, 58°C for 30 s, 72°C for 30 s for 35 cycles and final extension at 72°C for 10 min	(Carbone & Kohn, 1999)
EF1-986R	5' TAC TTG AAG GAA CCC TTA CC 3'		
GPD1	5' CAA CGG CTT CGG TCG CAT TG 3'	94°C for 3 min; 94°C for 30 s, 54°C for 30 s, 72°C for 30 s for 35 cycles and final extension at 72°C for 10 min	(Berbee et al., 1999)
GPD2	5' GCC AAG CAG TTG GTT GTG C 3'		
OPA 10-2R	5' GAT TCG CAG CAG GGA AAC TA 3'	94°C for 3 min; 94°C for 30 s, 62°C for 30 s, 72°C for 30 s for 35 cycles and final extension at 72°C for 10 min	(Andrew et al., 2009)
OPA 10-2L	5' TCG CAG TAA GAC ACA TTC TAC G 3'		

The PCR amplifications were performed on a GeneAmp PCR System 9700 (Applied Biosystems, Monza-Brianza, Italy). All PCR reactions were carried out by using the Taq DNA polymerase recombinant (Invitrogen™) in a total volume of 25 µl containing: PCR Buffer (1X), dNTP mix (0.2 mM), MgCl₂ (1.5 mM), forward and reverse primers (0.5 µM each), Taq DNA Polymerase (1 U) and 1 µL of genomic DNA. Reaction conditions were 94°C for 3 min; followed by 35 cycles of 94°C for 30 s, 55°C (ITS region)/58°C (EF-1α)/54°C (GAPDH)/62°C (OPA10-2) for 30 s, and 72°C for 30 s, followed by an additional 10-min extension at 72°C.

The amplicons were detected on 1% agarose gel and purified products were sequenced with both forward and reverse primers by MacroGen Europe (Amsterdam, The Netherlands).

Sequences were analyzed by using FinchTV v.1.4.0 (*FinchTV v.1.4.0. Available on line: <https://digitalworldbiology.com/FinchTV> (accessed on May 18, 2020)*, n.d.) and the consensus sequences were deposited in Genbank (Table 2).

For the molecular identification, sequences obtained in the present study and validated sequences of CBS representative strains of species within *Alternaria* sect. *Alternaria*, were phylogenetically analysed. Before analyses, the complete panel of reference sequences was tested utilizing the Elim Dupes software (*Elim Dupes software. Available on line: <http://hcv.lanl.gov/content/sequence/ELIMDUPES/elimdupes.html>*(accessed on June 15, 2020), n.d.) to delete multiple identical sequences. Identical reference sequences were included in the panel when representative of different *Alternaria* species (Woudenberg et al., 2015). Sequences were aligned using MUSCLE and introduced to MEGA6 for phylogenetic analysis with the Maximum Likelihood method using the Tamura-Nei model (Hall et al., 2013). Analyses were performed with 1000 bootstrap replications. In order to maximize the effectiveness of the investigation into the genetic diversity within isolates obtained

in the present study, the phylogenetic analysis was conducted using a combined data set of all sequenced markers (ITS, EF-1 α , GPDH and OPA10-2).

5.2.4 Pathogenicity tests

The pathogenicity of two *A. arborescens* isolates (AaMDc1A and AaMDc1d) and six *A. alternata* isolates, one for each morphotype from 2 to 5 (AaMR2b, AaMR5b, AaMDc3a and AaMDc1a) plus two for morphotype 1 (M95 A2 and AaMP3, from Apulia and Sicily, respectively), was tested in a commercial farm at Lentini (Syracuse, Sicily) on pomegranate fruits ‘Wonderful’ using the injection method described by Luo et al. (Luo et al., 2017). In detail, on 15th August 2020 a conidial suspension (5 μ l of 2×10^5 conidia ml⁻¹) was injected with a syringe into one side of a pomegranate fruits (10 fruits per each isolate). Control fruits were injected with sterile distilled water. Ten weeks later fruits were cut open longitudinally into two halves to observe heart rot symptoms.

5.2.5 Extraction and analyses of secondary metabolites

Isolates were tested for production of secondary metabolites using a modified Czapek-Dox liquid medium: 10 g/L glucose, 0.162 g/L NH₄NO₃, 1.7 g/L KH₂PO₄, 0.85 g/L MgSO₄, 0.425 g/L NaCl, 0.425 g/L KCl, 0.017 g/L FeSO₄, 0.017 g/L ZnSO₄ and 1.7 g/L yeast extract, pH 5.5. Cultures were inoculated with three mycelial plugs in 50 mL of medium. All cultures were performed in triplicate and incubated in the dark at 28 °C. After 8 days, cultures were filtered and *Alternaria* toxins in the clear medium were extracted by liquid-liquid extraction. Each sample was adjusted to pH 2 with HCl and an aliquot (5 mL) was transferred in a separating funnel. Ten mL of dichloromethane were added three times and the mixture was shaken for 1 min, then the dichloromethane extracts were collected in a flask. The final extract was evaporated to dryness in a rotary evaporator at 35 °C. The residue was dissolved in 1 mL of H₂O:CH₃OH 1:1 for the HPLC-MS/MS simultaneous detection of the main five *Alternaria* toxins. Analyses were carried out according to a previously validated method (Siciliano et al., 2015).

Standards of TeA (tenuazonic acid) copper salt from *A. alternata* (Purity \geq 98%), AOH (alternariol) from *Alternaria* spp. (Purity \geq 94%), AME (alternariol monomethyl ether) from *Alternaria alternata* (Purity \geq 98%), ALT (altenuene) from *Alternaria* spp. (Purity \geq 98%) and TEN (tentoxin) from *Alternaria tenuis* (Purity 99%) were purchased from Sigma-Aldrich in crystallized form. A stock solution of 1 mg/mL and a working solution of 10 μ g/mL were prepared in methanol for each molecule and kept at -20 °C. Standards for HPLC calibration and standards for addition experiment were prepared by diluting the working solution and a calibration curve was built for each analyte. Good linearity was obtained for all analytes ($R^2 > 0.999$). Recovery experiments were done spiking the matrix before extractions with a standard solution and the calculated recovery ranged between 80 and 100%.

5.3 Results

5.3.1 Morphological characterization of isolates

All 42 isolates were grouped according to macro- and microscopic features on PDA and MEA, along with reference strains of *A. alternata* and *A. arborescens* from CBS-KNAW. A higher variability in colony morphology was observed on PDA, as compared to MEA (**Figure 2**), allowing the differentiation of six morphotypes.

In particular, on PDA twenty isolates (AaMMH7d, AaMDc5d, AaMP3, M24-BB1, AaMMH6b, AaMMH6a, AaMR9a, AaMR7, AaMR11, AaMDc5b, AaMMH7a, AaMMH7b, M103 A2-1, M109 3, M95 A2, AaMMH6d, AaMP7a, AaMP10, AaMMH6e and AaMP9) showed colonies that were flat, woolly, with colors ranging from brown to black, and an average diameter of 65 mm. They produced dark brown conidia arranged in branched chains. Conidia appeared oval-ellipsoidal with 3–5 transverse septa. These features matched those of *A. alternata* ex-type reference strain CBS 916.96 (morphotype 1).

Nine isolates (AaMR2b, M80 B5, AaMP4, AaMR4, AaMR14a, AaMR14b, AaMP14b, AaMR12, AaMP14a) showed greenish colonies with white margins. Conidia appeared elongated with a long-tapered beak. The characteristic sporulation pattern matched that of the reference strain of *A. alternata* (ex *A. tenuissima*) CBS 112252 (morphotype 2).

One isolate (AaMR5b) exhibited a colony pale brown, flat, granulated with undulating edges. Conidia appeared long and ellipsoidal with 1–3 transverse septa. The sporulation pattern resembled that of *A. alternata* (ex *A. limoniasperae*) CBS 102595 (morphotype 3).

Four isolates (AaMDc3a, AaMDc3b, AaMDc3c, AaMDc3d) exhibited a sporulation pattern resembling that of the reference strain of *A. alternata* (ex *A. citri*) CBS 102.47, with elliptical and subglobose conidia (morphotype 4);

Four isolates (AaMDc2a, AaMDc2b, AaMP6b, AaMR6b) exhibited wide and long conidia, with a sporulation pattern resembling that of *A. alternata* (ex *A. toxicogenica*) CBS 102600 (morphotype 5).

Four isolates (AaMDc1a, AaMRa1, AaMDc1d, AaMDc1b) showed colonies varying from greenish grey to brown, characterized by a lower growth rate (average diameter 45 mm after 7 days on PDA). Conidia appeared oval or ellipsoidal with 1–4 transverse septa and 1–2 longitudinal septa. They were borne by long primary conidiophores, occasionally presenting sub-terminal branches. These characteristics matched those of the reference strain for *A. arborescens* CBS 109730 (morphotype 6).

5.3.2 Molecular characterization

Alternaria isolates from pomegranate sourced in southern Italy and reference isolates from CBS (Woudenberg et al., 2015) were grouped on the basis of a four-gene phylogeny, including ITS, EF-1 α , GAPDH and OPA 10-2 sequences. According to this analysis, 38 out of the 42 isolates were associated with *A. alternata*. They were from both the two sampling geographical areas, Sicily and Apulia, and clustered with reference isolates of *A. alternata*, including the isolates CBS 916.96, ex-type, and CBS 112252 (**Figure 3**). The *A. alternata* phylogenetic group included morphotypes from 1 to 5. The most

numerous phylogenetic sub-groups, corresponding to morphotype 1, included the ex-type isolate of *A. alternata* CBS 916.96.

Conversely, four isolates, namely AaMDc1a, AaMRa1, AaMDc1d and AaMDc1b, all from Sicily albeit from two different pomegranate cultivars, clustered within the *A. arborescens* species complex along with strains CBS 109730 from *Solanum lycopersicum*, CBS 105.24 from *Solanum tuberosum*, CBS 108.41 from wood, CBS 112749 from *Malus domestica*, CBS 118389 from *Pyrus pyrifolia* and CBS 115517 from *Malus domestica*. This group of isolates corresponded to the morphotype 6.

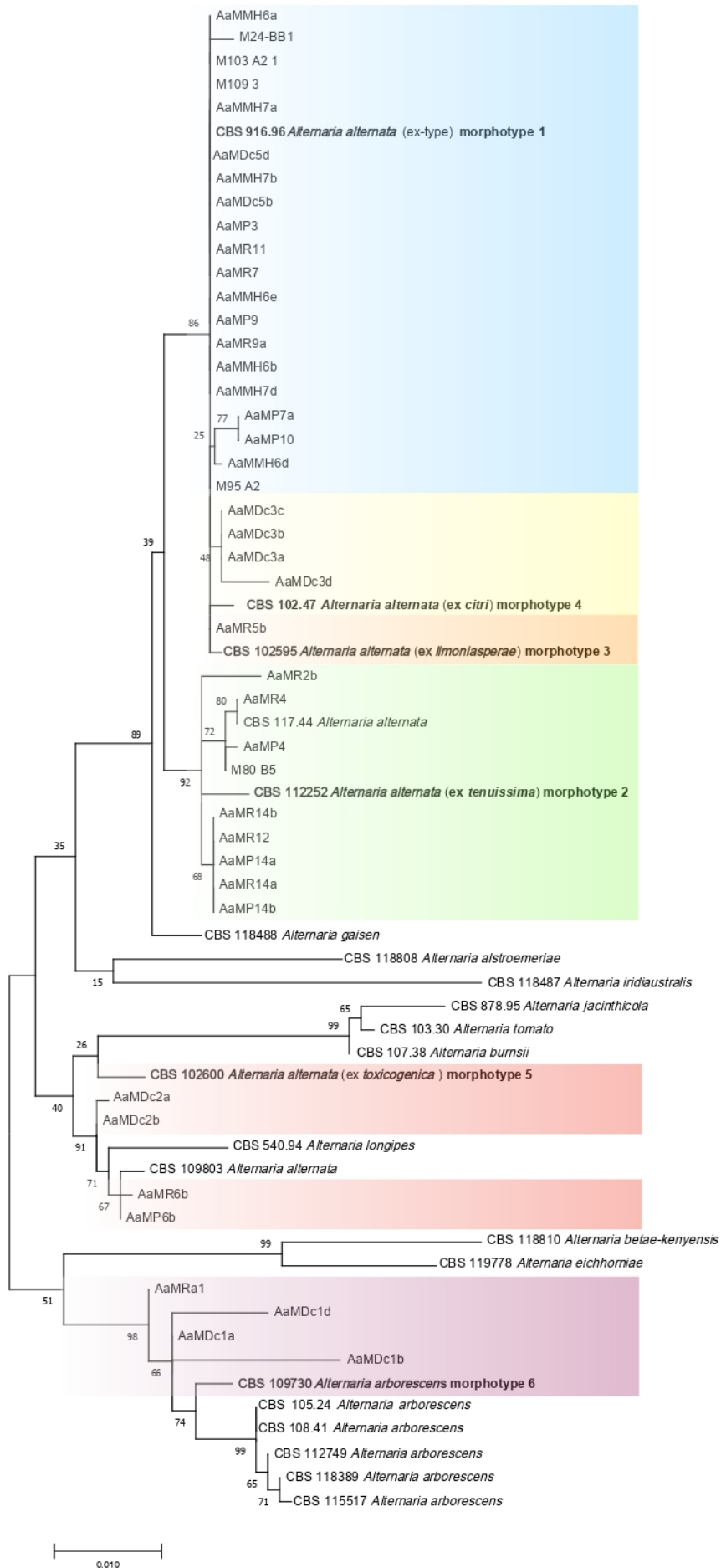


Figure 3. - Internal transcribed spacer (ITS), glyceraldehyde-3-phosphate dehydrogenase (GAPDH), translation elongation factor 1- α (EF-1 α) and one SCAR marker (OPA 10-2) multi-locus phylogenetic tree developed using the Maximum Likelihood Method, based on the Tamura–Nei model. The tree with the greatest log likelihood (-3746.14) is shown. Relationships between the 42 isolates from pomegranate sourced in southern Italy and the CBS reference isolates of *Alternaria alternata*, *A. arborescens* (in bold CBS isolates used as reference for diverse morphotypes) and other *Alternaria* spp. The six morphotypes are highlighted in different colors.

5.3.3 Pathogenicity tests

All eight tested isolates of *A. alternata* and *A. arborescens* induced typical symptoms of heart rot on artificially inoculated pomegranate fruits and were reisolated from rotten arils. The proportion of symptomatic fruits for each isolate ranged from 88 to 100%, not to count inoculated fruits that dropped before harvesting (from one to two per each isolate). In each symptomatic fruit the rot extended to about half of the entire longitudinal section (**Figure 4**). No symptoms were observed on control fruit.



Figure 4. – Symptoms of heart rot in a pomegranate fruits artificially inoculated by injecting a suspension of *Alternaria* conidia, 10 weeks after inoculation.

5.3.5. Analyses of *Alternaria* mycotoxins

The toxigenic potential of the 42 *Alternaria* spp. isolates was investigated *in vitro* on liquid culture medium, and the concentration levels of the five mycotoxins extracted from culture fluids are reported in Table 4. All isolates produced TeA, which was the prevalent mycotoxin found in culture extracts, with the only exception of isolates AaMR9a and AaMP9 of morphotype 1. Benzopyrone derivatives, AOH and AME, were produced by about 70% of the isolates. However, the amount of these two mycotoxins varied greatly

among isolates and within morphotypes and species. The isolates that produced AOH also produced AME, but the concentrations of the two toxins in culture filtrates were not correlated. ALT, a third toxin in the class of dibenzo- α -pyrones, was quantified in less than 50% of samples; it was not detected in culture fluids of isolates that did not produce AOH and AME. TEN, a cyclic tetrapeptide, was produced by 34 out of 38 *A. alternata* isolates, but its amount varied greatly, ranging from 3.09 to 2434 $\mu\text{g/L}$. None of the four morphotype 6 (*A. arborescens*) isolates tested produced TEN. Two isolates, AaMR14b and AaMP14a, both of morphotype 2, produced only TeA. Overall, however, no correlation was found between the toxigenic profile of the isolates and their specific phylogenetic identity, morphotype and geographical origin.

Table 4. *In vitro* mycotoxin production [$\mu\text{g/mL}$] by *Alternaria* isolates after 8 days of incubation at 28 °C in the dark.

Isolate	Morphotype	Origin	Mycotoxin concentration ($\mu\text{g/L}$) ^a				
			TeA	AOH	AME	ALT	TEN
AaMR7	1	Italy, Sicily	5133±561	9.141±1.46	2.094±0.22	9.177±1.32	167.5±31.9
AaMP7a	1	Italy, Sicily	1555±139	41.44±7.22	26.56±4.01	307.8±34.7	303.2±13.6
AaMP10	1	Italy, Sicily	1066±125	n.d. ^b	n.d.	n.d.	91.85±1.76
AaMR11	1	Italy, Sicily	1889±146	38.73±3.95	23.98±8.38	131.41±13.5	214.4±13.1
AaMMH6e	1	Italy, Sicily	279.4±44.6	5.619±0.44	4.735±0.42	n.d.	1.378±0.12
AaMP3	1	Italy, Sicily	495.6±50.3	n.d.	n.d.	n.d.	3.16±0.25
AaMR9a	1	Italy, Sicily	25.61±0.48	n.d.	n.d.	n.d.	30.77±2.28
AaMP9	1	Italy, Sicily	24.13±2.02	7.734±0.17	4.462±0.18	17.98±0.79	34.05±4.67
AaMDc5b	1	Italy, Sicily	839.2±65.7	n.d.	n.d.	n.d.	12.99±2.02
AaMDc5d	1	Italy, Sicily	3146±256	26.50±0.32	12.34±1.65	83.59±2.33	40.80±4.32
AaMMH6b	1	Italy, Sicily	786.8±111	6.604±0.29	2.451±0.40	8.236±1.31	n.d.
AaMMH7a	1	Italy, Sicily	2799±132	55.49±3.16	14.41±1.21	36.82±1.57	13.77±0.72
AaMMH7d	1	Italy, Sicily	1004±67.9	4.010±1.14	3.978±0.72	3.464±0.32	1.295±0.01
AaMMH6a	1	Italy, Sicily	1606±168	57.24±5.39	24.06±0.35	44.33±4.31	19.37±2.13
AaMMH6d	1	Italy, Sicily	1553±70.8	83.28±4.30	22.71±2.29	17.08±0.54	3.455±0.58
AaMMH7b	1	Italy, Sicily	2189±149	11.64±0.20	4.932±0.05	n.d.	31.82±0.25
M24-BB1	1	Italy, Apulia	4204±650	222.3±0.14	472.7±1.21	n.d.	1957±2.67
M95 A2	1	Italy, Apulia	5204±233	161.2±0.25	407.3±1.97	n.d.	2434±2.78
M103 A2-1	1	Italy, Apulia	1267±198	547.7±0.73	604.2±0.60	n.d.	1655±28.8
M109 3	1	Italy, Apulia	3258±7.78	384.9±0.09	196.5±0.36	n.d.	n.d.
AaMR4	2	Italy, Sicily	1950±56.5	23.82±1.77	24.12±4.32	n.d.	87.62±4.76
AaMR12	2	Italy, Sicily	1117±20.9	n.d.	n.d.	n.d.	20.80±0.31
AaMR2b	2	Italy, Sicily	1177±44.6	3.922±0.64	2.209±0.38	6.019±0.27	3.09±0.86
AaMP4	2	Italy, Sicily	789.3±113	n.d.	n.d.	n.d.	15.19±1.13
AaMR14b	2	Italy, Sicily	952.9±0.34	n.d.	n.d.	n.d.	n.d.
AaMP14a	2	Italy, Sicily	488.2±22.3	n.d.	n.d.	n.d.	n.d.
AaMR14a	2	Italy, Sicily	1169±33.8	n.d.	n.d.	n.d.	3.542±0.66
AaMP14b	2	Italy, Sicily	9227±904	44.87±2.87	6.603±0.27	n.d.	5.986±0.59
M80 B5	2	Italy, Apulia	2987±1.09	39.15±0.55	73.27±0.68	n.d.	8621±37.1
AaMR5b	3	Italy, Sicily	1264±73.0	18.29±1.63	23.59±1.36	112.5±2.51	153.2±15.4

AaMDc3a	4	Italy, Sicily	1762±38.6	37.64±1.16	4.853±0.01	17.97±1.06	51.69±5.91
AaMDc3b	4	Italy, Sicily	2887±195	89.64±2.97	10.77±0.10	7.465±0.28	27.94±2.72
AaMDc3c	4	Italy, Sicily	2336±154	n.d.	n.d.	n.d.	64.26±2.55
AaMDc3d	4	Italy, Sicily	2532±214	32.55±0.60	4.905±0.28	9.409±0.40	77.48±7.63
AaMR6b	5	Italy, Sicily	1460±83.6	n.d.	n.d.	n.d.	235.7±38.1
AaMP6b	5	Italy, Sicily	1115±24.9	1.848±0.01	4.928±0.43	94.28±8.51	201.4±20.3
AaMDc2a	5	Italy, Sicily	2028±92.3	n.d.	n.d.	n.d.	116.1±6.53
AaMDc2b	5	Italy, Sicily	1840±159	n.d.	n.d.	n.d.	51.42±0.19
AaMDc1a	6	Italy, Sicily	2769±207	56.18±6.82	7.050±1.71	425.97±33.2	n.d.
AaMDc1b	6	Italy, Sicily	3918±473	18.04±2.17	4.074±0.04	43.23±0.92	n.d.
AaMDc1d	6	Italy, Sicily	1680±171	33.12±4.62	2.984±1.26	67.54±2.91	n.d.
AaMRa1	6	Italy, Sicily	2666±19.5	76.98±1.37	9.974±1.29	384.92±42.3	n.d.

^a Means ± standard error of three independent biological experiments consisting of three technical replicates each.

^b n.d.= not detected.

5.4 Discussion

Results evidenced the complexity of *Alternaria* populations associated to heart rot of pomegranate fruits. According to the classification system proposed recently by Woudenberg et al. (Woudenberg et al., 2015) for the small-spored *Alternaria* species in the *Alternaria* section *Alternaria*, the isolates recovered from symptomatic pomegranate fruit sampled in two major producing regions of southern Italy, Apulia and Sicily, were referred to *A. alternata* and *A. arborescens* species complex (AASC) (Woudenberg et al., 2015), the former being by far the prevalent species. Despite the morphological and genetic variability, all isolates of both *A. alternata* and *A. arborescens* tested were pathogenic and induced typical symptoms of heart rot in pomegranate fruit artificially inoculated by injecting separately a conidial suspension of these two fungi into the fruit. These results indicate that *A. alternata* and *A. arborescens* are responsible for pomegranate heart rot disease in southern Italy. According to the available information, this is the first report of *A. arborescens* as a pathogen of pomegranate in Italy. Both species are known as plant pathogens and mycotoxin producers on a wide range of host plants (Andersen et al., 2015; Troncoso-Rojas & Tiznado-Hernández, 2014). Due to their growth even at low temperature, these *Alternaria* species are also responsible for spoilage of fruits and processed plant products during refrigerated transport and storage (Faedda et al., 2016).

In agreement with a previous study aimed at identifying *Alternaria* species associated to brown spot of tangerines in southern Italy (Garganese et al., 2016), *A. alternata* isolates recovered from pomegranate fruit showed a great morphological and molecular variability and were separated into six morphotypes corresponding to distinct albeit phylogenetically related clusters. Our results confirmed previous findings of other authors in California showing that diverse species of *Alternaria* are associated to heart rot of pomegranate (Luo et al., 2017; Michailides et al., 2008). Although in California heart rot is regarded as a minor disease of pomegranate, the correct identification of *Alternaria* species associated to this disease is considered a crucial aspect as *A. gaisen*, included in the section *Alternaria* and closely related to *A. arborescens*, is a quarantine pathogen and its presence might impose export restrictions (Luo et al., 2017).

In the present study, multi-locus phylogenetic analysis based on the four gene regions ITS, EF-1 α , GPDH and OPA 10-2, clearly separated *A. alternata*, *A. arborescens* and *A. gaisen*. However, neither ITS or EF-1 α and GPDH, alone or in combination, were able to discriminate these three species. Consistently with the results of this study aimed at characterizing the diversity of *Alternaria* species associated to heart rot of pomegranate, *A. alternata* and *A. arborescens* were the species associated to the brown fruit rot of tangerines and mandarins in southern Italy and California, and also in these cases *A. alternata* was the prevalent species (Garganese et al., 2016; F. Wang et al., 2020). It was demonstrated that the virulence of the *Alternaria* isolates recovered from citrus was positively correlated with the expression level of the ACTT1 and ACTT2 genes encoding for phytotoxins ACTT1 and ACTT2, respectively (Michailides et al., 2008). Several *formae speciales* of *A. alternata* infecting fruit and vegetable crops and producing host specific toxins are currently recognized, including *A. alternata* f. sp. *lycopersici* producing AAL-toxins and causing necrotic lesions on tomato, *A. alternata* f. sp. *mali* producing the AM toxin, *A. alternata* f. sp. *fragariae* producing the AF-toxin, and *A. alternata* f. sp. *citri* with two pathotypes, i.e. pathotype rough lemon for isolates producing the ACR-toxin, and pathotype tangerine for isolates producing the ACT-toxins (Hickert et al., 2016, Masunaka et al., 2005). No f. sp. or pathotype of *A. alternata* have so far been identified within the *A. alternata* populations associated to pomegranate fruits.

In standard laboratory conditions, isolates of both *A. alternata* and *A. arborescens* recovered from pomegranate fruit with symptoms of heart rot were able to produce mycotoxins, mainly tenuazonic acid (TeA), a tetramic acid derivative, and to a lesser extent alternariol (AOH), alternariol monomethyl ether (AME) and altenuene (ALT), in the structural group of dibenzopyrone derivatives. The majority of *A. alternata* produced also the cyclic tetrapeptide tentoxin (TEN) while none of the *A. arborescens* isolates tested produced this metabolite. The results of the present study are consistent with previous reports indicating that small-spored species in the section *Alternaria* (*A. tenuissima*, *A. arborescens* and *A. alternata* species groups) share a common secondary metabolite profile, but only a small proportion of *A. arborescens* isolates are able to produce TEN (Pinto & Patriarca, 2017; Patriarca et al., 2019). TeA, AOH, AME and TEN have a broad host range (Thomma, 2003) and in pomegranate heart rot disease they might act as virulence factors (Elhariry et al., 2016; Logrieco et al., 2009). Some of these non-host-specific toxins, such as TeA, AOH and AME, have been reported to induce harmful effects in mammals (Wenderoth et al., 2019). *In vitro* tests provided clear evidence of genotoxicity or acute toxicity in animals or rodent cells of AOH, AME ALT and TeA (“Scientific Opinion on the risks for animal and public health related to the presence of *Alternaria* toxins in feed and food,” 2011). Moldy arils of fresh pomegranate fruits affected by heart rot are usually removed by the consumer as they are not appropriate for human consumption. However, toxins can move from the rotten part to the surrounding tissues or processed fruit products. This may occur more frequently in *Alternaria* diseases that go unnoticed, as symptoms are internal such as heart rot. Moreover, current industrial processing methods do not exclude the risk of juice contamination by *Alternaria* toxins (Elhariry et al., 2016; Logrieco et al., 2009). As a consequence, the occurrence of heart rot on pomegranate fruits and of *Alternaria* toxins as contaminants in juice may be a risk factor for

consumer health. In a comprehensive study of EFSA (European Food Safety Authority) aimed at investigating the distribution of *Alternaria* toxins across the food categories and groups, AOH, AME, ALT, TeA and TEN were the toxins occurring most commonly in fruit and vegetable juices (“Scientific Opinion on the risks for animal and public health related to the presence of *Alternaria* toxins in feed and food,” 2011). In this study the ability of *Alternaria* species associated to heart rot of pomegranate to produce toxins has been investigated for the first time in Europe.

5.5 References

- Andersen, B., Nielsen, K. F., Fernández Pinto, V., & Patriarca, A. (2015). Characterization of *Alternaria* strains from Argentinean blueberry, tomato, walnut and wheat. *International Journal of Food Microbiology*, *196*, 1–10. <https://doi.org/10.1016/j.ijfoodmicro.2014.11.029>
- Andrew, M., Peever, T. L., & Pryor, B. M. (2009). An expanded multilocus phylogeny does not resolve morphological species within the small-spored *Alternaria* species complex. *Mycologia*, *101*, 95–109. <https://doi.org/10.3852/08-135>
- Armitage, A. D., Barbara, D. J., Harrison, R. J., Lane, C. R., Sreenivasaprasad, S., Woodhall, J. W., & Clarkson, J. P. (2015). Discrete lineages within *Alternaria alternata* species group: Identification using new highly variable loci and support from morphological characters. *Fungal Biology*, *119*, 994–1006. <https://doi.org/10.1016/j.funbio.2015.06.012>
- Barkai-Golan, R., & Paster, N. (2008). Mycotoxins in Fruits and Vegetables. In R. Barkai-Golan & P. Nachman (Eds.), *Mycotoxins in Fruits and Vegetables*. Academic Press. <https://doi.org/10.1016/B978-0-12-374126-4.X0001-0>
- Belgacem, I., Pangallo, S., Abdelfattah, A., Romeo, F. V., Cacciola, S. O., Li Destri Nicosia, M. G., Ballistreri, G., & Schena, L. (2019). Transcriptomic analysis of orange fruit treated with pomegranate peel extract (PGE). *Plants*, *8*, 101. <https://doi.org/10.3390/plants8040101>
- Benagi, V. I., Ravi Kumar, M. R., Gowdar, S. B., & Pawar, B. B. (2011). Survey on diseases of pomegranate in Northern Karnataka, India. *Acta Horticulturae*, *890*, 509–511.
- Berbee, M. L., Pirseyedi, M., & Hubbard, S. (1999). *Cochliobolus* phylogenetics and the origin of known, highly virulent pathogens, inferred from ITS and glyceraldehyde-3-phosphate dehydrogenase gene sequences. *Mycologia*, *91*, 964–977. <https://doi.org/10.2307/3761627>
- Carbone, I., & Kohn, L. M. (1999). A method for designing primer sets for speciation studies in filamentous ascomycetes. *Mycologia*, *91*, 553–556. <https://doi.org/10.2307/3761358>
- Chen, J., Liao, C., Ouyang, X., Kahramanoğlu, I., Gan, Y., & Li, M. (2020). Antimicrobial Activity of Pomegranate Peel and Its Applications on Food Preservation. In *Journal of Food Quality* (p. Article ID 8850339). <https://doi.org/10.1155/2020/8850339>
- Crous, P. W., Verkley, G. J. M., Groenwald, E., & Houbaken, J. (2009). *Fungal biodiversity, Westerdijk Laboratory Manual Series vol.1*.
- Day, K. R., & Wilkins, E. D. (2011). Commercial pomegranate (*Punica granatum* L.) production in California. *Acta Horticulturae*, *890*, 275–285.
- Elhariry, H. M., Khiralla, G. M., Gherbawy, Y., & Abd Elrahman, H. (2016). Natural occurrence of alternaria toxins in pomegranate fruit and the influence of some technological processing on their levels in juice. *Acta Alimentaria*, *45*, 380–389. <https://doi.org/10.1556/066.2016.45.3.9>

Elim Dupes software. Available on line: <http://hcv.lanl.gov/content/sequence/ELIMDUPES/elimdupes.html> (accessed on June 15, 2020). (n.d.).

Escrivá, L., Oueslati, S., Font, G., & Manyes, L. (2017). *Alternaria* Mycotoxins in Food and Feed: An Overview. *Journal of Food Quality*, *5*, 1–20. <https://doi.org/10.1155/2017/1569748>

Ezra, D., Shulhani, R., Bar Ya'akov, I., Harel-Beja, R., Holland, D., & Shtienberg, D. (2019). Factors affecting the response of pomegranate fruit to *Alternaria alternata*, the causal agent of heart rot. *Plant Disease*, *103*, 315–323. <https://doi.org/10.1094/PDIS-01-18-0147-RE>

Ezra, David, Kirshner, B., Hershovich, M., Shtienberg, D., & Kosto, I. (2015). Heart rot of pomegranate: Disease etiology and the events leading to development of symptoms. *Plant Disease*, *99*, 496–501. <https://doi.org/10.1094/PDIS-07-14-0707-RE>

Faemma, R., D'Aquino, S., Granata, G., Pane, A., Palma, A., Sanzani, S. M., Schena, L., & Cacciola, S. O. (2016). Postharvest fungal diseases of cactus pear fruit in southern Italy. *Acta Horticulturae*, *1144*, 215–218. <https://doi.org/10.17660/ActaHortic.2016.1144.31>

Faemma, R., Granata, G., Massimino Cocuzza, G. E., Lo Giudice, V., Audoly, G., Pane, A., & Cacciola, S. O. (2015). First report of heart rot of pomegranate (*Punica granatum*) caused by *Alternaria alternata* in Italy. *Plant Disease*, *99*, 1446. <https://doi.org/10.1094/PDIS-02-15-0238-PDN>

FinchTV v.1.4.0. Available on line: <https://digitalworldbiology.com/FinchTV> (accessed on May 18, 2020). (n.d.).

Fraeyman, S., Croubels, S., Devreese, M., & Antonissen, G. (2017). Emerging fusarium and alternaria mycotoxins: Occurrence, toxicity and toxicokinetics. *Toxins*, *9*, 228. <https://doi.org/10.3390/toxins9070228>

Garganese, F., Schena, L., Siciliano, I., Prigigallo, M. I., Spadaro, D., De Grassi, A., Ippolito, A., & Sanzani, S. M. (2016). Characterization of citrus-associated *Alternaria* species in Mediterranean areas. *PLoS ONE*, *11*(9), e0163255. <https://doi.org/10.1371/journal.pone.0163255>

Hall, M. P., Nagel, R. J., Fagg, W. S., Shiue, L., Cline, M. S., Perriman, R. J., Donohue, J. P., & Ares, M. (2013). Quaking and PTB control overlapping splicing regulatory networks during muscle cell differentiation. *RNA*, *19*(5), 627–638. <https://doi.org/10.1261/rna.038422.113>

Hickert, S., Bergmann, M., Ersen, S., Cramer, B., & Humpf, H. U. (2016). Survey of *Alternaria* toxin contamination in food from the German market, using a rapid HPLC-MS/MS approach. *Mycotoxin Research*, *32*, 7–18. <https://doi.org/10.1007/s12550-015-0233-7>

Holland, D., Hatib, K., & Bar-Ya'akov, I. (2009). Pomegranate: Botany, Horticulture, Breeding. *Horticultural Reviews*, *35*, 127–191. <https://doi.org/10.1002/9780470593776.ch2>

Istat.it. (2020). <http://dati.istat.it/Index.aspx?QueryId=33705>

Johnson, L. J., Johnson, R. D., Akamatsu, H., Salamiah, A., Otani, H., Kohmoto, K., & Kodama, M. (2001). Spontaneous loss of a conditionally dispensable chromosome from the *Alternaria alternata* apple pathotype leads to loss of toxin production and pathogenicity. *Current Genetics*, *40*, 65–72. <https://doi.org/10.1007/s002940100233>

Kusaba, M., & Tsuge, T. (1995). Phology of *Alternaria* fungi known to produce host-specific toxins on the basis of variation in internal transcribed spacers of ribosomal DNA. *Current Genetics*, *28*, 491–498. <https://doi.org/10.1007/BF00310821>

Lawrence, D. P., Rotondo, F., & Gannibal, P. B. (2016). Biodiversity and taxonomy of the pleomorphic genus *Alternaria*. *Mycological Progress*, *15*, 1–22. <https://doi.org/10.1007/s11557-015-1144-x>

Logrieco, A., Moretti, A., & Solfrizzo, M. (2009). *Alternaria* toxins and plant diseases: An overview of origin, occurrence and risks. *World Mycotoxin Journal*, 129–140. <https://doi.org/10.3920/WMJ2009.1145>

Luo, Y., Hou, L., Förster, H., Pryor, B., & Adaskaveg, J. E. (2017). Identification of *Alternaria* species causing heart rot of pomegranates in California. *Plant Disease*, *101*, 421–427. <https://doi.org/10.1094/PDIS-08-16-1176-RE>

Magangana, T. P., Makunga, N. P., Fawole, O. A., & Opara, U. L. (2020). Processing factors affecting the phytochemical and nutritional properties of pomegranate (*Punica granatum* L.) peel waste: A review. *Molecules*, *25*, 4690. <https://doi.org/10.3390/molecules25204690>

Masiello, M., Somma, S., Susca, A., Ghionna, V., Logrieco, A. F., Franzoni, M., Ravaglia, S., Meca, G., & Moretti, A. (2020). Molecular identification and mycotoxin production by *Alternaria* species occurring on durum wheat, showing black point symptoms. *Toxins*, *12*, 275. <https://doi.org/10.3390/toxins12040275>

Masunaka, A., Ohtani, K., Peever, T. L., Timmer, L. W., Tsuge, T., Yamamoto, M., Yamamoto, H., & Akimitsu, K. (2005). An isolate of *Alternaria alternata* that is pathogenic to both tangerines and rough lemon and produces two host-selective toxins, ACT- and ACR-toxins. *Phytopathology*, *95*, 241–247. <https://doi.org/10.1094/PHYTO-95-0241>

Michailides, T., Morgan, D., Quist, M., & Reyes, H. (2008). Infection of pomegranate by *Alternaria* spp. causing black heart. *Phytopathology*, *98*, S105.

Pangallo, S., Li Destri Nicosia, M. G., Raphael, G., Levin, E., Ballistreri, G., Cacciola, S. O., Rapisarda, P., Droby, S., & Schena, L. (2017). Elicitation of resistance responses in grapefruit and lemon fruits treated with a pomegranate peel extract. *Plant Pathology*, *66*, 633–640. <https://doi.org/10.1111/ppa.12594>

Pangallo, Sonia, Li Destri Nicosia, M. G., Agosteo, G. E., Abdelfattah, A., Romeo, F. V., Cacciola, S. O., Rapisarda, P., & Schena, L. (2017). Evaluation of a pomegranate peel extract as an alternative means to control olive anthracnose. *Phytopathology*, *107*, 1462–1467. <https://doi.org/10.1094/PHYTO-04-17-0133-R>

Pangallo, Sonia, Li Destri Nicosia, M. G., Scibetta, S., Strano, M. C., Cacciola, S. O., Agosteo, G. E., Belgacem, I., & Schena, L. (2020). Pre- and postharvest applications of a pomegranate peel extract to control citrus fruit decay during storage and shelf life. *Plant Disease*. <https://doi.org/10.1094/pdis-01-20-0178-re>

Pareek, S., Valero, D., & Serrano, M. (2015). Postharvest biology and technology of pomegranate. *Journal of the Science of Food and Agriculture*, *95*(12), 2360–2379. <https://doi.org/10.1002/jsfa.7069>

Patriarca, A. (2016). *Alternaria* in food products. *Current Opinion in Food Science*, *11*, 1–9. <https://doi.org/10.1016/j.cofs.2016.08.007>

Peever, T. L., Su, G., Carpenter-Boggs, L., & Timmer, L. W. (2004). Molecular systematics of citrus-associated *Alternaria* species. *Mycologia*, *96*, 119–134. <https://doi.org/10.1080/15572536.2005.11833002>

Prasad, R. N., Chandra, R., & Teixeira da Silva, J. A. (2010). Postharvest handling and processing of pomegranate. In R. Chandra (Ed.), *Pomegranate, Fruit, Vegetable and Cereal Science and Biotechnology* (pp. 88–95).

Prelle, A., Spadaro, D., Garibaldi, A., & Gullino, M. L. (2013). A new method for detection of five *Alternaria* toxins in food matrices based on LC-APCI-MS. *Food Chemistry*, *140*, 161–167. <https://doi.org/10.1016/j.foodchem.2012.12.065>

Pryor, B. M., & Gilbertson, R. L. (2000). Molecular phylogenetic relationships amongst *Alternaria* species and related fungi based upon analysis of nuclear ITS and mt SSU rDNA sequences. *Mycological Research*, *104*, 1312–1321. <https://doi.org/10.1017/S0953756200003002>

Pryor, Barry M., & Bigelow, D. M. (2003). Molecular characterization of *Embellisia* and *Nimbya* species and their relationship to *Alternaria*, *Ulocladium* and *Stemphylium*. *Mycologia*, *95*(6), 1141–1154. <https://doi.org/10.1080/15572536.2004.11833024>

Pryor, Barry M., & Michailides, T. J. (2002). Morphological, pathogenic, and molecular characterization of *Alternaria* isolates associated with alternaria late blight of pistachio. *Phytopathology*, *92*, 406–416. <https://doi.org/10.1094/PHYTO.2002.92.4.406>

Scientific Opinion on the risks for animal and public health related to the presence of *Alternaria* toxins in feed and food. (2011). *EFSA Journal*, *9*(10), 2407. <https://doi.org/10.2903/j.efsa.2011.2407>

Siciliano, I., Ortu, G., Gilardi, G., Gullino, M. L., & Garibaldi, A. (2015). Mycotoxin production in liquid culture and on plants infected with *Alternaria* spp. Isolated from rocket and cabbage. *Toxins*, *7*, 743–754. <https://doi.org/10.3390/toxins7030743>

Simmons, E. G. (1999). *Alternaria* themes and variations (236-243) host-specific toxin producers. *Mycotaxon*, *70*, 325–369.

Simmons, E. G. (2007). *Alternaria: an identification manual: fully illustrated and with catalogue raisonné 1796-2007* (E. G. Simmons (Ed.); CBS biodiv).

Tehranifar, A., Selahvarzi, Y., Kharrazi, M., & Bakhsh, V. J. (2011). High potential of agro-industrial by-products of pomegranate (*Punica granatum* L.) as the powerful antifungal and antioxidant substances. *Industrial Crops and Products*, *34*, 1523–1527. <https://doi.org/10.1016/j.indcrop.2011.05.007>

Thomidis, T. (2014). Fruit rots of pomegranate (cv. Wonderful) in Greece. *Australasian Plant Pathology*, *43*, 583–588. <https://doi.org/10.1007/s13313-014-0300-0>

Thomma, B. P. H. J. (2003). *Alternaria* spp.: From general saprophyte to specific parasite. *Molecular Plant Pathology*, *4*, 225–236. <https://doi.org/10.1046/j.1364-3703.2003.00173.x>

Troncoso-Rojas, R., & Tiznado-Hernández, M. E. (2014). *Alternaria alternata* (Black Rot, Black Spot). In *Postharvest Decay: Control Strategies* (pp. 147–187). <https://doi.org/10.1016/B978-0-12-411552-1.00005-3>

Tziros, G. T., Lagopodi, A. L., & Tzavella-Klonari, K. (2008). *Alternaria alternata* fruit rot of pomegranate (*Punica granatum*) in Greece. *Plant Pathology*, *57*, 379. <https://doi.org/10.1111/j.1365-3059.2007.01668.x>

Wang, F., Saito, S., Michailides, T., & Xiao, C.-L. (2020). Phylogenetic, Morphological, and Pathogenic Characterization of *Alternaria* Species Associated with Fruit rot of Mandarin in California. *Plant Disease*. <https://doi.org/10.1094/pdis-10-20-2145-re>

Wang, R., Ding, Y., Liu, R., Xiang, L., & Du, L. (2010). Pomegranate: constituents, bioactivities and pharmacokinetics. In R. Chandra (Ed.), *Pomegranate,- Fruit, Vegetable and Cereal Science and Biotechnology* (pp. 77–87).

White, T. J., Bruns, T., Lee, S., & Taylor, J. W. (1990). Amplification and direct sequencing of fungal ribosomal RNA genes for phylogenetics. In M. A. Innis, D. H. Gelfand, J. J. Sninsky, & T. J. White (Eds.), *PCR protocols: a guide to methods and applications* (Vol. 18, Issue 1, pp. 315–322). Academic Press, Inc. [http://msafungi.org/wp-content/uploads/Inoculum/64\(1\).pdf](http://msafungi.org/wp-content/uploads/Inoculum/64(1).pdf)

Woudenberg, J. H. C., Seidl, M. F., Groenewald, J. Z., de Vries, M., Stielow, J. B., Thomma, B. P. H. J., & Crous, P. W. (2015). *Alternaria* section *Alternaria*: Species, formae speciales or pathotypes? *Studies in Mycology*, *82*, 1–21. <https://doi.org/10.1016/j.simyco.2015.07.001>





Zhang, L., & McCarthy, M. J. (2012). Black heart characterization and detection in pomegranate using NMR relaxometry and MR imaging. *Postharvest Biology and Technology*, *67*, 96–101. <https://doi.org/10.1016/j.postharvbio.2011.12.018>

Chapter 6.

**Shoot dieback of citrus, a new disease caused by *Colletotrichum* species. Published on
Cells 2021, 10(2), 449; <https://doi.org/10.3390/cells10020449>**

Article

Twig and Shoot Dieback of Citrus, a New Disease Caused by *Colletotrichum* Species

Mario Riolo ^{1,2,3,†} , Francesco Aloï ^{1,4,†}, Antonella Pane ^{1,†} , Magdalena Cara ^{5,*}  and Santa Olga Cacciola ^{1,*} 

- ¹ Department of Agriculture, Food and Environment, University of Catania, 95123 Catania, Italy; mario.riolo@unirc.it (M.R.); francesco.aloi@unipa.it (F.A.); apane@unict.it (A.P.)
- ² Council for Agricultural Research and Agricultural Economy Analysis, Research Centre for Olive, Citrus and Tree Fruit- Rende CS (CREA- OFA), 87036 Rende, Italy
- ³ Department of Agricultural Science, Mediterranean University of Reggio Calabria, 89122 Reggio Calabria, Italy
- ⁴ Department of Agricultural, Food and Forest Sciences, University of Palermo, 90128 Palermo, Italy
- ⁵ Department of Plant Protection, Faculty of Agriculture and Environment, Agriculture University of Tirana (AUT), 1029 Tirana, Albania
- * Correspondence: magdacara@ubt.edu.al (M.C.); olgacacciola@unict.it (S.O.C.)
- † These authors have equally contributed to the study.

Abstract: (1) Background: This study was aimed at identifying the *Colletotrichum* species associated with twig and shoot dieback of citrus, a new syndrome occurring in the Mediterranean region and also reported as emerging in California. (2) Methods: Overall, 119 *Colletotrichum* isolates were characterized. They were recovered from symptomatic trees of sweet orange, mandarin and mandarin-like fruits during a survey of citrus groves in Albania and Sicily (southern Italy). (3) Results: The isolates were grouped into two distinct morphotypes. The grouping of isolates was supported by phylogenetic sequence analysis of two genetic markers, the internal transcribed spacer regions of rDNA (ITS) and β -tubulin (TUB2). The groups were identified as *Colletotrichum gloeosporioides* and *C. karstii*, respectively. The former accounted for more than 91% of isolates, while the latter was retrieved only occasionally in Sicily. Both species induced symptoms on artificially wound inoculated twigs. *C. gloeosporioides* was more aggressive than of *C. karstii*. Winds and prolonged drought were the factor predisposing to *Colletotrichum* twig and shoot dieback. (4) Conclusions: This is the first report of *C. gloeosporioides* and *C. karstii* as causal agents of twig and shoot dieback disease in the Mediterranean region and the first report of *C. gloeosporioides* as a citrus pathogen in Albania.

Keywords: *Colletotrichum gloeosporioides*; *Colletotrichum karstii*; ITS; TUB2; pathogenicity; citrus



Citation: Riolo, M.; Aloï, F.; Pane, A.; Cara, M.; Cacciola, S.O. Twig and Shoot Dieback of Citrus, a New Disease Caused by *Colletotrichum* Species. *Cells* **2021**, *10*, 449. <https://doi.org/10.3390/cells10020449>

Academic Editor:

Suleyman Allakhverdiev

Received: 31 January 2021

Accepted: 18 February 2021

Published: 20 February 2021

Publisher's Note: MDPI stays neutral with regard to jurisdictional claims in published maps and institutional affiliations.



Copyright: © 2021 by the authors. Licensee MDPI, Basel, Switzerland. This article is an open access article distributed under the terms and conditions of the Creative Commons Attribution (CC BY) license (<https://creativecommons.org/licenses/by/4.0/>).

1. Introduction

Albania with around 2000 ha of citrus groves is a relatively small citrus growing country, but has an old tradition in the production of citrus, primarily represented by mandarins and prevalently concentrated in the districts of Vlorë, Berat, Elbasan, Durrës, Tiranë, Lezhë, Shkodër and Gjirokastrë [1]. Italy ranks second among European citrus producer countries, with Sicily and Calabria regions (southern Italy) accounting for approximately 63 and 19% of total domestic production of oranges and 53 and 20% of production of tangerines, respectively [2]. Sicily alone accounts for around 86% of total domestic production of lemons [2]. Moreover, Italy is the leading producer country of organic citrus fruit globally, with over 35,000 ha, corresponding to about one third of the total domestic citrus growing area [3]. Over the last years in both Albania and southern Italy, outbreaks of citrus twig and shoot dieback were observed to occur in major orange and mandarin growing areas following extreme weather events whose frequency in the Mediterranean region has increased due to climate change [4]. The disease, here named twig and shoot dieback of citrus or *Colletotrichum* twig and shoot dieback to stress its association with pathogenic *Colletotrichum* species, was recently described as an emerging new disease of

citrus in Central Valley, California, distinct from the typical anthracnose of fruit, leaves and twigs [5,6]. Symptoms of dieback caused by *Colletotrichum* included chlorosis, crown thinning, necrotic blotches on leaves, blight and frequently gummosis of apical twigs, shoot and branch dieback [6]. Two *Colletotrichum* species, *C. gloeosporioides* and *C. karstii*, were associated with *Colletotrichum* dieback in California. Overall, neither species clearly prevailed over the other and, in pathogenicity tests, both species were able to infect twigs, although not all field symptoms were reproduced [5]. In pathogenicity tests performed in California, *C. karstii* was more aggressive than *C. gloeosporioides* [5]. Symptoms similar to twig and shoot dieback described in California were reported from countries of the Mediterranean region, including Algeria, Morocco and Tunisia, but they were always associated with other symptoms typical of anthracnose on fruits and leaves [7–9]. In a recent survey of citrus groves in Portugal aimed at identifying the *Colletotrichum* species associated with typical anthracnose on fruits, leaves and twigs, *C. gloeosporioides*, the dominant species, was isolated preferentially from fruits and leaves while *C. karstii* was isolated preferentially from twigs and leaves, suggesting the hypothesis of differences in host-plant organ specificity between these two species [10]. Differences in host-plant organ preference between *Colletotrichum* species complex have long been known [11]. Two of the best-known examples of host and organ specificity are provided by *C. abscissum* and *C. limeticola*, both in the *C. acutaum* complex, associated to post-bloom fruit drop (PFD) of citrus and Key Lime Anthracnose (KLA), respectively, occurring in the Americas [12–16]. According to the new molecular taxonomy of the genus *Colletotrichum*, based on multi-locus phylogeny and a polyphasic approach, 25 distinct *Colletotrichum* species have been so far identified to be associated to *Citrus* and allied genera worldwide. Seven of these, including *C. aenigma*, *C. ciggaro* (syn. *C. kahawae* subsp. *ciggaro*), *C. gloeosporioides sensu stricto (s.s.)* and *C. hystricis*, within the *C. gloeosporioides* species complex, *C. catinaense* and *C. karstii*, within the *C. boninense* species complex, and *C. acutatum s.s.*, within the *C. acutatum* species complex, have been reported from Italy [9,10,17–28], while in the literature there is no record of *Colletotrichum* infecting citrus from Albania. The objectives of this study were to identify the *Colletotrichum* species associated with the new disease twig and shoot dieback or *Colletotrichum* twig and shoot dieback of citrus in Albania and Sicily and evaluate the pathogenicity of these *Colletotrichum* species on different plant organs, including fruit, leaves and shoots.

2. Materials and Methods

2.1. Sampling and Isolation

During 2017 and 2018, citrus orchards were surveyed for twig and shoot dieback in six municipalities (Augusta, Lentini, Mineo, Misterbianco, Ramacca and Scordia) of the provinces of Catania and Syracuse (Sicily, southern Italy), and in the municipality of Xarrë, prefecture of Vlorë (Vlorë, Albania). *Colletotrichum* isolates were obtained from twigs with symptoms of blight and gumming and from leaves showing necrotic patches and mesophyll collapse. Overall, samples were collected from 10 citrus groves in Albania and six citrus groves (one for each municipality) in Sicily and from diverse citrus species and cultivars, including Clementine mandarin (*Citrus x clementina*), three cultivars of sweet orange (*Citrus x sinensis*), “Tarocco Lempso”, “Tarocco Scirè” and “Lane Late”, and two mandarin-like hybrids, “Fortune” (*C. x clementina* × “Orlando” tangelo) and “Mandared” (*C. x clementina* “Nules” × *C. x sinensis* “Tarocco”).

To obtain fungal isolates, twig and leaf fragments (5 mm) were washed with tap water, surface sterilised with a sodium hypochlorite solution (10%) for 1 min, immersed in 70% ethanol for 30 s and rinsed in sterile distilled water (s.d.w.). After disinfection, the fragments were blotted dry on sterilised filter paper, placed in Petri dishes on potato-dextrose-agar (PDA; Oxoid Ltd., Basingstoke, UK) amended with 150 µg/mL streptomycin and incubated at 25 °C until typical *Colletotrichum* colonies were observed. Sporulating conidiomata from subcultures were collected, crushed in a drop of s.d.w. and spread in Petri dishes over the surface of PDA amended with streptomycin to obtain single-conidium isolates. After 24 h incubation at 25 °C, germinating conidia were individually transferred

to Petri dishes onto PDA. Stock cultures of single-conidium isolates were maintained on PDA slants under mineral oil at 5–10 °C in the culture collection of the Molecular Plant Pathology laboratory of the Department of Agriculture, Food and Environment of the University of Catania, Italy.

2.2. Fungal Isolates

A total of 119 single-conidium isolates of *Colletotrichum* from citrus, representing a population of mass isolates around ten-fold larger, was characterised in this study (Table 1).

Table 1. Isolates of *Colletotrichum* sourced from different cultivars of *Citrus* species in Sicily (southern Italy) and Albania and characterized in this study. * Tetraploid hybrid clementine ‘Nules’x sweet orange ‘Tarocco’.

Isolate Code	Species	Host (Species and Cultivar)	Organ	Geographical Origin	Genbank Accession	
					ITS-rDNA	β-tubulin 2
AC1	<i>C. gloeosporioides</i>	Sweet orange ‘Tarocco Lempso’	twig	Ramacca (Ct)-Sicily	MT997785	MW001517
AC2	<i>C. gloeosporioides</i>	Sweet orange ‘Tarocco Lempso’	twig	Ramacca (Ct)-Sicily	MT997786	MW001518
AC3	<i>C. gloeosporioides</i>	Sweet orange ‘Tarocco Lempso’	twig	Ramacca (Ct)-Sicily	MT997787	MW001519
AC4	<i>C. gloeosporioides</i>	Sweet orange ‘Tarocco Lempso’	twig	Ramacca (Ct)-Sicily	MT997788	MW001520
AC5	<i>C. gloeosporioides</i>	Sweet orange ‘Tarocco Lempso’	twig	Ramacca (Ct)-Sicily	MT997789	MW001521
AC6	<i>C. gloeosporioides</i>	Sweet orange ‘Tarocco Lempso’	twig	Ramacca (Ct)-Sicily	MT997790	MW001522
AC7	<i>C. gloeosporioides</i>	Sweet orange ‘Tarocco Lempso’	twig	Ramacca (Ct)-Sicily	MT997791	MW001523
AC8	<i>C. gloeosporioides</i>	Sweet orange ‘Tarocco Lempso’	twig	Ramacca (Ct)-Sicily	MT997792	MW001524
AC9	<i>C. gloeosporioides</i>	Sweet orange ‘Tarocco Lempso’	twig	Ramacca (Ct)-Sicily	MT997793	MW001525
AC10	<i>C. gloeosporioides</i>	Sweet orange ‘Tarocco Lempso’	twig	Ramacca (Ct)-Sicily	MT997794	MW001526
AC11	<i>C. gloeosporioides</i>	Sweet orange ‘Tarocco Lempso’	twig	Ramacca (Ct)-Sicily	MT997795	MW001527
AC12	<i>C. gloeosporioides</i>	Sweet orange ‘Tarocco Lempso’	twig	Ramacca (Ct)-Sicily	MT997796	MW001528
AC13	<i>C. gloeosporioides</i>	Sweet orange ‘Tarocco Lempso’	twig	Ramacca (Ct)-Sicily	MT997797	MW001529
AC14	<i>C. gloeosporioides</i>	Sweet orange ‘Tarocco Lempso’	twig	Ramacca (Ct)-Sicily	MT997798	MW001530
AC15	<i>C. gloeosporioides</i>	Sweet orange ‘Tarocco Lempso’	twig	Ramacca (Ct)-Sicily	MT997799	MW001531
AC16	<i>C. gloeosporioides</i>	Sweet orange ‘Tarocco Lempso’	twig	Ramacca (Ct)-Sicily	MT997800	MW001532
AC17	<i>C. gloeosporioides</i>	Sweet orange ‘Tarocco Lempso’	twig	Ramacca (Ct)-Sicily	MT997801	MW001533
AC18	<i>C. gloeosporioides</i>	Sweet orange ‘Tarocco Lempso’	twig	Ramacca (Ct)-Sicily	MT997802	MW001534
AC19	<i>C. gloeosporioides</i>	Sweet orange ‘Tarocco Lempso’	twig	Ramacca (Ct)-Sicily	MT997803	MW001535
AC20	<i>C. gloeosporioides</i>	Sweet orange ‘Tarocco Lempso’	twig	Ramacca (Ct)-Sicily	MT997804	MW001536
AC21	<i>C. gloeosporioides</i>	Sweet orange ‘Tarocco Lempso’	twig	Ramacca (Ct)-Sicily	MT997805	MW001537
AC22	<i>C. gloeosporioides</i>	Sweet orange ‘Tarocco Lempso’	twig	Ramacca (Ct)-Sicily	MT997806	MW001538

Table 1. Cont.

Isolate Code	Species	Host (Species and Cultivar)	Organ	Geographical Origin	Genbank Accession	
AC23	<i>C. gloeosporioides</i>	Sweet orange 'Tarocco Lempso'	twig	Ramacca (Ct)-Sicily	MT997807	MW001539
AC24	<i>C. gloeosporioides</i>	Sweet orange 'Tarocco Lempso'	twig	Ramacca (Ct)-Sicily	MT997808	MW001540
AC25	<i>C. gloeosporioides</i>	Sweet orange 'Tarocco Lempso'	twig	Ramacca (Ct)-Sicily	MT997809	MW001541
AC26	<i>C. gloeosporioides</i>	Sweet orange 'Tarocco Lempso'	twig	Ramacca (Ct)-Sicily	MT997810	MW001542
AC27	<i>C. gloeosporioides</i>	Sweet orange 'Tarocco Lempso'	twig	Ramacca (Ct)-Sicily	MT997811	MW001543
AC28	<i>C. gloeosporioides</i>	Sweet orange 'Tarocco Lempso'	twig	Ramacca (Ct)-Sicily	MT997812	MW001544
AC29	<i>C. gloeosporioides</i>	Sweet orange 'Tarocco Lempso'	twig	Ramacca (Ct)-Sicily	MT997813	MW001545
AC30	<i>C. gloeosporioides</i>	Sweet orange 'Tarocco Lempso'	twig	Ramacca (Ct)-Sicily	MT997814	MW001546
AC31	<i>C. gloeosporioides</i>	Sweet orange 'Tarocco Lempso'	twig	Ramacca (Ct)-Sicily	MT997815	MW001547
AC32	<i>C. gloeosporioides</i>	Sweet orange 'Tarocco Lempso'	twig	Ramacca (Ct)-Sicily	MT997816	MW001548
AC33	<i>C. gloeosporioides</i>	Sweet orange 'Tarocco Lempso'	twig	Ramacca (Ct)-Sicily	MT997817	MW001549
AC34	<i>C. gloeosporioides</i>	Sweet orange 'Tarocco Lempso'	twig	Ramacca (Ct)-Sicily	MT997818	MW001550
AC35	<i>C. gloeosporioides</i>	Sweet orange 'Tarocco Lempso'	leaf	Ramacca (Ct)-Sicily	MT997819	MW001551
AC36	<i>C. gloeosporioides</i>	Sweet orange 'Tarocco Lempso'	leaf	Ramacca (Ct)-Sicily	MT997820	MW001552
AC37	<i>C. gloeosporioides</i>	Sweet orange 'Tarocco Lempso'	leaf	Ramacca (Ct)-Sicily	MT997821	MW001553
AC38	<i>C. gloeosporioides</i>	Sweet orange 'Tarocco Lempso'	leaf	Ramacca (Ct)-Sicily	MT997822	MW001554
ALL1A	<i>C. gloeosporioides</i>	Sweet orange 'Lane late'	leaf	Augusta (Sr)-Sicily	MT997843	MW001575
ALL1B	<i>C. gloeosporioides</i>	Sweet orange 'Lane late'	leaf	Augusta (Sr)-Sicily	MT997844	MW001576
ALL1C	<i>C. gloeosporioides</i>	Sweet orange 'Lane late'	leaf	Augusta (Sr)-Sicily	MT997845	MW001577
ALL1D	<i>C. gloeosporioides</i>	Sweet orange 'Lane late'	leaf	Augusta (Sr)-Sicily	MT997846	MW001578
ALL1E	<i>C. gloeosporioides</i>	Sweet orange 'Lane late'	twig	Augusta (Sr)-Sicily	MT997847	MW001579
ALL1F	<i>C. gloeosporioides</i>	Sweet orange 'Lane late'	twig	Augusta (Sr)-Sicily	MT997848	MW001580
ALL1G	<i>C. gloeosporioides</i>	Sweet orange 'Lane late'	twig	Augusta (Sr)-Sicily	MT997849	MW001581
ALL1H	<i>C. gloeosporioides</i>	Sweet orange 'Lane late'	twig	Augusta (Sr)-Sicily	MT997850	MW001582
ALL1I	<i>C. gloeosporioides</i>	Sweet orange 'Lane late'	twig	Augusta (Sr)-Sicily	MT997851	MW001583
ALL1L	<i>C. gloeosporioides</i>	Sweet orange 'Lane late'	twig	Augusta (Sr)-Sicily	MT997852	MW001584
ALL2A	<i>C. karstii</i>	Sweet orange 'Lane late'	twig	Augusta (Sr)-Sicily	MT997853	MW001545
ALL2B	<i>C. gloeosporioides</i>	Sweet orange 'Lane late'	twig	Augusta (Sr)-Sicily	MT997854	MW001585
ALL2C	<i>C. gloeosporioides</i>	Sweet orange 'Lane late'	twig	Augusta (Sr)-Sicily	MT997855	MW001586

Table 1. Cont.

Isolate Code	Species	Host (Species and Cultivar)	Organ	Geographical Origin	Genbank Accession	Genbank Accession
ALL2D	<i>C. gloeosporioides</i>	Sweet orange 'Lane late'	twig	Augusta (Sr)-Sicily	MT997856	MW001587
ALL2E	<i>C. gloeosporioides</i>	Sweet orange 'Lane late'	twig	Augusta (Sr)-Sicily	MT997857	MW001588
ALL2F	<i>C. gloeosporioides</i>	Sweet orange 'Lane late'	twig	Augusta (Sr)-Sicily	MT997858	MW001589
ALL2G	<i>C. gloeosporioides</i>	Sweet orange 'Lane late'	twig	Augusta (Sr)-Sicily	MT997859	MW001590
ALL2H	<i>C. gloeosporioides</i>	Sweet orange 'Lane late'	twig	Augusta (Sr)-Sicily	MT997860	MW001591
ALL2I	<i>C. karstii</i>	Sweet orange 'Lane late'	twig	Augusta (Sr)-Sicily	MT997861	MW001546
ALL2L	<i>C. karstii</i>	Sweet orange 'Lane late'	twig	Augusta (Sr)-Sicily	MT997862	MW001547
ALL2M	<i>C. karstii</i>	Sweet orange 'Lane late'	twig	Augusta (Sr)-Sicily	MT997863	MW001548
ALL2N	<i>C. karstii</i>	Sweet orange 'Lane late'	twig	Augusta (Sr)-Sicily	MT997864	MW001549
ALL2O	<i>C. karstii</i>	Sweet orange 'Lane late'	twig	Augusta (Sr)-Sicily	MT997865	MW001550
ALL2P	<i>C. karstii</i>	Sweet orange 'Lane late'	twig	Augusta (Sr)-Sicily	MT997866	MW001551
ALL2Q	<i>C. karstii</i>	Sweet orange 'Lane late'	twig	Augusta (Sr)-Sicily	MT997867	MW001552
ALL2R	<i>C. karstii</i>	Sweet orange 'Lane late'	twig	Augusta (Sr)-Sicily	MT997868	MW001553
ALL2S	<i>C. karstii</i>	Sweet orange 'Lane late'	twig	Augusta (Sr)-Sicily	MT997869	MW001554
ALL2T	<i>C. karstii</i>	Sweet orange 'Lane late'	twig	Augusta (Sr)-Sicily	MT997870	MW001555
ALL3A	<i>C. gloeosporioides</i>	Sweet orange 'Lane late'	twig	Augusta (Sr)-Sicily	MT997871	MW001592
ALL3B	<i>C. gloeosporioides</i>	Sweet orange 'Lane late'	twig	Lentini (Sr)-Sicily	MT997872	MW001593
ALL3C	<i>C. gloeosporioides</i>	Sweet orange 'Lane late'	twig	Lentini (Sr)-Sicily	MT997873	MW001594
ALL4A	<i>C. gloeosporioides</i>	Sweet orange 'Lane late'	twig	Lentini (Sr)-Sicily	MT997874	MW001595
ALL4B	<i>C. gloeosporioides</i>	Sweet orange 'Lane late'	twig	Lentini (Sr)-Sicily	MT997875	MW001596
ALL4C	<i>C. gloeosporioides</i>	Sweet orange 'Lane late'	twig	Lentini (Sr)-Sicily	MT997876	MW001597
ALL4D	<i>C. gloeosporioides</i>	Sweet orange 'Lane late'	twig	Scordia (Ct)-Sicily	MT997877	MW001598
F169	<i>C. gloeosporioides</i>	Mandarin 'Fortune'	twig	Scordia (Ct)-Sicily	MW506960	MW513961
F170	<i>C. gloeosporioides</i>	Mandarin 'Fortune'	twig	Scordia (Ct)-Sicily	MW506961	MW513962
F172	<i>C. gloeosporioides</i>	Mandarin 'Fortune'	twig	Scordia (Ct)-Sicily	MW506962	MW513963
F189	<i>C. gloeosporioides</i>	Mandarin 'Fortune'	twig	Scordia (Ct)-Sicily	MW506963	MW513964
F190	<i>C. gloeosporioides</i>	Mandarin 'Fortune'	twig	Scordia (Ct)-Sicily	MW506964	MW513965
F191	<i>C. gloeosporioides</i>	Mandarin 'Fortune'	twig	Misterbianco (Ct)-Sicily	MW506965	MW513966
F224	<i>C. gloeosporioides</i>	Sweet orange 'Tarocco Scirè'	twig	Misterbianco (Ct)-Sicily	MW506966	MW513967
F225	<i>C. gloeosporioides</i>	Sweet orange 'Tarocco Scirè'	twig	Misterbianco (Ct)-Sicily	MW506967	MW513968
F226	<i>C. gloeosporioides</i>	Sweet orange 'Tarocco Scirè'	twig	Misterbianco (Ct)-Sicily	MW506968	MW513969

Table 1. Cont.

Isolate Code	Species	Host (Species and Cultivar)	Organ	Geographical Origin	Genbank Accession	
F227	<i>C. gloeosporioides</i>	Sweet orange 'Tarocco Scirè'	twig	Misterbianco (Ct)-Sicily	MW506969	MW513970
F239	<i>C. gloeosporioides</i>	Sweet orange 'Moro'	twig	Carlentini (Sr)-Sicily	MW506970	MW513971
F253	<i>C. gloeosporioides</i>	Sweet orange 'Tarocco Scirè'	twig	Misterbianco (Ct)-Sicily	MW506971	MW513972
F254	<i>C. gloeosporioides</i>	Sweet orange 'Tarocco Scirè'	twig	Misterbianco (Ct)-Sicily	MW506972	MW513973
F256	<i>C. gloeosporioides</i>	Sweet orange 'Tarocco Scirè'	leaf	Misterbianco (Ct)-Sicily	MW506973	MW513974
SR 5	<i>C. gloeosporioides</i>	Sweet orange 'Tarocco Scirè'	twig	Mineo (Ct)-Sicily	MW506974	MW513975
SR6	<i>C. gloeosporioides</i>	Sweet orange 'Tarocco Scirè'	twig	Mineo (Ct)-Sicily	MW506975	MW513976
SR8	<i>C. gloeosporioides</i>	Sweet orange 'Tarocco Scirè'	twig	Mineo (Ct)-Sicily	MW506976	MW513977
SR12	<i>C. gloeosporioides</i>	Sweet orange 'Tarocco Scirè'	twig	Mineo (Ct)-Sicily	MW506977	MW513978
SR 15	<i>C. gloeosporioides</i>	Sweet orange 'Tarocco Scirè'	twig	Mineo (Ct)-Sicily	MW506978	MW513979
SR 19	<i>C. gloeosporioides</i>	Sweet orange 'Tarocco Scirè'	twig	Mineo (Ct)-Sicily	MW506979	MW513980
SF 2	<i>C. gloeosporioides</i>	Sweet orange 'Tarocco Scirè'	leaf	Mineo (Ct)-Sicily	MW506980	MW513981
SF 3	<i>C. gloeosporioides</i>	Sweet orange 'Tarocco Scirè'	leaf	Mineo (Ct)-Sicily	MW506981	MW513982
SR 21	<i>C. gloeosporioides</i>	Mandarin-like hybrid 'Mandared' *	twig	Mineo (Ct)-Sicily	MW506982	MW513983
SR 23	<i>C. gloeosporioides</i>	Mandarin-like hybrid 'Mandared' *	twig	Mineo (Ct)-Sicily	MW506983	MW513984
SR 25	<i>C. gloeosporioides</i>	Mandarin-like hybrid 'Mandared' *	twig	Mineo (Ct)-Sicily	MW506984	MW513985
SR 28	<i>C. gloeosporioides</i>	Mandarin-like hybrid 'Mandared' *	leaf	Mineo (Ct)-Sicily	MW506985	MW513986
Citrus Ctrl 1	<i>C. gloeosporioides</i>	Clementine mandarin	twig	Xarre-Albania	MT997823	MW001555
Citrus Ctrl 2	<i>C. gloeosporioides</i>	Clementine mandarin	twig	Xarre-Albania	MT997824	MW001556
Citrus Ctrl 3	<i>C. gloeosporioides</i>	Clementine mandarin	twig	Xarre-Albania	MT997825	MW001557
Citrus Ctrl 4	<i>C. gloeosporioides</i>	Clementine mandarin	twig	Xarre-Albania	MT997826	MW001558
Citrus Ctrl 5	<i>C. gloeosporioides</i>	Clementine mandarin	twig	Xarre-Albania	MT997827	MW001559
Citrus Ctrl 6	<i>C. gloeosporioides</i>	Clementine mandarin	twig	Xarre-Albania	MT997828	MW001560
Citrus Ctrl 7	<i>C. gloeosporioides</i>	Clementine mandarin	twig	Xarre-Albania	MT997829	MW001561
Citrus Ctrl 8	<i>C. gloeosporioides</i>	Clementine mandarin	twig	Xarre-Albania	MT997830	MW001562
Citrus Ctrl 9	<i>C. gloeosporioides</i>	Clementine mandarin	twig	Xarre-Albania	MT997831	MW001563
Citrus Ctrl 10	<i>C. gloeosporioides</i>	Clementine mandarin	twig	Xarre-Albania	MT997832	MW001564
Citrus Ctrl 11	<i>C. gloeosporioides</i>	Clementine mandarin	twig	Xarre-Albania	MT997833	MW001565
Citrus Ctrl 12	<i>C. gloeosporioides</i>	Clementine mandarin	twig	Xarre-Albania	MT997834	MW001566
Citrus Ctrl 13	<i>C. gloeosporioides</i>	Clementine mandarin	twig	Xarre-Albania	MT997835	MW001567
Citrus Ctrl 14	<i>C. gloeosporioides</i>	Clementine mandarin	twig	Xarre-Albania	MT997836	MW001568
Citrus Ctrl 15	<i>C. gloeosporioides</i>	Clementine mandarin	twig	Xarre-Albania	MT997837	MW001569
Citrus Ctrl 16	<i>C. gloeosporioides</i>	Clementine mandarin	twig	Xarre-Albania	MT997838	MW001570

Table 1. Cont.

Isolate Code	Species	Host (Species and Cultivar)	Organ	Geographical Origin	Genbank Accession	Genbank Accession
Citrus Ctrl 17	<i>C. gloeosporioides</i>	Clementine mandarin	twig	Xarre-Albania	MT997839	MW001571
Citrus Ctrl 18	<i>C. gloeosporioides</i>	Clementine mandarin	twig	Xarre-Albania	MT997840	MW001572
Citrus Ctrl 19	<i>C. gloeosporioides</i>	Clementine mandarin	twig	Xarre-Albania	MT997841	MW001573
Citrus Ctrl 20	<i>C. gloeosporioides</i>	Clementine mandarin	twig	Xarre-Albania	MT997842	MW001574
UWS 149	<i>C. acutatum</i>	<i>Olea europaea</i>	fruit	Agonis Ridge WA-Australia	JN121186	JN121273
C2	<i>C. gloeosporioides</i>	<i>Citrus x limon</i>	fruit	Lamezia Terme (CZ)-Calabria	JN121211	JN121298
CAM	<i>C. karstii</i>	<i>Camellia</i> sp.	leaf	Sicily	KC425664	KC425716

* holotype; ** epitype.

Mass isolates were obtained from symptomatic twigs and leaves and were preliminarily separated into two groups on the basis of morphotype, i.e., colony morphology, radial growth rate on PDA at 25 °C and microscopical traits, such as the shape and size of conidia and the presence of setae. About 10% of mass isolates of each morphotype and from each site were selected randomly and a single-conidium isolate was obtained from each selected mass isolate. A *C. acutatum* s.s. isolate (UWS 149) from olive (*Olea europaea*) sourced in Australia and a *C. gloeosporioides* s.s. isolate (C2) from lemon (*Citrus × limon*), sourced in Calabria [29], as well as a *C. karstii* (CAM) from *Camellia* sp., sourced in Sicily [26], were used as references in growth and pathogenicity tests.

2.3. Morphological Characteristics and Optimum Growth Temperature of Isolates

Agar plugs (5-mm-diam) were taken from the edge of actively growing cultures on PDA and transferred to the centre of 9-cm diameter Petri dishes containing PDA. Dishes were incubated at 25 °C either in the dark for 10 d to determine both the colony morphology and radial growth rate or with continuous fluorescent light to observe microscopical morphological traits. Conidial and mycelial suspensions were prepared in s.d.w. from 10-day-old cultures and examined microscopically.

Optimum temperature for radial growth was determined only for a restricted number of isolates of the two morphotypes and also for isolates of *C. acutatum* (UWS 149), *C. gloeosporioides* (C2) and *C. karstii* (CAM) used as references. Agar plugs (5-mm-diam) were taken from the edge of actively growing cultures on PDA and transferred to the centre of 9-cm diameter Petri dishes containing PDA. Dishes were incubated at 20, 25 and 30 °C in the dark (three replicates per each temperature and per each isolate). Two orthogonal diameters were measured per each colony after 3 and 7 d incubation. The experiment was repeated once with similar results, so results of only one experiment are reported.

2.4. DNA Extraction, PCR Amplification and Sequencing

Genomic DNA was extracted from single-conidium *Colletotrichum* isolates using the method described in Cacciola et al. [30]. The ITS1–58S–ITS2 region and the fragment of the β -tubulin 2 gene (TUB2) between exons 2 and 6 were amplified and sequenced from a complete panel of isolates as described in a previous paper [30]. Amplified products were analyzed by electrophoresis and single bands of the expected size were purified with the QIAquick PCR Purification Kit (Qiagen, Hilden, Germany) and sequenced with both forward and reverse primers by MacroGen Europe (Amsterdam, The Netherlands). The ChromasPro v. 1.5 software [31] was used to evaluate the reliability of sequences and to create consensus sequences. Unreliable sequences in which both forward and reverse sequences, or one or the other, were not successful or contained doubtful bases were re-

sequenced. The ITS and TUB2 sequences obtained in the present study were deposited in GenBank and the relative accession numbers are reported in Table 1. Validated sequences representative of all species identified within the *C. boninense* and *C. gloeosporioides* species complexes were phylogenetically analysed to determine the relationship between different isolates and define their taxonomic status. Sequences from ex-type or authentic culture were included in the analysis as a reference (Table 2).

Table 2. GenBank accession numbers of sequences of the isolates of worldwide origin used as references in phylogenetic analyses.

Species	Isolate	Clade	Origin	Host	Source	GenBank Accession Number	
						ITS-rDNA	β -tubulin 2
<i>C. acutatum</i> **	IMI 117620	<i>acutatum</i>	Australia	<i>C. papaya</i>	[32]	FJ788417	FJ788419
<i>C. aenigma</i> *	ICMP 18608	<i>gloeosporioides</i>	USA	<i>Persea americana</i>	[23]	JX010244	JX010389
<i>C. aeschynomenes</i> *	ICMP 17673	<i>gloeosporioides</i>	USA	<i>A. virginica</i>	[23]	JX010176	JX010392
<i>C. alatae</i> *	CBS 304.67	<i>gloeosporioides</i>	India	<i>Dioscorea alata</i>	[23]	JX010190	JX010383
<i>C. alienum</i> *	ICMP 12071	<i>gloeosporioides</i>	New Zealand	<i>Malus domestica</i>	[23]	JX010251	JX010411
<i>C. annellatum</i> *	CBS 129826	<i>boninense</i>	Colombia	<i>Hevea brasiliensis</i>	[14]	JQ005222	JQ005656
<i>C. aotearoa</i> *	ICMP 18537	<i>gloeosporioides</i>	New Zealand	<i>Coprosma</i> sp.	[23]	JX010205	JX010420
<i>C. beeveri</i> *	CBS 128527	<i>boninense</i>	New Zealand	<i>B. repanda</i>	[14]	JQ005171	JQ005605
<i>C. boninense</i> *	CBS 123755	<i>boninense</i>	Japan	<i>C. asiaticum</i> var. <i>sinicum</i>	[14]	JQ005153	JQ005588
<i>C. brasiliense</i> *	CBS 128501	<i>boninense</i>	Brazil	<i>Passiflora edulis</i>	[14]	JQ005235	JQ005669
<i>C. brisbaniense</i> *	CBS 292.67	<i>acutatum</i>	Australia	<i>C. annuum</i>	[22]	JQ948291	JQ949942
<i>C. carthami</i> **	SAPA100011	<i>acutatum</i>	Japan	<i>C. tinctorium</i>	[33]	AB696998	AB696992
<i>C. clidemiae</i> *	ICMP 18658	<i>gloeosporioides</i>	USA	<i>Clidemia hirta</i>	[23]	JX010265	JX010438
<i>C. colombiense</i> *	CBS 129818	<i>boninense</i>	Colombia	<i>Passiflora edulis</i>	[14]	JQ005174	JQ005608
<i>C. fiorinae</i> *	CBS 128517	<i>acutatum</i>	USA	<i>Fiorinia externa</i>	[22]	JQ948292	JQ949943
<i>C. gloeosporioides</i> **	CBS 112999	<i>gloeosporioides</i>	Italy	<i>Citrus sinensis</i>	[14]	JQ005152	JQ005587
<i>C. gloeosporioides</i> *	STE-U4295	<i>gloeosporioides</i>	Italy	<i>Citrus</i> sp.	[34]	AY376532	AY376580
<i>C. godetiae</i> *	CBS 133.44	<i>gloeosporioides</i>	Denmark	<i>Clarkia hybrida</i>	[14]	JQ948402	JQ950053
<i>C. karstii</i> *	CBS 132134/ CORCG6	<i>boninense</i>	China	<i>Vanda</i> sp.	[35]	HM585409	HM585428
<i>C. paspali</i> *	MAFF 305403	<i>graminicola</i>	Japan	<i>P. notatum</i> Fluegge	[36]	EU554100	JX519244;
<i>C. truncatum</i> **	CBS 151.35	<i>truncatum</i>	USA	<i>Phaseolus lunatus</i>	[36]	GU227862	GU228156

* ex-holotype; ** epitype.

Phylogenetic analysis was conducted for the ITS and TUB2 sequences, as well as for the combined data set of the two markers using maximum likelihood and Bayesian methods. TOPALi v2 [37] was used to determine the substitution model that best fitted the data. The model HKY + I + G was selected for the Bayesian and maximum likelihood phylogenetic analysis using MrBayes v. 3.1.1 and PhyML v. 2.4.5, respectively, implemented in TOPALi. Bayesian analysis was performed with four runs conducted simultaneously for 500,000 generations with 10% sampling frequency and burn-in of 30%. Maximum likelihood was performed with 100 bootstrap replicates.

2.5. Pathogenicity Test

The pathogenicity of all 119 single-conidium isolates of *Colletotrichum* from citrus and the reference isolates of *C. acutatum*, *C. gloeosporioides* and *C. karstii* was tested on mature apple fruits (*Malus domestica*) 'Fuji' and 'Cripps Pink'. The assay on apples was included in this study as it was often used as a standard method to evaluate the pathogenicity of *Colletotrichum* spp. from various host-plants [38]. Apples (three apples per fungal isolate) were wounded inoculated by removing aseptically a piece of tissue (3 mm side) using a scalpel, then inserting a mycelium plug of the same size upside down into the pulp of the fruit and putting back in place the piece of tissue. A sterile agar plug was inserted into control apples. Apples were incubated at 25 °C and the area of the external lesion was measured seven days post inoculation (d.p.i.). In a preliminary test using a set of isolates, including the reference isolates of *C. acutatum* (UW 149), *C. gloeosporioides* (C2) and

C. karstii (CAM), no difference in susceptibility was observed between ‘Fuji’ and ‘Cripps Pink’ apples, so in subsequent tests of the 119 *Colletotrichum* isolates sourced from citrus during the survey and the reference isolates of the three *Colletotrichum* species fruits of the two apple cultivars were used indifferently depending on the availability.

The pathogenicity of a more restricted subset of isolates, including four *C. gloeosporioides* isolates from citrus (one, Citrus ctrl 1, sourced in Albania, and three, AC5 and AC24 from twigs and AC38 from leaf, sourced in Italy) two *C. karstii* isolates (ALL2I and ALL2S sourced in Italy) and the reference isolates of *C. acutatum* from olive (UWS 149), *C. gloeosporioides* (C2) from lemon and *C. karstii* (CAM) from camellia, was tested on different citrus plant organs, including young twigs of sweet orange ‘Tarocco Scirè’, lemon (*C. × limon*) ‘Femminello 2Kr’ and bergamot (*C. × bergamia*) ‘Fantastico’, young and mature expanded leaves of sweet orange ‘Moro’ and ‘Navelina’, mature fruit of sweet orange ‘Tarocco Meli’ and lemon ‘Femminello 2Kr’ as well as green fruitlets of lemon ‘Femminello 2Kr’.

On 1 June 2020, twigs (around 0.5 cm diameter) were wounded inoculated using a scalpel to lift a strip of bark and insert under the bark, upside down and in contact with the cambium, a mycelium plug (3 mm side) taken from the edge of an actively growing culture on PDA. A plug of sterile agar was inserted under the bark of control twigs. The wounds were sealed tightly with Parafilm®. Inoculations were carried out on four-year-old trees in an experimental field in the municipality of Mineo. Six twigs on each tree were inoculated and six served as a control. The length of necrotic lesions was recorded at 14 d.p.i. The experimental design was a complete randomized block with three replicates (trees) per each citrus variety and *Colletotrichum* isolate combination. The experiment was repeated on June 30th and the data of the two experiments were analyzed separately.

The same *Colletotrichum* isolates were used to inoculate fruits and leaves, to test their ability to produce symptoms of anthracnose. Ripe sweet orange and lemon fruits were surface disinfected with 70% ethanol, rinsed with s.d.w., blotted dry and inoculated by wounding and without wounding. Unwounded fruits were inoculated by putting mycelium plugs (3 mm side) directly on the peel (two plugs on the upper side of each fruit placed horizontally, four cm apart from each other). Control fruits received sterile agar plugs. The same number of fruits was inoculated using a scalpel to remove aseptically two small pieces (3 mm side) of peel, four cm apart from each other. Mycelium plugs of the same size were inserted upside down into the albedo and the peel pieces were replaced to cover the wounds. Sterile agar plugs were inserted into the albedo of control fruits. After inoculation, fruits were placed in humid chambers (plastic boxes with air-tight lid) on plastic rings to avoid direct contact with the humid paper and incubated at 25 °C under 16/8 h light/dark photoperiod and 90% RH. Symptoms were recorded three, six and 12 d.p.i. Four replicated fruits for each inoculation method (wounding and without wounding) and *Colletotrichum* isolate combination were included in each of the two separate experiments, one with mature sweet orange fruit and the other with mature lemon fruit, respectively. In a separate trial the same *Colletotrichum* isolates were inoculated on unripe fruitlets of lemon ‘Femminello 2Kr’. Differently from tests on mature fruit, each fruitlet was inoculated with a single plug instead of two. Symptoms were recorded three and six d.p.i.

Expanded young (from summer vegetative flushing) and mature (from spring or previous year vegetative flushing) leaves of sweet orange ‘Moro’ and ‘Navelina’ were collected on 2 October 2020 in the same citrus orchard, surface disinfected with 70% ethanol, washed with s.d.w., blotted dry and transferred to a humid chamber (plastic boxes with air-tight lid) on blotting paper soaked with s.d.w. and covered with aluminium foil to avoid direct contact between leaves and water. Leaves were inoculated on the abaxial side by wounding and without wounding. A razor blade was used to gently scrape the surface of the leaf lamina so as to create small (2 mm side) superficial lesions (six lesions per leaf, three on each side of the midrib). A mycelium plug (3 mm side) taken from the edge of an actively growing culture on PDA was put on each lesion with the side covered

by mycelium in contact with the leaf surface. Six mycelium plugs (three on each side of the midrib) were placed on the lamina of unwounded leaves. Sterile agar plugs were placed on both wounded and unwounded leaves used as controls. Leaves were incubated in humid chamber at 25 °C under 16/8 h light/dark photoperiod and 90% RH and symptoms were recorded at five d.p.i. The experimental design was a complete randomized block with four replicates (leaves) for each citrus variety, type of leaf (young or mature), inoculation method (wounded or unwounded) and *Colletotrichum* isolate combination.

Colletotrichum isolates used in pathogenicity tests were re-isolated from the lesions and identified based on colony morphology to fulfil Koch's postulates. The identity of the isolates obtained from artificially inoculated symptomatic twigs, fruit and leaves was also confirmed by sequencing the ITS and TUB2 regions.

2.6. Statistical Analysis

Data from pathogenicity tests were analyzed using RStudio v.1.2.5 (R) [39]. The means of surface areas of necrotic lesions induced by different *Colletotrichum* isolates were compared and analyzed by one-way Analysis of Variance (ANOVA) coupled with Tukey-Kramer Honestly Significant Difference (HSD) test. Likewise, ANOVA and Tukey-Kramer Honestly Significant Difference (HSD) test were applied for statistical analysis of the differences between mean colony diameters in radial growth tests of isolates at different temperatures. When comparing independent groups, Student's t-test was used. Levene's test was used to determine the homogeneity of variance between independent trials. No heterogeneity was detected and data from independent trials were combined.

3. Results

In all surveyed orchards, outbreaks of *Colletotrichum* twig and shoot dieback of citrus were observed from April to October on both young and mature trees and always following strong winds, occurring on trees suffering because of water stress after prolonged drought. Symptoms included blight and gumming of twigs (Figure 1B,C), defoliation and crown thinning as well as necrotic blotches, russetting of the abaxial side and mesophyll collapse of leaves remained still attached to the twigs (Figure 1D). In most severe cases, dieback of entire branches (Figure 1A) and death of young (one- to three-year-old) trees were observed. The incidence of the disease in a single orchard varied greatly irrespective of the age of the trees. In most orchards, affected trees were scattered and only a few twigs or shoots were symptomatic within a tree while in a few orchards more than 80% of trees were more or less seriously affected.

Symptoms were often severe on the top of the canopy of mature trees and on trees exposed to wind and suffering because of drought. Overall, about 1200 *Colletotrichum* isolates were sourced in Sicily, 93% from twigs and 7% from leaves. About 180 isolates were sourced in Albania, all from twigs. All the isolates from Albania showed the same morphology.

Colonies of these isolates on PDA were low-convex, fast-growing (10–11 mm average growth per day at 25 °C), with entire margin and dense, cottony, aerial mycelium, initially white turning to pale grey and salmon pink conidial mucilaginous masses in the centre of the colony, dark acervuli scattered over all the surface in old colonies. Colony reverse was pale orange to uniformly grey. Single-celled conidia were, hyaline, smooth, cylindrical with both ends rounded; the range of their dimensions was 11–15 × 4–6 µm. Setae were common in most isolates. Conversely, *Colletotrichum* isolates from Italy were separated into two clearly distinct groups on the basis of morphotype (Figure 2). The first group, encompassing the majority of isolates and including isolates from both twigs and leaves, showed the same morphotype as isolates from Albania. The second group, encompassing about 100 mass isolates from twigs sourced from sweet orange 'Lane Late' in the municipality of Augusta, showed a different morphotype. Colonies on PDA were less fast growing (8 mm average growth per day at 25 °C) and flat, with entire margin, mycelium appressed and moderately dense, white-orange to pale gray-orange, minute salmon orange conidium masses scattered

over all the surfaces. The colony reverse was pale orange. Conidia were single-celled, hyaline, smooth, cylindrical with both ends rounded; the range of their dimensions was $10\text{--}17 \times 4\text{--}6 \mu\text{m}$. Setae were exceedingly rare or absent in most isolates.

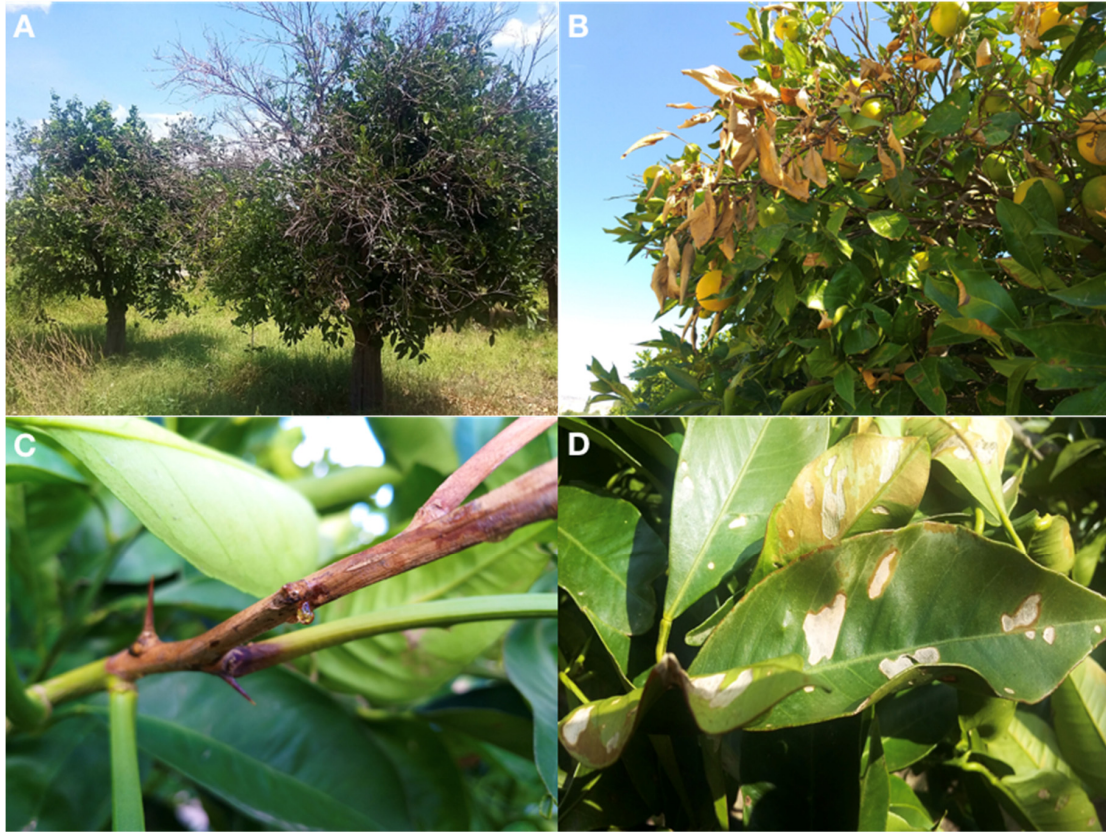


Figure 1. (A). Shoot blight and dieback of entire branches on Sweet orange ‘Tarocco Scirè’ injured by wind. (B) Symptoms of shoot blight incited by *Colletotrichum* infections on Sweet orange ‘Tarocco Scirè’ injured by wind. (C) Gumming associated with citrus shoot blight on Sweet orange ‘Tarocco Scirè’. (D) Leaf mesophyll collapse and necrosis caused by wind on leaves of ‘Tarocco Scirè’ sweet orange. Conidiomata of *Colletotrichum* are visible on necrotic lesions as black pin point-dots.

The phylogenetic analysis of the combined data set of sequences from ITS and TUB2 regions of all single-conidium *Colletotrichum* isolates from citrus sourced in Albania and southern Italy (Table 1), along with sequences of the isolates of *C. acutatum* (UWS 149), *C. gloeosporioides* (C2) and *C. karstii* (CAM) used as references and the reference sequences of *Colletotrichum* species separated within the *C. gloeosporioides* and *C. boninense* species complexes, produced a phylogenetic tree (Figure 3) with a similar topology and high concordance with those reported by the authors who revised the systematics of these species complexes using multigene sequence analysis [14,22,23].

All the isolates from Albania and the isolates from southern Italy with the same morphotype were identified as *C. gloeosporioides* because they clustered (bootstrap values 100%) with the ex-type isolate of this species. Conversely, the 10 single-conidium isolates from the municipality of Augusta showing a distinct morphotype clustered (bootstrap values 100%) with ITS and TUB2 region sequences of reference isolates of *C. karstii*, including the culture from holotype isolate CBS 132134/CORCG6 and the isolate CAM from camellia sourced in Sicily. Sequences of isolates of both *C. gloeosporioides* and *C. karstii* were clearly distinct from reference sequences of *C. acutatum*.

All selected isolates of both *C. gloeosporioides* and *C. karstii* as well as the reference isolate of *C. acutatum* grew faster at 25 than at 30 and 35 °C. However, at 30 and 35 °C the *C. gloeosporioides* isolates were less inhibited than isolates of the other two species, indicating they were more thermophilic. In particular, the radial growth of *C. gloeosporioides*

isolates at 30 °C was reduced only by 7 to 11% compared to the growth at 25 °C, and by 16 to 30% at 35 °C. Conversely, the growth of *C. karstii* isolates was reduced by 55 to 60% at 30 °C and by 75 up to 79 % at 35 °C. The growth of the reference isolate of *C. acutatum* was dramatically reduced at 30 and 35 °C, by 79 and 88% respectively (Table 3).

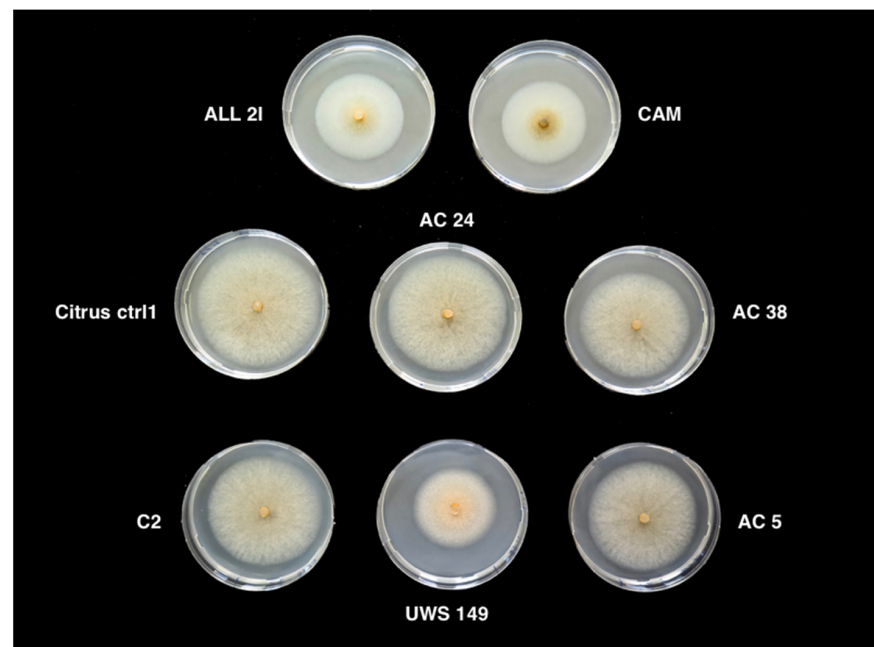


Figure 2. Morphology of 6-day-old colonies of *Colletotrichum gloeosporioides* (AC24, AC38, AC5, C2 and Citrus ctrl1), *C. acutatum* (UWS 149) and *C. karstii* (ALL 2I and CAM) grown on potato-dextrose-agar at 25 °C in the dark.

Table 3. Mean radial growth rates of colonies of *Colletotrichum* spp., isolates on PDA at three different temperatures, as determined after 7 d of incubation.

<i>Colletotrichum</i> spp.	Isolate	25 °C (mm d ⁻¹) Mean ± S.D. ^a	30 °C (mm d ⁻¹) Mean ± S.D. ^a	35 °C (mm d ⁻¹) Mean ± S.D. ^a
<i>C. acutatum</i>	UWS 14	57 ± 0.6	12 ± 0.5	8 ± 0.3
<i>C. gloeosporioides</i>	AC 24	79 ± 0.5	70 ± 0.8	64 ± 1.2
<i>C. gloeosporioides</i>	Citrus ctrl1	76 ± 0.6	70 ± 1.6	53 ± 17.6
<i>C. gloeosporioides</i>	AC 5	75 ± 0.6	69 ± 0.6	63 ± 1.8
<i>C. gloeosporioides</i>	C2	75 ± 0.8	68 ± 0.3	63 ± 0.3
<i>C. gloeosporioides</i>	AC 38	73 ± 1.1	67 ± 1.3	62 ± 0.6
<i>C. karstii</i>	ALL 2I	57 ± 5.4	26 ± 1.9	12 ± 0
<i>C. karstii</i>	CAM	56 ± 1.1	22 ± 0.8	25 ± 0.3

^a Mean of three replicate Petri dishes.

In pathogenicity tests on apples, all isolates were pathogenic. However, symptoms induced on apples by isolates of the three tested *Colletotrichum* species were different. Necrotic lesions induced by the *C. gloeosporioides* isolates were dark brown, with a definite margin and black conidiomata emerging from the surface in concentric rings (Figure 4A).

Lesions induced by the *C. acutatum* isolate were pale brown with an irregular margin, a faint white aerial mycelium around the inoculation wound and point-like orange masses of conidia scattered over the surface of the lesion (Figure 4B). Lesions on apples inoculated with *C. karstii* isolates were restricted, dark brown with a faint white mycelium emerging from the wound and without sign of sporulation (Figure 4C). No significant difference in virulence was found between isolates of the same species irrespective of their origin, so data of all isolates belonging to the same species were pooled together. *C. gloeosporioides* isolates

and the reference isolate of *C. acutatum* were significantly more virulent than isolates of *C. karstii* (Figure 5).

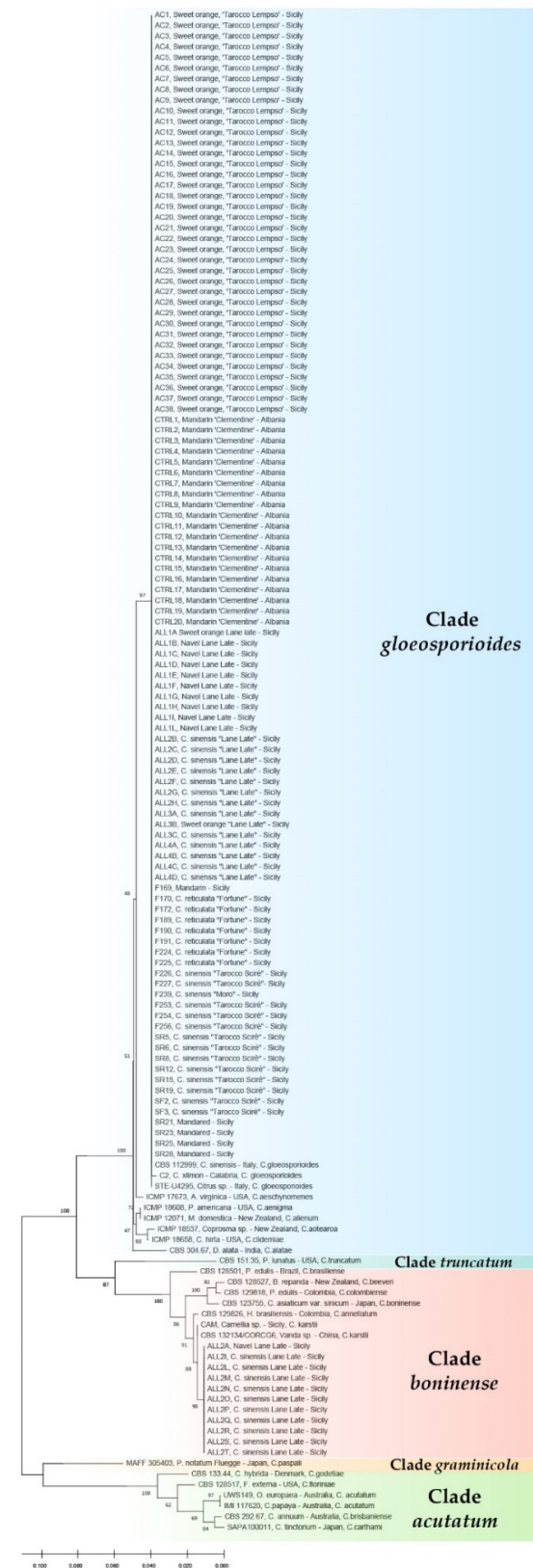


Figure 3. Phylogenetic tree obtained using combined internal transcribed spacers (ITS) and β -tubulin (TUB2) sequences of isolates of *Colletotrichum* spp. collected in the present study along with reference isolates of *C. karstii*, *C. gloeosporioides*, and other representative species of the other *Colletotrichum*

boninense, *C. gloeosporioides* and *C. acutatum* species complex. The evolutionary history was inferred using the maximum likelihood method based on the Tamura–Nei model and the tree with the highest log likelihood is shown. The percentage of trees in which the associated taxa clustered together is shown next to the branches.



Figure 4. (A) Necrotic lesion induced by a *Colletotrichum gloeosporioides* isolate on a wound inoculated apple seven d.p.i. (B) Necrotic lesion induced by the *Colletotrichum acutatum* reference isolate on a wound inoculated apple seven d.p.i. (C) Necrotic lesion induced by a *Colletotrichum karstii* isolate on a wound inoculated apple seven d.p.i.

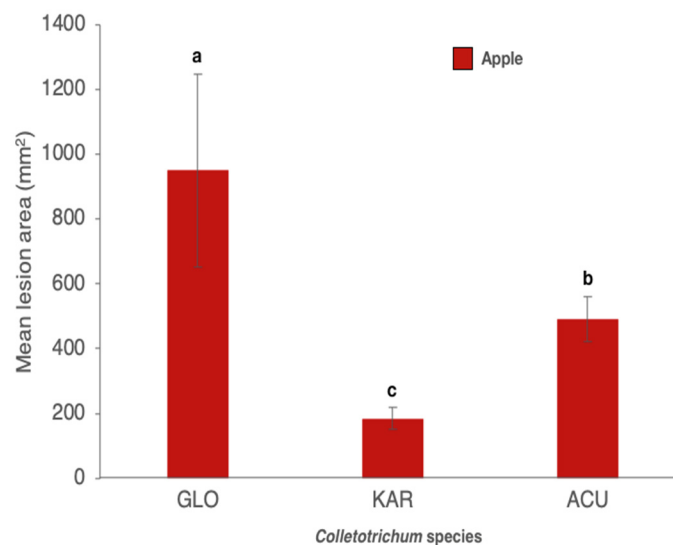


Figure 5. Mean area (\pm SD) of necrotic lesions (mm²) induced by *Colletotrichum gloeosporioides* (GLO), *C. karstii* (KAR) and *C. acutatum* (ACU) isolates on wound inoculated apples, seven d.p.i. Values sharing same letters are not statistically different according to Tukey's honestly significant difference (HSD) test ($p \leq 0.05$).

In in-field tests on twigs of sweet orange, lemon and bergamot the isolates of *C. gloeosporioides* and *C. acutatum* were more aggressive than isolates of *C. karstii*. Isolates of *C. acutatum* and *C. gloeosporioides* induced gumming in twigs of all three citrus species while isolates of *C. karstii* induced gumming only in bergamot twigs (Figure 6A–C).

Mean length of necrotic lesion of the bark induced by the *C. gloeosporioides* and *C. acutatum* isolates was significantly higher than the length of lesions induced by the *C. karstii* isolates (Figure 7). In twigs inoculated with *C. karstii* isolates, the necrotic lesion was localized around the inoculation point and the wound healed rapidly. No significant difference in lesion size was observed between sweet orange, lemon and bergamot twigs. Likewise, no significant difference in virulence, as determined on the basis of the size of the necrotic lesion, was observed between isolates of the same *Colletotrichum* species so data of all

isolates belonging to the same species were pooled together. On control twigs, inoculation wounds healed rapidly without any symptoms of necrosis or gummosis.



Figure 6. (A) Gumming on a twig of lemon ‘Femminello 2Kr’ wound inoculated with a *Colletotrichum gloeosporioides* isolate 14 d.p.i. (B) Gumming on a twig of bergamot ‘Fantastico’ wound inoculated with a *Colletotrichum gloeosporioides* isolate 14 d.p.i. (C) Twigs of bergamot ‘Fantastico’ wound inoculated with *Colletotrichum karstii* (left) and *C. gloeosporioides* (right) 14 d.p.i. The bark was removed to show the internal symptoms: the twig on the left shows a gum impregnation of the young xylem and a cicatricial tissue around the inoculation point while the twig on the right shows a profuse gumming extending beyond the inoculation point.

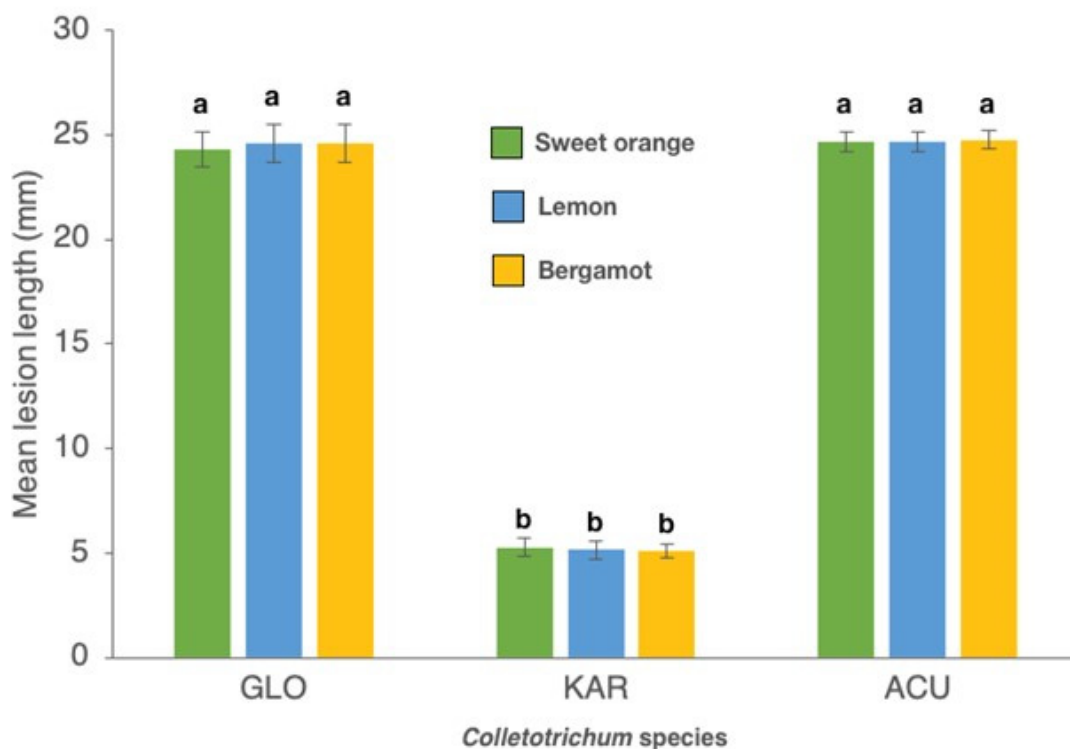


Figure 7. Mean length (mm) of necrotic lesions of six twigs per each of three replicated trees (\pm SD) induced by isolates of *Colletotrichum gloeosporioides* (GLO) (five isolates, means of 90 replicates), *C. karstii* (KAR) (three isolates, means of 54 replicates) and *C. acutatum* (ACU) (one isolate, means of 18 replicates) on in-field artificially inoculated twigs of sweet orange ‘Tarocco Scirè VCR’, lemon ‘Femminello 2Kr’ and bergamot ‘Fantastico’, 14 d.p.i. Values sharing same letters are not statistically different according to Tukey’s honestly significant difference (HSD) test ($p \leq 0.05$).

In tests on green and mature fruit as well as on tender and mature leaves *Colletotrichum* isolates were able to induce lesions only after wounding. In pathogenicity tests on mature fruit of sweet orange and lemon, *C. gloeosporioides* isolates were more aggressive than isolates of *C. karstii* even on fruits. Isolates of both species induced a brown necrotic halo around the inoculation wound and the necrosis extended deep into the albedo (Figure 8A,B), but the mean size of lesions induced by the *C. gloeosporioides* isolates was greater than the mean size of lesions induced by the *C. karstii* isolates on both sweet orange and lemon (Figure 9). No significant difference in virulence, as determined based on the average size of the necrotic lesion, was observed between isolates of the same *Colletotrichum* species so data of isolates belonging to the same species were pooled together (Figure 9).



Figure 8. (A) Necrotic lesions around the inoculation point in a fruit of sweet orange ‘Tarocco Meli’ wound inoculated with an isolate of *Colletotrichum gloeosporioides* 12 d.p.i.; the peel has been removed to show that the necrosis extends into the albedo. (B) Necrotic lesions around the inoculation point in a fruit of lemon ‘Femminello 2Kr’ wound inoculated with an isolate of *Colletotrichum gloeosporioides* 12 d.p.i.; the peel has been removed to show that the necrosis extends into the albedo. (C) Aerial mycelium developed on the two inoculation points in a fruit of sweet orange ‘Tarocco Meli’ wound inoculated with the reference isolate of *Colletotrichum acutatum* 12 d.p.i.; the peel has been removed to show the necrotic lesion extending into the albedo lined by an orange coloured cicatricial tissue. (D). Aerial mycelium growing on the two inoculation points in a fruit of lemon ‘Femminello 2Kr’ wound inoculated with the reference isolate of *Colletotrichum acutatum* 12 d.p.i.; the peel has been removed to show the necrotic lesion extending into the albedo.

The reference isolate of *C. acutatum* induced quite peculiar symptoms on both sweet orange and lemon fruit as the inoculation wounds were covered by a white, cottony aerial mycelium, which masked the lesion. The necrosis extended into the albedo and reached its maximum extent 6 d.p.i., but did not expand further (Figure 8C,D).

As a consequence, the area of the external necrotic lesion cannot be measured and direct comparison with isolates of the other two *Colletotrichum* species was not possible in terms of virulence. No symptoms were observed on control fruits.

On green fruitlets of lemon differences of symptoms induced by isolates of the three *Colletotrichum* species were almost exclusively qualitative. All *C. gloeosporioides* and *C. karstii* isolates induced gumming and a very restricted necrotic lesion around the inoculation point (Figure 10A,C) while fruitlets inoculated with the *C. acutatum* isolate showed gumming and an abundant white aerial mycelium covering the lesion (Figure 10B). Symptom appeared three d.p.i. and did not evolve further over the next three days. The only symptom on

control fruitlets was the necrosis of tissue plug removed temporarily to inoculate the fruitlets and replaced to plug the inoculation wound.

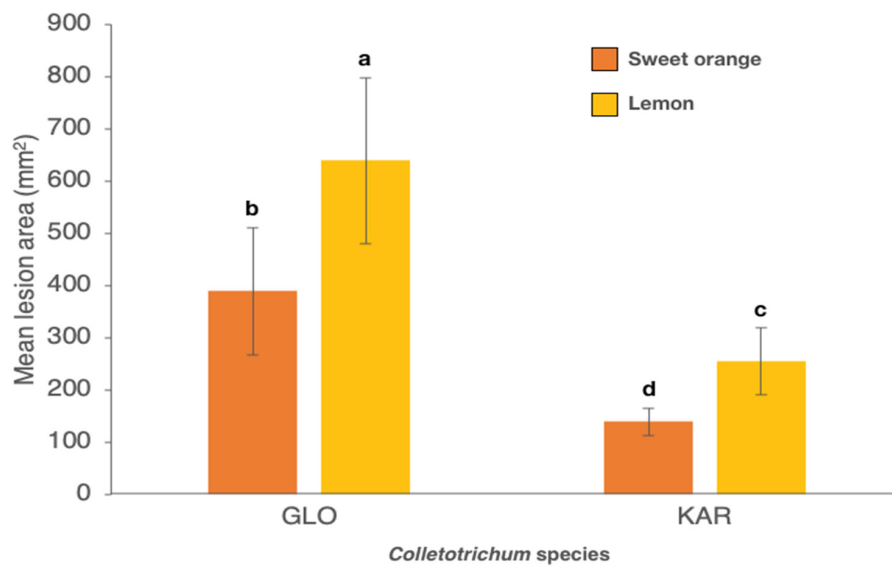


Figure 9. Mean area (mm²) of necrotic lesions (\pm SD) induced by isolates of *Colletotrichum gloeosporioides*^b (GLO) (five isolates) and *C. karstii*^c (KAR) (three isolates)^a on wound inoculated fruits of sweet orange ‘Tarocco Meli’ and lemon ‘Femminello 2Kr’, 12 d.p.i. Values sharing same letters are not statistically different according to Tukey’s honestly significant difference (HSD) test ($p \leq 0.05$). ^a Four fruits for each citrus species and two inoculation wounds per fruit. ^b Means of 40 replicates. ^c Means of 24 replicates.



Figure 10. (A) Aerial gray mycelium and gum exudate on green fruitlets of lemon ‘Femminello 2Kr’ wound inoculated with an isolate of *Colletotrichum gloeosporioides* 6 d.p.i. (B) Aerial white mycelium and gum exudate on green fruitlets of lemon ‘Femminello 2Kr’ wound inoculated with the reference isolate of *Colletotrichum acutatum* 6 d.p.i. (C) Aerial gray mycelium and gum exudate on green fruitlets of lemon ‘Femminello 2Kr’ wound inoculated with an isolate of *Colletotrichum karstii* 6 d.p.i.

All *Colletotrichum* isolates induced circular necrotic lesions on young leaves of both ‘Navelina’ and ‘Moro’ (Figure 11A–D) while the only symptom induced on mature leaves of these two sweet orange cultivars was a translucent, very restricted dark brown halo around the inoculation point. No symptoms were observed on both young and mature control leaves.

Slight, albeit significant, differences in susceptibility were observed between ‘Moro’ and ‘Navelina’, the latter being more susceptible to the infection of aggressive isolates. There were, in fact, significant differences in virulence among the *Colletotrichum* isolates tested. Unexpectedly, the two heterologous isolates, i.e., the *C. acutatum* reference isolate from olive and the *C. karstii* reference isolate from camellia, were the most aggressive. Both the *C. karstii* isolates recovered from ‘Lane Late’ showed an intermediate virulence while

the *C. gloeosporioides* isolates were slightly less virulent and did not differ significantly between each other (Figure 12).



Figure 11. (A) Necrotic lesions induced by the heterologous *Colletotrichum karstii* isolate from camellia on wound inoculated young leaves of sweet orange ‘Navelina’ 5 d.p.i. (B) Necrotic lesions induced by the heterologous reference isolate of *Colletotrichum acutatum* from olive on wound inoculated young leaves of sweet orange ‘Navelina’ 5 d.p.i. (C) Necrotic lesions induced by an isolate of *Colletotrichum karstii* from citrus on wound inoculated young leaves of sweet orange ‘Moro’ 5 d.p.i. (D) Necrotic lesions induced by an isolate of *Colletotrichum gloeosporioides* from citrus on wound inoculated young leaves of sweet orange ‘Moro’ 5 d.p.i.

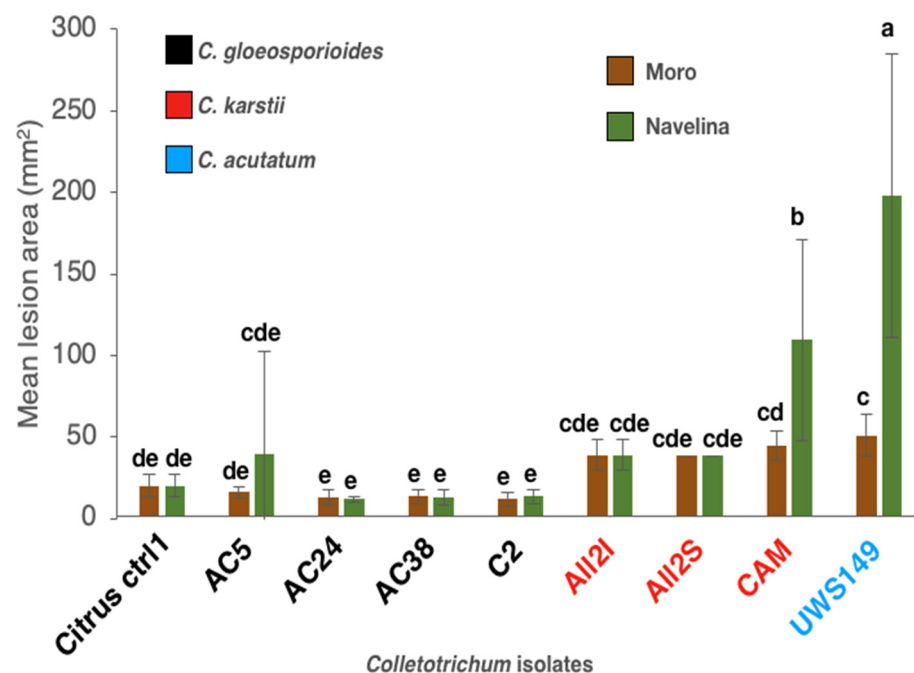


Figure 12. Mean area of 24 replicates (four leaves with six lesions each) of necrotic lesions (mm²) (\pm SD) incited by isolates of *C. gloeosporioides* (Citrus ctr1, AC5, AC24, AC38 and C2), *C. karstii* (All2I, All2S and CAM) and *C. acutatum* (UWS149) on wound inoculated young leaves of sweet orange ‘Moro’ and ‘Navelina’, five d.p.i. Values sharing same letters are not statistically different according to Tukey’s honestly significant difference (HSD) test ($p \leq 0.05$).

4. Discussion

A new disease of citrus, named twig and shoot dieback or *Colletotrichum* twig and shoot dieback to stress its association with pathogenic *Colletotrichum* species, and recently observed in California, is reported for the first time from two citrus growing countries of

the Mediterranean region, Albania and Italy, where it was found to be quite common and widespread. According to the modern taxonomy of *Colletotrichum* based prevalently on multilocus sequence phylogeny and consistently with the results obtained in California, the *Colletotrichum* species associated with twig and shoot dieback of citrus in Albania and Italy were identified as *C. gloeosporioides* s.s., in the *C. gloeosporioides* species complex, and *C. karstii*, in the *C. boninense* species complex. *Colletotrichum gloeosporioides* was the only species associated with twig and shoot dieback in Albania and by far the prevalent species associated with this syndrome in Sicily. *C. gloeosporioides* is reported for the first time as a pathogen of citrus in Albania. Differently from *C. gloeosporioides*, *C. karstii* was found only sporadically, accounting for just around one third of the *Colletotrichum* isolates retrieved from a single sampling site in Sicily. The results of in-field tests provided evidence that both *Colletotrichum* species were pathogens on twigs of different citrus species, but *C. gloeosporioides* was more aggressive than *C. karstii*, indicating the former species was the main causative agent of twig and shoot dieback in surveyed areas. By contrast, in California *C. karstii* was proved to be more virulent than *C. gloeosporioides* [5]. To explain this discrepancy one can only speculate that populations of *C. gloeosporioides* and *C. karstii* associated to citrus in California are different from populations of these two species from the Mediterranean region. However, no general conclusion can be drawn as in pathogenicity tests performed in California only a single isolate of *C. gloeosporioides* and a single isolate of *C. karstii* were compared [5]. In agreement with our results, previous studies aimed at identifying the *Colletotrichum* species associated to citrus anthracnose in China and Europe, showed that among the *Colletotrichum* species recovered from citrus groves *C. gloeosporioides* was the most common and the most virulent on detached citrus fruits [17,25,27]. No significant intraspecific variability in virulence was observed among the isolates of *C. gloeosporioides* and *C. karstii* recovered from citrus in Albania and Italy. However, evidence from other studies indicate the pathogenicity of isolates of both *C. gloeosporioides* and *C. karstii* may vary even within populations originating from the same host-plant and geographic area. Marked differences in pathogenicity were reported among isolates of *C. gloeosporioides* from citrus sourced in Tunisia as well as among *C. gloeosporioides* isolates from olive sourced in Italy [19,26]. In Portugal, an isolate of *C. karstii* from sweet orange was as virulent as an isolate of *C. gloeosporioides* from lemon when inoculated on sweet orange fruits and significantly less virulent when inoculated on lemon and mandarin fruits [10]. In this study, all tested isolates of *C. gloeosporioides* were more aggressive on twigs than isolates of *C. karstii* irrespective of their origin.

Colletotrichum gloeosporioides, both in a broad (*C. gloeosporioides* species complex) and in a strict sense (*C. gloeosporioides* s.s.), has a wide host range and is the most common *Colletotrichum* species associated to symptoms of citrus anthracnose globally [8,17,23–25,40–42]. In this study, all isolates of *C. gloeosporioides* recovered from trees with symptom of twig and shoot dieback in Albania and Sicily were overly aggressive and were able of inducing anthracnose symptoms on fruits and leaves, as well as necrosis and gumming on twigs of different citrus species.

C. karstii is also a polyphagous species and among the species in the *C. boninense* complex it is the most common and the one reported from a greater number of countries and different geographical areas [14]. In Italy, it was recovered from several host-plants including olive (*Olea europaea*), and there is evidence of it as a citrus inhabitant in southern Italy since the 1990s [26,43]. In this study, isolates of *C. karstii* retrieved from citrus were less virulent than isolates of *C. gloeosporioides* on artificially inoculated fruits and twigs of both sweet orange and lemon. However, isolates of *C. karstii* from citrus demonstrated to be more virulent than *C. gloeosporioides* isolates on young leaves of sweet orange. This agrees with previous reports indicating this *Colletotrichum* species is a common foliar pathogen of citrus [10,23–25]. In a previous study aimed at characterizing the *Colletotrichum* species in the *C. gloeosporioides* and *C. boninense* complexes associated with olive anthracnose, *C. karstii* isolates from olive showed a low level of virulence on olive drupes, suggesting this species was an occasional pathogen on olive [26].

Overall the results of this survey do not support the hypothesis of organ specificity as a factor determining the prevalence of a *Colletotrichum* species over another in citrus trees affected by twig and shoot dieback. It is likely that the proportion of *C. gloeosporioides* and *C. karstii* isolates recovered in this study and the distribution of these two *Colletotrichum* species in surveyed areas depend on other factors conditioning their fitness and adaptative capacity. In the years following the revision of the systematics of *C. gloeosporioides* and *C. boninense* species complexes that led to the segregation of *C. karstii* as a distinct species within the *C. boninense* complex, *C. karstii* has been increasingly reported from several citrus growing countries, including China, Iran, Italy, New Zealand, Portugal, South Africa, Tunisia, Turkey and USA, always in association with other *Colletotrichum* species, mainly *C. gloeosporioides* [5,10,19,20,23,24,27,28]. This does not imply necessarily that *C. karstii* is an emerging pathogen *sensu* [4]. It seems more likely that the proliferation of reports of this *Colletotrichum* species on citrus from diverse and distant geographical areas is a consequence of the taxonomic revision of the *C. gloeosporioides* and *C. boninense* species complexes based on multilocus phylogenetic analysis, which provided a framework for a correct identification of already present cryptic species.

In the present study, a third *Colletotrichum* species included as a reference, *C. acutatum* *s.s.*, was shown to be as virulent as *C. gloeosporioides* on artificially inoculated twigs of different citrus species while on fruits of sweet orange and lemon induced symptoms different from the typical anthracnose. Interestingly, shoot blight is one of the symptoms of KLA, a disease caused by *C. limetticola*, also a species in the *C. acutatum* complex and affecting exclusively Key lime [14,44]. The only report of *C. acutatum* *s.s.* on citrus in Europe is from a small island of the Aeolian archipelago, north of Sicily, where it was recovered from leaves of lemon and sweet orange [17]. Yet this polyphagous *Colletotrichum* species, probably originating from the southern hemisphere, is already established in southern Italy on different host-plants and is replacing *C. godetiae* (syn. *C. clavatum*) as the main causal agent of olive anthracnose in Calabria [45–47]. In addition, there is evidence of its presence on oleander in Sicily since 2001 [29]. The threat posed by this exotic *Colletotrichum* species as a potential citrus pathogen in the Mediterranean region deserves particular attention.

The sudden outbreak of twig and shoot dieback in vast areas following winds and prolonged drought presupposes an inoculum already present and widespread throughout the citrus orchards. As a matter of fact, *Colletotrichum gloeosporioides* and *C. karstii*, like many other *Colletotrichum* species, may have different lifestyles. They may be latent pathogens, endophytes, epiphytes or saprobes and switch to a pathogenic lifestyle when host plants are under stress [48]. As stress factors have a fundamental role in triggering the infection by *Colletotrichum* species, twig and shoot dieback may be regarded as a complex disease, a definition also encompassing other emerging citrus diseases, such as dry root rot incited by species of *Fusarium* *s.l.* [49–51]. A common feature of this type of diseases is the difficulty in reproducing the syndrome in experimental conditions as even wounding may only partially substitute environmental stresses and cannot reproduce alone the effects of different stressors acting simultaneously on host-plant. This may explain the failure in reproducing all field symptoms of *Colletotrichum* twig and shoot dieback by artificial inoculations [5].

5. Conclusions

This study provided evidence that the new disease of citrus named twig and shoot dieback emerging in the Mediterranean region is caused by *Colletotrichum gloeosporioides*, and occasionally by *C. karstii*. Consistently with the results of this study, both *C. gloeosporioides* and *C. karstii* were found to be associated with the disease in Central Valley in California, but the proportion and distribution of the two *Colletotrichum* species in citrus groves of California, Albania and Italy were different. In Albania and Italy, winds and drought were identified as the stress factors predisposing the host-plant to the infections by *Colletotrichum* spp. and allowing these ubiquitous fungi to switch from an endophytic or saprophytic to a pathogenic lifestyle, while in California the predisposing stress factors

have not yet been precisely determined [5,52]. A better understanding of both the diversity of *Colletotrichum* species, associated with twig and shoot dieback of citrus, and the factors triggering the outbreaks of this disease is basilar for developing effective management strategies. In California, the effectiveness of chemical treatments with fungicides, including strobilurins (azoxystrobin, pyraclostrobin and trifloxystrobin), triazoles (fenbuconazole) and copper fungicides, are being investigated as part of an integrated disease management strategy. A more sustainable management strategy, compatible with organic farming, should privilege measures aimed at both preventing or mitigating the effect of predisposing factors and reducing the amount of inoculum of *Colletotrichum* in the orchard, such as proper management of the irrigation to avoid water stress, use of windbreaks to protect the trees from winds and pruning to remove withered twigs and branches and stimulate new vegetation flushing.

Author Contributions: Conceptualization, S.O.C., A.P. and M.C.; methodology, A.P., S.O.C., M.R. and F.A.; software, F.A. and M.R.; validation, S.O.C., A.P. and M.C.; formal analysis, F.A. and M.R.; investigation, M.R., F.A. and A.P.; resources, S.O.C., A.P. and M.C.; data curation, F.A. and M.R.; writing—original draft preparation, F.A. and M.R.; writing—review and editing, S.O.C., A.P. and M.C.; visualization, S.O.C.; supervision, S.O.C., A.P. and M.C.; project administration, S.O.C. and A.P.; funding acquisition, S.O.C., A.P. and M.C. All authors have read and agreed to the published version of the manuscript.

Funding: This research was funded by the University of Catania, Italy “Investigation of phytopathological problems of the main Sicilian productive contexts and eco-sustainable defense strategies (MEDIT-ECO)” PiaCeRi - PIAno di inCentivi per la Ricerca di Ateneo 2020-22 linea 2” “5A722192155”; “F.A. has been granted a Ph.D. fellowship “Scienze Agrarie, Alimentari, Forestali e Ambientali—XXXIII cycle”, University of Palermo; M.R. has been granted a fellowship by CREA “OFA” (Rende, Italy), this study is part of his activity as PhD, in “Agricultural, Food, and Forestry Science”, University Mediterranean of Reggio Calabria, XXXV cycle”.

Institutional Review Board Statement: Not pertinent.

Informed Consent Statement: Not pertinent.

Data Availability Statement: Not pertinent.

Acknowledgments: The authors are grateful to Jordan Merkuri, “Didactic and Scientific Research Center—Durrës, Albania” for his help in isolating the pathogen; and to V. Lo Giudice for the encouragement to focus on this emerging phytopathological problem of citrus; the authors wish also to thank Anna Davies for the English revision of the text and G. Gozzo for providing assistance during the collection of samples.

Conflicts of Interest: The authors declare no conflict of interest. The funders had no role in the design of the study; in the collection, analyses, or interpretation of data; in the writing of the manuscript, or in the decision to publish the results.

References

1. Shkreli, E.; Imami, D. *Citrus Sector Study*; ASF Project Office: Tiranë, Albania, 2019.
2. Istat.it. Available online: <http://dati.istat.it/Index.aspx?QueryId=33705> (accessed on 18 September 2020).
3. Sinab.it. Available online: <http://www.sinab.it/node/22428> (accessed on 18 September 2020).
4. Cacciola, S.O.; Gullino, M.L. Emerging and re-emerging fungus and oomycete soil-borne plant diseases in Italy. *Phytopathol. Mediterr.* **2019**, *58*, 451–472.
5. Mayorquin, J.S.; Nouri, M.T.; Peacock, B.B.; Trouillas, F.P.; Douhan, G.W.; Kallsen, C.; Eskalen, A. Identification, Pathogenicity, and Spore Trapping of *Colletotrichum karstii* Associated with Twig and Shoot Dieback in California. *Plant Dis.* **2019**, *103*, 1464–1473. [CrossRef] [PubMed]
6. Eskalen, A.; Dohuan, G.W.; Craig, K.; Mayorquin, J.S. *Colletotrichum* dieback of mandarins and Navel oranges in California: A new twig and shoot disease in the Central Valley. *Citrograph* **2019**, *10*, 50–54.
7. Benyahia, H.; Ifia, A.; Smaili, C.; Afellah, M.; Lamsetef, Y.; Timmer, L.W.; Ifi, A. First report of *Colletotrichum gloeosporioides* causing withertip on twigs and tear stain on fruit of citrus in Morocco. *Plant Pathol.* **2003**, *52*, 798. [CrossRef]
8. Rhaiem, A.; Taylor, P.W.J. *Colletotrichum gloeosporioides* associated with anthracnose symptoms on citrus, a new report for Tunisia. *Eur. J. Plant Pathol.* **2016**, *146*, 219–224. [CrossRef]

9. Mahiout, D.; Bendahmane, B.S.; Youcef Benkada, M.; Mekouar, H.; Berrahal, N.; Rickauer, M. First report of *Colletotrichum gloeosporioides* on citrus in Algeria. *Phytopathol. Mediterr.* **2018**, *57*, 355–359.
10. Ramos, A.P.; Talhinhos, P.; Sreenivasaprasad, S.; Oliveira, H. Characterization of *Colletotrichum gloeosporioides*, as the main causal agent of citrus anthracnose, and *C. karstii* as species preferentially associated with lemon twig dieback in Portugal. *Phytoparasitica* **2016**, *44*, 549–561. [[CrossRef](#)]
11. Dowling, M.; Peres, N.; Villani, S.; Schnabel, G. Managing *Colletotrichum* on fruit crops: A “complex” challenge. *Plant Dis.* **2020**, *104*, 2301–2316. [[CrossRef](#)]
12. Brown, A.E.; Sreenivasaprasad, S.; Timmer, L.W. Molecular characterization of slow-growing orange and key lime anthracnose strains of *Colletotrichum* from citrus as *C. acutatum*. *Phytopathology* **1996**, *86*, 523–527. [[CrossRef](#)]
13. Peres, N.A.; Timmer, L.W.; Adaskaveg, J.E.; Correll, J.C. Lifestyles of *Colletotrichum acutatum*. *Plant Dis.* **2005**, *89*, 784–796. [[CrossRef](#)]
14. Damm, U.; Cannon, P.; Woudenberg, J.; Johnston, P.; Weir, B.; Tan, Y.; Shivas, R.; Crous, P. The *Colletotrichum boninense* species complex. *Stud. Mycol.* **2012**, *73*, 1–36. [[CrossRef](#)] [[PubMed](#)]
15. Bragança, C.A.; Damm, U.; Baroncelli, R.; Júnior, N.S.M.; Crous, P.W. Species of the *Colletotrichum acutatum* complex associated with anthracnose diseases of fruit in Brazil. *Fungal Biol.* **2016**, *120*, 547–561. [[CrossRef](#)]
16. Savi, D.C.; Rossi, B.J.; Rossi, G.R.; Ferreira-Maba, L.S.; Bini, I.H.; Trindade, E.D.S.; Goulin, E.H.; Machado, M.A.; Glienke, C. Microscopic analysis of colonization of *Colletotrichum abscissum* in citrus tissues. *Microbiol. Res.* **2019**, *226*, 27–33. [[CrossRef](#)]
17. Guarnaccia, V.; Groenewald, J.; Polizzi, G.; Crous, P. High species diversity in *Colletotrichum* associated with citrus diseases in Europe. *Persoonia* **2017**, *39*, 32–50. [[CrossRef](#)] [[PubMed](#)]
18. Moges, A.; Belew, D.; Admassu, B.; Yesuf, M.; Maina, S.; Ghimire, S. Frequent association of *Colletotrichum* species with citrus fruit and leaf spot disease symptoms and their genetic diversity in Ethiopia. *J. Plant Pathol. Microbiol.* **2017**, *8*. [[CrossRef](#)]
19. Ben Hadj Daoud, H.; Baraldi, E.; Iotti, M.; Leonardi, P.; Boughalleb-M’Hamdi, N. Characterization and pathogenicity of *Colletotrichum* spp. causing citrus anthracnose in Tunisia. *Phytopathol. Mediterr.* **2019**, *58*, 175–185.
20. Uysal, A.; Kurt, Ş. First report of *Colletotrichum karstii* causing anthracnose on citrus in the Mediterranean region of Turkey. *J. Plant Pathol.* **2019**, *101*, 753. [[CrossRef](#)]
21. Lima, W.G.; Spósito, M.B.; Amorim, L.; Gonçalves, F.P.; De Filho, P.A.M. *Colletotrichum gloeosporioides*, a new causal agent of citrus post-bloom fruit drop. *Eur. J. Plant Pathol.* **2011**, *131*, 157–165. [[CrossRef](#)]
22. Damm, U.; Cannon, P.; Woudenberg, J.; Crous, P. The *Colletotrichum acutatum* species complex. *Stud. Mycol.* **2012**, *73*, 37–113. [[CrossRef](#)]
23. Weir, B.; Johnston, P.; Damm, U. The *Colletotrichum gloeosporioides* species complex. *Stud. Mycol.* **2012**, *73*, 115–180. [[CrossRef](#)]
24. Peng, L.; Yang, Y.; Hyde, K.D.; Bahkali, A.H.; Liu, Z. *Colletotrichum* species on Citrus leaves in Guizhou and Yunnan provinces, China. *Cryptogam. Mycol.* **2012**, *33*, 267–283.
25. Huang, F.; Chen, G.Q.; Hou, X.; Fu, Y.S.; Cai, L.; Hyde, K.D.; Li, H.Y. *Colletotrichum* species associated with cultivated citrus in China. *Fungal Divers.* **2013**, *61*, 61–74. [[CrossRef](#)]
26. Schena, L.; Mosca, S.; Cacciola, S.O.; Faedda, R.; Sanzani, S.M.; Agosteo, G.E.; Sergeeva, V.; Magnano di San Lio, G. Species of the *Colletotrichum gloeosporioides* and *C. boninense* complexes associated with olive anthracnose. *Plant Pathol.* **2014**, *63*, 437–446. [[CrossRef](#)]
27. Aiello, D.; Carrieri, R.; Guarnaccia, V.; Vitale, A.; Lahoz, E.; Polizzi, G. Characterization and Pathogenicity of *Colletotrichum gloeosporioides* and *C. karstii* Causing Preharvest Disease on Citrus *sinensis* in Italy. *J. Phytopathol.* **2015**, *163*, 168–177. [[CrossRef](#)]
28. Taheri, H.; Javan-Nikkhah, M.; Elahinia, S.A.; Khodaparast, S.A.; Golmohammadi, M. Species of *Colletotrichum* associated with citrus trees in Iran. *Mycol. Iran.* **2016**, *3*, 1–14.
29. Faedda, R.; Agosteo, G.E.; Schena, L.; Mosca, S.; Frisullo, S.; Magnano Di San Lio, G.; Cacciola, S.O. *Colletotrichum clavatum* sp. nov. identified as the causal agent of olive anthracnose in Italy. *Phytopathol. Mediterr.* **2011**, *50*, 283–302.
30. Cacciola, S.O.; Gilardi, G.; Faedda, R.; Schena, L.; Pane, A.; Garibaldi, A.; Gullino, M.L. Characterization of *Colletotrichum ocimi* Population Associated with Black Spot of Sweet Basil in Northern Italy. *Plants* **2020**, *9*, 654. [[CrossRef](#)]
31. ChromasPro v. 1.5 Software. Available online: <http://www.technelysium.com.au/> (accessed on 15 October 2020).
32. Shivas, R.G.; Tan, Y.P. A taxonomic re-assessment of *Colletotrichum acutatum*, introducing *C. fiorinae* comb. at stat. nov. and *C. simmondsii* sp. nov. *Fungal Divers.* **2009**, *39*, 111–112.
33. Uematsu, S.; Kageyama, K.; Moriwaki, J.; Sato, T. *Colletotrichum carthami* comb. nov., an anthracnose pathogen of safflower, garland chrysanthemum and pot marigold, revived by molecular phylogeny with authentic herbarium specimens. *J. Gen. Plant Pathol.* **2012**, *78*, 316–330. [[CrossRef](#)]
34. Lubbe, C.M.; Denman, S.; Cannon, P.F.; Groenewald, J.Z.; Lamprecht, S.C.; Crous, P.W. Characterization of *Colletotrichum* Species Associated with Diseases of Proteaceae. *Mycologia* **2004**, *96*, 1268–1279. [[CrossRef](#)]
35. Yang, Y.; Cal, L.; Yu, Z.; Liu, Z.; Hyde, K.D. *Colletotrichum* species on Orchidaceae in Southwest China. *Cryptogam. Mycol.* **2011**, *32*, 229–253.
36. Cannon, P.F.; Damm, U.; Johnston, P.R.; Weir, B.S. *Colletotrichum*—Current status and future directions. *Stud. Mycol.* **2012**, *73*, 181–213. [[CrossRef](#)]
37. TOPALi v2. Available online: <http://www.topali.org/> (accessed on 15 October 2020).

38. Freeman, S.; Katan, T.; Shabi, E. Characterization of *Colletotrichum* Species Responsible for Anthracnose Diseases of Various Fruits. *Plant Dis.* **1998**, *82*, 596–605. [[CrossRef](#)]
39. R Core Team. *R: A Language and Environment for Statistical Computing*; R Foundation for Statistical Computing: Vienna, Austria, 2018. Available online: <https://www.R-project.org> (accessed on 18 October 2020).
40. Timmer, L.W.; Brown, G.E. Biology and control of anthracnose diseases of citrus. In *Host Specificity*; Prusky, D., Freeman, S., Dickman, M.B., Eds.; The American Phytopathological Society: St. Paul, MN, USA, 2000; pp. 300–316.
41. Phoulivong, S.; Cai, L.; Chen, H.; McKenzie, E.H.C.; Abdelsalam, K.; Chukeatirote, E.; Hyde, K.D. *Colletotrichum gloeosporioides* is not a common pathogen on tropical fruits. *Fungal Divers.* **2010**, *44*, 33–43. [[CrossRef](#)]
42. Douanla-Meli, C.; Unger, J.-G. Phylogenetic study of the *Colletotrichum* species on imported citrus fruits uncovers a low diversity and a new species in the *Colletotrichum gigasporum* complex. *Fungal Biol.* **2017**, *121*, 858–868. [[CrossRef](#)]
43. Abdelfattah, A.; Nicosia, M.G.L.D.; Cacciola, S.O.; Droby, S.; Schena, L. Metabarcoding Analysis of Fungal Diversity in the Phyllosphere and Carposphere of Olive (*Olea europaea*). *PLoS ONE* **2015**, *10*, e0131069. [[CrossRef](#)] [[PubMed](#)]
44. Peres, N.A.; MacKenzie, S.J.; Peever, T.L.; Timmer, L.W. Postbloom Fruit Drop of Citrus and Key Lime Anthracnose Are Caused by Distinct Phylogenetic Lineages of *Colletotrichum acutatum*. *Phytopathology* **2008**, *98*, 345–352. [[CrossRef](#)]
45. Mosca, S.; Nicosia, M.G.L.D.; Cacciola, S.O.; Schena, L. Molecular Analysis of *Colletotrichum* Species in the Carposphere and Phyllosphere of Olive. *PLoS ONE* **2014**, *9*, e114031. [[CrossRef](#)] [[PubMed](#)]
46. Schena, L.; Abdelfattah, A.; Mosca, S.; Nicosia, M.G.L.D.; Agosteo, G.E.; Cacciola, S.O. Quantitative detection of *Colletotrichum godetiae* and *C. acutatum* sensu stricto in the phyllosphere and carposphere of olive during four phenological phases. *Eur. J. Plant Pathol.* **2017**, *149*, 337–347. [[CrossRef](#)]
47. Pangallo, S.; Nicosia, M.G.L.D.; Agosteo, G.E.; Abdelfattah, A.; Romeo, F.V.; Cacciola, S.O.; Rapisarda, P.; Schena, L. Evaluation of a Pomegranate Peel Extract as an Alternative Means to Control Olive Anthracnose. *Phytopathology* **2017**, *107*, 1462–1467. [[CrossRef](#)] [[PubMed](#)]
48. Crous, P.W.; Groenewald, J.Z.; Slippers, B.; Wingfield, M.J. Global food and fibre security threatened by current inefficiencies in fungal identification. *Philos. Trans. R. Soc. B Biol. Sci.* **2016**, *371*, 20160024. [[CrossRef](#)] [[PubMed](#)]
49. Yaseen, T.; D’Onghia, A. *Fusarium* spp. Associated to citrus dry root rot: An emerging issue for mediterranean citriculture. *Acta Hort.* **2012**, *940*, 647–655. [[CrossRef](#)]
50. Adesemoye, A.; Eskalen, A.; Faber, B.; Bender, G.; Connell, N.O.; Kallsen, C.; Shea, T. Current knowledge on *Fusarium* dry rot of citrus. *Citrograph* **2011**, *2*, 29–33.
51. Sandoval-Denis, M.; Guarnaccia, V.; Polizzi, G.; Crous, P. Symptomatic Citrus trees reveal a new pathogenic lineage in *Fusarium* and two new *Neocosmospora* species. *Persoonia* **2018**, *40*, 1–25. [[CrossRef](#)] [[PubMed](#)]
52. Li, T.; Fan, P.; Yun, Z.; Jiang, G.; Zhang, Z.; Jiang, Y. β -Aminobutyric Acid Priming Acquisition and Defense Response of Mango Fruit to *Colletotrichum gloeosporioides* Infection Based on Quantitative Proteomics. *Cells* **2019**, *8*, 1029. [[CrossRef](#)] [[PubMed](#)]

Chapter. 7

General conclusions

Fungal plant pathogens are among the foremost biotic factors that cause devastating diseases in crops (Doehlemann et al., 2017). About 8,000 species of fungi and oomycetes are responsible for diseases in plants (Horst, 2008; Fisher et al., 2020). Pathogenic fungi infect plants at any phase from the seedling stage to the seed maturity stage under natural environmental conditions, either alone or in concert with other pathogens (Narayanasamy, 2011).

Case studies included in this PhD thesis describe diseases that can cause significant losses in yield, quality and quantity in various agricultural systems of economically important horticultural and forest plant species.

Accurate diagnosis of diseases, i.e. the identification of causative agents, is a prerequisite for the development of rational and effective disease management strategies (Hariharan & Prasannath, 2021). This PhD thesis illustrates original examples of applications of molecular techniques based on PCR in the diagnosis of fungal plant diseases. Examples include the validation of different specific diagnostic methods for routine detection of *Fusarium circinatum*, a pathogen of quarantine concern in Europe. But it also reports examples of the correct identification of fungal pathogens, causing emerging or re-emerging diseases of crops of relevant economic importance in the Mediterranean macroregion, such as scabby canker of cactus pear, whose causal agent was identified as *Neofusicoccum batangarum*, twig and shoot dieback of citrus, a complex disease caused by *Colletotrichum* species, bot gummosis of lemon, whose causal agent in southern Italy was identified as *Neofusicoccum parvum*, and heart rot of pomegranate incited by *Alternaria alternata* and *A. arborescens*. As regards *F. circinatum*, the objective was to participate in an international European network which is seeking for a practical, sensitive and robust detection method that can be used routinely and universally by phytosanitary national and regional services to avoid the introduction and spread of this destructive quarantine pathogen in the EPPO area. Conversely, as far as the other diseases are concerned the main objective was to identify precisely the causal agents according to the modern molecular fungal taxonomy based on DNA sequencing and multi-locus phylogenetic analysis. The advent of DNA sequencing technology, in fact, has revolutioned the taxonomy and nomenclature of fungi. In particular, the multi-locus sequence phylogeny resulted in a substantial taxonomic and nomenclatural revision of families and genera encompassing also important plant pathogens, including among others the *Botryosphaeriaceae* family and the genera *Alternaria* and *Colletotrichum* (Andrew et al., 2009; Armitage et al., 2015; Cannon et al., 2012, Damm et al., 2012a; Damm et al., 2012b; Dissanayake et al., 2016; Lawrence et al., 2016; Phillips et al., 2013; Phillips et al., 2019; Shivas et al., 2009; Weir et al., 2012; Woudenberg et al., 2015; Zhang et al., 2021). Numerous cryptic species have been described and phylogenetic frameworks have been provided which prelude to the identification of new taxa as well as to a more accurate identification of pathogen genotypes and a more fine tuning of disease management strategies. However, due to the increasing number of DNA loci analysed and the number of

fungus isolates examined, molecular taxonomy of fungi is still evolving and defining species boundaries is still challenging. Moreover, not all fungi associated with plants are pathogens: most of them are saprobes, endophytes, opportunistic or latent pathogens and shift to an aggressive pathogenic lifestyle when environmental conditions are favorable or the host-plant is stressed. As a consequence, molecular diagnosis must be integrated with a more complete characterization of the fungus biology and ecology as well as of the fungus-plant genetic interaction. These aspects, including the differential expression of pathogenesis-related genes in pine seedlings inoculated with *F. circinatum* and *Phytophthora* species (as a model-system of multiple infections), the host range of *N. batangarum*, the ability of distinct *Colletotrichum* species to infect different organs of citrus plants and the toxigenic profile of *A. alternata*, *A. arborescens* and *N. batangarum* have been also considered in this thesis.

The study on *Fusarium circinatum* (Ioos et al., 2019) evaluated the transferability and the performance of nine molecular diagnostic protocols based on conventional or real-time PCR, involving an international collaborative team of 23 partners. Diagnostic sensitivity, specificity and accuracy of the nine protocols all reached values >80%, and the diagnostic specificity was the only parameter differing significantly between protocols. The rates of false positives and of false negatives were computed and only the false positive rates differed significantly, ranging from 3.0% to 17.3%. Considering that participating laboratories were free to use their own reagents and equipment, this study demonstrated that the diagnostic protocols for *F. circinatum* were not easily transferable to end users. More generally, obtained results suggested that the use of protocols using conventional or real-time PCR outside their initial development and validation conditions should require careful characterization of the performance data prior to use under modified conditions (i.e. reagents and equipment). These results highlight the difficulty still encountered in the large-scale routine application of molecular diagnosis for the detection of quarantine pathogens and the need of validation of published protocols retrieved from the literature using the ring test-lab system to evaluate their performance.

In this study a combined molecular and biochemical approach has been used to obtain a better insight into a peculiar disease of cactus pear named scabby canker, which constitutes a serious limit to the cultivation of this Cactacea in minor islands around Sicily. Despite its regional and worldwide economic importance as a fruit crop the diseases of cactus pear have been only occasionally studied. Scabby canker was first reported about 50 years ago and the causal agent was originally identified as *Dothiorella ribis*, an epithet no longer used in the modern taxonomy of *Botryosphaeriaceae* and recently put in synonymy with *N. ribis* (Somma et al., 1973). Subsequently in a comprehensive recent review of cactus pear diseases the cosmopolitan fungus *Lasiodiplodia thebromae* (*Botryosphaeriaceae*) was cited as the causal agent of this disease (Granata et al., 2017). In this study, using multi-locus phylogenetic analysis and according with the modern molecular taxonomy of *Botryosphaeriaceae*, the causal agent of scabby canker of cactus pear was identified as *N. batangarum*, a species reported for the first time in Europe (Aloi et al., 2020). Quite interestingly, in a very recent critical review of the taxonomy of *Botryosphaeriaceae* (Zhang et al., 2021), the species concept of *N. ribis* was broadened and *N. batangarum*, although genetically distinct, was put in

synonymy with *N. ribis*, a species with a very broad host range, confirming that the modern molecular taxonomy of fungi is still in a continuous evolution. Apart from the purely taxonomic aspects, the presently restricted host- and geographical range of *N. batangarum* despite its potentially wide host range shown in pathogenicity tests, its aggressiveness and exclusive presence on cactus pear are epidemiological and ecological aspects deserving further investigation. An additional aspect with phytosanitary implications, deserving particular attention is the threat this pathogen poses for cactus pear cultivation in Sicily, the first cactus pear fruit producer in Europe and the second globally.

The ability of *N. batangarum* to produce phytotoxic secondary metabolites, including (–)-(R)-mellein (1); (±)-botryoisocoumarin A; (–)-(3R,4R)- and (–)-(3R,4S)-4-hydroxymellein; (–)-terpestacin; and (+)-3,4-dihydro-4,5,8-trihydroxy-3-methylisocoumarin, named (+)-neoisocoumarin (Masi et al., 2020), is consistent with the literature concerning the production of secondary metabolites by *Botryosphaeriaceae* and expands the list of biologically active metabolites produced by *Neofusicoccum* species (recently reviewed by Salvatore et al., 2021). The most active compounds were (±)-botryoisocoumarin A, (–)-terpestacin, and (+)-neoisocoumarin, that showed phytotoxicity on both cactus pear and a non-host and taxonomically not related plant (tomato), suggesting these metabolites can have an active role as wide-spectrum virulence factors in scabby canker and other plant diseases caused by *Botryosphaeriaceae*. The ability to produce such a large arsenal of phytotoxins may, at least in part, explain the polyphagy of *Botryosphaeriaceae* in general and the potential wide host-range of *N. batangarum*, in particular. Moreover, it has been hypothesized that (–)-terpestacin, due to its allelopathic, anti-fungal and anti-bacterial, activity may help *N. batangarum* to compete with other components of the microbiota in colonizing the plant. The ecological functions of secondary metabolites produced by *Neofusicoccum* and possible applications of their allelopathic activity, as herbicides or antimicrobial compounds, have been little explored so far. Masi et al. (2018) questioned the possibility to use (–)-terpestacin as an herbicide due to its phytotoxicity. Another *Neofusicoccum* species that has been characterized in this study using multi-locus phylogenetic analysis, is *N. parvum*, a very polyphagous and aggressive plant pathogen. In a survey of lemon groves of the two major lemon production regions of southern Italy *N. parvum* has been identified as the prevalent causal agent of bot gummosis of lemon, for the first time in this country. Pathogenicity tests carried out to fulfill Koch's postulates showed differences in susceptibility between the two tested lemon cultivars, suggesting that a screening of a larger number of commercial lemon cultivars for the susceptibility to this disease could be interesting for developing a sustainable disease management strategy based on genetic resistance.

Another topical aspect addressed by this thesis was the role of opportunistic pathogens such as *Colletotrichum* spp. in the etiology of complex plant diseases, as a consequence of the ability of these fungi to shift from a saprobic or endophytic into a pathogenic life style on stressed plants. In this respect, the attitude of *Colletotrichum* spp. to behave as latent, opportunistic pathogens is similar to that of *Neofusicoccum* spp. and other *Botryosphaeriaceae* (Slippers and Wingfield, 2007). Using multi-locus phylogenetic analysis and completing Koch's postulates, *C. gloeosporioides* and *C. karstii*, two

polyphagous and common species, were identified as the causal agents of a new syndrome named twig and shoot dieback of citrus. However, winds and drought were the environmental stressors that triggered the shift of this fungi into an aggressive pathogenic life style. This case-study clearly exemplify the possibility of new plant diseases emerging in the Mediterranean region as a result of climate change.

Finally, multi-locus phylogenetic analysis allowed to clearly identify as *A. alternata* and *A. arborescens*, the species associated to heart rot, a complex disease that has emerged recently in commercial pomegranate orchards in California and the Mediterranean basin (Riolo et al., 2021). This study also highlighted another aspect of *Alternaria* heart rot of pomegranate, namely the toxigenic potential of *Alternaria* species associated with the disease, which has practical implications for the juice industry and the EU regulations of the limits of mycotoxins in foods. Food security, in general, is a topical aspect of the UE policy. The actual risk and level of contamination of pomegranate juice by *Alternaria* toxins during the industrial processing have not yet been quantified and deserve to be thoroughly investigated.

The diversity of case-studies addressed in this study offered the opportunity to apply different molecular approaches spanning from molecular techniques based on PCR in the diagnosis of plant diseases or in the study of the transcriptomic response of plant in a model pathosystem, to the multi-gene sequencing and phylogenetic analysis to precisely identify the pathogens. Another interesting aspect was the application of these molecular techniques to better understand the complex interactions host-plant/pathobiome in multiple infections and host-plant/pathogens/ environment in complex diseases, in which environmental stressors have a still unexplored key-role.

In previous paragraphs, main results have been summarized and discussed for each case-study, moreover potential applications and further developments of each research line have been suggested or hypothesized. A general aspect that as a PhD student I would like to highlight is the formative aspect of the thesis in the way it was conceived; it oriented me toward a problem-solving attitude using modern technologies and a multi-disciplinary approach.

References

- Adams, I.P.; Fox, A.; Boonham, N.; Massart, S.; Jonghe, K.D. 2018. The impact of high throughput sequencing on plant health diagnostics. *Eur. J. Plant Pathol.* 152: 909-919.
- Aloi, F., Giambra, S., Schena, L., Surico, G., Pane, A., Gusella, G., Stracquadiano, C., Burrano, S., & Cacciola, S. O. (2020). New insights into scabby canker of *Opuntia ficus-indica*, caused by *Neofusicoccum batangarum*. *Phytopathologia Mediterranea*, 59, 269–284. <https://doi.org/10.14601/Phyto-11225>
- Barba, M., Czosnek, H.; Hadidi, A. 2014. Historical perspective, development and applications of next-generation sequencing in plant virology. *Viruses* 6: 106-136.
- Bartlett, J.M.; Stirling, D., 2003. A short history of the polymerase chain reaction. *Methods Mol. Biol.* 226: 3-6.
- Chen, K; Wang, Y.; Zhang, R.; Zhang, H., Gao, C. 2019. CRISPR/Cas genome editing and precision plant breeding in agriculture. *Annu. Rev. Plant Biol.* 70: 667-697.
- Cooke, D.E.L.; Schena, L.; Cacciola, S.O. 2007. Tools to detect, identify, and monitor *Phytophthora* species in natural ecosystems. *J. Plant Pathol.* 89: 13-28.
- Crous, P.W. 2005. Impact of molecular phylogenetics on the taxonomy and diagnostics of fungi. *Bulletin OEPP/EPPO Bulletin* 35: 47-51.
- Crous, P.W.; Hawksworth, D.L.; Wingfield, M.J. 2015. Identifying and naming plant-pathogenic fungi: past, present and future. *Annu. Rev. Phytopathol.* 53: 247-267.
- Doehlemann, G., Ökmen, B., Zhu, W., and Sharon, A. 2017. Plant Pathogenic Fungi. *Microbiol. Spectr.* 5 (1), FUNK-0023-2016. doi: 10.1128/microbiolspec.FUNK-0023-2016
- Fisher, M. C., Gurr, S. J., Cuomo, C. A., Blehert, D. S., Jin, H., Stukenbrock, E. H., et al. 2020. Threats Posed by the Fungal Kingdom to Humans, Wildlife, and Agriculture. *mBio* 11 (3), e00449–e00420. doi: 10.1128/mBio.00449-20
- Frantzeskakis, L.; Di Pietro, A.; Rep, M.; Schirawsk, J.; Wu, C.H.; Panstruga, R. 2020. Rapid evolution in plant–microbe interactions – a molecular genomics perspective. *New Phytologist* 225: 1134-1142.
- Guarnaccia, V.; Groenewald, J.Z.; Woodhall, J.; Armengol, J. *et al.* 2018. *Diaporthe* diversity and pathogenicity revealed from a broad survey of grapevine diseases in Europe. *Persoonia* 40: 135-153.
- Gupta, R.; Lee, S.E.; Agrawal, G.K.; Rakwal, R.; Park, S.; Wang, Y.; Kim, S.T. 2015. Understanding the plant-pathogen interactions in the context of proteomics-generated apoplastic proteins inventory. *Front. Plant Sci.* 6:352. doi: 10.3389/fpls.2015.00352
- Hariharan G, Prasannath K. Recent Advances in Molecular Diagnostics of Fungal Plant Pathogens: A Mini Review. *Front Cell Infect Microbiol.* 2021 Jan 11;10:600234. doi: 10.3389/fcimb.2020.600234. PMID: 33505921; PMCID: PMC7829251.
- Horst, R. (2008). “Classification of plant pathogens,” in Westcott’s Plant Disease Handbook. Ed. R. Horst (Dordrecht: Springer), 43–79. doi: 10.1007/978-1-4020-4585-1_2
- Ioos, R., Aloi, F., Piškur, B. *et al.* Transferability of PCR-based diagnostic protocols: An international collaborative case study assessing protocols targeting the quarantine pine pathogen *Fusarium circinatum*. *Sci Rep* 9, 8195 (2019). <https://doi.org/10.1038/s41598-019-44672-8>

- Kaunitz, J.D., 2015. The discovery of PCR: ProCuRement of Divine Power. *Dig. Dis. Sci.* 60: 2230-2231.
- Lindahl, B.D.; Nilsson, R.H.; Tedersoo, L.; Abarenkov, K. *et al.* 2013. Fungal community analysis by high-throughput sequencing of amplified markers – a user’s guide. *New Phytologist*: 199: 288–299.
- Masi, M.; Nocera, P.; Reveglia, P.; Cimmino, A.; Evidente, A. Fungal metabolites antagonists towards plant pests and human pathogens: Structure-activity relationship studies. *Molecules* 2018, 23, 834.
- Masi, M., Aloï, F., Nocera, P., Cacciola, S. O., Surico, G., & Evidente, A. . Phytotoxic Metabolites Isolated from *Neofusicoccum batangarum*, the Causal Agent of the Scabby Canker of Cactus Pear (*Opuntia ficus-indica* L.). *Toxins* 2020, 12, 126. <https://doi.org/10.3390/toxins12020126>
- Muñoz, I.V.; Sarrocco, S.; Malfatti, L.; Baroncelli, R.; Vannacci, G. 2020. CRISPS/Cas for fungal genome editing: a new tool for the management of plant diseases. *Front. Plant Sci.* doi: <https://doi.org/10.3389/fpls.2019.00135>
- Narayananamy, P. (2011). “Diagnosis of fungal diseases of plants,” in *Microbial plant pathogens-detection and disease diagnosis* (Dordrecht: Springer), 273–284. doi: 10.1007/978-90-481-9735-4_5
- Peyraud, R.; Dubiella, U.; Barbacci, A.; Genin, S.; Raffaele, S.; Roby, D. 2017. Advances on plant-pathogen interactions from molecular toward systems biology perspectives. *Plant J.* 90: 720-737.
- Raja, H.A.; Miller, A.N.; Pearce, C.J.; Oberlies, N.H. 2017. Fungal identification using molecular tools: a primer for the natural products research community. *J. Nat. Prod.* 80: 756-770.
- Riolo, M., Aloï, F., Pane, A., Cara, M., & Cacciola, S. O. (2021). Twig and Shoot Dieback of Citrus, a New Disease Caused by *Colletotrichum* Species. *Cells*, 10(2), 449.
- Ruvishika, S.; Jayawardena, R.S., Hyde, K.D., Chen, Y.J. *et al.* 2020. One stop shop IV: taxonomic update with molecular phylogeny for important phytopathogenic genera: 76–100. *Fungal Diversity* 103: 87–218.
- Salvatore, M.M.; Alves, A.; Andolfi, A. Secondary Metabolites Produced by *Neofusicoccum* Species Associated with Plants: A Review. *Agriculture* 2021, 11, 149. <https://doi.org/10.3390/agriculture11020149>
- Sanzani, S.M.; Li Destri Nicosia, M.G.; Faedda, R.; Cacciola, S.O.; Schena, L. 2014. Use of PCR detection methods to study biocontrol agents and phytopathogenic fungi and oomycetes in environmental samples. *J. Phytopathol.* 162: 1-13.
- Schena, L.; Li Destri Nicosia, M.G., Sanzani, S.M.; Faedda, R.; Ippolito, A.; Cacciola, S.O. 2013. Development of quantitative PCR detection methods fo phytopathogenic fungi and oomycetes. *J. Plant Pathol.* 95, 7-24.
- Schenke, D.; Cai, D. 2020. Applications of CRISPS/Cras to improve crop disease resistance: beyond inactivation of susceptibility factors. *iScience* 23, 101478.
- Williams, P.M., 2009. The beginning of Real-Time PCR. *Clinical Chemistry* 55(4): 833-834.